Investigation of the essential role of *S. cerevisiae MEC1*

Caroline Louise Earp

A thesis submitted to University College London in fulfilment of the requirements for the degree of Doctor of Philosophy

May 2008

Division of Stem Cell Biology and Developmental Genetics
National Institute for Medical Research
The Ridgeway
Mill Hill
London
NW7 1AA

ProQuest LLC
789 East Eisenhower Parkway
P.O. Box 1346
Ann Arbor, MI 48106-1346

Declaration

"I, **Caroline Earp**, confirm that the work presented in this thesis is my own. Where information has been derived from other sources, I confirm that this has been indicated in the thesis"

Signed ..... **Date** 28/05/08

Abstract

S. cerevisiae Mec1 is an essential, chromosome-based, signal transduction protein, which is involved in DNA replication, repair, and recombination. The Mec1-dependent checkpoint response to genotoxic stress has been widely investigated. However the essential role, which is believed to be to upregulate dNTP synthesis for DNA replication, remains less well understood. I have used two independent approaches to investigate the essential role of *MEC1* further.

Firstly, the possibility that Mec1 controls local dNTP synthesis at the replication fork was examined. It is known that in the absence of Mec1 function, chromosome breakage occurs in specific regions of the genome called "replication slow zones". Given the importance of Mec1 in upregulating dNTP synthesis, this phenotype could be explained by an essential requirement for Mec1 to couple dNTP synthesis with replication fork progression in these regions. This possibility was examined using chromatin immunoprecipitation to look for association of Mec1 with the DNA during S-phase. Although Mec1 recruitment to the DNA in response to replication stress was observed, no recruitment was seen during unchallenged S-phase.

Secondly, a novel multicopy suppressor of the lethality of the temperature sensitive *mec1* alleles, *mec1-4* and *mec1-40*, was characterised. This suppressor, *GIS2*, encodes a retroviral-like zinc-finger protein, homologous to mammalian CNBP. *GIS2* has been previously suggested to be a negative regulator of the RAS-cAMP-PKA signalling pathway, which is important for coupling growth and cell cycle progression. Therefore, other conditions expected to downregulate PKA activity were tested for their ability to suppress lethality of *mec1-4*. As predicted, both deletion of *RAS2* and growth on alternative carbon sources can suppress the lethality of *mec1-4*. The only known mechanism of suppressing the loss of *MEC1* function is to increase dNTP levels. However, increased *GIS2* expression did not have any significant effects on the known mechanisms of upregulating dNTP synthesis.

Overall, I describe a novel genetic interaction between *mec1-4* and *GIS2*. Possible mechanisms for this interaction are also discussed.

Table of Contents

List of Figures

List of Tables

List of Abbreviations

1C	one cell (haploid) DNA content
2C	two cell (diploid) DNA content
^{32}P	32-phosporous
4-NQO	4-nitroquinoline
5'FOA	5'-fluoro-orotic acid
5'UTR	5'-untranslated region
ACS	ARS consensus sequence
αF	alpha factor
Amp	ampicillin
AMP	adenosine monophosphate
APC/C	anaphase promoting complex or cyclosome
APC/C^{Cdc20}	Cdc20-bound APC/C
APC/C^{Cdh1}	Cdh1-bound APC/C
APS	ammonium persulphate
ARS	autonomously replicating sequence
A-T	ataxia telangiectasia
ATM	ataxia telangiectasia mutated
ATP	adenosine triphosphate
ATR	ataxia telangiectasia and Rad3 related
ATRIP	ATR interacting protein
bp	base pair(s)
BSA	bovine serum albumin
cAMP	cyclic-AMP
CDK	cyclin-dependent kinase
ChIP	chromatin immunoprecipitation
CNBP	cellular nucleic acid binding protein
DAPI	4,6-diamino-2-phenylindole
dATP	deoxyadenosine triphosphate
dCTP	deoxycytidine triphosphate
dGTP	deoxyguanosine triphosphate

DMSO	dimethyl sulphoxide
DNA	deoxyribonucleic acid
dNTP	deoxynucleotide triphosphate
DSB	double-strand break
dsDNA	double-stranded DNA
dTTP	deoxythymidine triphosphate
E. coli	*Eschericia coli*
ECL	enhanced chemiluminescence
EDTA	ethlenediaminetetra-acetic acid
FACS	fluorescence activated cell scan
FEAR	CDC fourteen early anaphase release
G1	gap 1
G2	gap 2
GAP	GTPase activating protein
GDP	guanosine diphosphate
GEF	guanine nucleotide exchange factor
GFP	green fluorescent protein
GIG	glucose inhibition of gluconeogenic growth
GIS	*gig* suppressor
hCNBP	human CNBP
γH2AX	phosphorylated *S. cerevisiae* H2A or vertebrate H2AX
GPCR	G-protein coupled receptor
GTP	guanosine triphosphate
HEPES	4-(2-hydroxyethyl)-1-piperazineethanesulphonic acid
HR	homologous recombination
HU	hydroxyurea
IR	ionising radiation
kb	kilo base (s)/ kilo base pair (s)
kd	kinase-dead
L	DNA ladder
LB	Luria Bertani
LMP	low melting point
M	mitosis
MAT	mating type locus

MBF	MCB-binding factor
MCB	*Mlu*I cell cycle box
MEN	mitotic exit network
MES	2-(N-morpholino)ethanesulphonic acid
MMS	methyl methanesulphonate
MOPS	3-(N-morpholino)propanesulphonic acid
mRNA	messenger RNA
NER	nucleotide excision repair
NHEJ	non-homologous end-joining
OD_{600}	optical density at 600 nm
ORC	origin recognition complex
ORF	open reading frame
PAGE	polyacrylamide gel electrophoresis
PBS	phospho-buffered saline
PCNA	proliferating cell nuclear antigen
PCR	polymerase chain reaction
PDS	post diauxic shift
PEG	polyethylene glycol
PFGE	pulsed-field gel electrophoresis
PIKK	phosphatidylinositol-3-OH kinase-like kinase
PKA	protein kinase A
PMSF	phenylmethylsulphonyl fluoride
pre-RC	pre-replicative complex
R1	RNR large subunit
R2	RNR small subunit
rDNA	ribosomal DNA
RFC	replication factor C
RNA	ribonucleic acid
RNase	ribonuclease
RNR	ribonucleotide reductase
rp	ribosomal protein
RPA	replication protein A
rpm	revolutions per minute
RSZ	replication slow zone

S	DNA synthesis
S. cerevisiae	*Saccharomyces cerevisiae*
S. pombe	*Schizosaccharomyces pombe*
SBF	SCB-binding factor
SC	synthetic complete
SCB	Swi4/Swi6-dependent cell cycle box
SD	synthetic dextrose
SDS	sodium dodecyl sulphate
SPB	spindle pole body
SPM	sporulation media
ssDNA	single-stranded DNA
SSPE	sodium chloride sodium phosphate EDTA
STRE	stress response element
TAE	Tris-acetate EDTA
TBE	Tris-borate EDTA
TBS	Tris-buffered saline
TCA	trichloroacetic acid
TE	Tris-EDTA
TEMED	N,N,N',N'-tetramethyl-ethylenediamine
TOP	terminal oligopyrimidine
tRNA	transfer RNA
ts	temperature sensitive
UV	ultra violet
WCE	whole cell extract
wt	wild type
YEP	yeast extract peptone
YPD	yeast extract peptone dextrose
YPG	yeast extract peptone glycerol

Acknowledgements

Firstly I would like to thank my supervisor, Rita Cha, for giving me the opportunity to do this project, and for her continued support, ideas, and advice through out. Secondly, I would like to thank everyone from Yeast Genetics, past and present, who has contributed to this project. In particular, Jesus Carballo, Marco Geymonat, Steve Sedgwick, Ad Spanos, and especially Tony Johnson, who has been an incredible source of "yeast" knowledge. I would also like to thank Jonathan Millar and Tony Carr for their ideas and guidance.

Thank you to Oscar Aparicio, Marco Foiani, Mingxia Huang, Doug Koshland, and Maria Pia Longhese who all kindly supplied yeast strains or plasmids used in this project. Additionally, thank you to Sam Rowbotham, who carried out the initial genetic screen in which *GIS2* was isolated.

On a more personal note, a huge thank you to Mary and Nadia for keeping me sane!

Finally, thanks to Jim for his love, support, and patience.

Chapter 1

Introduction

1.1 The eukaryotic cell cycle

1.1.1 Overview

The survival of any organism depends on the ability of its cells to proliferate. Individual cells grow in size by taking up nutrients from the extracellular environment and converting these into biological macromolecules (Hartwell, 1974). This growth can only occur if the essential nutrients are supplied in sufficient quantities. If this condition is met, a population of cells will expand by individual cells undergoing the mitotic cell division cycle. Successful passage though the cell cycle requires accurate and timely completion of two key events: genome duplication followed by segregation of the two copies of the cell's genetic material (Hartwell, 1974). Progression through the cell cycle follows a highly ordered sequence of events and is tightly coupled to cell growth (Hartwell & Weinert, 1989; Johnston *et al.*, 1977). If anything goes wrong in the cellular machinery that co-ordinates these processes then cell viability and genome stability will be compromised; in multicellular organisms this can lead to tumourigenesis (Lengauer *et al.*, 1998).

A considerable amount of the understanding of the eukaryotic mitotic cell cycle has come from detailed genetic studies of the yeasts *Saccharomyces cerevisiae* (*S. cerevisiae*) and *Schizosaccharomyces pombe* (*S. pombe*) (Hartwell *et al.*, 1970; Nurse & Thuriaux, 1980). The cell division cycle is simply viewed in four main phases: G1 (gap 1), S (DNA synthesis), G2 (gap 2) and M (mitosis) (Hartwell, 1974). Progression through the cell cycle is driven by cyclin-dependent kinases (CDKs), whose activity is controlled by the periodic transcription of the regulatory cyclin subunits (Mendenhall & Hodge, 1998).

1.1.2 Initiation of the cell cycle

In each cell cycle there is a decision point that determines a commitment for that cell to undergo an entire cell division cycle. This point is called START in *S. cerevisiae* and the restriction point in mammalian cells (Blagosklonny & Pardee, 2002; Hartwell, 1974). Three conditions must be met for an *S. cerevisiae* cell to pass START (Johnston *et al.*, 1977): i) cells must reach a critical size, ii) there must be sufficient nutrients available, and iii) for haploid cells, there must be no mating factor present. Exactly how a cell senses the critical size threshold remains unclear, but Cln3 protein levels are an important factor. Cln3 is one of three G1 cyclins that control Cdc28, which is the only CDK in *S. cerevisiae* (Mendenhall & Hodge, 1998). Cln3 protein levels do not vary during the cell cycle (Tyers *et al.*, 1993). But, expression of *CLN3* is strongly downregulated, at both the transcriptional and translational level, under poor nutrient conditions (Hall *et al.*, 1998; Polymenis & Schmidt, 1997). Since Cln3 is a potent activator of START (Tyers *et al.*, 1993), downregulating *CLN3* expression in poor nutrient conditions prevents entry into the cell cycle when cells cannot grow in size. There are also nutrient sensing pathways that communicate information on nutrient status to the cell cycle machinery independently of Cln3. One of these pathways, the Ras-cAMP-PKA pathway, is covered in more detail in Section 1.6.

The third condition, the absence of mating factor, is a condition that is regularly used during experimental investigations of the *S. cerevisiae* cell cycle. *S. cerevisiae* has two mating types, **a** and α, which are determined by the allele encoded at the mating type (*MAT*) locus (reviewed by Herskowitz, 1988). Haploid cells sense the presence of the opposite mating type by a secreted mating pheromone. So, **a**-cells secrete **a**-factor, which is sensed by **a**-factor receptors expressed by α-cells, and vice versa (Herskowitz, 1988). Mating factor receptor stimulation by mating factor activates a signal transduction cascade that causes arrest in G1 before START, and polarised cell growth in anticipation of cell fusion to make a diploid cell (Herskowitz, 1988; Zhao *et al.*, 1995). Experimentally, a culture of **a**-cells can be arrested in G1 by adding chemically synthesised α-factor (αF). Then, assuming the other growth conditions are sufficient to pass START, the cells will progress synchronously through the cell cycle upon removal of the αF.

If growth conditions are not good enough to support proliferation then cells will enter a more specialised, non-dividing, resting state called stationary phase (reviewed by Herman, 2002). Cells at low density in rich media progress rapidly from one cell cycle to the next, generating energy by fermenting glucose to ethanol. This is called log phase growth and in this case G1 is very short. As the glucose supply in the media is exhausted, cells switch to respiratory growth and now use the ethanol produced during fermentative growth as a carbon source. This switch is called the post-diauxic shift. During the post-diauxic phase, growth rate is significantly slowed. Cells also start to show some stationary phase characteristics, such as stress resistance and accumulation of storage carbohydrates. Complete entry into stationary phase follows the post-diauxic phase. Growth rate is shut down further; ribosome production ceases and protein degradation and organelle turnover increases.

1.1.3 The G1/S transition

The G1/S transition is the period after START when cells prepare to initiate DNA replication (reviewed by Toone *et al.*, 1997). It is characterised by an increase in CDK activity, controlled by the G1 cyclins. Firstly, passage through START requires a threshold level of Cln3-Cdc28 kinase activity to be reached. The Cln3-Cdc28 complex activates two transcription factors SCB-binding factor (SBF) and MCB-binding factor (MBF) (Mendenhall & Hodge, 1998). These transcription factors are dimeric complexes that both contain a Swi6 subunit, along with a Swi4 subunit for SBF and a Mbp1 subunit for MBF (Dirick *et al.*, 1992; Koch *et al.*, 1993). SBF (Swi4-Swi6) and MBF (Mbp1-Swi6) bind to Swi4/Swi6-dependent cell cycle box (SCB) promoter elements and *Mlu*I cell cycle box (MCB) promoter elements respectively.

SBF activates the transcription of the other G1 cyclins, *CLN1* and *CLN2* (Nasmyth & Dirick, 1991). This generates a positive feedback loop by activating the Cln1/2-Cdc28 kinase, which in turn further activates SBF/MBF-dependent transcription and promotes other START events (Cross & Tinkelenberg, 1991; Dirick & Nasmyth, 1991). SBF also activates genes required for bud formation, and membrane and cell wall biosynthesis. Experimentally in *S. cerevisiae*, passage through START can be monitored by the formation of cells with small buds. MBF activates the transcription

of the S-phase cyclins, *CLB5* and *CLB6*, and other genes required for DNA replication, such as the ribonucleotide reductase subunit *RNR1* and the polymerase subunit *POL1* (Koch *et al.*, 1993; Lowndes *et al.*, 1991).

1.1.4 S-phase

1.1.4.1 Defining replication origins

Replication in eukaryotes initiates from multiple origins. In *S. cerevisiae* there are around 300-400 active replication origins (Toone *et al.*, 1997). In mammalian cells there can be thousands of replication origins, but they are not defined by specific *cis*-acting sequences as in *S. cerevisiae*. Replication origins in *S. cerevisiae* are defined by autonomously replicating sequence (*ARS*) elements, which were initially shown to confer the stable maintenance of a selectable plasmid (Newlon & Theis, 1993). However, *ARS* elements that function in the plasmid context do not always function in the chromosomal context, showing that additional levels of regulation are required to form an active replication origin. All *ARS* elements share an 11 bp *ARS* consensus sequence (ACS), which is bound by a six subunit complex called the origin recognition complex (ORC) (Bell & Stillman, 1992). In *S. cerevisiae* ORC binds to *ARS* elements throughout the cell cycle (Liang & Stillman, 1997).

ORC binding also defines replication origins in mammalian cells and *S. pombe*, despite the lack of sequence specificity (Chuang & Kelly, 1999; Schaarschmidt *et al.*, 2004). Instead of *ARS* elements, A/T rich DNA seems to be important for ORC binding in other organisms. The cell cycle regulation of ORC binding is less well understood in mammalian cells, but Orc1 (at least) dissociates from the DNA at the end of S-phase and rebinds in G1 (Natale *et al.*, 2000).

Interestingly, in yeast and mammalian cells, the function of ORC extends beyond defining replication origins: additional roles for ORC in gene silencing, sister chromatid cohesion, and ribosome biogenesis have been suggested (Du & Stillman, 2002; Foss *et al.*, 1993; Shimada & Gasser, 2007).

1.1.4.2 The dynamics of replication origin firing

In general, the mechanisms that control the dynamics of replication origin firing are poorly understood. Some understanding comes from experimental observations on the behaviour of specific replication origins. For example, the nature of the surrounding chromatin structure is known to be important in controlling the timing of origin firing. So, origins located near actively transcribing genes tend to fire early in S-phase, whereas origins located near telomeres or regions of heterochromatin fire late in S-phase (Friedman *et al.*, 1997; Reynolds *et al.*, 1989). There are also differences in the efficiency of origin firing: some origins fire almost every cell cycle, whereas others only fire very occasionally (Raghuraman *et al.*, 2001). How the subset of origins that fire in any one cell cycle are selected is unclear.

Replication origin firing in *S. cerevisiae* occurs in a continuum throughout S-phase (Raghuraman *et al.*, 2001), although a practical distinction is often made between early- and late-firing origins. So, some replication origins, such as *ARS305*, reproducibly fire early in S-phase (Reynolds *et al.*, 1989). Others, such as *ARS501*, only fire later in S-phase. Under conditions where DNA replication is inhibited, firing of these late origins is delayed (Santocanale & Diffley, 1998). Thus, temporal patterns of replication origin firing can be clearly defined in *S. cerevisiae*. However, this temporal pattern is unlikely to reflect a set temporal program of replication origin firing. Single molecule DNA combing techniques were used to look at the timing of replication origin firing on single chromosome fibres. At this level, significant variation was seen in the temporal pattern of origin firing, suggesting there is no strictly controlled temporal program (Czajkowsky *et al.*, 2008). Thus, the observed temporal pattern of replication origin firing is most likely to be based on the averaged effects of the probability of origin firing across a population.

1.1.4.3 Building the replication fork

Stable association of the replicative polymerases with the replication origin requires several highly regulated transitional stages (reviewed by Sclafani & Holzen, 2007; Toone *et al.*, 1997) (Figure 1.1). The first stage is to build a pre-replicative complex (pre-RC) on the ORC-bound replication origin, which is composed of Cdc6, Cdt1

and MCM2-7 (Toone *et al.*, 1997). The association of these proteins with the replication origin is controlled by CDK activity so that pre-RC formation can only occur in a very specific time window: as cells enter G1 after mitotic exit, but before START (Piatti *et al.*, 1996). Restricting pre-RC formation to this specific time window in G1 ensures that once cells have passed START no origin can initiate replication twice. This regulation is critical to ensure genomic stability by preventing any hazardous re-replication.

So, the pre-RC is built in G1 before the decision to enter the cell cycle is taken. After cells have passed START, a larger initiation complex containing several essential replication factors, is built around the pre-RC (reviewed by Sclafani & Holzen, 2007). These replication factors include Sld2, Sld3, Dpb11, Cdc45, Mcm10 and the GINS complex (Kamimura *et al.*, 2001; Ricke & Bielinsky, 2004; Takayama *et al.*, 2003). The assembly of the initiation complex is controlled by CDK activity. The CDK-dependent phosphorylation of Sld2 and Sld3 is essential for the stable association of the other replication factors with the initiation complex (Tanaka *et al.*, 2007; Zegerman & Diffley, 2007). The components of this initiation complex ultimately form an integral part of the active replication fork. So, they are required for both the establishment and progression of replication forks.

The next stage is to initiate origin firing and to assemble the replicative machinery. First, Dbf4-Cdc7 kinase activity is required to initiate local unwinding of the DNA duplex (Lei *et al.*, 1997). One known target of the Dbf4-Cdc7 kinase is the MCM2-7 complex, which is assumed to be the helicase that unwinds the DNA duplex during DNA replication. Experimental evidence to show that MCM2-7 has helicase activity has been elusive. Recently however, helicase activity was observed for the larger MCM-Cdc45-GINS complex purified from *Drosophila* (Moyer *et al.*, 2006). Presumably therefore, Dbf4-Cdc7 phosphorylates MCM2-7, which activates the MCM2-7 helicase activity in the context of the initiation complex and promotes local unwinding of the DNA duplex. The single-stranded DNA that is exposed at the replication origin upon unwinding is bound by the heterotrimeric replication protein A (RPA) (reviewed by Bell & Dutta, 2002). RPA binding promotes further unwinding and is important for the association of DNA polymerase α (pol α). DNA pol α is the only enzyme that can initiate DNA synthesis *de novo*, and does so by

synthesising an RNA primer for the replicative polymerases, pol δ and pol ε, to extend (reviewed by Bell & Dutta, 2002). The processive polymerase machinery is then built around the initial RNA primer. The replication factor C (RFC) clamp-loader binds to the primer-DNA duplex and then loads the proliferating cell nuclear antigen (PCNA) heterotrimeric clamp. PCNA is a processivity factor for pol δ. PCNA also forms a scaffold for many other proteins, such as DNA repair factors, that may need to interact with the replication fork (Moldovan *et al.*, 2007).

This multi-protein replication complex that promotes the polymerisation of the new DNA strands is called the replisome. The replicative polymerases can only catalyse DNA synthesis in a 5'-3' direction. However, as the two DNA template stands are of opposite polarity, only the strand that is of the same polarity as the polymerisation process can be synthesised in a continuous manner. This strand is called the leading strand. The other strand is called the lagging strand and new DNA must be synthesised as short fragments as the DNA duplex is unwound. These fragments are called Okazaki fragments are subsequently ligated together to form a continuous DNA strand (reviewed by Waga & Stillman, 1998).

The two replication forks that are assembled at the origin then synthesise the new DNA strands, bi-directionally away from the replication origin. DNA synthesis at several replication forks is co-ordinated spatially and temporally in replication factories, and these can be seen as nuclear foci that contain replisome proteins (Kitamura *et al.*, 2006). Thus, once assembled, the replisome eventually forms part of this larger, fixed, replication structure, into which the template DNA is fed, and out of which come the newly synthesised strands (Falaschi, 2000).

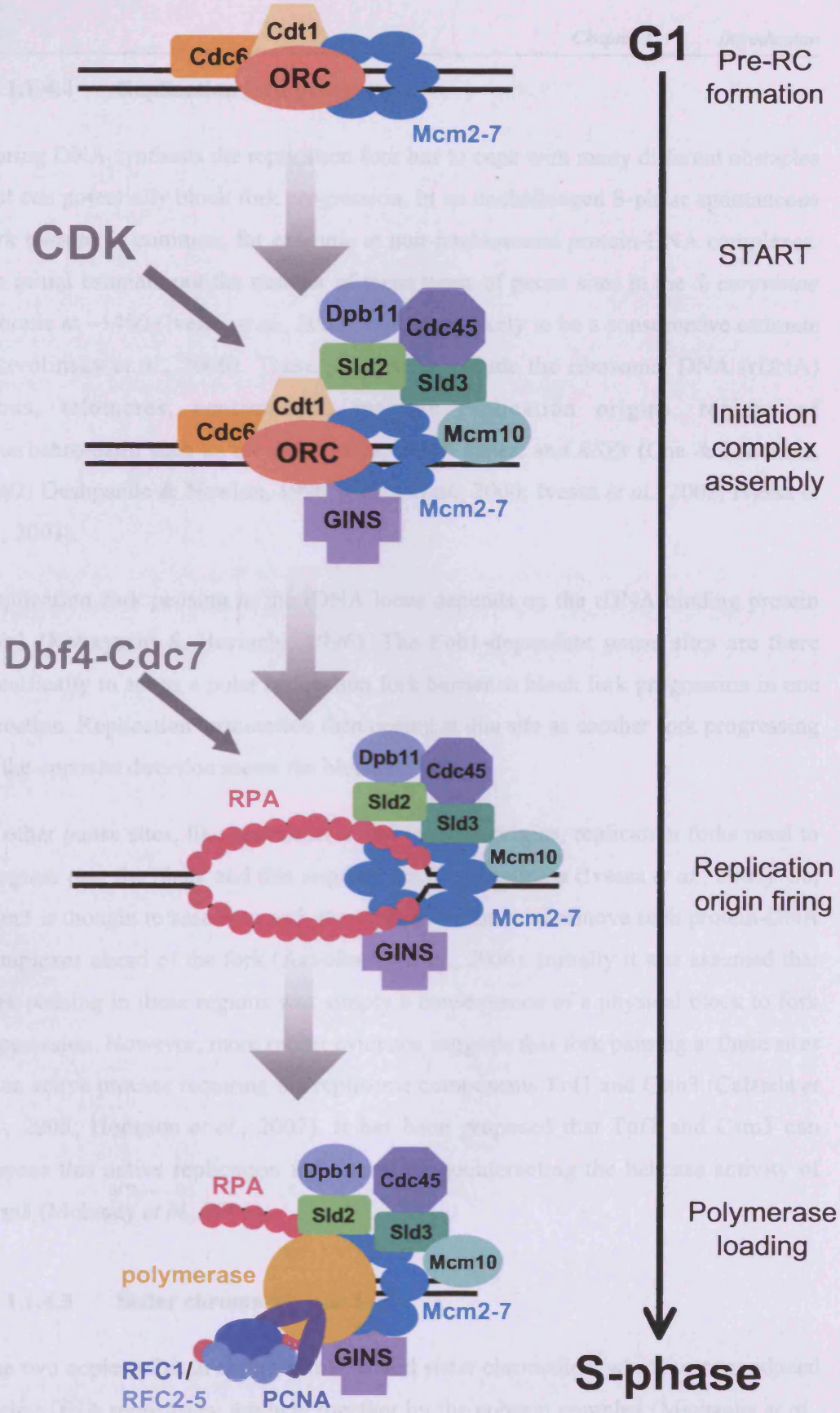
G1
Pre-RC formation
Cdt1
Cdc6
ORC
Mcm2-7
CDK
START
Dpb11
Cdc45
Sld2
Sld3
Cdt1
Cdc6
ORC
Mcm10
GINS
Mcm2-7
Initiation complex assembly
Dbf4-Cdc7
Dpb11
Cdc45
RPA
Sld2
Sld3
Mcm10
Mcm2-7
GINS
Replication origin firing
Dpb11
Cdc45
RPA
Sld2
Sld3
Mcm10
polymerase
Mcm2-7
GINS
RFC1/
RFC2-5
PCNA
Polymerase loading
S-phase

1.1.4.4 Replication fork progression

During DNA synthesis the replication fork has to cope with many different obstacles that can potentially block fork progression. In an unchallenged S-phase spontaneous fork pausing is common, for example at non-nucleosomal protein-DNA complexes. An initial estimate put the number of these types of pause sites in the *S. cerevisiae* genome at ~1400 (Ivessa *et al.*, 2003), but this is likely to be a conservative estimate (Azvolinsky *et al.*, 2006). These pause sites include the ribosomal DNA (rDNA) locus, telomeres, centromeres, inactive replication origins, regions of heterochromatin such as the *MAT* locus, tRNA genes, and *RSZs* (Cha & Kleckner, 2002; Deshpande & Newlon, 1996; Ivessa *et al.*, 2000; Ivessa *et al.*, 2002; Ivessa *et al.*, 2003).

Replication fork pausing in the rDNA locus depends on the rDNA binding protein Fob1 (Kobayashi & Horiuchi, 1996). The Fob1-dependent pause sites are there specifically to act as a polar replication fork barrier to block fork progression in one direction. Replication termination then occurs at this site as another fork progressing in the opposite direction meets the blocked fork.

In other pause sites, like centromeres and inactive origins, replication forks need to progress past the block and this requires the Rrm3 helicase (Ivessa *et al.*, 2003). So, Rrm3 is thought to associate with the replication fork and remove such protein-DNA complexes ahead of the fork (Azvolinsky *et al.*, 2006). Initially it was assumed that fork pausing in these regions was simply a consequence of a physical block to fork progression. However, more recent evidence suggests that fork pausing at these sites is an active process requiring the replisome components Tof1 and Csm3 (Calzada *et al.*, 2005; Hodgson *et al.*, 2007). It has been proposed that Tof1 and Csm3 can impose this active replication fork arrest by counteracting the helicase activity of Rrm3 (Mohanty *et al.*, 2006).

1.1.4.5 Sister chromatid cohesion

The two copies of each chromosome, called sister chromatids, which were produced during DNA replication, are held together by the cohesin complex (Michaelis *et al.*,

1997). The cohesin complex is composed of four subunits, Smc1, Smc3, Scc1 and Scc3 (Haering *et al.*, 2002). The cohesin complex is loaded onto chromosomes in G1, before DNA replication (Ciosk *et al.*, 2000). As DNA replication proceeds a physical connection is established between sister chromatids, dependent on the cohesin complex (Uhlmann & Nasmyth, 1998). However, the precise molecular mechanism of how the cohesin complex joins sister chromatids remains unclear (Gregan & Rumpf, 2006). This physical connection between sister chromatids is essential for ensuring each daughter cell receives a complete and single copy of the genome.

1.1.5 Mitosis

G2 marks the period after the completion of DNA replication as cells prepare to segregate the replicated chromosomes. Mitosis is the whole process of nuclear division and cytokinesis, which comprises several sub-stages (reviewed by Zachariae & Nasmyth, 1999).

1.1.5.1 Nuclear division

Firstly the replicated chromosomes condense, although in *S. cerevisiae* chromosome condensation is not as extensive as in mammalian cells (Vas *et al.*, 2007). The condensed sister chromatids then align perpendicular to the axis of the mitotic spindle in preparation for segregation (Zachariae & Nasmyth, 1999). The microtubules, which make up the mitotic spindle, nucleate from spindle pole bodies (SPBs) that are positioned on opposite sides of the nucleus (reviewed by Winey & O'Toole, 2001). These microtubules attach to the chromosomes, through a multi-protein complex called the kinetochore, so that one sister chromatid of each pair is attached to the mitotic spindle from opposite SPBs (Zachariae & Nasmyth, 1999).

Separation of the sister chromatids occurs during anaphase, and it depends on two processes (Zachariae & Nasmyth, 1999). First, the dissolution of the cohesion between sister chromatids allows their physical separation. Second, the elongation of the mitotic spindle spatially segregates the separated sister chromatids into the mother and daughter cells.

After nuclear division the cell needs to exit mitosis and undergo cytokinesis.

1.1.5.2 Progression through mitosis

Progression through mitosis is controlled by a large multi-subunit complex, the anaphase promoting complex or cyclosome (APC/C), which promotes the ubiquitin-mediated proteolysis of key cell cycle regulators (reviewed by Morgan, 1999). There are two regulatory co-factors, Cdc20 and Cdh1, that activate the APC/C and control its substrate specificity (Visintin *et al.*, 1997). Temperature sensitive mutations in APC/C subunits cause a cell cycle arrest before anaphase onset (Kramer *et al.*, 1998), showing that this is the first transition regulated by the APC/C. So, what are the protein(s) that need to be targeted for destruction at this stage?

It is the cleavage of the Scc1 cohesin subunit that promotes the segregation of sister chromatids to opposite poles, dependent on the pulling force of the mitotic spindle (Uhlmann *et al.*, 1999). Scc1 is cleaved by Esp1 (separase) and the separase activity of Esp1 is inhibited by Pds1 (securin) (Ciosk *et al.*, 1998). Degradation of Pds1 is mediated by APC/C^{Cdc20}, which then releases Esp1 to cleave Scc1 (Ciosk *et al.*, 1998).

1.1.5.3 Mitotic exit

In molecular terms, mitotic exit marks the completion of one cell cycle and the transition into G1 of the next cell cycle (Zachariae & Nasmyth, 1999). Essentially, mitotic exit requires inactivation of mitotic CDK activity to allow events in G1 of the next cell cycle, such as pre-RC formation, to occur. There are two mechanisms to inactivate mitotic CDK activity. One is upregulation of the CDK inhibitor, Sic1 (Knapp *et al.*, 1996). The second is APC/C^{Cdh1}-dependent destruction of mitotic cyclin, Clb2 (Schwab *et al.*, 1997). Both of these events depend upon the phosphatase activity of Cdc14 (Visintin *et al.*, 1998). From G1 to late mitosis Cdc14 is sequestered in the nucleolus, by its inhibitor Net1, to keep it inactive (Visintin *et al.*, 1999). Release of active Cdc14 from the nucleolus depends on two tightly regulated networks: the *CDC* fourteen early anaphase release (FEAR) network and the mitotic exit network (MEN).

The FEAR network is a non-essential signalling cascade that contributes to an initial release of Cdc14 from the nucleolus at the onset of anaphase (reviewed by Stegmeier & Amon, 2004). The FEAR network includes the separase Esp1, the protein kinase Cdc5, the kinetochore protein Slk19, and Spo12 (Stegmeier *et al.*, 2002). The role of Esp1 in the FEAR network is independent of its protease activity that is used to cleave Scc1 (Sullivan & Uhlmann, 2003). How these components of the FEAR network function together is currently poorly understood.

The MEN is essential for mitotic exit and it promotes the sustained and irreversible release of Cdc14 from the nucleolus (reviewed by Stegmeier & Amon, 2004). The MEN genes include *TEM1*, *LTE1*, *CDC15*, *CDC5*, and *DBF2* (Jaspersen *et al.*, 1998). The MEN is a GTPase signalling cascade (reviewed by Stegmeier & Amon, 2004). A two-component GTPase activating protein (GAP), Bub2-Bfa1, maintains Tem1 in an inactive state until mitotic exit. After nuclear division, Tem1 is activated by Lte1. Lte1 was initially assumed to be a guanine nucleotide exchange factor (GEF) for Tem1, although there are no data to support this assertion (Geymonat *et al.*, 2002; Yoshida *et al.*, 2003). Therefore, how Lte1 activates Tem1 remains unclear. Tem1 then activates the Cdc15 kinase, which in turn activates the Dbf2 kinase. Dbf2 then promotes the release of Cdc14, although the molecular details of how this is achieved are not clear. Cdc5 is also considered a MEN gene; it does activate MEN in multiple ways, although it is not a core component of the signalling cascade.

1.2 The role of *MEC1*^{ATR}

S. cerevisiae MEC1, and the closely related *TEL1*, are members of the phosphatidylinositol-3-OH kinase-like kinase (PIKK) super-family (Abraham, 2004). Despite the similarity of their C-terminal kinase domain to the phosphatidylinositol-3-OH lipid kinases, the PIKKs are protein kinases. Homologs of *MEC1* include mammalian ATR (ataxia telangiectasia and Rad3 related) and *S. pombe rad3+*. Homologs of *TEL1* include mammalian ATM (ataxia telangiectasia mutated) and *S. pombe tel1+*. Mutations in ATR or ATM in humans cause the rare genetic disorders Seckel syndrome and ataxia telangiectasia (A-T) respectively (Chun & Gatti, 2004;

O'Driscoll *et al.*, 2003). These disorders are characterised by neurological defects and a predisposition to cancer. Human cell lines that are compromised in ATR or ATM function show defects in the DNA damage response and are sensitive to genotoxic stress (Jeggo *et al.*, 1998; O'Driscoll *et al.*, 2003). Overall, numerous studies have shown that the critical role of $Mec1^{ATR}/Tel1^{ATM}$ is to maintain genomic integrity (Casper *et al.*, 2002; Craven *et al.*, 2002). So, in response to lesions that compromise DNA integrity, these PIKKs initiate a protein kinase cascade that can reversibly arrest the cell cycle and promote repair of damaged DNA (Figure 1.2).

In higher eukaryotes, both ATR and ATM are important in responding efficiently to genotoxic stress. In *S. cerevisiae*, Tel1 plays a secondary role to Mec1 in maintaining genomic integrity and the main role of Tel1 is maintaining telomere length (Greenwell *et al.*, 1995; Morrow *et al.*, 1995). Deletion of *TEL1* alone does not confer sensitivity to genotoxic stress. However, deletion of *TEL1* in a strain lacking Mec1 function causes increased sensitivity to genotoxic stress (Craven *et al.*, 2002; Morrow *et al.*, 1995). Conversely, over-expression of *TEL1* rescues the lethality, and partially rescues the DNA damage sensitivity, of *mec1Δ* (Morrow *et al.*, 1995). Therefore, as for ATM and ATR, there is partial functional overlap between *MEC1* and *TEL1*, although Mec1 is the more dominant of the two.

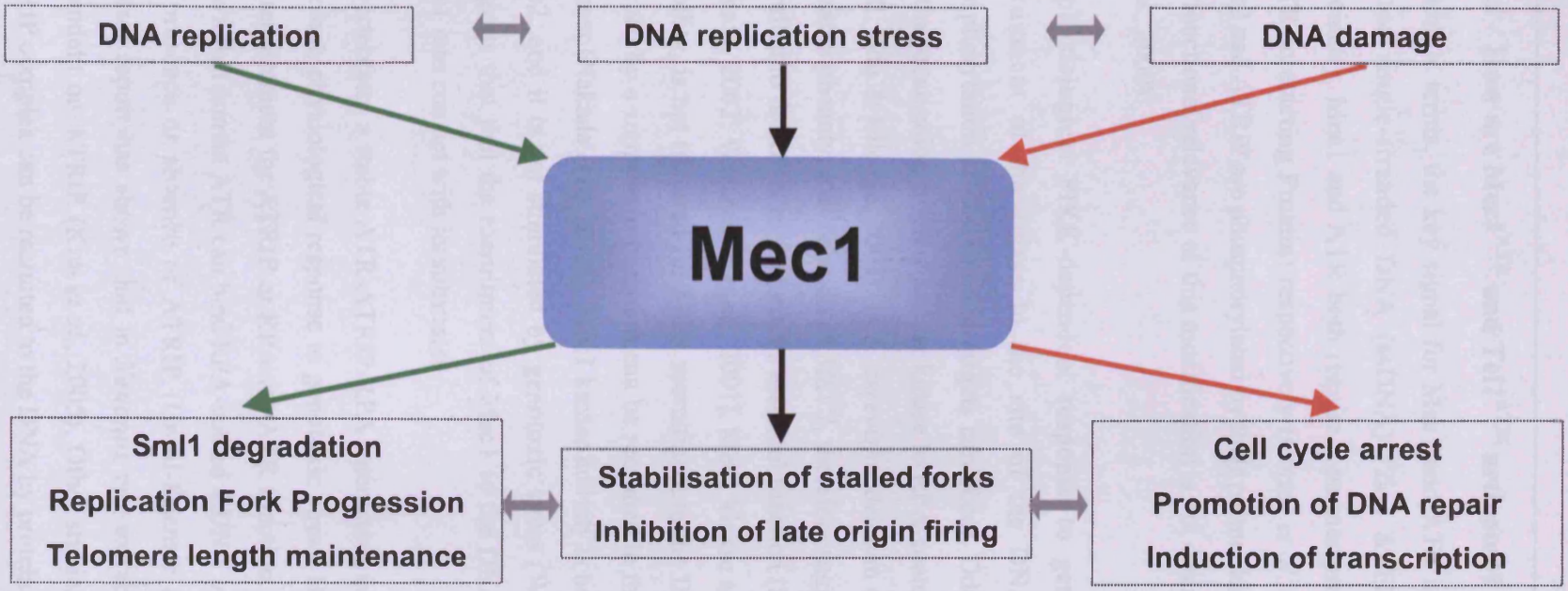

Figure 1.2 *MEC1* is essential for maintaining genomic stability. *S .cerevisiae* Mec1 is required to maintain DNA integrity during normal DNA replication, under conditions of replication stress and following DNA damage. In each case Mec1 co-ordinates different downstream responses that are appropriate to the initial stimulus. During DNA replication (green arrows) Mec1 promotes the degradation of the RNR inhibitor Sml1, promotes replication fork progression through areas of the genome that are difficult to replication (such as *RSZs*) and promotes that extension of shortened telomeres. Under conditions of replication stress (black arrows) Mec1 initiates a checkpoint response that promotes the stabilisation of stalled replication forks and inhibits late origin firing. In response to DNA damage (red arrows) Mec1 initiates a checkpoint response that promotes cell cycle arrest, promotes DNA repair and activates DNA damage-induced transcription. For clarity these responses are depicted and described as separate pathways. However, in the context of a living cell some temporal overlap between these stimuli and the Mec1-dependent response is expected (grey arrows). Precisely how Mec1 co-ordinates differential downstream responses, depending on the initial stimulus/stimuli, is not currently understood.

1.2.1 How are Mec1^{ATR} and Tel1^{ATM} activated?

In simple terms, the key signal for Mec1 and ATR activation is binding to RPA-coated single-stranded DNA (ssDNA) (Zou & Elledge, 2003). To function efficiently, Mec1 and ATR both require a partner protein, called Ddc2 or ATRIP (ATR Interacting Protein) respectively (Cortez *et al.*, 2001; Paciotti *et al.*, 2000). Ddc2 and ATRIP are phosphorylated by their partner kinase, Mec1 or ATR, although the functional relevance of this modification is not clear (Cortez *et al.*, 2001; Paciotti *et al.*, 2000).

A physiological PIKK-dependent response to genotoxic stress requires the recruitment of the kinase to the site of the DNA lesion, so that efficient phosphorylation of downstream targets can occur. Ddc2 and ATRIP are important for the localisation of their partner kinase to RPA-coated ssDNA (Rouse & Jackson, 2002; Zou & Elledge, 2003). In *S. cerevisiae* deletion of *DDC2* is lethal and shows the same phenotype as deletion of *MEC1*, therefore suggesting that Mec1 needs to be recruited to the DNA to perform its essential function (Paciotti *et al.*, 2000; Rouse & Jackson, 2002; Wakayama *et al.*, 2001). Mec1 kinase activity, although essential for viability, is not required for Mec1 recruitment to the DNA. So, a kinase-dead allele rescued by a suppressor mutation can be recruited to the DNA in a Ddc2-dependent manner (Nakada *et al.*, 2005). Mec1 kinase activity is not dependent on its binding to Ddc2, and it is not stimulated by genotoxic stress (Wakayama *et al.*, 2001). This suggests that that the recruitment of Mec1 to the DNA is required solely to bring Mec1 into contact with its substrates

In vertebrates a stable ATR-ATRIP-RPA interaction is also an important part of an efficient, physiological response to genotoxic stress. However, reports do differ on the requirement for ATRIP or RPA for ATR function. For example, one report has shown that human ATR can bind RPA-coated ssDNA *in vitro* with similar affinity in the presence or absence of ATRIP (Unsal-Kacmaz & Sancar, 2004). However, another report has shown that in *Xenopus* egg extracts DNA binding by ATR is dependent on ATRIP (Kim *et al.*, 2005). Other studies have shown that the ATR-ATRIP complex can be recruited to the DNA by proteins other than RPA, such as the mis-match repair machinery (Bomgarden *et al.*, 2004; Yoshioka *et al.*, 2006). Unlike

S .cerevisiae Mec1, ATR kinase activity can be stimulated by DNA binding in *Xenopus* egg extracts (Guo *et al.*, 2000). Additionally, the vertebrate Dpb11 homolog, TopBP1, which is a component of the replisome, has been shown to strongly stimulate ATR kinase activity (Kumagai *et al.*, 2006).

Experimentally, different methods can be used to induce Mec1 or ATR activation, but as a general rule these all work by generating ssDNA. For example, damage to DNA bases caused by ultra violet (UV) irradiation is recognised and repaired by the nucleotide excision repair (NER) pathway (Sancar *et al.*, 2004). In wild type *S. cerevisiae* cells, UV irradiation in G1 activates Mec1 and induces a G1/S cell cycle arrest. But, this only happens if there is an intact NER pathway that processes the damaged DNA to generate ssDNA (Neecke *et al.*, 1999). A similar requirement for NER to generate a PIKK-dependent response to UV stress has been shown in human fibroblasts (Marti *et al.*, 2006). In a *rad14Δ* mutant, which is not proficient for NER, there is no Mec1-dependent G1/S cell cycle arrest. Instead there is a Mec1-dependent response in S-phase, when Mec1 senses ssDNA accumulation at stalled replication forks caused by replication of a damaged template (Neecke *et al.*, 1999) .

Tel1 and ATM also require a partner protein complex, the Mre11-Rad50- Xrs2/Nbs1 complex (*S. cerevisiae* MRX or vertebrate MRN), to respond efficiently to genotoxic stress (Usui *et al.*, 2001; Uziel *et al.*, 2003). The recruitment of Tel1 or ATM to DNA lesions depends on a C-terminal motif in Xrs2 or Nbs1 respectively (Falck *et al.*, 2005). The MRN complex stimulates ATM kinase activity, and is thought to do so by facilitating stable substrate binding (Lee & Paull, 2004).

In humans, hypomorphic alleles of MRE11 or NBS1 cause similar genetic disorders to A-T, which is caused by loss of ATM (Chun & Gatti, 2004). Experimentally, A-T cell lines are sensitive to DNA damaging agents, like ionizing radiation (IR), that induce double-strand breaks (DSBs) (Jeggo *et al.*, 1998). Likewise, *S. cerevisiae* Tel1 can initiate a signalling response to DSBs. However, its role is less prominent than that of ATM, due to the dominance of the Mec1 response. For example, if ssDNA formation is prevented at the site of a DSB using a *rad50S* mutant where the ends of the DNA are not resected, there is a Mec1-independent but Tel1-dependent response (Usui *et al.*, 2001). Also, UV irradiation in G1 in *mec1Δ* cells does not

cause a cell cycle arrest in G1 or S-phase, but does activate a G2/M cell cycle arrest dependent on Tel1 and the MRX complex (Clerici *et al.*, 2004). It is inferred that replication of a damaged template generates DSBs which, in the absence of Mec1, can be detected after replication by Tel1.

Overall, the simple picture is that in mammalian cells ATR responds to replication stress and other forms of damage that generate ssDNA, whilst ATM responds primarily to DSBs. In *S. cerevisiae*, although a similar functional division applies, Mec1 is more dominant than Tel1. In reality $Mec1^{ATR}$ and $Tel1^{ATM}$ probably respond to genotoxic stress in a more co-ordinated fashion. For example, in mammalian cells IR can activate ATR in an ATM-dependent manner (Jazayeri *et al.*, 2006). So, following IR, ATM and the MRN complex are recruited to the site of a DSB. ATM then stimulates the nuclease activity of Mre11 and the resultant resection of the DNA ends produces the RPA-coated ssDNA required for ATR activation.

Also, the nature of the signals that activate $Mec1^{ATR}$ and $Tel1^{ATM}$ are probably more complex that the simple ssDNA/DSB picture described above. For example, ATM can be activated by changes in chromatin structure, independently of DSB formation (Bakkenist & Kastan, 2003). Additionally, the chromatin structure in the DNA flanking the break site has been shown to be important for ATM activation (You *et al.*, 2007). The authors of this study suggested that it is histone modifications or changes in nucleosome structure around the break site that are actually the direct signal for ATM activation.

ATM is also regulated by autophosphorylation. So, in its inactive form ATM is found as a dimer (Bakkenist & Kastan, 2003). DNA damage induces intermolecular phosphorylation on serine 1981 (S1981) and dimer dissociation (Bakkenist & Kastan, 2003). Serine 1981 phosphorylation is often used as a marker for ATM activation. However, full ATM activation is dependent on the MRN complex and recruitment to the DNA (You *et al.*, 2005) and ATM S1981 autophosphorylation is separable from its stable recruitment to DNA damage sites (Falck *et al.*, 2005). Currently, the precise relationship between ATM autophosphorylation, recruitment to the DNA and ATM activation is not clear (Lee & Paull, 2005; You *et al.*, 2005).

1.2.2 The essential role of *MEC1*^{ATR}

MEC1 and its mammalian homolog, ATR, are both essential genes (Brown & Baltimore, 2000; Cortez *et al.*, 2001; Kato & Ogawa, 1994; Zhao *et al.*, 1998). *TEL1* and its mammalian homolog, ATM, are not essential (Chun & Gatti, 2004; Greenwell *et al.*, 1995). Cells lacking Mec1 function, either *mec1Δ* cells rescued by a suppressor mutation or cells with a hypomorphic *mec1* allele, are highly sensitive to genotoxic stress (Weinert *et al.*, 1994; Zhao *et al.*, 1998). However, the essential role of *MEC1* is not its ability to respond to genotoxic stress. In addition to co-ordinating the response to genotoxic stress, Mec1 is required for upregulating intracellular dNTP levels for DNA replication (Zhao *et al.*, 1998). It is this role of regulating dNTP levels that is believed to be the essential role of *MEC1*. So, mutations that increase dNTP levels, such as over-expression of the ribonucleotide reductase (RNR) subunit *RNR1* or deletion of the RNR inhibitor *SML1*, rescue the lethality of *mec1Δ* (Desany *et al.*, 1998; Zhao *et al.*, 1998). Increasing dNTP levels enables *mec1Δ* cells to proliferate with wild type kinetics in unstressed conditions, albeit with increased rates of genomic instability (Craven *et al.*, 2002). The *S. pombe MEC1* homolog, *rad3+*, is a non-essential gene (Bentley *et al.*, 1996). *S. pombe rad3+* is required to co-ordinate the cellular response to genotoxic stress (Bentley *et al.*, 1996), but there is currently no known role for *rad3+* in upregulating intracellular dNTP levels for DNA replication (Liu *et al.*, 2003).

In contrast, there is an essential requirement for the genotoxic stress response of metazoan ATR (Brown & Baltimore, 2000; Cortez *et al.*, 2001; Garcia-Muse & Boulton, 2005). The exact reason for the difference between metazoan and yeast cells in the essential requirement for a functional genotoxic stress response is not clear. It could be due to the more complex nature of a higher eukaryotic genome, which has regions, such as repetitive sequences that are especially difficult to replicate (Callahan *et al.*, 2003; Dart *et al.*, 2004). In this case, the genotoxic stress response of ATR would be required during unchallenged DNA replication (see Section 1.4 for a discussion on the roles of Mec1 and ATR in maintaining replication fork stability). In support of this idea, studies in *Xenopus* suggest that ATR can associate with the replication fork (Dart *et al.*, 2004). No equivalent association of Mec1 with the replication fork has been shown for *S. cerevisiae*.

1.2.3 *MEC1*^{ATR} and fragile site stability

In mammalian cells common fragile sites are regions of the genome that are prone to forming gaps or breaks in metaphase chromosomes after being cultured under conditions of replication stress (reviewed by Schwartz *et al.*, 2006). Common fragile sites are hotspots of genomic instability and these regions often show translocations or deletions in tumour cells (Schwartz *et al.*, 2006). This genomic instability is thought to arise from DNA features in these regions, such as the tendency to form secondary structure, which makes them difficult to replicate and prone to break formation. ATR is important for maintaining genomic stability at fragile sites, presumably by regulating replication through these difficult-to-replicate regions (Casper *et al.*, 2002).

S. cerevisiae replication slow zones (*RSZs*) are used as a model for mammalian fragile sites (Cha & Kleckner, 2002). Replication proceeds slower in *RSZs* than in other regions of the genome in wild type cells, suggesting these regions are intrinsically difficult to replicate. DNA DSBs form in *RSZs* when cells expressing a temperature sensitive allele of *mec1*, *mec1-4* or *mec1-40*, undergo replication at the restrictive temperature (Cha & Kleckner, 2002). *RSZs* are relatively large regions of the genome (~10kb) and, where break points have been mapped on chromosome III, they occur between highly active replication origins (Cha & Kleckner, 2002). *RSZs* are genetically defined regions, since altering the pattern of replication by deleting replication origins does not alter the pattern of break formation (Cha & Kleckner, 2002).

Deletion of *SML1* suppresses the temperature sensitivity of *mec1-4* and *mec1-40* and also suppresses break formation in *RSZs* (Cha & Kleckner, 2002). This suggests that in strains expressing the *mec1-4* or *mec1-40* alleles the replication stress induced by the altered regulation of dNTP synthesis contributes to the eventual formation of DSBs in *RSZs*. However, the nature of the chromosomal break formation in *RSZs* is different to that which occurs following replication stress induced by exogenous dNTP depletion. In the latter situation DSBs can form due to the processing of unprotected, stalled replication forks by the homologous recombination (HR) machinery (Section 1.3.5.1). Chromosomal break formation in *RSZs* does not require

the cell to have functional HR machinery (N. Hashash and R. Cha, unpublished data). Instead, break formation in *RSZs* follows a prolonged period of replication fork pausing and depends on currently unidentified events that happen in the G2/M transition. Replication forks paused in *RSZs* before break formation are competent to resume replication, as *mec1-4* and *mec1-40* cells retain viability if they are returned to the permissive temperature. This suggests that Mec1 function is required to promote continued replication through these regions. Whether this function is simply to ensure a sufficient supply of dNTPs to complete replication, or if it reflects another role of Mec1 is unclear.

1.2.4 Telomeres

Telomeres are specialised nucleoprotein structures that protect the end of linear chromosomes (Smogorzewska & de Lange, 2004). They consist of a unique repeat sequence that, due to the difficulty of replicating the end of a linear structure, is synthesised by a reverse transcriptase called telomerase. In the absence of telomerase or protective telomere binding proteins, telomeres shorten. Unstable telomeres ultimately lead to cellular senescence, where a cell loses its capacity to proliferate (Smogorzewska & de Lange, 2004). The DNA structures at telomeres closely resemble those recognised by DNA damage sensors. Therefore it is not surprising that many proteins involved in maintaining genomic integrity also play a role in telomere maintenance. Tel1 is important for maintaining telomere length, and in a *tel1Δ* strain telomeres are short, but stable (Ritchie *et al.*, 1999). The Tel1 homolog ATM has also been shown to have a role in maintaining telomere length in mammalian cells (Pandita, 2002). In the absence of Mec1 and Tel1 function however, telomeres become unstable and cells senesce (Ritchie *et al.*, 1999). Therefore *S. cerevisiae* Mec1 can contribute to maintaining telomere length.

1.3 The DNA damage response

1.3.1 Cell cycle checkpoints

Problems may arise during the cell cycle where control mechanisms, additional to the cell cycle machinery described in Section 1.1, are required to ensure genomic

stability. These control mechanisms are called cell cycle checkpoints (Hartwell & Weinert, 1989). Hartwell and Weinert initially defined a checkpoint as a process that promoted cell cycle arrest or delay, presumably to allow time to correct the initial problem. For example, a checkpoint exists to arrest the cell cycle in G2/M to prevent anaphase onset with damaged DNA (Gardner *et al.*, 1999). Further study of checkpoint function has shown that checkpoint proteins are also involved in additional processes to maintain cell viability under stressful conditions (Harrison & Haber, 2006). These include the recruitment and activation of proteins that carry out DNA repair and the induction of an altered transcriptional program. All checkpoint responses to DNA damage or replication stress are dependent on $Mec1^{ATR/ATM}$. There are other cell cycle checkpoints, for example the spindle assembly checkpoint that responds to defects in the mitotic spindle, which are not dependent on $Mec1^{ATR/ATM}$.

Failure to delay cell cycle progression in the presence of DNA damage poses the risk of cell death or transmitting mutations to future generations. In multicellular organisms failure to respond efficiently to DNA damage can cause accumulation of mutations that is linked with tumourigenesis (Motoyama & Naka, 2004).

1.3.2 Checkpoint sensors

The checkpoint sensors are the proteins that recognise abnormal DNA structures and initiate the checkpoint response (Figure 1.3). $Mec1^{ATR}$ and $Tel1^{ATM}$ both fall into this category and their roles in sensing DNA damage were discussed previously in Section 1.2.1. Checkpoint activation additionally requires the heterotrimeric PCNA-like clamp, Mec3-Rad17-Ddc1 (or the 9-1-1 complex, Rad9-Rad1-Hus1, in mammalian cells) and the RFC-like $Rad24^{Rad17}$-RFC2-5 clamp loader (Harrison & Haber, 2006). Recruitment of the checkpoint clamp and clamp-loader to DNA damage sites requires RPA-coated ssDNA (Lucca *et al.*, 2004; Zou *et al.*, 2003), but does not require extensive resection of the DNA ends (Nakada *et al.*, 2004). Thus, the clamp and clamp-loader, like the PIKK sensors, are recruited to DNA damage sites early in the DNA damage response.

The PIKKs and the clamp/clamp-loader are recruited independently to the DNA damage site (Melo *et al.*, 2001). Once localised to the DNA damage site they then

co-operate in relaying the downstream checkpoint signal. So, phosphorylation of downstream Mec1 targets depends on the presence of the clamp and clamp-loader (Emili, 1998; Paciotti *et al.*, 1998). The clamp and clamp-loader most likely recruit the Mec1 substrates to the damage site, where they come into contact with the independently recruited Mec1 kinase. Having two independent sensor systems in this way guards against inappropriate checkpoint activation.

The PIKKs and the checkpoint clamp and clamp-loader complex are important for initiating the DNA-damage-signalling cascade. However, whether they truly detect the initial DNA damage is more difficult to determine. Recently a role for chromatin remodeling complexes as an early sensor of DSBs has been described. The *S. cerevisiae* RSC chromatin remodeling complex is required for the recruitment of Mec1 and Tel1 to the DNA damage site (Liang *et al.*, 2007). Mutations of RSC subunits impair the loss of core histones at the break site, impair the association of Mre11 with the break site, and delay the nucleolytic processing required to from 3' ssDNA tails (Liang *et al.*, 2007). These observations suggest a model where early chromatin remodeling is required for DNA processing enzymes and checkpoint proteins to associate with the damage site and initiate a timely DNA damage response.

1.3.3 Checkpoint transducers

The checkpoint transducers are the proteins that amplify and transmit the checkpoint signal to the downstream effectors (Figure 1.3). There are two key transducer kinases, $Rad53^{Chk2}$ and $Chk1^{Chk1}$, that function downstream of Mec1. Adaptor proteins, such as Rad9, are required to bring Rad53 and Chk1 into contact with Mec1. Rad9 is hyperphosphorylated by Mec1, which is the stimulus to recruit Rad53 (Schwartz *et al.*, 2002).

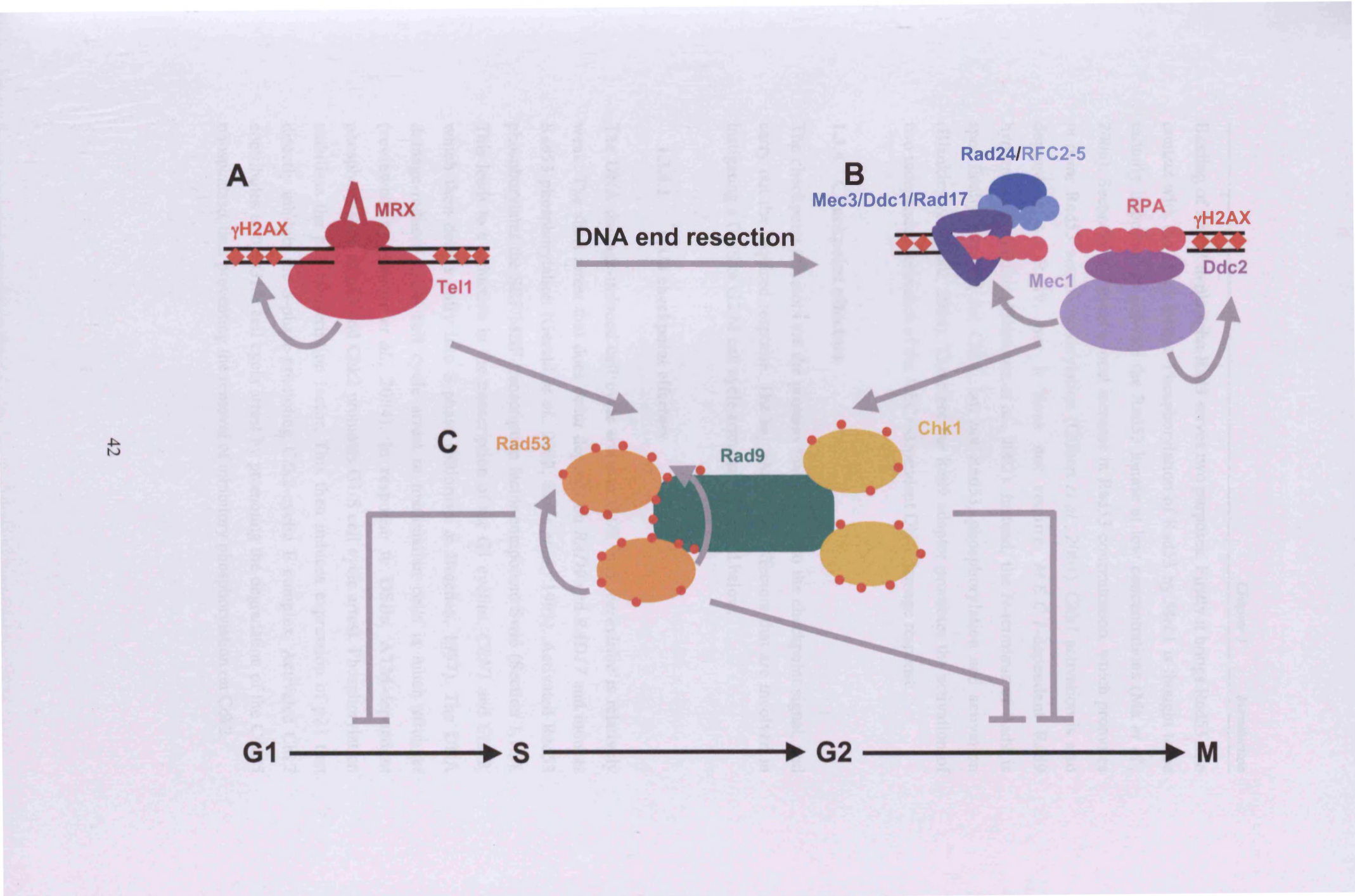
A
γH2AX
MRX
Tel1
DNA end resection
B
Rad24/RFC2-5
Mec3/Ddc1/Rad17
RPA
γH2AX
Ddc2
Mec1
C
Rad53
Rad9
Chk1
G1
S
G2
M

Binding of Rad53 to phospho-Rad9 serves two purposes. Firstly it brings Rad53 into contact with the Mec1 kinase. Phosphorylation of Rad53 by Mec1 is thought to be initially important to activate the Rad53 kinase at low concentrations (Ma *et al.*, 2006). Secondly it creates a local increase in Rad53 concentration, which promotes *in trans* Rad53 autophosphorylation (Gilbert *et al.*, 2001). Chk1 activation is also dependent on Rad9, but it does not require *MEC1*-dependent Rad9 hyperphosphorylation (Schwartz *et al.*, 2002). Instead, the N-terminus of Rad9 is specifically required for Chk1, but not Rad53, phosphorylation and activation (Blankley & Lydall, 2004). Therefore the Rad9 adaptor promotes the activation of two independent branches of the *MEC1*-dependent DNA damage response.

1.3.4 Checkpoint effectors

The checkpoint effectors are the proteins that respond to the checkpoint signal, and carry out the required response. The key checkpoint effectors that are involved in instigating a G1/S or G2/M cell cycle arrest are described below.

1.3.4.1 G1/S checkpoint effectors

The DNA damage-induced cell cycle arrest at G1/S in *S. cerevisiae* is relatively weak. The short arrest that does occur depends on *RAD9* and *RAD17* and induces Rad53 phosphorylation (Gerald *et al.*, 2002; Siede *et al.*, 1993). Activated Rad53 phosphorylates the SBF/MBF transcription factor component Swi6 (Section 1.1.3). This leads to a reduction in the transcription of the G1 cyclins, *CLN1* and *CLN2*, which then delays entry into S-phase (Sidorova & Breeden, 1997). The DNA damage-induced G1/S cell cycle arrest in mammalian cells is much stronger (reviewed by Sancar *et al.*, 2004). In response to DSBs, ATM-dependent phosphorylation of p53 and Chk2 promotes G1/S cell cycle arrest. Phosphorylation stabilises the p53 transcription factor. This then induces expression of p21 that directly inhibits the S-phase-promoting Cdk2-cyclin E complex. Activated Chk2 contributes to the G1/S cell cycle arrest by promoting the degradation of the Cdc25 phosphatase, thus preventing the removal of inhibitory phosphorylation on Cdk2.

1.3.4.2 G2/M checkpoint effectors

In *S. cerevisiae*, Rad53 and Chk1 act in parallel pathways downstream of Mec1 to execute the G2/M cell cycle arrest (Gardner *et al.*, 1999; Liang & Wang, 2007). Chk1 phosphorylates the anaphase-inhibitor Pds1, which prevents APC/C^{Cdc20}-dependent ubiquitination of Pds1 and consequently reduces Pds1 proteolysis (Agarwal *et al.*, 2003; Wang *et al.*, 2001). Stabilisation of Pds1 prevents the release of active Esp1, which has two independent effects on the G2/M cell cycle arrest. Firstly, maintaining Esp1 in an inactive state inhibits anaphase by preventing cleavage of the cohesin subunit Scc1 and therefore separation of sister chromatids (Section 1.1.5.1). Secondly, it blocks activation of the FEAR pathway to inhibit the release of Cdc14 from the nucleolus (Liang & Wang, 2007).

Rad53 activation contributes to Pds1 stabilisation by inhibiting the interaction of Pds1 with the APC/C co-factor Cdc20 (Agarwal *et al.*, 2003). Currently it is not known whether Cdc20 is a direct target of the Rad53 kinase. Another effect of Rad53 activation is to block mitotic exit by inhibiting the MEN (Section 1.1.5.3). The precise mechanism by which Rad53 blocks MEN activation remains unclear, but phosphorylation of Bfa1 is a likely target (Hu *et al.*, 2001; Liang & Wang, 2007). Additionally the polo-like kinase Cdc5 is phosphorylated in a *RAD53*-dependent manner, although this does not inhibit the role of Cdc5 in promoting mitotic exit (Cheng *et al.*, 1998). Instead, phosphorylation of the cohesin subunit Scc1 by Cdc5 is required for efficient degradation of Scc1 by Esp1 (Alexandru *et al.*, 2001). So, Rad53-dependent phosphorylation of Cdc5 probably contributes to the inhibition of anaphase onset. Therefore both Chk1 and Rad53, through different downstream signalling pathways, contribute to the inhibition of anaphase onset and the inhibition of mitotic exit.

In mammalian cells, the DNA-damage-dependent G2/M cell cycle arrest is achieved by inhibiting the mitosis-promoting Cdc2-Cyclin B complex (reviewed by Sancar *et al.*, 2004). Inhibitory phosphorylation of the mitotic CDK, Cdc2, is promoted by Chk1- and Chk2-dependent upregulation of the Wee1 kinase. Activated Chk1 and Chk2 also promote inhibition of Cdc25 phosphatase activity, which prevents the removal of the inhibitory phosphorylation on Cdc2. The DNA damage-dependent

G2/M cell cycle arrest in *S. pombe* is also achieved by activation of equivalent pathways to inhibit mitotic CDK activity (Rhind & Russell, 1998).

1.3.5 Promoting DNA repair

One of the earliest detectable responses to checkpoint activation is the phosphorylation of the histone H2A (or the histone variant, H2AX, in higher eukaryotes) by $Mec1^{ATR}$ or $Tel1^{ATM}$ (Downs *et al.*, 2000; Paull *et al.*, 2000; Rogakou *et al.*, 1998). The phosphorylated species is referred to as γH2AX and can be detected in large regions around a DSB site. So, in *S. cerevisiae* γH2AX covers regions up to at least 10 kb adjacent to a DSB site (Downs *et al.*, 2004), and in mammalian cells it can cover megabase length regions adjacent to a DSB site (Rogakou *et al.*, 1999). The formation of γH2AX is important for the stable recruitment of proteins that promote the repair process (Paull *et al.*, 2000). For example, Nbs1 binds directly to γH2AX and this is important for the stable recruitment of the MRN complex to a DNA lesion (Kobayashi *et al.*, 2002).

In *S. cerevisiae* chromatin modifying enzymes, such as the NuA4 histone acetyltransferase complex and the ATP-dependent chromatin remodeling complexes INO80 and SWR1, are recruited to a DSB via the binding of a common Arp4 subunit to γH2AX (Downs *et al.*, 2004). The recruitment of these chromatin modifying activities to the damaged DNA is thought to be important for regulating access of the repair machinery to the damaged DNA, and for restoring normal chromatin structure after DNA repair (Peterson & Cote, 2004). Also in *S. cerevisiae*, the *de novo* association of cohesin around the DSB site depends on γH2AX formation (Unal *et al.*, 2004), and this is important for promoting repair by homologous recombination between sister chromatids (Xie *et al.*, 2004).

In accordance with the important role played by γH2AX in promoting DNA repair, mammalian cells that lack H2AX show increased levels of genomic instability (Bassing *et al.*, 2002; Celeste *et al.*, 2002).

1.3.5.1 Homologous recombination

There are two main pathways by which a DSB can be repaired, non-homologous end-joining (NHEJ) and homologous recombination (HR). In NHEJ the two DNA ends are religated, with minimal processing (reviewed by Lieber *et al.*, 2003). In this case there will be some loss of DNA sequence information from the damaged DNA ends and this pathway is therefore considered an error-prone repair pathway. HR on the other hand uses a homologous template to ensure accurate repair of the DSB break (reviewed by West, 2003). In diploid cells this template can either be a homologous chromosome or a sister chromatid. During proliferation the sister chromatid is the preferred template, as it prevents potential loss of heterozygosity where there are mutant gene alleles, and so repair of a DSB by HR is therefore favoured in late S/G2.

For repair by HR to take place, the ends of the DSB must be resected by nucleases. At a DSB site the Mre11 and Exo1 exonucleases co-operate in this process to generate 3' ssDNA tails (Nakada *et al.*, 2004). These 3' ssDNA tails are initially bound by RPA, but the Rad51 recombinase later replaces RPA (West, 2003). Rad52 is another essential HR protein that promotes Rad51 binding and stimulates the HR process (West, 2003). The Rad51-DNA filament promotes homologous pairing and DNA strand exchange with another DNA duplex, most commonly the sister chromatid (West, 2003). The repair process then requires DNA synthesis using the homologous DNA as a template, followed by separation of the repaired duplexes (West, 2003).

In response to DNA damage the homologous recombination machinery, along with other repair proteins, is rapidly relocalised to repair foci that are built around the DNA lesions (Lisby *et al.*, 2004; Paull *et al.*, 2000). Thus, HR is important for the accurate repair of DSBs. But, the HR process must be carefully regulated, as unscheduled HR can contribute to genomic instability (Admire *et al.*, 2006; Lambert & Carr, 2005; Lemoine *et al.*, 2005). This idea is discussed further in Section 1.4.5.

1.3.6 Maintaining checkpoint activation

The presence of RPA-coated ssDNA activates the $Mec1^{ATR}$-dependent checkpoint response (Section 1.2.1). However, the presence of RPA-coated ssDNA alone is not sufficient to generate a sustained checkpoint response (Byun *et al.*, 2005; Ira *et al.*, 2004). Instead, continued ssDNA generation and Mec1 activation are required to ensure checkpoint signalling is not turned off prematurely (Pellicioli *et al.*, 2001; Vaze *et al.*, 2002).

1.3.7 Turning off the checkpoint

Once the problem that initially caused cell cycle arrest has been successfully addressed, the cell needs to be able to re-enter the cell cycle. To do this checkpoint signalling needs to be shut down. The process of switching off the checkpoint is not as well understood as that of activating it. What is understood however suggests that reversal of some of the activation processes is important. For example, the PP2C-type phosphatases, Ptc2 and Ptc3, can bind to activated Rad53, which presumably results in Rad53 dephosphorylation and inactivation (Leroy *et al.*, 2003). A human PP2C-type phosphatase, Wip1, can also reverse ATM/ATR-dependent phosphorylation of p53 and Chk1 (Lu *et al.*, 2005). Another important target for checkpoint recovery is γH2AX. In *S. cerevisiae*, dephosphorylation of γH2AX by the Pph3 phosphatase is important for checkpoint recovery (Keogh *et al.*, 2005). In mammalian cells, the PP2A phosphatase is important for dephosphorylating γH2AX, although the equivalent defect in checkpoint recovery in the absence of this dephosphorylation has not been shown (Chowdhury *et al.*, 2005).

1.3.8 Gene expression response

One of the less well characterised aspects of the DNA damage response is the major change in gene expression that occurs. Microarray analysis has shown that treatment with DNA damaging agents alters the transcription of hundreds of genes in *S. cerevisiae* (Gasch *et al.*, 2001; Jelinsky & Samson, 1999). The Dun1 kinase is activated in a Mec1- and Rad53-dependent manner (Zhou & Elledge, 1993). Dun1 is an important mediator of some, but not all, of the DNA-damage-induced transcriptional response (de la Torre Ruiz & Lowndes, 2000). Important targets of

the Dun1-controlled transcriptional response that have been investigated in detail are the genes encoding subunits of the RNR enzyme (Section 1.5.2).

Gene expression at the post-transcriptional level is regulated in response to DNA damage, by modulating the activity of mRNA deadenylase enzymes that regulate mRNA polyA tail length and mRNA stability (Hammet *et al.*, 2002; Traven *et al.*, 2005; Woolstencroft *et al.*, 2006).

Finally, post-translational regulation of Sml1, an inhibitor of RNR, is another important response to DNA damage in *S. cerevisiae*. This response is covered in more detail in Section 1.5.3.

1.4 Responding to replication stress

There are many factors, both exogenous and endogenous, that can impede replication fork progression during the replication process (Lambert & Carr, 2005). Challenges to replication fork progression such as encountering protein-DNA complexes and DNA secondary structure, or collisions with RNA polymerases happen routinely every S-phase (Section 1.1.4.4). Also, various genotoxic insults can impede replication fork progression in different ways (Lambert & Carr, 2005). So, limiting the supply of dNTP precursors, for example by inhibiting RNR with hydroxyurea (HU), can block DNA synthesis. Similarly, inhibition of polymerase α by aphidicolin will also block DNA synthesis. Genotoxic agents that cause DNA inter-strand cross-links will block the DNA helicase, and therefore progression of the whole replisome. Genotoxic agents that cause damage to DNA bases, such as the alkylating agent methyl methanesulphonate (MMS) or UV irradiation, can inhibit the polymerisation of the new DNA strand. Exogenous genotoxic agents, such as HU, MMS or UV irradiation, are commonly used to study the replication stress response. This replication stress response is dependent on a $Mec1^{ATR}$ and $Rad53^{Chk2}$ signalling cascade and is commonly referred to as the S-phase checkpoint (Longhese *et al.*, 2003).

When faced with a block to progression, several things can happen to the replication fork (Lambert & Carr, 2005) (Figure 1.4). Firstly, the fork can pause, in a state

competent to continue DNA replication, and in *S. cerevisiae* this does not require activation of the S-phase checkpoint. This type of physiological fork pausing was described in Section 1.1.4.4. Secondly, a replication fork can stall when DNA synthesis is prevented in a non-physiological manner, for example by genotoxic stress-inducing chemicals. In this case the S-phase checkpoint is required to maintain the replication fork in a state competent to continue DNA replication (Lopes *et al.*, 2001; Sogo *et al.*, 2002). The worst-case scenario is when the replication fork collapses and the polymerase dissociates from the DNA (Cobb *et al.*, 2003; Lucca *et al.*, 2004). In *S. cerevisiae* there is no essential requirement for a system to guard against replication fork collapse, or to promote replication fork restart during unchallenged replication (Desany *et al.*, 1998; Lisby *et al.*, 2004; Zhao *et al.*, 1998). However, in higher eukaryotes there is an essential requirement for the S-phase checkpoint and the ability to restart collapsed replication forks (Trenz *et al.*, 2006). Presumably therefore, replication fork stalling and collapse during unchallenged replication is more prevalent in higher eukaryotes than in yeast.

The consequences of failing to ensure the accurate completion of DNA replication in the face of all these potential problems are very serious (Myung *et al.*, 2001). This is because any genetic mutations that are acquired during S-phase will be transmitted directly to daughter cells. Therefore, the response to replication stress is particularly important in ensuring cellular survival and genome stability (Tourriere & Pasero, 2007). In the first instance, the cell needs to be able to detect any replication stress problems (Section 1.4.1). Next, the cell needs to ensure that DNA replication can be completed with minimal errors. Often there is a trade-off here, so that the cell allows reduced DNA replication accuracy in the interests of continuing and completing replication. The cell also needs to ensure that there are a sufficient number of replication forks to complete replication.

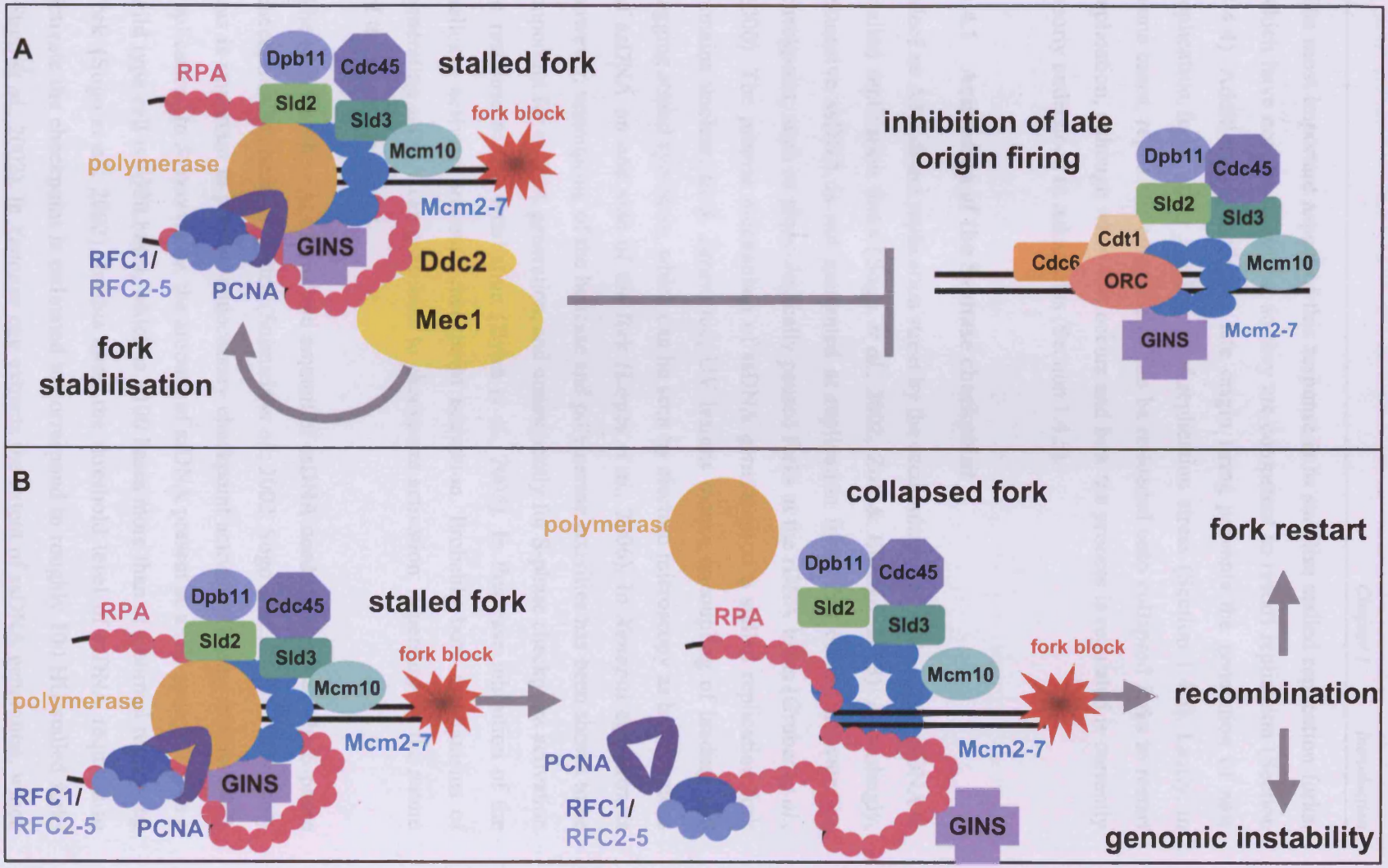
A
stalled fork
RPA
Dpb11
Cdc45
Sld2
Sld3
fork block
polymerase
Mcm10
Mcm2-7
GINS
RFC1/
RFC2-5
PCNA
Ddc2
Mec1
fork
stabilisation
inhibition of late
origin firing
Dpb11
Cdc45
Sld2
Sld3
Cdt1
Cdc6
ORC
Mcm10
GINS
Mcm2-7
B
collapsed fork
polymerase
fork restart
RPA
Dpb11
Cdc45
Sld2
Sld3
stalled fork
fork block
polymerase
Mcm10
Mcm2-7
GINS
RFC1/
RFC2-5
PCNA
recombination
genomic instability

The most important aspect of this response is to stabilise stalled replication forks, which have not yet collapsed, so they are competent to restart replication (Section 1.4.4). Additionally, inhibiting late origin firing prevents the generation of new replication forks under conditions of replication stress (Section 1.4.3). Lastly, in some cases, replisome components can be re-loaded onto collapsed forks to restart replication, although when this occurs and how the process is regulated is currently poorly understood in eukaryotes (Section 1.4.5).

1.4.1 Activation of the S-phase checkpoint

Mec1 or ATR detect replication stress by the accumulation of RPA-coated ssDNA at stalled replication forks (Sogo *et al.*, 2002; Zou & Elledge, 2003). Accordingly, extensive ssDNA is not generated at replication forks that do not activate the checkpoint, such as physiologically paused forks at the rDNA locus (Gruber *et al.*, 2000). The precise mechanism of ssDNA generation at a stalled replication fork remains unclear. In *S. cerevisiae*, UV lesions induce uncoupling of leading and lagging strand synthesis, which can be seen by electron microscopy as large regions of ssDNA on one side of the fork (Lopes *et al.*, 2006). In *Xenopus* egg extracts however, uncoupling of the helicase and polymerase activities has been shown to be important for ssDNA generation, and consequently for S-phase checkpoint activation in response to UV irradiation (Byun *et al.*, 2005). In this case inhibition of the helicase activity prevents checkpoint activation. Probably both mechanisms of generating ssDNA can contribute to checkpoint activation, depending on the nature of the replication stress.

The idea that there is a threshold amount of ssDNA needed to activate the S-phase checkpoint has been suggested (Shimada *et al.*, 2002; Sogo *et al.*, 2002). Presumably this is important to prevent unnecessary checkpoint activation during normal DNA replication. In *S. cerevisiae*, the amount of ssDNA present at a HU-stalled fork in a wild type cell is ~320 bases, which is ~100 bases more than at a normal replicating fork (Sogo *et al.*, 2002). In this case, the threshold level of ssDNA required to activate the checkpoint is estimated to correspond to roughly 100 HU-stalled forks (Sogo *et al.*, 2002). In *Xenopus* egg extracts the extent of ssDNA generation, which

can be thousands of bases at a stalled fork, correlates with the level of ATR activation, as measured by Chk1 phosphorylation (Byun *et al.*, 2005).

1.4.2 S-phase checkpoint proteins

Many of the proteins required for the S-phase checkpoint response, like Mec1, Rad53, the PCNA-like clamp and the 9-1-1 clamp loader, overlap with those required for the DNA damage response (Section 1.3). However, Mrc1, a component of the replisome, takes the place of Rad9 as an S-phase specific adaptor to activate Rad53 (Osborn & Elledge, 2003). Additionally other components of the replisome are required for an efficient S-phase checkpoint response. For example, mutations in pol α, RPA, pol ε and Dpb11 all show an impaired S-phase checkpoint response (Araki *et al.*, 1995; Longhese *et al.*, 1996; Marini *et al.*, 1997; Wang & Elledge, 1999), suggesting the replisome itself plays a role in activating the replication stress response.

1.4.3 Inhibition of late origin firing

Activation of the S-phase checkpoint slows down, but does not stop, progression through S-phase. So, in *S. cerevisiae* replication at 23°C in 200 mM HU proceeds at a steady rate over at least 6 hours, whereas replication at 23°C in the absence of HU is complete within 1 hour (Alvino *et al.*, 2007). This increase in the length of time spent in S-phase is achieved by delaying origin firing. In an unperturbed S-phase at 25°C the late origin *ARS501* fires about 15 minutes after the early origin *ARS305* (Alcasabas *et al.*, 2001; Feng *et al.*, 2006; Santocanale & Diffley, 1998). In wild type cells challenged with 200 mM HU, replication intermediates can be detected from the *ARS305*, but not from *ARS501*, 90 minutes after release from α-factor (Santocanale & Diffley, 1998). No such delay in origin firing is observed in checkpoint mutants. So, *rad53* mutants undergoing replication in 200 mM HU show the same relative timing of origin activation of *ARS305* and *ARS501* as in an unperturbed wild type S-phase (Alcasabas *et al.*, 2001; Feng *et al.*, 2006; Santocanale & Diffley, 1998).

The molecular mechanism for delaying origin firing is thought to require Rad53-dependent phosphorylation of Dbf4 (Weinreich & Stillman, 1999). So, phosphorylation of Dbf4 reduces the kinase activity of the S-phase promoting Dbf4-Cdc7 complex to prevent origin firing (Section 1.4.3). A similar mechanism of regulating the timing of replication origin firing has been suggested to occur during unchallenged replication in *Xenopus* egg extracts (Marheineke & Hyrien, 2004; Shechter *et al.*, 2004). In this model, limited activation of ATR, by RPA-coated ssDNA at active regions of replication, feeds back to inhibit late origin firing. Thus, suggesting that the temporal pattern of replication origin firing is a self-regulatory process, mediated by ATR-dependent feedback.

Although checkpoint mutants do not delay origin firing under conditions of replication stress, there is still some, checkpoint-independent, slowing of S-phase (Paulovich & Hartwell, 1995; Tercero & Diffley, 2001). In wild type cells treated with 200 mM HU forks progress at roughly 50 base pairs (bp)/min (Sogo *et al.*, 2002) and in 0.03% MMS at roughly 300 bp/min (Tercero & Diffley, 2001). This is compared with an estimated average fork rate during unchallenged DNA replication of 2.9 kb/min, although this average does represent a dramatic variation in fork rates across the genome (Raghuraman *et al.*, 2001). These slower fork rates presumably reflect the physical impediment to the replisome caused by limiting dNTPs in the case of HU treatment and alkylation damage in the case of MMS treatment.

1.4.4 Stabilisation of stalled replication forks

In the absence of a functional S-phase checkpoint replication stress induces replication fork collapse, defined as the loss of the association of the replicative polymerases with the DNA (Cobb *et al.*, 2003; Lucca *et al.*, 2004). In this situation abnormal DNA replication structures, such as extensive single stranded gaps and hemi-replicated bubbles, can be observed (Lopes *et al.*, 2001; Sogo *et al.*, 2002). This type of unprotected, stalled replication fork is a substrate for recombination events that can contribute to genomic instability (Admire *et al.*, 2006; Lambert & Carr, 2005; Lemoine *et al.*, 2005). During replication stress, the S-phase checkpoint is important to prevent the dissociation of the replisome from the DNA at the fork.

This ensures that replication can later be resumed and also protects the fork from undesirable DNA processing events (Cotta-Ramusino *et al.*, 2005).

Precisely how the S-phase checkpoint stabilises the replisome in wild type cells is unknown. Though presumably checkpoint-dependent phosphorylation of replisome components, such as Mrc1, plays a role (Katou *et al.*, 2003; Osborn & Elledge, 2003). Mrc1 and Tof1 also contribute to replisome stability independently of the S-phase checkpoint (Katou *et al.*, 2003). So, in *mrc1Δ* or *tof1Δ* cells treated with HU, the replisome does not dissociate from the DNA as it does in cells lacking Mec1 or Rad53 function. Instead, it becomes uncoupled from the site to DNA synthesis.

The stabilisation of stalled replication forks is the most important factor for maintaining viability under conditions of replication stress. This is illustrated by the *mec1-100* hypomorphic mutant, which cannot slow S-phase progression, but is still viable in MMS (Paciotti *et al.*, 2001). As no MMS-induced slowing of S-phase is seen, the *mec1-100* mutant presumably cannot inhibit late origin firing. However, *mec1-100* cells do retain some ability to stabilise stalled replication forks (Cobb *et al.*, 2005), which will therefore allow them to resume replication and minimise loss of viability.

1.4.5 Replication fork restart

Recombination-mediated replication fork restart is essential in bacteria (reviewed by Cox, 2002). Bacteria initiate replication of their circular chromosome from a single replication origin. The two replication forks then progress in opposite directions until they meet at a defined termination site on the opposite side of the chromosome. The irreversible collapse of either of the two replication forks would be lethal and so having a mechanism to restart collapsed replication forks is essential. This process of replication fork collapse and recombination-mediated restart are considered a normal part of bacterial replication.

The extent to which similar mechanisms of recombination-mediated replication fork restart are employed in eukaryotic cells is less clear. HR is essential in mammalian cells, but not in *S. cerevisiae* cells. However, *S. cerevisiae* cells with mutations that cause defects in DNA synthesis become dependent on the recombination machinery

for viability (Merrill & Holm, 1998; Merrill & Holm, 1999). So, there is indirect evidence that in eukaryotes, as in bacteria, recombination can be important for promoting replication fork restart.

In *S. cerevisiae* Rad52 foci are observed in *mec1Δ sml1Δ* or *rad53Δ sml1Δ* cells, and not in wild type cells, treated with HU (Lisby *et al.*, 2004). In S-phase checkpoint mutants under conditions of replication stress replication forks collapse to form abnormal DNA structures (Section 1.4.4). Therefore, the HR machinery is recruited to collapsed replication forks, presumably because they are recognised as DSBs. However, HR has also been proposed to play a role in replication fork stabilisation in wild type cells, for example by protecting the nascent DNA strands from degradation (Lambert *et al.*, 2005). This proposed role of HR in protecting replication forks could be important even in the absence of promoting strand exchange and undergoing the complete HR process.

In higher eukaryotes the restart of collapsed replication forks is also thought to be essential for viability. In *Xenopus* egg extracts ATM- and ATR-dependent repair and restart of collapsed replication forks is essential to prevent the accumulation of DSBs during replication (Trenz *et al.*, 2006). This process is dependent on the Mre11 subunit of the MRN complex (Trenz *et al.*, 2006). Though, whether this ATM/ATR- and MRN-dependent promotion of replication fork restart requires recombination or not was not addressed in this study.

Previously it was described how unscheduled recombination at the replication fork can contribute to genomic instability (Admire *et al.*, 2006; Lambert *et al.*, 2005; Lemoine *et al.*, 2005). However, the specific circumstances in which recombination can contribute to viability, and how this process is regulated remains unclear. Recombination during replication is therefore viewed as a "double-edged sword": it can help promote viability, but at the expense of genomic stability (Lambert *et al.*, 2005).

1.5 dNTP synthesis

The ability of a cell to synthesise balanced amounts of the four deoxyribonucleotide triphosphate (dNTP) precursors (dATP, dGTP, dCTP and dTTP) is essential for replication and maintenance of the genome (Reichard, 1988). If dNTP levels are too low there is a risk of cell death due to an inability to complete DNA replication or repair (Zhao *et al.*, 1998). On the other hand, dNTP levels must not be too high as this increases the risk of spontaneous mutations (Chabes *et al.*, 2003a). For example, mammalian cell lines that have undergone oncogenic transformation contain dNTP pools that are 3-4 fold higher than normal diploid cells, and this results in an increased mutation rate (Martomo & Mathews, 2002). Defects in nucleotide metabolism have also been shown to be the underlying cause of human genetic diseases that affect mitochondrial function (Bourdon *et al.*, 2007; Mathews, 2006). Therefore, there are rigorous control mechanisms to ensure that the amount of dNTPs synthesised correctly meets the cells needs.

The rate-limiting step in the formation of deoxyribonucleotides is the reduction of the 2'-OH in the ribose sugar of ribonucleotides and the reaction is catalysed by ribonucleotide reductase (RNR) (reviewed by Nordlund & Reichard, 2006). *E. coli* RNR is the archetypal RNR enzyme and is a tetrameric complex composed of two large R1 subunits and two small R2 subunits (Mathews *et al.*, 1987). In *S. cerevisiae* there are four RNR genes. *RNR1* and *RNR3* encode the large R1 subunits (Elledge & Davis, 1990), and *RNR2* and *RNR4* encode the small R2 subunits (Elledge & Davis, 1987; Huang & Elledge, 1997; Wang *et al.*, 1997). *RNR3* expression is induced in response to cellular stress (Elledge & Davis, 1990; Tadi *et al.*, 1999). Therefore under normal growth conditions, when *RNR3* is not expressed, Rnr1 is the only large subunit. *RNR2* and *RNR4* are both expressed under normal growth conditions and function as an Rnr2-Rnr4 heterodimer (Perlstein *et al.*, 2005). The precise functional stoichiometry of the eukaryotic RNR enzyme is not clear (Kashlan & Cooperman, 2003).

Most of the control mechanisms for regulating the availability of dNTPs converge on the activity of RNR (Figure 1.5). These are described in the following sections.

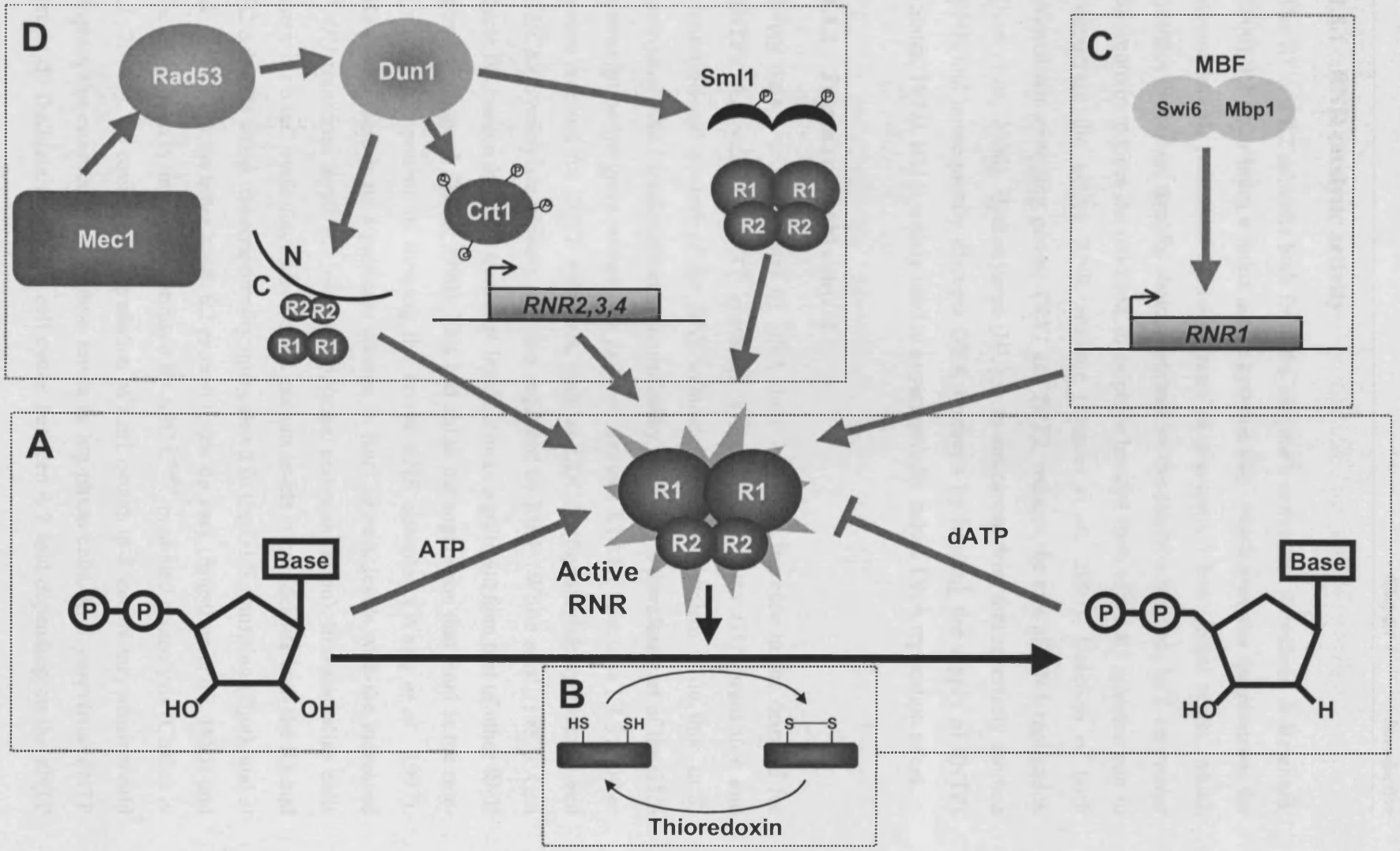
D
Rad53
Dun1
Sml1
Mec1
Crt1
N
C
R2 R2
R1 R1
RNR2,3,4
R1 R1
R2 R2
C
MBF
Swi6 Mbp1
RNR1
A
R1 R1
R2 R2
Active
RNR
ATP
dATP
Base
P P
HO OH
Base
P P
HO H
B
HS SH
S S
Thioredoxin

1.5.1 RNR catalytic activity

The R1 and R2 subunits both form the enzyme's active site (Nordlund & Reichard, 2006). R1 contributes a redox active cysteine pair, which provides the electrons for ribonucleotide reduction. R2 contributes an iron-tyrosyl free radical centre, which initiates the radical transfer chain important for the catalytic reaction. In *S. cerevisiae* thioredoxin reduces the oxidised, di-sulphide bonded form of the R1 cysteine pair to regenerate the active RNR enzyme (Camier *et al.*, 2007). Deletion of both thioredoxin-encoding genes, *TRX1* and *TRX2*, reduces the rate of DNA replication (Koc *et al.*, 2006). Hydroxyurea (HU) is an anticancer drug that reversibly inhibits RNR and consequently disrupts DNA synthesis by limiting the supply of dNTPs (Slater, 1973). HU is widely used to experimentally induce DNA replication stress.

1.5.2 Transcriptional control

Every time a cell replicates its DNA there is a large increase in the demand for dNTPs. Accordingly, dNTP synthesis is upregulated at the G1/S transition and transcriptional control of the RNR subunits is one mechanism to do this. In *S. cerevisiae RNR1* transcription is controlled by MBF and is therefore part of the G1/S transcription program induced as cells go through START (Section 1.1.3). Other genes required for dNTP synthesis, such as *CDC21* (thymidylate synthetase) and *CDC8* (thymidylate kinase), are also regulated by MBF (White *et al.*, 1987). Cell cycle fluctuation in *RNR1* transcript levels is more significant than that of other RNR genes (Elledge & Davis, 1990). This had led to the suggestion that Rnr1 is the rate-limiting component in forming the active RNR complex (Wang *et al.*, 1997). However, there is no significant change in Rnr1 protein levels with the increased *RNR1* transcript levels (L. Johnston, personal communication). In mammalian cells there is no cell cycle fluctuation in R1 protein levels either, despite both the R1 and R2 subunits being transcriptionally upregulated in the G1/S transition (Bjorklund *et al.*, 1990). On the other hand, R2 protein levels do vary (Engstrom *et al.*, 1985) and the R2 protein is degraded in mitosis by APC/C^{Cdh1}-mediated proteolysis (Chabes *et al.*, 2003b). No equivalent degradation of Rnr1 occurs in *S. cerevisiae*, which would explain the constant Rnr1 protein levels in log phase cells. In *S. cerevisiae* dNTP levels do fluctuate during the cell cycle: between 4-9 fold depending on the dNTP

(Koc *et al.*, 2003; Koc *et al.*, 2004). The fluctuation in dNTP levels depends mostly, but not entirely, on MCB-dependent gene induction (Koc *et al.*, 2003).

The ability to upregulate dNTP synthesis is also important for survival following genotoxic stress in yeast and mammalian cells (Chabes *et al.*, 2003a; Hakansson *et al.*, 2006b; Tanaka *et al.*, 2000). This requirement is presumably to provide dNTPs for the repair of damaged DNA. Additional transcriptional mechanisms are required to increase dNTP synthesis following genotoxic stress. In *S. cerevisiae RNR2*, *RNR3* and *RNR4* are coordinately induced upon activation of the Mec1-Rad53-Dun1 signalling cascade, which targets the Crt1 transcriptional repressor (Huang *et al.*, 1998). Dun1-dependent phosphorylation of Crt1 leads to removal of Crt1 from the chromatin and increases the expression of Crt1-controlled genes (Huang *et al.*, 1998). In mammalian cells, activation of p53 leads to transcription of an alternative R2 protein, p53R2 (Tanaka *et al.*, 2000).

1.5.3 Post translational control

S. cerevisiae RNR is inhibited by Sml1 (Chabes *et al.*, 1999). Sml1 is a small protein that binds to R1 large subunit and inhibits the catalytic cycle by preventing regeneration of the reduced cysteine pair (Zhang *et al.*, 2007). Sml1 protein levels are cell cycle regulated, being degraded as cells enter S-phase and reappearing after the completion of DNA replication (Zhao *et al.*, 2001). Therefore removal of Sml1 presumably contributes to the increase in dNTP levels as cells enter S-phase. The fluctuation in Sml1 protein levels is dependent on the Mec1-Rad53-Dun1 signalling cascade (Zhao *et al.*, 2001) and Sml1 is the only direct substrate of Dun1 that has been identified to date (Uchiki *et al.*, 2004; Zhao & Rothstein, 2002). The essential role of Mec1 is believed to be to upregulate dNTP synthesis for DNA replication by removing Sml1-dependent RNR inhibition (Zhao *et al.*, 1998). Deletion of Sml1 results in 2.5-fold higher dNTP levels in log phase cells and this can rescue the lethality of a *mec1Δ* strain (Zhao *et al.*, 1998). There is also a rapid decrease in Sml1 protein levels after exposure to DNA damage, again dependent on the Mec1-Rad53-Dun1 signalling cascade (Zhao *et al.*, 2001).

There is no known equivalent protein inhibitor of RNR in mammalian cells. The *S. pombe* Spd1 protein is an inhibitor of *S. pombe* RNR activity (Hakansson *et al.*, 2006a). Therefore, there appears to be a functional equivalent to *S. cerevisiae* Sml1 in *S. pombe*, although it is not an ortholog of Sml1. Like Sml1, Spd1 is degraded during S-phase and in response to DNA damage (Liu *et al.*, 2003; Woollard *et al.*, 1996). Unlike Sml1 however, Spd1 degradation is only dependent on $Rad3^{Mec1}$ in response to DNA damage (Liu *et al.*, 2003). Instead, Spd1 degradation, both during S-phase and in response to DNA damage, is dependent on the COP9 signalosome, which activates the ubiquitin ligase that targets Spd1 for degradation (Liu *et al.*, 2003).

1.5.4 Sub-cellular location

Deoxyribonucleotide synthesis is thought to take place in the cytoplasm, with the dNTPs then being supplied to the site of DNA polymerisation by diffusion (Reichard, 1988). In *S. cerevisiae*, under normal growth conditions the R1 subunit, Rnr1, is primarily located in the cytoplasm, whereas the R2 subunits, Rnr2 and Rnr4, are located in the nucleus (Huang & Elledge, 1997; Yao *et al.*, 2003). After genotoxic stress there is a Mec1-Rad53-Dun1-dependent relocalisation of the small subunits from the nucleus to the cytoplasm (Yao *et al.*, 2003). Yao *et al.* (2003) also showed a similar relocalisation upon S-phase entry, although this effect is less pronounced. The compartmentalisation of the R1 and R2 subunits into different cellular locations is achieved by active transport of the R2 subunits into the nucleus (An *et al.*, 2006) followed by Wtm1-dependent nuclear sequestration (Lee & Elledge, 2006; Zhang *et al.*, 2006).

A similar model of nuclear sequestration of the R2 subunit, dependent on Spd1, has been proposed in *S. pombe*: Spd1 degradation is required for relocalisation of the *S. pombe* R2 subunit from the nucleus to the cytoplasm (Liu *et al.*, 2003). Therefore two roles have been proposed for proposed for Spd1: one as an RNR inhibitor (equivalent to *S. cerevisiae* Sml1) and one as an R2 nuclear anchor (equivalent to *S. cerevisiae* Wtm1). These roles are not mutually exclusive, and degradation of Spd1 before S-phase and in DNA damage conditions could upregulate dNTP synthesis by both relocalisation of the R2 subunit and removal of the inhibition of the R1 subunit.

Most analyses of the subcellular localisation of mammalian RNR show it to be cytoplasmic (Engstrom *et al.*, 1984; Engstrom & Rozell, 1988). However translocation of the R1 and R2 subunits to the nucleus is thought to be important for the synthesis of dNTPs following genotoxic stress (Tanaka *et al.*, 2000; Xue *et al.*, 2003).

1.5.5 Allosteric feedback

A model for how allosteric feedback influences RNR activity has been described in detail by Reichard and Thelander (Reichard *et al.*, 2000; Thelander & Reichard, 1979). Binding of dNTP products to sites in the R1 subunit can influence the preference of RNR for different types of nucleotide. This specificity control is therefore important for maintaining balanced dNTP pools. The overall enzymatic activity of RNR is regulated positively by ATP and negatively by dATP. The model described by Reichard and Thelander has more recently been extended by the discovery that the activity of RNR is also regulated by changes in the oligomeric state of R1, induced by nucleotide binding to the allosteric binding sites (Kashlan & Cooperman, 2003).

For mammalian RNR, physiological levels of dATP (~20μM) inhibit its activity (Reichard *et al.*, 2000). Therefore mammalian RNR activity will only increase as dATP levels fall, for example as it is used in DNA replication or repair. The threshold for inhibitory dATP feedback is higher in *S. cerevisiae* (~50μM) (Domkin *et al.*, 2002), but it still contributes to the control of RNR activity: an *rnr1-D57N* mutant, where this dATP binding site has been mutated, shows 1.6-2.0 fold higher dNTP levels in a log phase culture (Chabes *et al.*, 2003a). This difference in the dATP feedback threshold might explain why *S. cerevisiae* has Sml1 as an RNR inhibitor, whereas no equivalent inhibitor has been identified in mammalian cells.

1.6 The Ras-cAMP-PKA pathway

The Ras-cyclic AMP-protein kinase A (Ras-cAMP-PKA) pathway is one of the cellular signalling pathways that couples cell growth with nutrient availability (Thevelein *et al.*, 2000). The amount of cAMP synthesised by the cell needs to reach

a certain threshold level for the cell to enter the cell cycle. So, under conditions of nutrient limitation cAMP synthesis is downregulated and cells arrest in G1 before START (Hubler *et al.*, 1993). Upon prolonged nutrient starvation cells will enter stationary phase (Section 1.1.2). Genetic mutants that decrease signalling in the Ras-cAMP-PKA pathway mimic the effects of nutrient starvation (Tatchell *et al.*, 1985; Toda *et al.*, 1987b). For example, by showing stationary phase characteristics, such as heat shock resistance and the accumulation of storage carbohydrates, during mitotic growth. Conversely genetic mutants that increase signalling in the Ras-cAMP-PKA pathway prevent the acquisition of stationary phase characteristics (Toda *et al.*, 1987a). These cells show decreased viability under conditions of nutrient limitation, presumably due to their defect in accumulating storage carbohydrates.

1.6.1 Core components of the *S. cerevisiae* Ras-cAMP-PKA pathway

Signalling through the Ras-cAMP-PKA pathway ultimately regulates the activity of the cAMP-dependent PKA (Figure 1.6). PKA is a tetrameric complex of any two of the three PKA catalytic subunits (Tpk1, Tpk2, or Tpk3) and two inhibitory Bcy1 subunits (Cannon & Tatchell, 1987; Toda *et al.*, 1987a; Toda *et al.*, 1987b). The three *TPK* genes have overlapping functions, as only one of them is required for normal growth (Toda *et al.*, 1987b). However phenotypic differences are seen in their ability to complement other mutants in the Ras-cAMP-PKA pathway (Toda *et al.*, 1987b). Binding of cAMP to the PKA inhibitory subunit, Bcy1, reduces its affinity for PKA and therefore increases PKA activity (Johnson *et al.*, 1987; Taylor *et al.*, 1990; Toda *et al.*, 1987a). Cellular levels of cAMP are controlled by adenylate cyclase (Cyr1), which synthesises cAMP from ATP (Casperson *et al.*, 1985). Cyclic AMP is broken down to AMP by the phosphodiesterases Pde1 and Pde2 (Nikawa *et al.*, 1987; Sass *et al.*, 1986).

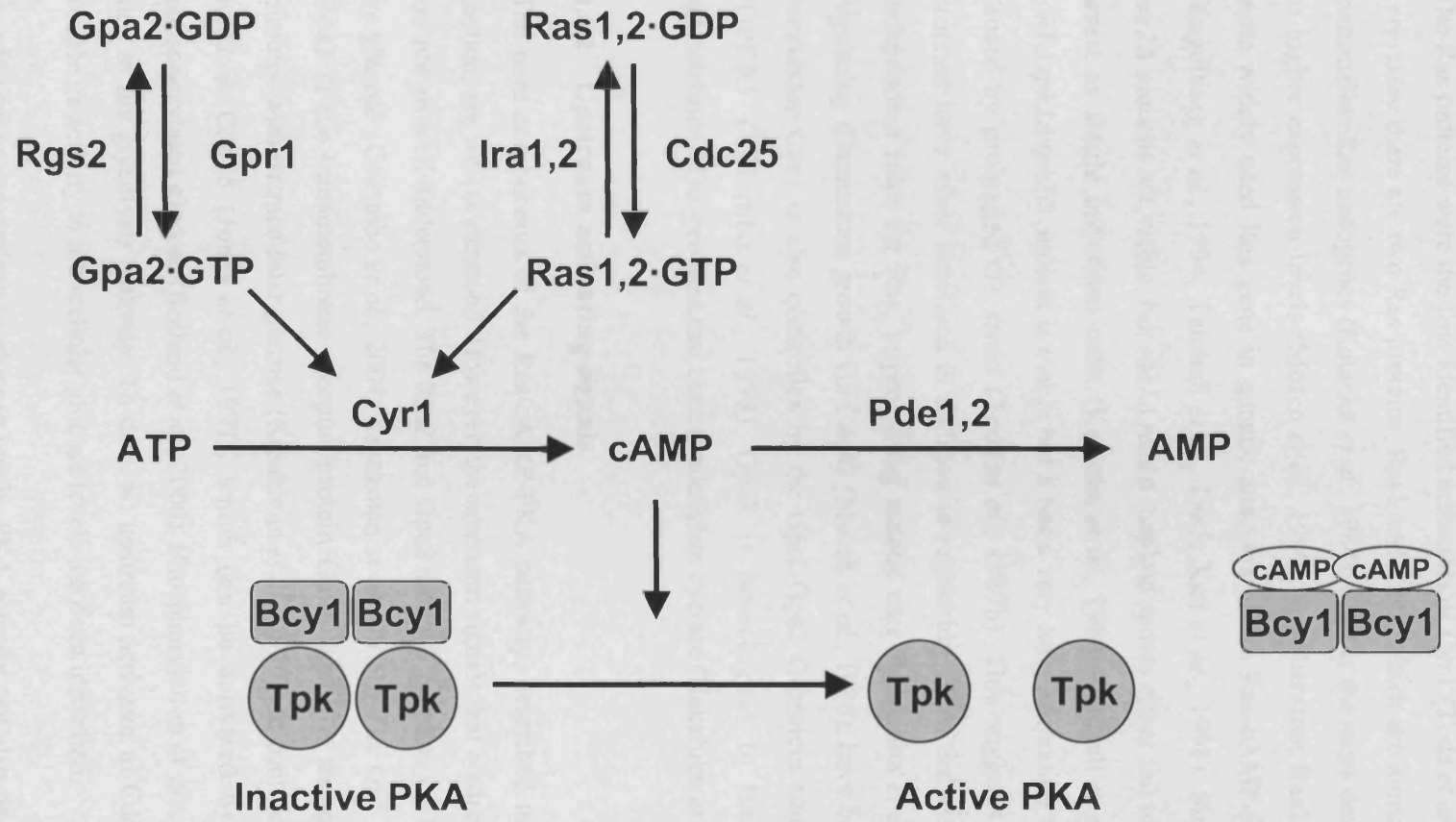

Figure 1.6 The core components of the *S. cerevisiae* Ras-cAMP-PKA pathway. Inactive PKA is a heterotetramer composed of two Tpk subunits and two inhibitory Bcy1 subunits. The inhibitory Bcy1 subunits dissociate upon binding of cAMP to release the active Tpk subunits. Adenylate cyclase (Cyr1) synthesises cAMP from ATP. The phosphodiesterases, Pde1 and Pde2 break down cAMP into AMP. Cyr1 activity is stimulated by the small GTP-binding proteins, Ras1, Ras2 and Gpa2. The guanine nucleotide exchange factors, Cdc25 and Gpr1, activate Ras1,2 and Gpa2 repectively. The GTPase activating proteins Ira1,2 and Rgs2 convert the active GTP-bound from of Ras1,2 and Gpa2 into the inactive GDP-bound form.

The Ras proteins were the first identified activators of Cyr1 (Toda *et al.*, 1985). In *S. cerevisiae* there are two Ras proteins, Ras1 and Ras2, which are homologous to the mammalian Ras oncogenes (Kataoka *et al.*, 1984). Ras2 is the more dominant, due to its higher expression levels (Mosch *et al.*, 1999), and therefore Ras2 has been the more widely used Ras gene in genetic analyses of the Ras-cAMP-PKA pathway (Engelberg *et al.*, 1994; Tatchell *et al.*, 1985; Xue *et al.*, 1998). Single *ras1Δ* or *ras2Δ* mutants are viable, but *ras1Δ ras2Δ* haploid spores either fail to germinate or arrest as single unbudded cells (Kataoka *et al.*, 1984; Tatchell *et al.*, 1985). A *tpk1Δ tpk2Δ tpk3Δ* mutant is viable but it has a very long generation time, which is caused by prolonged G1 arrest (Toda *et al.*, 1987b). This suggests that the Ras proteins have other functions in addition to regulating PKA. Subsequently PKA-independent roles for Ras, in promoting mitotic exit (Morishita *et al.*, 1995) and regulating filamentous growth via Cdc42 (Mosch *et al.*, 1996), have been shown. *S. cerevisiae* Cyr1 is also controlled by the Gpr1-Gpa2 G-protein coupled receptor (GPCR) (Colombo *et al.*, 1998). Gpa2 is homologous to the mammalian heterotrimeric Gα-proteins that control adenylate cyclase (Nakafuku *et al.*, 1988).

1.6.2 Upstream activating signals

The core components of the Ras-cAMP-PKA pathway, described in the previous section, are well understood. However, the upstream signals that control their activity are not so well understood. The Ras2 and Gpa2 small G proteins are both activated by glucose (Colombo *et al.*, 2004; Kraakman *et al.*, 1999). The GEF that activates Gpa2 is the transmembrane receptor protein Gpr1, which is thought to interact directly with extracellular glucose (Kraakman *et al.*, 1999). In contrast, the GEF for Ras2 is Cdc25 (Jones *et al.*, 1991), which can be activated by intracellular phosphorylated glucose (Rolland *et al.*, 2000). Phosphorylation of glucose is the first step in the glycolysis pathway. To date, no upstream activator of Cdc25 that could couple its activity to intracellular glucose levels has been identified.

In addition to responding to glucose levels, PKA activity can also be modulated by other nutrients (Thevelein *et al.*, 2005). In rich media with glucose as a carbon source, yeast cells grow rapidly by fermenting the glucose to ethanol. The absence of

any essential nutrient, such as nitrogen, will stop fermentative growth (Hirimburegama *et al.*, 1992). Addition of nitrogen to cells starved of nitrogen in glucose media will restore fermentative growth and activate PKA (Hirimburegama *et al.*, 1992). In this situation, PKA activation is independent of cAMP (Durnez *et al.*, 1994).

1.6.3 Downstream effectors

The phenotypic effects of variations in PKA activity are well known. For example, high PKA activity promotes glycolysis, promotes the synthesis of ribosomal protein genes and reduces stress resistance (Klein & Struhl, 1994; Martinez-Pastor *et al.*, 1996; Pernambuco *et al.*, 1996). On the other hand, low PKA activity increases the level of storage carbohydrates and increases stress resistance (Charizanis *et al.*, 1999; Engelberg *et al.*, 1994; Tatchell *et al.*, 1985). Despite having a good understanding of these phenotypic effects, specific targets of the PKA kinase are less well known. For many of the clearly identified targets, phosphorylation by PKA directly modulates their enzymatic activity. For example, phosphorylation of trehalase by PKA promotes the break down of the storage carbohydrate trehalose (Uno *et al.*, 1983), and phosphorylation of phosphofructokinase-2 by PKA promotes glycolysis (Francois *et al.*, 1984).

Variations in PKA activity also cause large changes in the transcriptional profile of the cell (Thevelein & de Winde, 1999). A reduction in PKA activity promotes the expression of genes required for stress resistance and entry into stationary phase. These genes fall into two large transcriptional regulons: the post diauxic shift (PDS) regulon and the stress response element (STRE) regulon (Boorstein & Craig, 1990; Marchler *et al.*, 1993). Expression of PDS genes is dependent on the Gis1 transcription factor and is induced at the diauxic shift (Pedruzzi *et al.*, 2000). Expression of STRE genes is dependent on the Msn2 and Msn4 transcription factors and can also be induced independently of PKA by cellular stresses such as oxidative or osmotic stress (Martinez-Pastor *et al.*, 1996; Smith *et al.*, 1998).

1.6.4 PKA-dependent control of cell cycle progression

PKA activity can influence the major cell cycle transitions at G1/S and G2/M. Cells arrest in G1 if the level of cAMP is too low and this correlates with inhibition of *CLN1* and *CLN2* transcription (Hubler *et al.*, 1993). So, addition of exogenous cAMP to cells arrested in G1, which are unable to synthesise cAMP, causes induction of *CLN1* and *CLN2* expression (Hubler *et al.*, 1993). The signalling pathway by which cAMP causes *CLN1* and *CLN2* expression is not known. However, it must be more complex that just direct transcriptional activation by PKA, as inhibition of *CLN1* and *CLN2* expression can also occur upon increased PKA activity (Baroni *et al.*, 1994; Tokiwa *et al.*, 1994). This is a specific response seen in cells growing in raffinose to the addition of glucose. Cells have a larger critical cell size for cell cycle entry when grown in rich media (Johnston *et al.*, 1979). So, delaying *CLN1* and *CLN2* transcription serves to increase the length of G1, allowing a longer period of growth to increase the cell size.

PKA is a negative regulator of APC/C in mammalian cells and fission yeast via inhibitory phosphorylation of APC/C subunits (Kotani *et al.*, 1998; Yamada *et al.*, 1997). Negative regulation of APC/C by PKA in *S. cerevisiae* has not been shown directly, but it is inferred, as reducing PKA activity can rescue the lethality of some APC/C temperature sensitive mutants (Anghileri *et al.*, 1999; Bolte *et al.*, 2003; Irniger *et al.*, 2000). In mammalian cells cAMP levels and PKA activity contribute to cell cycle progression. So, PKA activity decreases at the onset of mitosis to allow APC/C activation (Grieco *et al.*, 1994). PKA activity then increases in late mitosis, and this is required for transition into the subsequent interphase (Grieco *et al.*, 1996). This peak in PKA activity going into G1 is required for efficient DNA replication in the following cell cycle (Costanzo *et al.*, 1999).

1.6.5 Ras and PKA in other systems

S. cerevisiae is unique in that the Ras proteins regulate Cyr1 activity (Toda *et al.*, 1985). Mammalian PKA controls cellular proliferation in response to hormone signals and is activated by a GPCR, similar to Gpr1-Gpa2 in *S. cerevisiae* (Gilman, 1984). Mammalian Ras activity is also important for cellular proliferation and there

are four different mammalian Ras proteins, which are classical oncogenes (Bos, 1989). Over-expression of mammalian H-ras can substitute for *S. cerevisiae* Ras deficiency (Kataoka *et al.*, 1985). *S. pombe* is more similar to the mammalian system, so *S. pombe* Cyr1 is controlled by a GPCR and not by Ras (Byrne & Hoffman, 1993). There is only one Ras protein in *S. pombe*, Ras1. Like *S. cerevisiae* Ras2, it signals to two different effector pathways. One pathway signals through Byr2 to control mating (Wang *et al.*, 1991). The other pathway signals though Cdc42 to control cellular morphology (Chang *et al.*, 1994), and this pathway is equivalent to the *S. cerevisiae* Cdc42 pathway that is controlled by Ras2 (Mosch *et al.*, 1996).

1.7 Aims of this project

Mec1 prevents genomic instability through its involvement in many different cellular processes. The Mec1-dependent checkpoint response to genotoxic stress has been widely investigated. However its essential role, thought to be in upregulating dNTP synthesis for DNA replication, remains less well understood. For example, although it is known that *mec1Δ* lethality can be suppressed by increasing dNTP levels, it is only assumed that cells lacking Mec1 function die because they have insufficient dNTP levels. I have used two independent approaches to investigate further the essential role of *S. cerevisiae MEC1*. Firstly, the possibility that Mec1 controls local dNTP synthesis at the replication fork was examined. Secondly, the mechanism of suppression of the lethality a temperature sensitive allele of *MEC1* by a novel multicopy suppressor, *GIS2*, was characterised.

Chapter 2

Materials and Methods

2.1 Commonly used buffers and solutions

The details of commonly used buffers and solutions are given in Table 2.1. All chemicals were purchased from Sigma unless otherwise indicated.

Table 2.1 Commonly used buffers and solutions

Buffer/Solution	Composition
PBS (1x)	137 mM NaCl, 2.7 mM KCl, 10 mM Na_2HPO_4, 1.8 mM KH_2PO_4
PCR[a] buffer (1x)	2.25 mM $MgCl_2$, 50 mM KCl, 10 mM Tris-HCl pH 8.4
Phosphate buffer pH6.5 (1M stock)	685 mM NaH_2PO_4, 315 mM Na_2HPO_4
SSPE (20x stock)	3 M NaCl, 200 mM NaH_2PO_4, 20 mM EDTA[b]
TAE (1x)	40 mM Tris base, 40 mM acetic acid, 1 mM EDTA
TBE (1x)	45 mM Tris base, 45 mM boric acid, 1 mM EDTA
TBS (1x)	20 mM Tris-HCl pH 7.6, 150 mM NaCl
TE (1x)	10 mM Tris-HCl pH 8.0, 1 mM EDTA

[a] polymerase chain reaction (PCR)

[b] ethlenediaminetetra-acetic acid (EDTA)

2.2 Bacterial techniques

2.2.1 Bacterial strains

Eschericia coli (*E. coli*) strain DH5α (*F' endA1 hsdR17* [$r_K^- m_K^+$] *supE44 thi-1 recA1 gyrA* [Nal^r] *relA1 Δ[lacZYA-argF]U169 deoR* [*ϕ80dlacΔ(lacZ)MI5]*) was used for all bacteriological work.

2.2.2 *E. coli* media and growth conditions

E. coli were grown in Luria-Bertani (LB) broth (1% [w/v] bacto-tryptone, 0.5% [w/v] yeast extract, 1% [w/v] NaCl pH 7.5) supplemented with 100 μg/ml ampicillin (LB-Amp) for plasmid selection. Liquid cultures were grown at 37°C in a gyratory shaker at 300 rpm. For solid LB media, 1.5% (w/v) bacto-agar was added to LB-broth. *E. coli* were grown on LB-agar plates in a constant temperature incubator at 37°C. For long-term storage at –80°C, stock cultures were made by adding 1 ml of an overnight *E. coli* culture grown in LB-Amp to 1 ml of 2x LB/glycerol (2x LB-broth, 50% [v/v] glycerol).

2.2.3 *E. coli* transformation

To make chemically competent *E. coli* cells for transformation, DH5α cells were grown overnight with shaking in 2 ml of LB broth (no selection) at 37°C. The following morning, 100 ml of LB broth (no selection) was inoculated with 0.5 ml of the overnight culture and grown to an OD_{600} of 0.5. The culture was chilled on ice before the cells were pelleted (10,000 rpm, 1 min, 4°C). The cells were resuspended in 30 ml of filter-sterilised ice-cold buffer 1 (10 mM potassium acetate, 50 mM $MnCl_2$, 100 mM RbCl, 10 mM $CaCl_2$, 15% [v/v] glycerol, adjusted to pH 5.8 with dilute acetic acid) and left on ice for 90-120 min at 4°C. The cells were pelleted (5000 rpm, 1 min, 4°C) and gently resuspended in 4 ml of filter-sterilised ice-cold buffer 2 (10 mM MOPS, 75 mM $CaCl_2$, 10 mM RbCl, 15% [v/v] glycerol, adjusted to pH 7.0 with HCl). After addition of 60 μl dimethyl sulphoxide (DMSO) to the cells in buffer 2, the mixture was divided into aliquots of 100 μl in pre-chilled microfuge tubes and stored at –80°C.

To transform *E. coli* cells, 50 μl of chemically competent cells was added to DNA (either 5 μl of a ligation mix or 10-100 ng of plasmid DNA) and incubated on ice for 20 minutes. The mixture was subjected to heat shock at 42°C for 1 minute. Then 1 ml of LB-broth was added and the cells were incubated at 37°C in a hot-block for 1 h to recover. Aliquots of 100 μl and 900 μl were plated onto LB-Amp agar and grown overnight at 37°C

2.2.4 Purification of *E. coli* plasmid DNA

Plasmid DNA was extracted from a 2 ml overnight culture using a QuantumPrep Plasmid Miniprep kit [BioRad] according to the manufacturer's instructions.

2.3 Yeast techniques

2.3.1 Yeast media and growth conditions

Details of the yeast media used in this study are described in Table 2.2.

Table 2.2 Yeast growth media

Medium	Composition
YEP	1% (w/v) yeast extract, 2% (w/v) bacto-peptone
YPD	1% (w/v) yeast extract, 2% (w/v) bacto-peptone, 2% (w/v) glucose
YPG agar	1% (w/v) yeast extract, 2% (w/v) bacto-peptone, 3% (v/v) glycerol, 2% (w/v) bacto-agar
Minimal	0.67% (w/v) yeast nitrogen base, with either appropriate amino acid supplements at 40 μg/ml or 0.8 g/L amino acid dropout mix
SD	0.67% (w/v) yeast nitrogen base, with either appropriate amino acid supplements at 40 μg/ml or 0.8 g/L amino acid dropout mix, 2% (w/v) glucose
Amino acid dropout mix	800 mg adenine, 800 mg arginine, 800 mg histidine, 2400 mg leucine, 1200 mg lysine, 800 mg methionine, 2000 mg phenylalanine, 8000 mg threonine, 800 mg tryptophan, 1200 mg tyrosine, 800 mg uracil (with the appropriate amino acid dropped out)
SPM	1% (w/v) potassium acetate, 2% (w/v) bacto-agar

Routinely, yeast strains were grown either in YPD rich media or, for auxotrophic selection, in synthetic dextrose (SD) media (Table 2.2). SD media supplemented with all the amino acids listed in the dropout mix in Table 2.2 (i.e. with no amino acid dropped out) is referred to as synthetic complete (SC) media. Where non-glucose carbon sources (raffinose, galactose or glycerol) were used, the indicated carbon source was added to YEP or minimal media (Table 2.2). Liquid cultures were grown in a gyratory shaker [New Brunswick] at 175 rpm. For growth on solid media 2% (w/v) bacto-agar was added to the media. Yeast strains were incubated on agar plates

in a constant temperature incubator. The standard growth temperature for wild type strains was 30°C. Temperature sensitive strains were grown at the permissive temperature of 23°C and the restrictive temperature as indicated.

Overnight growth on YPG agar (Table 2.2) was used to select against petite mutants.

To select for drug resistance, 200 μg/ml G-418 [GIBCO] or 300 μg/ml Hygromycin B was added to YPD agar.

Growth on 5'-fluoro-orotic acid (5'FOA) [Apollo] containing solid media (SD- or SC-media, 3% [w/v] bacto-agar, 1 mg/ml 5'FOA) was used to select against *URA3* gene expression.

To induce DNA replication stress or DNA damage, cells were grown in the presence of hydroxyurea (HU) or methyl methanesulphonate (MMS) respectively at the indicated concentration.

For long-term storage, yeast strain stocks were stored at -80°C. Stocks were made by adding freshly grown cells from an agar plate to 1.8 ml of 25% (v/v) glycerol.

2.3.2 Mating yeast strains

To generate diploid strains two haploid strains of opposite mating types were mixed in a patch on a YPD agar plate and incubated overnight at 23°C or 30°C, depending on the strain genotype.

Where possible diploids were isolated by auxotrophic selection. If auxotrophic selection was not possible, cells from the mating patch were streaked for single colonies on a YPD agar plate and diploids were selected by microscopic screening (Section 2.3.11) and their ability to sporulate.

2.3.3 Tetrad dissection

Diploid strains were incubated on minimal sporulation media (SPM; Table 2.2) at 23°C or 30°C for a minimum of 24 hours. Tetrads were digested for 30 minutes with 50 μl of 5 mg/ml Zymolyase-20T [ICN Biomedicals] in SCE buffer (1 M sorbitol,

100 mM sodium citrate, 60 mM EDTA) at 37°C. Tetrads were dissected using a Singer MSM micromanipulator.

The genotype of the resulting haploid strains after tetrad dissection was determined by replica plating onto the appropriate SD-dropout media.

The mating type of the resulting haploid strains after tetrad dissection was determined by their ability to mate with mating type tester strains (RCY313 and RCY314; Table 2.7) to produce a prototrophic diploid.

2.3.4 Determination of cell density

The cell density of yeast cultures was determined either by counting cell numbers or by the optical density at 600 nm (OD_{600}).

To obtain a cell count, 50 µl of liquid culture was diluted into 10 ml Casyton [Scharfe System] solution and sonicated using a Status US200 sonicator [Philip Harris Scientific] for 3 seconds at 20% power to separate the cells. Cell numbers were counted using a CASY1 (model TT) particle counter [Scharfe System] according to the manufacturer's instructions.

The OD_{600} of a culture was measured in a CO8000 cell density meter [WPA], using a cuvette [Fisherbrand] containing 1 ml of liquid culture (diluted up to 10x if necessary).

2.3.5 Logarithmic growth

To obtain a log phase culture, first a 5 ml liquid starter culture was inoculated with cells freshly grown on an agar plate from the strain stock. This culture was grown for a minimum of 8 hours, in selective media where strains carried a 2µm plasmid, and then the cell density was measured. The appropriate volume of starter culture was diluted into the required volume of YPD to reach mid-log phase (2-4 x 10^6 cells/ml or an OD_{600} of 0.05-0.15) after overnight growth (14-16 hours).

2.3.6 Growth synchronisation

To obtain a synchronous culture for cell cycle analysis, 5 μg/ml α-factor [Polypeptide synthesis lab, NIMR] was added to a mid-log phase culture and cells were arrested for 3-4 hours. To release from the G1 block, the cells were pelleted (3000 rpm, 2 min), washed twice with saline and resuspended in fresh pre-warmed YPD.

2.3.7 Fluorescence activated cell scan (FACS) analysis

Cells from 1 ml of a mid-log phase or synchronous culture were pelleted (13,000 rpm, 1 min) and resuspended in 1 ml of fixative (40% [v/v] ethanol, 0.1 M sorbitol). After a minimum of 3 hours in fixative, cells were pelleted (13,000 rpm, 1 min), resuspended in 250 μl ribonuclease (RNase) solution (50 mM Tris-HCl pH 7.5, 100 μg/ml RNaseA) and incubated overnight at 37°C. The next day the cells were pelleted (13,000 rpm, 1 min), resuspended in 500 μl pepsin solution (50 mM HCl, 5 mg/ml pepsin) and incubated for a minimum of 5 minutes at room temperature. The cells were then pelleted (13,000 rpm, 1 min), resuspended in 1 ml SYTOX solution (50 mM Tris-HCl pH 7.5, 1 μM SYTOX Green nucleic acid stain [Invitrogen Molecular Probes]) and incubated overnight at 4°C.

The samples were analysed using a FACScan fluorescence activated cell analyser [Becton Dickinson] according to the manufacturer's instructions.

2.3.8 Drug and temperature sensitivity assays

Yeast cultures were grown overnight to saturation. The following morning they were diluted to an OD_{600} of 0.5, and then used to make 10-fold serial dilutions. The growth media was used to make dilutions, except where dilutions were to be spotted onto agar plates containing a different carbon source. In this case growth media with no carbon source was used to make the dilution series. The dilution series was spotted (4-5 μl) onto solid media (type as indicated in the figure legends). Once dry, the agar plates were incubated at the indicated temperature for 1-5 days as necessary. All drug and temperature sensitivity assays were repeated at least twice, using independent

clones of each strain. One representative experiment is shown in each case in the Results chapters.

2.3.9 Yeast transformation

Yeast strains were transformed by a standard lithium acetate method as described in (Gietz & Woods, 2002). To prepare competent cells, a 50 ml culture was grown to mid-log phase. The cells were pelleted (3000 rpm, 2 min) and washed once with 25 ml sterile H_2O. The cells were resuspended at 10^9 cells/ml in sterile H_2O and 100 µl of this cell suspension was used per transformation. The cells were pelleted (13,000 rpm, 1 min) and resuspended in 360 µl of transformation mix (30% [w/v] polyethylene glycol $(PEG)_{3350}$, 100 mM lithium acetate, 100 µg single-stranded carrier DNA, 1-10 µg of transforming DNA). The cells were incubated in the transformation mixture at 42°C for 40 minutes. For auxotrophic selection, cells were pelleted (6000 rpm, 1 min) after the heat shock treatment and resuspended in 500 µl sterile H_2O. Aliquots of 200 µl were plated directly onto SD-dropout agar plates. To select for drug resistance, the cells were pelleted (6000 rpm, 1 min) after the heat shock treatment, resuspended in 1 ml YPD rich media and allowed to recover for 2-3 hours before plating onto selective media as before.

2.3.10 Isolation of yeast genomic DNA

Cells from a 2 ml overnight culture were pelleted (13,000 rpm, 1 min), washed with 500 µl H_2O, and resuspended in 100 µl breakage buffer (50 mM Tris-HCl pH 7.6, 20 mM EDTA, 1% [w/v] sodium dodecyl sulphate [SDS]). Glass beads (0.5 mm) [BioSpec Products] were added to the level of the liquid and the cells were lysed by two 10 second pulses at speed setting 4 in a RiboLyser [Hybaid] with 1 minute on ice between pulses. The lysate was collected by piercing the bottom of the tube with a red-hot needle, placing this tube inside a clean 1.5 ml tube supported by a 15 ml tube, and centrifuging for 30 seconds at 3000 rpm. The lysate was then incubated for 10 minutes at 70°C in a hot block. After mixing briefly using a vortex, 200 µl of 5 M potassium acetate and 150 µl of 5 M NaCl were added to the lysate and the mixture was incubated on ice for 20 minutes. The cell debris was removed by centrifugation

(13,000 rpm, 20 min, 4°C). The supernatant was transferred to a clean 1.5 ml tube and 150 µl 30% (w/v) PEG_{6000} was added. The mixture was incubated on ice for 10 minutes and then the DNA was recovered by centrifugation (13,000 rpm, 10 min, 4°C). The supernatant was removed and the DNA pellet resuspended in 40 µl of nuclease-free H_2O.

2.3.11 Microscopy

An Eclipse E200 phase-contrast microscope [Nikon] with a 40x objective was used to routinely view yeast cultures. An Olympus DP12 [Olympus Optics] digital camera was used to capture images.

2.4 DNA manipulations

2.4.1 Agarose gel electrophoresis

Routine agarose gel electrophoresis was carried out in 1% (w/v) agarose gels (electrophoresis grade) [Invitrogen] with TBE electrophoresis buffer (Table 2.1). Use of alternative percentage agarose gels is indicated in the Figure legends. Where the DNA fragments were to be subsequently purified, low melting point (LMP) agarose [Invitrogen] and TAE electrophoresis buffer (Table 2.1) were used.

DNA was loaded with 1/6 volume 6x DNA loading buffer (0.2% [w/v] bromophenol blue, 30% [v/v] glycerol) and run with a constant voltage of 75 volts. DNA was stained using 0.05% (w/v) ethidium bromide [GIBCO] (which was added directly to the molten agarose before pouring the gel) and visualised under short wave ultra-violet radiation using a BioDoc-It System transilluminator [UVP]. The size of DNA fragments was estimated by comparison to the DNA markers in a 1 kilo base pair (kb) DNA ladder [Invitrogen].

2.4.2 Recovery of DNA fragments from agarose gels

DNA fragments were extracted from TAE agarose gels using a Wizard PCR Preps DNA purification system [Promega] according to the manufacturer's instructions.

2.4.3 Pulsed-field gel electrophoresis (PFGE)

Chromosome-sised-DNA containing agarose plugs were prepared for PFGE from cell pellets (~10^9 cells) collected and stored in 1 ml 50 mM EDTA. The cell pellet was weighed and the amount of cells adjusted to the same amount for each sample to be analysed. For each plug 0.1 g cells was used. To the cell pellet, 25 µl of solution I (1 M sorbitol, 100 mM sodium citrate, 60 mM EDTA, 5% [v/v] β-mercaptoethanol, 5 mg/ml zymolyase-20T) per plug (i.e. per 0.1 g cells) was added and stirred into the cell pellet. Next 75 µl of melted 1.5% (w/v) LMP agarose [Invitrogen] was added per plug and mixed into the cell pellet. The mixture was placed into plug moulds and left to set for 30 minutes. Plugs were removed from the mould into a 2 ml plastic tube. To the plugs, 1 ml of solution II (0.45 M EDTA, 10 mM Tris-HCl pH 7, 7.5% [v/v] β-mercaptoethanol, 10 µg/ml RNaseA) was added and incubated at 37°C for a minimum of 6 hours. The tube was incubated on ice for 10 minutes, before removing solution II and replacing it with 1 ml solution III (0.25 M EDTA, 10 mM Tris-HCl pH 7, 1% [w/v] sarkosyl, 1 mg/ml Proteinase K [Roche]). The plugs were incubated overnight in solution III at 37°C. The next day the tube was incubated on ice for 10 minutes, before removing solution III and replacing it with 1 ml storage solution (50 mM EDTA, 50% [v/v] glycerol). The prepared agarose plugs were stored at –20°C.

Electrophoresis was performed using 1/3 plug per lane at 14°C in a Bio-Rad CHEF Mapper with the following conditions: a voltage gradient of 5.5 V/cm^2, switch times of 5- to 30-sec, a switch angle of 120%, in a 1% (w/v) agarose gel (Pulsed Field Certified Agarose) [Bio-Rad] in 0.5x TBE for 24 hours.

2.4.4 Southern blot analysis

The agarose gel to be blotted was rinsed in water for 10 minutes, followed by depurination in 0.25 M HCl for 20 minutes. The gel was then rinsed again in water and denatured in 0.4 M NaOH for 30 minutes. The gel was blotted overnight in 0.4 M NaOH onto Hybond-N+ positively charged nylon transfer membrane [GE Healthcare].

The blotted membrane was rinsed with 50 mM sodium phosphate buffer pH 6.5 for 15 minutes. The membrane was then placed in a hybridisation tube [Hybaid] with 15

ml of prehybridisation buffer (7% [w/v] SDS, 0.5 M sodium phosphate buffer pH 6.5, 1 mM EDTA) rotating at 65°C for a minimum of 10 minutes. DNA probes were made either by restriction enzyme digest (Sections 2.4.2 and 2.4.5) or by PCR (Section 2.4.7). The DNA probe was labelled with ^{32}P-dCTP [GE Healthcare] using a Prime-It RmT Random Primer Labeling kit [Stratagene] according to the manufacturer's instructions. Before addition to a fresh 15 ml of prehybridisation buffer, the ^{32}P-labelled probe was denatured by incubation in a hot block at 95°C for 5 minutes. The prehybridisation buffer containing the denatured ^{32}P-labelled probe was then transferred to the hybridisation tube with the membrane. The membrane was incubated with the ^{32}P-labelled probe overnight, rotating at 65°C.

To remove non-specific signal the membrane was washed twice for 20 minutes in ~300 ml wash buffer (1% [w/v] SDS, 40 mM sodium phosphate buffer, 1 mM EDTA) before being wrapped in Saran wrap and exposed to a storage phosphor screen [Kodak] for 1-3 days.

The screen was scanned using a Storm 860 Phosphorimager and band intensity was quantified with ImageJ software [NIH].

See Table 2.4 for a list of DNA probes used in this study.

2.4.5 Restriction endonuclease digestions

DNA was incubated with the required restriction endonuclease enzyme(s) [New England Biolabs or Roche] in the appropriate restriction endonuclease buffer according to the manufacturer's instructions at 37°C for a minimum of 2 hours.

2.4.6 DNA ligations

Following restriction enzyme digestion (Section 2.4.5), plasmid vector DNA to be used for ligation was incubated with 1 U calf intestine alkaline phosphatase [Roche] at 37°C for 1 hour.

Ligation of DNA fragments was carried out in a 20 µl reaction mixture containing 1x T4 DNA ligase buffer [Promega], 1.5 U T4 DNA ligase [Promega] and a 1:5 molar

ratio of vector:insert DNA (roughly estimated from an ethidium bromide stained agarose gel). A control reaction without any insert DNA was carried out alongside. Ligation reactions were incubated overnight at 18°C and 5 µl of the reaction mix was transformed into competent *E. coli* cells (Section 2.2.3) the following day.

2.4.7 Polymerase chain reaction (PCR)

Polymerase chain reactions were carried out in a Biometra T3 thermocycler [Thistle Scientific].

DNA fragments for genomic modifications were made by PCR (as described in (Longtine *et al.*, 1998) in a 100 µl reaction containing 1x PCR buffer, 2 µM of each primer, 200 µM dNTPs [GE healthcare], 5 U Taq polymerase [Abgene] and 100 ng template plasmid DNA. The PCR program was an initial denaturation at 94°C for 5 minutes, followed by 20 cycles of 94°C (1 min), 55°C (30 sec), 72°C (1 min), and a final elongation step at 72°C for 10 minutes.

DNA probes for Northern blot or Southern blot analysis were made as above except with 1 µl of a genomic DNA prep from a wild type yeast strain (Section 2.3.10) as the template DNA.

Diagnostic colony PCR was carried out in 50 µl reactions containing 1x PCR buffer, 1 µM of each primer, 100 µM dNTPs, 2.5 U Taq polymerase. The yeast colony was smeared onto the bottom of the PCR tube and microwaved for 1 minute on full power (900 W), before being resuspended in the reaction mixture. The colony PCR program was an initial denaturation at 94°C for 5 minutes, followed by 30 cycles of 94°C (1 min), 50°C (30 sec), 72°C (1 min), and a final elongation step at 72°C for 10 minutes.

PCR analysis of DNA from chromatin immunoprecipitation (ChIP) experiments (Section 2.7) was carried out in 25 µl reactions containing 1x PCR buffer, 0.5 µM of each primer, 100 µM dNTPs, 1.25 U Taq polymerase and 2.5 µl of purified DNA. The ChIP PCR program was an initial denaturation at 94°C for 5 minutes, followed

by 40 cycles of 94°C (1 min), 58°C (30 sec), 72°C (1 min), and a final elongation step at 72°C for 10 minutes.

Details of the primers [Eurogentec] used in this study are shown in Table 2.3. All primers were supplied desalted.

Table 2.3 Primers used in this study

Name	Sequence 5'-3'	Source
P521	AGCTGCATCAGGTCGGAGAC	Cha lab
P531	TTTCAGAGCCTTCTTTGGAG	Kamimura, 2001
P532	CAAACTCCGTTTTTAGCCCC	Kamimura, 2001
P533	GAAGATGCTAAGAAATGCAG	Kamimura, 2001
P534	AGTTGAGGCGCAGAATCCCA	Kamimura, 2001
P537	TCGACGTACCTGACCAACCC	This study
P539	GTGACAAGCTCACGCAAGTC	This study
P540	TTCGCTAGAAAATGAGTAAG	Kamimura, 2001
P541	CAGCTATGAAAGATGCGTAG	Kamimura, 2001
P586	AGAAACTATTCATTCGAACG	This study
P587	CACCTCCAATCTGCTTCAAG	This study
P590	TCCGACTCTTCTGATATCGAAGTTGACCATACGA AAAGCACCGATCCTCGGATCCCCGGGTTAATTAA	This study
P591	CATATTGCATCGAATAGTAATTACATAGCAATAA TAGCAACAACATGAATTCGAGCTCGTTTTCG	This study
P592	GCGCAGTGTGGCAAGCTTGC	This study
P593	CTCTCTTCAACTGCTCAATAATTTCCCGCTATGC AAAATAGGGAACAAAAGCTGG	This study
P594	TTGTTGTTGTTGGCAGCGATTTTGAGCGTAAAAG TAGTCTTGGGACTGTAGGGCGAATTGGG	This study
P595	GAGTCTCTCCTCCAAATCC	This study
P596	GGAACATCGCCCGTTTCGCC	This study
P636	ATTCCGATGCTGACTTGC	This study
P637	ATGCTCTTTCTGCTTTGGGGGCACTTGAGGATTG TATTATTTTAACGGATCCCCGGGTTAATTAA	This study

Name	Sequence 5'-3'	Source
P639	CATGATAAGTGATTGTTCCTTTGTTTTTTTCAGTG GATGTTTCACGAATTCGAGCTCGTTTAAAC	This study
P643	CGCAAGTGTATGTTAACC	This study
P645	TATGCTCCGCATTGGTCTTG	This study
P648	AGGATGCTAGCCTATGAC	This study
P657	AGTAAAGGGGCTTAACATACAGTAAAAAAGGCAA TTATAGTGAAGCGGATCCCCGGGTTAATTAA	This study
P658	AAAATCCAGATTCAAACAATGTTTTTGAAATAATG CTTCTCATGTGAATTCGAGCTCGTTTAAAC	This study
P660	CTAGCAAGGTCTGGAGAA	This study
P664	CACCTCCGCTTACATCAA	This study
P672	ATTACCTCCCGTATCACCCG	This study
P673	ACCCTGGACACCAAGAGCAA	This study
P674	GAATGTTTCTACATCAACC	This study
P675	GAGTGTTTCTAGGTTTGAC	This study
P676	AAAACCAAGTTAACCGTTTTCGAATTGAAAGGAG ATATACAGCGGATCCCCGGGTTAATTAA	This study
P677	CAACTTTATAGAGTTCTTTTCGTCTTAGCGTTTCT ACAACTAGAATTCGAGCTCGTTTAAAC	This study
P678	TGACTCTCTGCAATGTCC	This study
S1	GGATCCACATGGTTAGGGTCCATGACG	Cha lab
S2	GGATCCATGGCGACTGGATACGCA	Cha lab

2.5 RNA manipulations

2.5.1 Control of ribonuclease activity

All glassware and plasticware were incubated with a 2% (v/v) solution of AbSolve [NEN Life Science Products] for a minimum of 30 minutes to remove any RNase contamination. Any disposable plasticware was certified RNase free and was used directly from a freshly opened packet. Gloves were worn at all times during RNA manipulations.

2.5.2 Preparation of RNA extracts

Total RNA was isolated from ~10^8 yeast cells using a FastRNA Pro Red Kit [Qbiogene] according to the manufacturer's instructions. The RNA concentration was calculated from the OD_{260nm} (1 OD_{260nm} = 40 µg/ml) measured using a Genesys 10-S spectrophotometer [Thermo Spectronic].

2.5.3 Northern blot analysis

To prepare RNA samples for electrophoresis, 12 µl of a mixture containing 8% (w/v) deionised glyoxyl, 65% (v/v) DMSO, and 15 mM sodium phosphate buffer pH 6.5 was added to 5 µg of RNA. The mixture was incubated at 50°C for 15 minutes to denature the RNA. The denatured RNA sample was cooled on ice immediately and 4 µl of loading buffer (50% [v/v] glycerol, 10 mM sodium phosphate buffer, 0.4% [w/v] bromophenol blue) was added. Electrophoresis was performed in a 1.2% (w/v) agarose gel in 15 mM sodium phosphate buffer pH 6.5, at a constant voltage of 4 volts per cm of gel length.

The agarose gel was blotted overnight in 25 mM sodium phosphate buffer onto Hybond-N+ positively charged nylon transfer membrane [GE Healthcare].

The blotted membrane was rinsed in 25 mM sodium phosphate buffer pH 6.5 for 5 minutes. The membrane was then placed in a hybridisation tube [Hybaid] with 15 ml of prehybridisation buffer (5x SSPE, 50% [v/v] formamide, 1% [w/v] SDS, 10% [w/v] dextran sulphate) rotating at 42°C for 4 hours. The DNA probe was labelled with ^{32}P-dCTP [GE Healthcare] using a Prime-It RmT Random Primer Labeling kit [Stratagene] according to the manufacturer's instructions. Before being added to the prehybridisation buffer in the tube with the membrane, the ^{32}P-labelled probe was denatured by incubation in a hot block at 95°C for 5 minutes. The membrane was incubated with the ^{32}P-labelled probe overnight, rotating at 42°C.

To remove non-specific signal, the membrane was rinsed once in 2x SSPE, washed twice for 20 minutes in ~300 ml wash buffer (2x SSPE, 2% [w/v] SDS), then rinsed in 0.1x SSPE before being wrapped in Saran wrap and exposed to a storage phosphor screen [Kodak] for 1-3 days.

The screen was scanned using a Storm 860 Phosphorimager and band intensity was quantified with ImageJ software [NIH].

Table 2.4 DNA probes used in this study

Probe name	Probe size (bp)	Source
ACT1	563	*Cla*I digest of pYA301
CHA1	~800	*Hind*III/*Kpn*I digest of pRSC38
GIS2	1012	PCR product using primers S1 and S2
RNR1	~2600	*Eco*RI digest of pSE738
RNR2	800	*Eco*RV digest of pMH172
RNR3	1481	PCR product using primers P672 and P673
RPB4	658	PCR product using primers P674 and P675

2.6 Protein techniques

2.6.1 Preparation of yeast TCA extracts

Yeast cells (~10^7-10^8cells) were pelleted (3000 rpm, 2 min) and resuspended in 1 ml 20% (w/v) trichloroacetic acid (TCA) [Fisher Scientific]. Cells were transferred to a 2 ml tube, pelleted (13,000 rpm, 1 min) and resuspended in 200 µl 20% (w/v) TCA. Glass beads (0.5 mm) [BioSpec Products] were added up to the level of the liquid and mixed vigorously for 4 minutes using a vortex. Next, 400 µl of 5% (w/v) TCA was added to the tube and the whole aqueous extract removed to a new 2 ml tube. The precipitated proteins were pelleted (3000 rpm, 10 min, 4°C) and the supernatant removed. To the protein pellet, 100 µl of 3x Laemmli buffer (150 mM Tris-HCl pH 6.8, 6% [w/v] SDS, 30% [v/v] glycerol, 0.3% [w/v] bromophenol blue, 15% [v/v] β-mercaptoethanol) and 50 µl of Tris-HCl pH 9.4 were added and mixed using a vortex for 10 seconds. The protein extract was incubated at 95°C in a hot block for 5 minutes. Insoluble material was pelleted (3000 rpm, 10 min, 4°C) and the soluble supernatant removed to a fresh tube for storage at -20°C.

2.6.2 SDS polyacrylamide gel electrophoresis

Proteins were separated by denaturing sodium-dodecyl-sulphate polyacrylamide gel electrophoresis (SDS-PAGE). Polyacrylamide gels (7 x 9 cm) were assembled in a Hoefer Dual Gel Caster vertical apparatus [Amersham Biosciences]. The resolving gel (% acrylamide [Protogel] as indicated, 0.04% [w/v] SDS, 375 mM Tris-HCl pH 8.8, polymerised with 0.1% [w/v] ammonium persulphate [APS] [Bio-Rad] and 0.05% [v/v] N,N,N',N'-tetramethyl-ethylenediamine [TEMED] [Bio-Rad]) was overlaid with stacking gel (5% [w/v] acrylamide, 0.04% [w/v] SDS, 375 mM Tris-HCl pH 6.8, polymerised as before) and left at room temperature to set with a well-forming comb in place. Protein samples were incubated in a hot block at 95°C for 5 minutes prior to loading on the gel and 5-10 µl of a TCA protein extract was loaded per lane. Electrophoresis was performed at a constant current of 35 mA in electrophoresis running buffer (365 mM glycine, 50 mM Tris base, 0.1% [w/v] SDS) until the bromophenol blue dye reached the bottom of the resolving gel. Proteins on the gel were detected by Western blot analysis (Section 2.6.3). The molecular weight of proteins was estimated by comparison with high-range rainbow molecular weight markers (5 µl per gel lane) [Amersham Biosciences].

2.6.3 Western blot analysis

The proteins separated by SDS-PAGE (Section 2.6.2) were transferred to a Protran nitrocellulose membrane [Schleicher & Schnell]. The V10-SDB semi-dry electroblotter apparatus [BDH] was assembled using Whatman 3MMChr filter paper, the membrane and the gel according to the manufacturer's instructions. The filter paper, membrane and gel were all pre-incubated in transfer buffer (40 mM glycine, 48.5 mM Tris base, 0.04% [w/v] SDS, 20% [v/v] methanol) for at least 10 minutes. The transfer was performed at 2-5 mA/cm^2 of gel area for 2 hours.

After transfer, the membrane was incubated with blocking buffer (phosphate-buffered-saline [PBS; Table 2.1] containing 0.2% [v/v] Tween-20 [PBS-T], 5% [w/v] dried milk [Marvel]) for 1 hour at room temperature. Then the membrane was probed with the indicated primary antibody (Table 2.5) at the appropriate dilution in blocking buffer, gently shaking overnight at 4°C. The next day the membrane was

washed in PSB-T (3 x 20 min), and then incubated with the appropriate horseradish peroxidase-conjugated secondary antibody [Sigma] at a 1:10,000 dilution in blocking buffer for 1 hour. The membrane was washed (3 x 10 min) in PBS and the signal visualised by enhanced chemiluminescence (ECL) [GE healthcare]. The two ECL reagents were mixed in a 1:1 ratio and the membrane was incubated with a total volume of 3 ml of the ECL reagents for 1 minute at room temperature. The excess liquid was drained off the membrane, which was then wrapped in Saran wrap and exposed to autoradiography film [Kodak] in the dark in an exposure cassette. The time of exposure varied depending on the intensity of the signal. Multiple exposures were taken when the signal was to be subsequently quantified to obtain a signal in the linear range. Films were developed in an X150 X-ray film processor [X-ograph Imaging Systems]. Developed films were scanned and the images were saved as TIFF files. The band intensity was quantified with ImageJ software [NIH].

Table 2.5 Antibodies used in this study

Antibody	Type	Dilution for Western blotting	Source
α-HA (12CA5)	mouse monoclonal	1:1000	NIMR, London
α-MYC (9E10)	mouse monoclonal	1:1000	NIMR, London
α-Rad53	rabbit polyclonal	1:1000	Marco Foiani
α-tubulin (YL1/2)	rat monoclonal	1:5000	Abcam

2.7 Chromatin Immunoprecipitation (ChIP)

The ChIP method used was adapted from that described in (Strahl-Bolsinger *et al.*, 1997). A sample of yeast cells (~10^8-10^9 cells) was taken from a mid-log phase or synchronous culture. Formaldehyde [Fisher Scientific] was then added to a final concentration of 1% (v/v) and the cross-linking reaction was allowed to proceed for 20 minutes at room temperature with occasional inversion. Next, glycine [BDH] was added to a final concentration of 125 mM and incubated for 5 minutes at room temperature. The cells were pelleted (3000 rpm, 2 min), washed with ice-cold Tris-buffered-saline (TBS; Table 2.1) and transferred to a clean 2 ml tube. The cells were resuspended in 500 µl of lysis buffer (50 mM HEPES-KOH pH 7.5, 140 mM NaCl, 1

mM EDTA, 1% [v/v] Triton X-100, 0.1% [w/v] sodium deoxycholate, 1x Complete EDTA-free protease inhibitor cocktail [Roche], 1 mM phenylmethylsulphonyl fluoride [PMSF]) and lysed in the presence of glass beads (0.5 mm) [Biospec Products] by three 10 second pulses at speed setting 4 in a RiboLyser [Hybaid], with a minimum of 1 minute on ice between pulses. The lysate was collected by piercing the bottom of the tube with a red-hot needle, placing this tube inside a clean 1.5 ml tube supported by a 15 ml sterilin tube, and centrifuging for 30 seconds at 3000 rpm. The supernatant was discarded and the pellet resuspended in 500 µl of lysis buffer.

The DNA was sheared by three pulses of 20 seconds at 20% power on a Status US200 sonicator [Philip Harris Scientific] and the sample was cooled on ice for at least 1 minute between pulses. The lysate was then clarified by two rounds of centrifugation (13,000 rpm, 4°C, first 5 min, then 15 min). For analysis of the input DNA, 20 µl of the cleared lysate was added to 230 µl of TE (Table 2.2) with 1% (w/v) SDS. The remaining lysate was incubated with 2 µl of the indicated antibody overnight at 4°C on a rotating wheel. The next day 20 µl of a 50% (w/v) slurry of Protein-A-sepharose beads [Amersham Biosciences] (blocked with bovine serum albumin [BSA]) was added and the lysate incubated for 4 hours at 4°C on a rotating wheel. The beads were pelleted (4000 rpm, 1 min) and washed as follows: twice with 1 ml lysis buffer (no protease inhibitors), once with 1 ml lysis buffer with 360 mM NaCl, once with 1 ml final wash buffer (10 mM Tris-HCl pH 8.0, 250 mM LiCl, 0.5% [v/v] Nonidet P-40 [BDH], 0.5% [w/v] sodium deoxycholate, 1 mM EDTA) and once with 1 ml TE.

The beads were then resuspended in 100 µl of elution buffer (50 mM Tris-HCl pH 8.0, 10 mM EDTA, 1% [w/v] SDS) and incubated at 65°C in a hot block for 15 minutes. The supernatant was transferred to a clean 1.5 ml tube and the beads were washed with 150 µl TE, 0.67% (w/v) SDS. To reverse the cross-links the combined 250 µl supernatant and the corresponding input DNA sample (taken earlier) were incubated at 65°C in a hot block overnight. The next day 250 µl TE, 5 µg glycogen and 100 µg proteinase K [Roche] were added and the extracts were incubated at 37°C for 1 hour in a hot block. Then 55 µl of 4 M LiCl was added and the DNA was purified by phenol/chloroform extraction. To the sample, 500 µl of

phenol:chloroform:isoamyl alcohol (25:24:1) was added, mixed briefly using a vortex and centrifuged (13,000 rpm, 5 min). The aqueous phase was removed to a clean tube and the process repeated with a second 500 µl of phenol:chloroform:isoamyl alcohol (25:24:1). Next, 1 ml of 100% (v/v) ethanol was added to the aqueous phase and incubated at -20°C for a minimum of 20 minutes. The precipitated DNA was pelleted (13,000 rpm, 15 min) and washed in 500 µl of 70% (v/v) ethanol. The DNA was pelleted again (13,000 rpm, 15 min), the ethanol removed and the DNA pellet dried at room temperature.

The purified DNA was resuspended in 30 µl of TE and analysed by PCR (Section 2.4.7).

2.8 Fluorescence microscopy

2.8.1 Preparation of cells expressing green fluorescent protein (GFP)

A 900 µl sample of a mid-log phase culture was incubated with 100 µl of 37% (w/v) formaldehyde [Fisher Scientific] for 10 minutes at room temperature. The cells were pelleted (5000 rpm, 1 min), washed twice with 1 ml PBS, and then resuspended in 200 µl PBS. A 10 µl sample of the cell suspension was spread onto a glass microscope slide and left to dry. Before application of the glass coverslip, 2 µl of 4,6-diamino-2-phenylindole (DAPI) solution (1.5 µg/ml DAPI [Sigma] in Vectashield mounting medium [Vector Lab]) was dotted onto the dried cells.

2.8.2 Preparation of immunostained nuclear spreads

Yeast cells were pelleted (5000 rpm, 1 min) from 5 ml of a mid-log phase culture, resuspended in 1 ml solution I (1.2 M sorbitol, 50 mM $MgCl_2$, 80 mM K_2HPO_4, 20 mM KH_2PO_4 pH 7.4) and stored on ice until preparation of nuclear spreads.

Cells were pelleted (5000 rpm, 1 min), resuspended in 200 µl of spheroplasting buffer (Solution I with 20 mM DTT, 1 mg/ml Zymolyase-20T) and incubated at 37°C for 30 minutes. Next, 1 ml of ice-cold Solution II (0.1 M MES-OH pH 6.4, 1 mM EDTA, 0.5 mM $MgCl_2$, 1 M sorbitol) was added and mixed gently by inversion. The spheroplasts were pelleted (1000 rpm, 8 min) and then resuspended in 200 µl of

ice-cold solution II. A 20 µl sample of the resuspended spheroplasts was placed onto a clean glass microscope slide. Then 120 µl of fixative solution (4% [w/v] paraformaldehyde, 3.4% [w/v] sucrose) and 80 µl of 1% (v/v) photoflo detergent [Kodak] were added to the spheroplasts on the slide. The mixture was spread over the area of the slide gently using a pipette tip. The nuclear spreads were left to dry overnight.

The dried nuclear spreads were washed for 10 minutes in PBS in a Coplin jar. After draining the excess PBS off the slide, 200 µl of blocking buffer (2% [w/v] dried milk in PBS) was added to the central area of the slide and the slide was incubated at room temperature for 10 minutes. Excess liquid was drained off the slide and 50 µl of blocking buffer with the primary antibody (1:100 dilution) was added. The slide was incubated at room temperature for 1 hour in a humidity chamber (dark plastic box containing damp paper towels). The slide was then washed twice in PBS in a Coplin jar for 10 minutes and 50 µl of PBS with an AlexaFluor-488 FITC-conjugated secondary antibody [Molecular Probes] (1:500 dilution) was added. The slide was incubated with the secondary antibody for 1 hour in a humidity chamber. Excess liquid was drained from the slide and 5 µl of DAPI solution (Section 2.7.1) was added to the centre of the slide. A coverslip was placed over the nuclear spread and the slide was ready for viewing.

2.8.3 Fluorescence microscopy

Fluorescence microscopy was performed on a Deltavision Spectris system containing a photometrics CH350L liquid cooled charge-coupled device camera and an Olympus IX70 inverted microscope with a 100x objective equipped with Deltavision data collection system [Applied Precision].

For nuclear spreads 5 images (0.1 µm apart) were acquired and for whole cells 18 images (0.2 µm apart) were acquired. Images were processed using SoftWoRx image processing suite [Applied Precision] and PhotoShop version CS [Adobe] software. Out of focus images were discarded prior to projecting the stack of images onto one plane. Exposure times varied and were dependent upon the intensity of the observed fluorescence.

2.9 Plasmid construction

The plasmids used in this study are summarised in Table 2.6. Details of plasmids constructed in this study are given in Sections 2.8.1-2.8.3.

Table 2.6 Plasmids used in this study

Plasmid Name	Details	Reference/Source
pAG32	PCR template for gene manipulation (pFA6a-hphMX4)	(Goldstein & McCusker, 1999)
pCLE4	Original library clone. YEp24-*GIS2*	Cha lab
pCLE5	Original library clone. YEp24-*MEC1*	Cha lab
pCLE8	YEp24-*GIS2* (*URA3*, 2 μm)	This study
pCLE9	pRS424-*GIS2* (*TRP1*, 2 μm)	This study
pCLE11	Original library clone. YEp24-*RNR1*	Cha lab
pFA6a-3HA-kanMX6	PCR template for gene manipulation	(Longtine *et al.*, 1998)
pFA6a-3HA-hphMX4	PCR template for gene manipulation	This study
pFA6a-TRP1	PCR template for gene manipulation	(Longtine *et al.*, 1998)
pFA6a-GFP-TRP1	PCR template for gene manipulation	(Longtine *et al.*, 1998)
pMH172	*RNR2* gene	Johnston lab stocks
pMH726	*HA-RNR1* integrative plasmid	(Yao *et al.*, 2003)
pMK9	YCp50-*MEC1* (*URA3*, ARS/CEN)	(Kato & Ogawa, 1994)
pMPY-3xMYC	PCR template for gene manipulation	(Schneider *et al.*, 1995)
pRS424	Multicopy cloning vector (*TRP1*, 2 μm)	(Christianson *et al.*, 1992)
pRSC38	pUC19-*CHA1*	Cha lab
pSE738	*RNR1* gene	Johnston lab stocks
pYA301	*ACT1* gene	Johnston lab stocks
YEp24	Multicopy cloning vector (*URA3*, 2 μm)	Johnston lab stocks
p306-*ORC1-HA/C*	*ORC1-HA* integrative plasmid	(Aparicio *et al.*, 1997)

2.9.1 pFA6a-3HA-hphMX4

The 1.7 kb DNA fragment containing the hygromycin resistance gene (*hph*^{R}) was excised from plasmid pAG32 by digestion with *Bgl*II and *Eco*RV. Plasmid pFA6a-3HA-kanMX6 was digested with *Bgl*II and *Pme*I to yield the 2.8 kb pFA6a-3HA plasmid backbone These DNA fragments were purified from an agarose gel and ligated to make the pFA6a-3HA-hphMX4 plasmid used as a PCR template for adding a 3HA epitope tag to *DPB3*.

2.9.2 YEp24-*GIS2*

An original library clone (pCLE4) containing the *GIS2* open reading frame (ORF) was subjected to 3 sequential restriction enzyme digests with *Nhe*I, *Pml*I and *Sal*I. After each restriction digest, the plasmid backbone was purified from an agarose gel and religated (Section 2.4.6). Finally plasmid pCLE8 was formed (Figure 2.1), where the only remaining expressed ORF was *GIS2*.

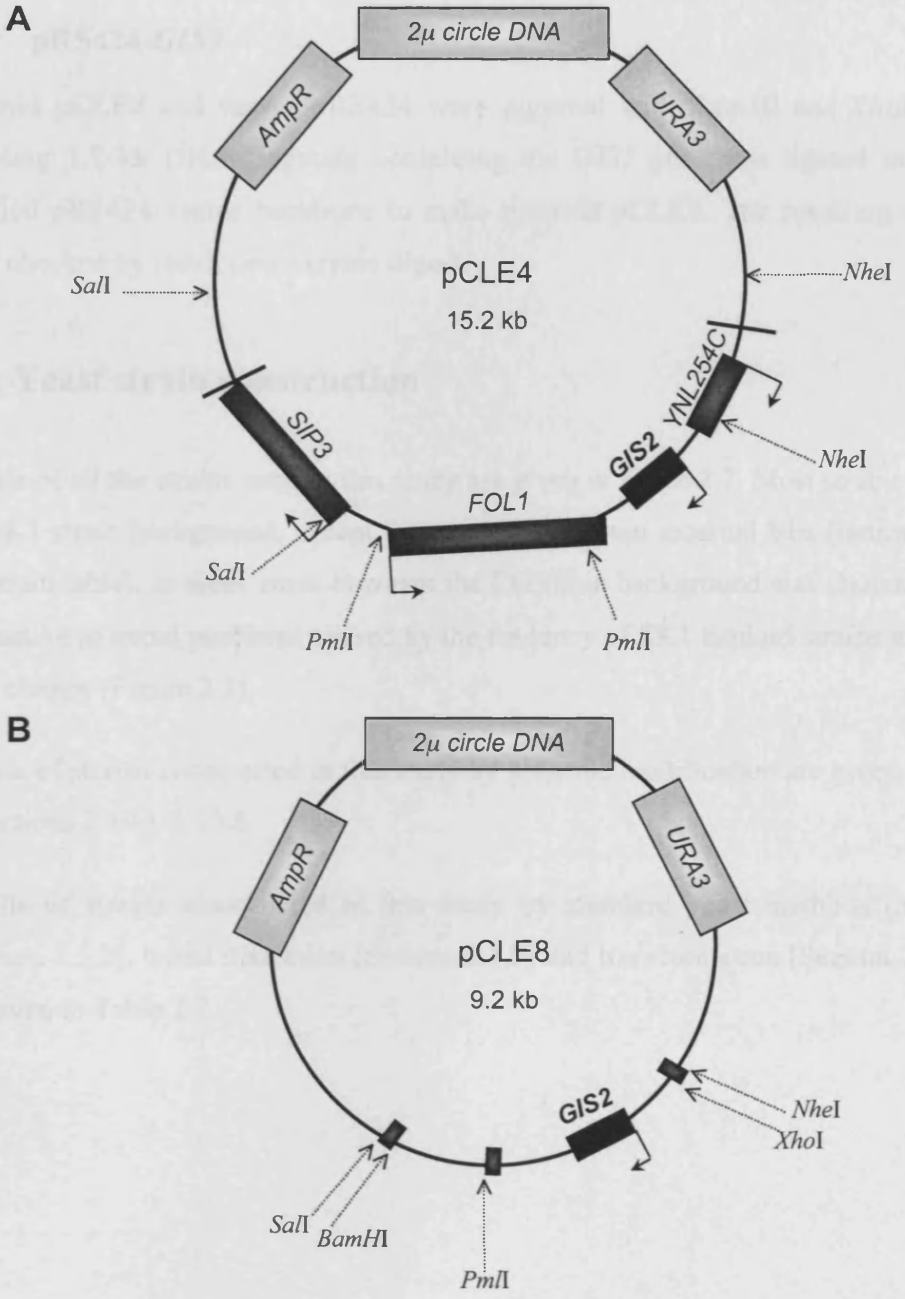

Figure 2.1 Construction of YEp24-*GIS2* (pCLE8). A) A diagram (not to scale) representing plasmid pCLE4. The bold lines (——) represent the boundaries between the YEp24 plasmid backbone and the chromosomal insert in the library plasmid pCLE4. The dark grey boxes represent genes, additional to *GIS2* (black box), found in the chromosomal insert. The arrows (↱) indicate the promoter end of each gene. The relative positions of the restriction enzyme sites (*Nhe*I, *Pml*I, *Sal*I) used to make plasmid pCLE8 are shown. **B)** A diagram (not to scale) representing plasmid pCLE8. The small dark gray boxes represent remaining (unexpressed) gene sequences. The positions of the remaining *Nhe*I, *Pml*I and *Sal*I restriction enzyme sites in pCLE8 are shown. The positions of the *Bam*HI and *Xho*I restriction enzyme sites used to generate pCLE9 are also shown.

2.9.3 pRS424-*GIS2*

Plasmid pCLE8 and vector pRS424 were digested with *Bam*HI and *Xho*I. The resulting 1.7 kb DNA fragment containing the *GIS2* gene was ligated into the purified pRS424 vector backbone to make plasmid pCLE9. The resulting clones were checked by restriction enzyme digest.

2.10 Yeast strain construction

Details of all the strains used in this study are given in Table 2.7. Most strains are of the SK1 strain background, except for some strains from external labs (indicated in the strain table). In some cases however the CG strain background was chosen as an alternative to avoid problems caused by the tendency of SK1 haploid strains to form tight clumps (Figure 2.2).

Details of strains constructed in this study by genomic modification are given below in Sections 2.10.1-2.10.8.

Details of strains constructed in this study by standard yeast methods (mating [Section 2.3.2], tetrad dissection [Section 2.3.3] and transformation [Section 2.3.9]) are given in Table 2.7.

Table 2.7 Yeast strains used in this study

Name	Genotype	Reference/Source
Cha Lab Stocks		
CY3217 [a]	*MAT***a** *ade2-1 leu2-3,112 his3-11,15 trp1-1 ura3-1 can1-100 ORC2-9myc::TRP1*	Marco Foiani
CY5677 [a]	*MAT***a** *ade2-1 leu2-3,112 his3-11,15 trp1-1 ura3-1 can1-100 pol2::POL2-3HA::LEU2*	Marco Foiani
JCY408	*MAT***a** *ho::hisG lys2 ura3 leu2::hisG his4 MEC1::mec1-kd sml1Δ::hphMX4*	
NHY30	*MAT***a** *ho::LYS2 lys2 ura3 leu2::hisG top2-1*	
NHY371	*MATα ho::LYS2 lys2 ura3 arg4 ycg1-2::KanMx4*	Doug Koshland
NHY372	*MATα ho::LYS2 lys2 ura3 leu2 arg4 esp1-1*	Doug Koshland
RCY298	*MAT***a** *ho::hisG lys2 ura3 leu2::hisG his4 sml1Δ::hphMX4*	
RCY308	*MAT***a** *ho::hisG lys2 ura3 leu2::hisG his4 sml1Δ::hphMX4 mec1Δ::LEU2*	
RCY313 [b]	*MAT***a** *ade8*	
RCY314 [b]	*MATα ade8*	
RCY315	*MATα ho::hisG lys2 ura3 leu2::hisG his4 arg4 sml1Δ::hphMX4 mec1Δ::LEU2*	
RCY406	*MAT***a** *ho::LYS2 lys2 ura3 leu2::hisG his4*	
RCY415	*MAT***a** *ho::LYS2 lys2 ura3 leu2::hisG his4 ade2::LK arg4::mec1-4-KanMX4 mec1Δ::LEU2*	
RCY416	*MATα ho::LYS2 lys2 ura3 leu2::hisG his4 ade2::LK arg4::mec1-4-KanMX4 mec1Δ::LEU2*	
RCY426	*MAT***a** *ho::LYS2 lys2 ura3 leu2::hisG his4 ade2::LK arg4::mec1-40-KanMX4 mec1Δ::LEU2*	
RCY483	*MAT***a** *ho::LYS2 lys2 ura3 leu2::hisG his4 ade2::LK arg4::MEC1-KanMX4 mec1Δ::LEU2*	
RCY620	*MAT***a** *ho::LYS2 lys2 ura3 leu2::hisG his4 ade2::LK arg4 mec1-4-ADE2*	
RCY1652	*MAT***a** *ho::LYS2 lys2 ura3 leu2::hisG his4 arg4*	
RCY1710	*MAT***a** *ho::LYS2 lys2 ura3 leu2::hisG his4 arg4::mec1-4-KanMX4 mec1Δ::LEU2 3MYC-SML1*	RCY416 x CEY96
RCY2026	*MATα ho::LYS2 lys2 ura3 leu2::hisG his4 trp1::hisG arg4 tel1Δ::hphMX4*	

Name	Genotype	Reference/Source
RCY2446	*MATα ho::LYS2 lys2 ura3 leu2::hisG his4 trp1::hisG arg4*	
RCY2447	*MAT***a** *ho::LYS2 lys2 ura3 leu2::hisG his4 trp1::hisG arg4*	
RCY2458	*MAT***a**/*MATα ho::LYS2/ho::LYS2 lys2/lys2 ura3/ura3 leu2::hisG/leu2::hisG*	
RCY2459	*MAT***a** *ho::LYS2 lys2 ura3 leu2::hisG*	
YLL476.34/2C [a]	*MAT***a** *ade2-1 leu2-3,112 his3-11,15 trp1-1 ura3-1 can1-100 MEC1-MYC18::LEU2::mec1*	Maria Pia Longhese
Johnston Lab Stocks		
CG378 [c]	*MAT***a** *can1 ade5-1 leu2-3,112 trp1-289 ura3-52*	
CLF25-2A [d]	*MAT***a** *leu2 ura3 trp1 ade5 dbf2-2*	
J2-22 [d]	*MAT***a** *ura1 or ura3 lys2 leu2 his7 trp1 dbf4-1*	
K1993 [a]	*MAT***a** *ura3 leu2 trp1 his3 cdc15-2*	
Strains constructed in this study		
CEY8	*MAT***a** *ho::LYS2 lys2 ura3 leu2::hisG orc1::ORC1-HA-URA3*	
CEY18	*MAT***a** *ho::LYS2 lys2 ura3 leu2::hisG DPB3-3HA-hph*	
CEY21	*MAT***a** *ho::LYS2 lys2 ura3 leu2::hisG rnr1::HA-RNR1-KanMX*	
CEY22	*MATα ho::LYS2 lys2 ura3 leu2::hisG rnr1::HA-RNR1-KanMX*	
CEY81	*MAT***a** *ho::LYS2 lys2 ura3 leu2::hisG arg4::mec1-4-KanMX4 mec1Δ::LEU2 DPB3-3HA-hph*	from CEY18 x RCY416
CEY82	*MAT***a** *ho::LYS2 lys2 ura3 leu2::hisG his4 arg4::mec1-4-KanMX4 mec1Δ::LEU2 rnr1::HA-RNR1-KanMX*	from CEY22 x RCY415
CEY96	*MAT***a** *ho::LYS2 lys2 ura3 leu2::hisG 3MYC-SML1*	
CEY131	RCY426 [YEp24]	
CEY149	RCY426 [pCLE5-*MEC1*]	

Name	Genotype	Reference/Source
CEY151	RCY426 [pCLE8-*GIS2*]	
CEY155	RCY415 [YEp24]	
CEY157	RCY483 [YEp24]	
CEY159	RCY415 [pCLE5-*MEC1*]	
CEY161	RCY483 [pCLE5-*MEC1*]	
CEY163	RCY415 [pCLE8-*GIS2*]	
CEY165	RCY483 [pCLE8-*GIS2*]	
CEY167	RCY620 [YEp24]	
CEY169	RCY1652 [YEp24]	
CEY171	RCY620 [pCLE5-*MEC1*]	
CEY173	RCY1652 [pCLE5-*MEC1*]	
CEY175	RCY620 [pCLE8-*GIS2*]	
CEY177	RCY1652 [pCLE8-*GIS2*]	
CEY187	*MAT***a**/*MATα ho::LYS2/ho::LYS2 lys2/lys2 ura3/ura3 leu2::hisG/leu2::hisG his4/his4 trp1::hisG/trp1::hisG arg4/arg4*	RCY2446 x RCY2447
CEY189	*MAT***a**/*MATα ho::hisG/ho::LYS2 lys2/lys2 ura3/ura3 leu2::hisG/leu2::hisG his4/his4 TRP1/ trp1::hisG ARG4/arg4 sml1Δ::hphMX4/ SML1 mec1Δ::LEU2/MEC1[pMK9-MEC1]*	from RCY308 x RCY2446

Name	Genotype	Reference/Source
CEY191	*MAT***a**/*MATα ho::hisG/ho::LYS2 lys2/lys2 ura3/ura3 leu2::hisG/leu2::hisG his4/his4 TRP/trp1::hisG ARG4/arg4 sml1Δ::hphMX4/SML1 MEC1::mec1-kd/MEC1[pMK9-MEC1]*	from JCY408 x RCY2446
CEY198	RCY1710 [YEp24]	
CEY202	RCY1710 [pCLE8-*GIS2*]	
CEY208	*MAT***a** *ho::LYS2 lys2 ura3 leu2::hisG his4 trp1::hisG arg4 gis2Δ::TRP1*	
CEY209	*MATα ho::LYS2 lys2 ura3 leu2::hisG his4 trp1::hisG arg4 gis2Δ::TRP1*	
CEY226	CEY82 [YEp24]	
CEY230	CEY82 [pCLE8-*GIS2*]	
CEY256	*MAT***a** *ho::hisG lys2 ura3 leu2::hisG his4 trp1::hisG mec1Δ::LEU2* [pMK9-*MEC1*] [pCLE9-*GIS2*]	from CEY189
CEY257	*MATα ho::hisG lys2 ura3 leu2::hisG his4 trp1::hisG mec1Δ::LEU2* [pMK9-*MEC1*] [pCLE9-*GIS2*]	from CEY189
CEY258	*MAT***a** *ho::hisG lys2 ura3 leu2::hisG his4 trp1::hisG* [pMK9-*MEC1*] [pCLE9-*GIS2*]	from CEY189
CEY259	*MATα ho::hisG lys2 ura3 leu2::hisG his4 trp1::hisG arg4 MEC1::mec1-kd* [pMK9-*MEC1*] [pCLE9-*GIS2*]	from CEY191
CEY260	*MAT***a** *ho::hisG lys2 ura3 leu2::hisG his4 trp1::hisG arg4 MEC1::mec1-kd* [pMK9-*MEC1*] [pCLE9-*GIS2*]	from CEY191
CEY261	*MATα ho::hisG lys2 ura3 leu2::hisG his4 trp1::hisG arg4* [pMK9-*MEC1*] [pCLE9-*GIS2*]	from CEY191
CEY266	*MATα ho::LYS2 lys2 ura3 leu2::hisG hisx trp1::hisG arg4::mec1-4-KanMX4 mec1Δ::LEU2*	from RCY415 x RCY2446
CEY267	*MAT***a** *ho::LYS2 lys2 ura3 leu2::hisG his4 trp1::hisG arg4::mec1-4-KanMX4 mec1Δ::LEU2*	from RCY415 x RCY2447
CEY268	*MAT***a** *ho::LYS2 lys2 ura3,leu2::hisG his4 trp1::hisG arg4::MEC1-KanMX4 mec1Δ::LEU2*	from RCY483 x RCY2448
CEY269	*MATα ho::LYS2 lys2 ura3 leu2::hisG his4 trp1::hisG arg4::MEC1-KanMX4 mec1Δ::LEU2*	from RCY483 x RCY2449
CEY293	*MAT***a** *ho::LYS2 lys2 ura3 leu2::hisG his4 arg4::MEC1-KanMX4 mec1Δ::LEU2 rnr1::HA-RNR1-KanMX*	from CEY22 x CEY483
CEY301	*MAT***a** *ho::LYS2 lys2 ura3 leu2::hisG his4 trp1::hisG arg4::mec1-4-KanMX4 mec1Δ::LEU2 gis2Δ::TRP*	from CEY208 x CEY266
CEY309	CEY267 [YEp24]	
CEY310	CEY267 [pCLE8-*GIS2*]	

Name	Genotype	Reference/Source
CEY311	CEY268 [YEp24]	
CEY322	CEY208 [YEp24]	
CEY330 [c]	*MAT***a** *can1 ade5-1 leu2-3,112 trp1-289 ura3-52 GIS2-GFP-TRP1*	
CEY334 [c]	*MAT***a** *can1 ade5-1 leu2-3,112 trp1-289 ura3-52 gis2Δ::TRP1*	
CEY342	*MAT***a** *ho::LYS2 lys2 ura3 leu2::hisG his4 arg4::MEC1-KanMX4 mec1Δ::LEU2*	from RCY483 x RCY2026
CEY346	*MAT***a** *ho::LYS2 lys2 ura3 leu2::hisG his4 arg4::mec1-4-KanMX mec1Δ::LEU2*	from RCY415 x RCY2026
CEY347	*MAT***a** *ho::LYS2 lys2 ura3 leu2::hisG his4 arg4::mec1-4-KanMX mec1Δ::LEU2 tel1Δ::hphMX4*	from RCY415 x RCY2026
CEY349	*MAT***a** *ho::LYS2 lys2 ura3 leu2::hisG his4 arg4::MEC1-KanMX4 mec1Δ::LEU2 3MYC-SML1*	from CEY96 x CEY269
CEY354 [c]	CG378 [YEp24]	
CEY355 [c]	CG378 [pCLE8-*GIS2*]	
CEY358	CEY268 [pCLE8-*GIS2*]	
CEY360	*MAT***a** *ho::LYS2 lys2 ura3 leu2::hisG his4 arg4::MEC1-KanMX4 mec1Δ::LEU2 tel1Δ::hphMX4*	from RCY483 x RCY2026
CEY364	*MAT***a** *ho::LYS2 lys2 ura3 leu2::hisG his4 trp1::hisG arg4 dun1Δ::TRP1*	
CEY368	CEY360 [YEp24]	
CEY371	CEY346 [YEp24]	
CEY373	CEY346 [pCLE8-*GIS2*]	
CEY374	CEY346 [pCLE11-*RNR1*]	
CEY377	CEY347 [YEp24]	
CEY379	CEY347 [pCLE8-*GIS2*]	
CEY380	CEY347 [pCLE11-*RNR1*]	
CEY382	CEY342 [YEp24]	
CEY414	CEY349 [YEp24]	

Name	Genotype	Reference/Source
CEY417	CEY349 [pCLE8-*GIS2*]	
CEY430	*MATα ho::LYS2 lys2 ura3 leu2::hisG his4 ade2::LK trp1::hisG arg4*	from RCY483 x RCY2446
CEY459	*MATα ho::LYS2 lys2 ura3 leu2::hisG his4 trp1::hisG arg4 ras2Δ::TRP1*	
CEY461	*MAT***a** *ho::LYS2 lys2 ura3 leu2::hisG his4 arg4*	from RCY620 x RCY2446
CEY468	*MAT***a** *ho::LYS2 lys2 ura3 leu2::hisG his4 ade2::LK arg4 mec1-4-ADE2*	from RCY620 x RCY2446
CEY471	*MATα ho::LYS2 lys2 ura3 leu2::hisG his4 ade2::LK trp1::hisG arg4 mec1-4-ADE2*	from RCY620 x RCY2446
CEY473 [c]	CEY334 [YEp24]	
CEY477	*MAT***a** *ho::LYS2 lys2 ura3 leu2::hisG his4 arg4::mec1-4-KanMX4 mec1Δ::LEU2*	from RCY415 x RCY2446
CEY480	*MAT***a** *ho::LYS2 lys2 ura3 leu2::hisG his4 arg4::MEC1-KanMX4 mec1Δ::LEU2*	from RCY483 x RCY2446
CEY482	RCY415 [pCLE11-*RNR1*]	
CEY511	*MAT***a** *ho::LYS2 lys2 ura3 leu2::hisG his4 trp1::hisG arg4::mec1-4-KanMX4 mec1Δ::LEU2 ras2Δ::TRP1*	from CEY267 x CEY459
CEY514	*MAT***a** *ho::LYS2 lys2 ura3 leu2::hisG his4 trp1::hisG arg4::MEC1-KanMX4 mec1Δ::LEU2 ras2Δ::TRP1*	from CEY268 x CEY459
CEY522	CEY461 [YEp24]	
CEY526	CEY486 [YEp24]	
CEY530	CEY490 [YEp24]	
CEY537	*MAT***a** *ho::LYS2 lys2 ura3 leu2::hisG his4 ade2::LK trp1::hisG arg4 dun1Δ::TRP1*	from CEY364 x CEY430
CEY542	RCY308 [YEp24]	
CEY544	RCY308 [pCLE5-*MEC1*]	
CEY545	RCY308 [pCLE8-*GIS2*]	
CEY547	RCY308 [pCLE11-*RNR1*]	
CEY565	CEY480 [YEp24]	
CEY575	CEY477 [YEp24]	

Name	Genotype	Reference/Source
CEY585	CEY511 [YEp24]	
CEY595	CEY514 [YEp24]	
CEY650	*MAT***a** *ho::LYS2 lys2 ura3 leu2::hisG his4 ade2::LK trp1::hisG arg4 dun1Δ::TRP1 mec1-4-ADE2*	from CEY537 x CEY471
CEY661	CEY480 [pCLE8-GIS2]	
CEY663	CEY514 [pCLE8-GIS2]	
CEY665	CEY477 [pCLE8-GIS2]	
CEY667	CEY511 [pCLE8-GIS2]	
CEY685	CEY364 [YEp24]	
CEY687	CEY364 [pCLE8-*GIS2*]	
CEY689	CEY468 [YEp24]	
CEY691	CEY468 [pCLE8-*GIS2*]	
CEY693	CEY650 [YEp24]	
CEY695	CEY650 [pCLE8-*GIS2*]	
CEY721	*MAT***a** *ho::LYS2 lys2 ura3 leu2::hisG his4 trp1::hisG arg4::mec1-4-KanMX4 mec1Δ::LEU2 gis2Δ::TRP ras2Δ::TRP1*	from CEY209 x CEY511
CEY723	*MAT***a** *ho::LYS2 lys2 ura3 leu2::hisG his4 trp1::hisG arg4::MEC1-KanMX4 mec1Δ::LEU2 gis2Δ::TRP*	from CEY208 x CEY269
CEY725 [d]	CLF25-2A [YEp24]	
CEY727 [d]	CLF25-2A [pCLE8-*GIS2*]	
CEY729 [a]	K1993 [YEp24]	
CEY731 [a]	K1993 [pCLE8-*GIS2*]	
CEY733	NHY371 [YEp24]	
CEY734	NHY371 [pCLE8-*GIS2*]	
CEY735	NHY30 [YEp24]	

Name	Genotype	Reference/Source
CEY736	NHY30 [pCLE8-*GIS2*]	
CEY737	NHY372 [YEp24]	
CEY738	NHY372 [pCLE8-*GIS2*]	
CEY739 [d]	J2-22 [YEp24]	
CEY740 [d]	J2-22 [pCLE8-*GIS2*]	
CEY741	CEY293 [YEp24]	
CEY743	CEY293 [pCLE8]	

[a] W303 strain background

[b] S288c strain background

[c] CG strain background

[d] mixed strain background

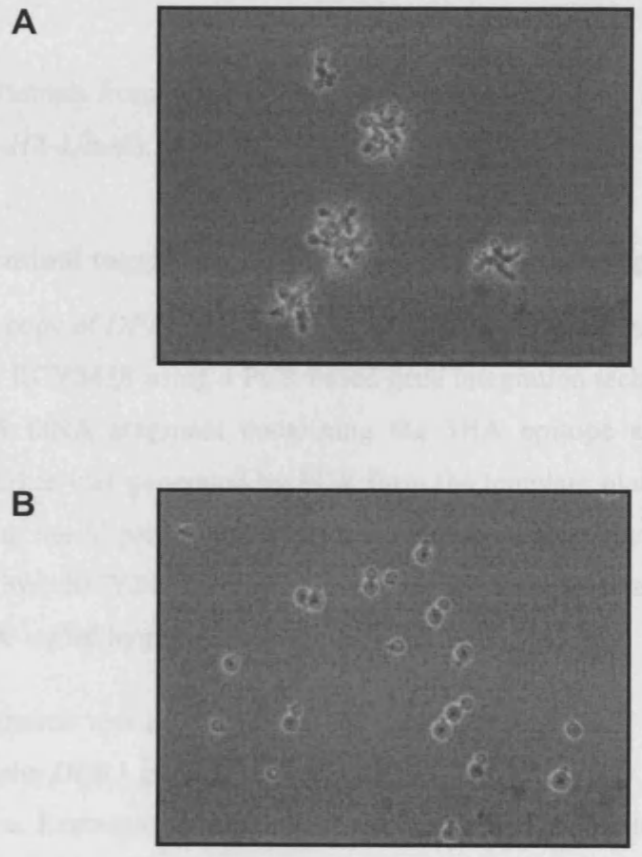

Figure 2.2 Haploid SK1 and CG *S. cerevisiae* cells. Images of log phase cultures of an SK1 haploid strain (RCY2459) **(A)** and a CG haploid strain (CG378) **(B)** viewed under a phase-contrast microscope.

2.10.1 Integration of an *ORC1-HA* containing plasmid

To construct strain CEY8, the integrative plasmid p306-*ORC1-HA* was digested with *Xba*I and transformed into RCY2458 (SK1 wild type diploid). Stable integrants were selected on SD-URA media. Expression of Orc1-HA was confirmed by Western blot analysis.

Dissection of tetrads from diploids that expressed Orc1-HA gave rise to strain CEY8 (*orc1::ORC1-HA-URA3*).

2.10.2 C-terminal tagging of *DPB3* with a 3HA epitope tag

The genomic copy of *DPB3* was tagged with a 3HA epitope tag in the SK1 wild type diploid strain RCY2458 using a PCR-based gene integration technique (Longtine *et al.*, 1998). A DNA fragment containing the 3HA epitope and a hygromycin resistance marker was generated by PCR from the template plasmid pFA6a-3HA-hphMX4 using the 5' primer P590 and the 3' primer P591. The PCR product was transformed into RCY2458 and stable integrants were selected on YPD media containing 300 μg/ml hygromycin B.

Correct integration was confirmed by colony PCR using the 5' primer P592 with homology to the *DPB3* gene the 3' primer P521 with homology to the hygromycin resistance gene. Expression of Dpb3-3HA was confirmed by Western blot analysis.

Dissection of tetrads from diploids that expressed Dpb3-3HA gave rise to strain CEY18 (*DPB3-3HA-hphMX4*).

2.10.3 Integration of an *HA-RNR1* containing plasmid

To construct strain CEY21, the integrative plasmid pMH726 was digested with *Mfe*I and transformed into RCY2458 (SK1 wild type diploid). Stable integrants were selected on YPD media containing 200 μg/ml G418. Expression of HA-Rnr1 was confirmed by Western blot analysis.

Dissection of tetrads from diploids that expressed Rnr1-HA gave rise to strains CEY21 (*MAT***a** *rnr1::HA-RNR1-KanMX4*)and CEY22 (*MATα rnr1::HA-RNR1-KanMX4*).

2.10.4 N-terminal tagging of *SML1* with a 3MYC epitope tag

Strain CEY96 was made by tagging the genomic copy of *SML1* with a 3MYC epitope tag in the SK1 wild type haploid strain RCY2459 using a PCR-based gene integration technique (Schneider *et al.*, 1995). A DNA fragment containing *two* copies of the 3MYC epitope flanking a *URA3* marker gene was generated by PCR from the template plasmid pMPY-3xMYC using the 5' primer P593 and the 3' primer P594. The PCR product was transformed into RCY2459 and stable integrants were selected on SD-URA media.

Correct integration was confirmed by colony PCR using the 5' primer P596 with homology to the region upstream of the *SML1* locus and the 3' primer P595 with homology to the *SML1* gene. The expected PCR product size was 1.8 kb. Correct integrants were grown overnight in a 2 ml liquid YPD culture and then plated onto SC agar containing 5'FOA to select for recombinants that had excised the *URA3* marker. Correct recombination was confirmed by colony PCR as above, but with an expected PCR product of 532 bp.

Expression of 3MYC-Sml1 was tested for by Western blot.

The *3MYC-SML1* strain could not rescue the lethality of a *mec1Δ* strain and the expected cell cycle-dependent fluctuation in 3MYC-Sml1 protein levels was seen (Zhao *et al.*, 2001) (Figure 2.3). Together these observations showed that the 3MYC-Sml1 protein was functional.

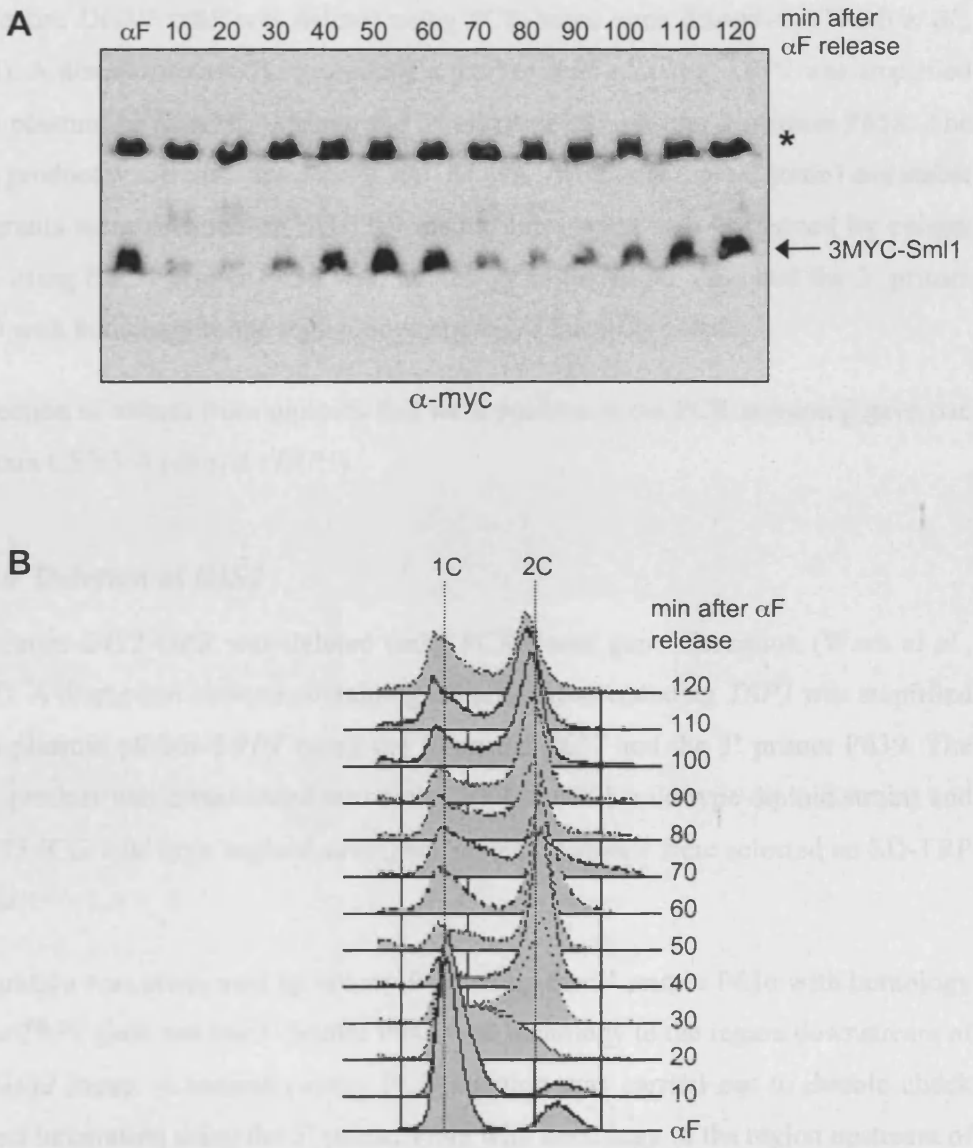

Figure 2.3 Cell cycle-dependent fluctuations in 3MYC-Sml1 protein levels. A log phase culture of strain CEY96, grown in YPD at 30°C, was arrested in G1 with αF for three hours. Cells were released into fresh YPD at 30°C and samples were taken every ten minutes for protein extraction and FACS analysis. **A)** Proteins were separated on a 15% polyacryamide gel and analysed by Western blot using an anti-MYC antibody. The non-specific band (*) serves as a loading control **B)** FACS analysis shows the distribution of cells in the population with a one cell DNA content, before replication (1C) and with a two cell DNA content, after replication (2C). Each FACS profile represents 50,000 counts.

2.10.5 Deletion of *DUN1*

The entire *DUN1* ORF was deleted using PCR-based gene disruption (Wach *et al.*, 1994). A disruption cassette containing a marker gene encoding *TRP1* was amplified from plasmid pFA6a-*TRP1* using the 5' primer P657 and the 3' primer P658. The PCR product was transformed into CEY187 (SK1 wild type diploid strain) and stable integrants were selected on SD-TRP media. Integration was confirmed by colony PCR using the 5' primer P636 with homology to the *TRP1* gene and the 3' primer P660 with homology to the region downstream of the *DUN1* locus.

Dissection of tetrads from diploids that were positive in the PCR screening gave rise to strain CEY364 (*dun1Δ::TRP1*).

2.10.6 Deletion of *GIS2*

The entire *GIS2* ORF was deleted using PCR-based gene disruption (Wach *et al.*, 1994). A disruption cassette containing a marker gene encoding *TRP1* was amplified from plasmid pFA6a-*TRP1* using the 5' primer P637 and the 3' primer P639. The PCR product was transformed into both CEY187 (SK1 wild type diploid strain) and CG378 (CG wild type haploid strain) and stable integrants were selected on SD-TRP media.

Integration was confirmed by colony PCR using the 5' primer P636 with homology to the *TRP1* gene and the 3' primer P643 with homology to the region downstream of the *GIS2* locus. A second colony PCR reaction was carried out to double check correct integration using the 5' primer P648 with homology to the region upstream of the *GIS2* locus and the 3' primer P664 with homology to the *TRP1* gene.

Strain CEY334 (*gis2Δ::TRP1*) gave a positive signal in both PCR screening reactions.

Dissection of tetrads from SK1 diploids that were positive in both PCR screening reactions gave rise to strains CEY208 (*MAT***a** *gis2Δ::TRP1*) and CEY209 (*MATα gis2Δ::TRP1*).

2.10.7 C-terminal tagging of *GIS2* with GFP

Strain CEY330 was made by tagging the genomic copy of *GIS2* in CG378 (CG wild type haploid strain) with the *GFP* gene using a PCR-based gene integration technique (Longtine *et al.*, 1998). A DNA fragment containing the *GFP* gene and the *TRP1* marker gene was generated by PCR from the template plasmid pFA6a-*GFP-TRP1* using the 5' primer P638 and the 3' primer P639. The PCR product was transformed into CG378 and stable integrants were selected on SD-TRP media.

Correct integration was confirmed by colony PCR using the 5' primer P636 with homology to the *TRP1* gene the 3' primer P643 with homology to the region downstream of the *GIS2* locus.

2.10.8 Deletion of *RAS2*

The entire *RAS2* ORF was deleted using PCR-based gene disruption (Wach *et al.*, 1994). A disruption cassette containing a marker gene encoding *TRP1* was amplified from plasmid pFA6a-*TRP1* using the 5' primer P676 and the 3' primer P677. The PCR product was transformed into CEY187 (SK1 wild type diploid strain) and stable integrants were selected on SD-TRP media. Integration was confirmed by colony PCR using the 5' primer P636 with homology to the *TRP1* gene and the 3' primer P678 with homology to the region downstream of the *RAS2* locus.

Dissection of tetrads from diploids that were positive in the PCR screening gave rise to strain CEY459 (*ras2Δ::TRP1*).

Chapter 3

The role of Mec1 in regulating dNTP availability during DNA replication

3.1 Introduction

The current thinking is that bulk dNTP synthesis in *S. cerevisiae* takes place in the cytoplasm (Yao *et al.*, 2003), and that the dNTP pool is freely diffusible between the cytoplasm and the nucleus (Reichard, 1988). In addition, it is possible that a proportion of dNTPs are synthesised locally in the nucleus and directly channelled to the replication fork. This is known to happen in prokaryotes (Mathews, 1993), and has also been suggested to occur in mammalian cells (Prem veer Reddy & Pardee, 1980). *S. cerevisiae* Mec1 is involved both in the regulation of dNTP synthesis via Sml1 and in promoting replication fork stability under conditions of replication stress (Sections 1.4.4 and 1.5.3). Thermal inactivation of temperature sensitive *mec1* alleles, *mec1-4* or *mec1-40*, causes chromosomal breaks specifically in replication slow zones (Section 1.2.3). Deleting *SML1* prevents these chromosomal breaks, presumably by increasing dNTP levels (Cha & Kleckner, 2002). In wild type cells replication forks progress more slowly through *RSZs* than other regions of the genome (Cha & Kleckner, 2002). It is possible that in a wild type cell Mec1 promotes increased dNTP synthesis specifically at *RSZs*. This increased dNTP synthesis would be coupled to increased polymerase processivity in these regions, so enabling DNA replication to be completed. In this case the phenotype of prolonged replication fork stalling and chromosomal breakage seen in *mec1-4* and *mec1-40* cells at the restrictive temperature would be due to a defect in the upregulation of local dNTP synthesis at *RSZs*. If Mec1 is required in this way for regulating local dNTP synthesis at the replication fork then Mec1, RNR, and Sml1 should associate with the replication fork, either throughout S-phase or specifically at *RSZs*. A

chromatin immunoprecipitation (ChIP) assay was set up to test this hypothesis by looking to see if these proteins were chromatin-associated during S-phase.

3.2 Results

3.2.1 Optimisation of the ChIP assay

The assay was set up to analyse the temporal association of proteins with five specific fragments within a region of chromosome III, spanning from the replication origin *ARS305* through the downstream *RSZ* (Figure 3.1). *ARS305* is a well-characterised, early-firing replication origin (Reynolds *et al.*, 1989). Therefore, synchronous replication fork progression should be observed after release from α-factor. Similar assays have been used previously to examine the timing of chromatin association of different replication proteins (Kamimura *et al.*, 2001; Lucca *et al.*, 2004).

The first step in setting up the ChIP assay was to select five primer pairs that would amplify PCR products from genomic DNA at the desired chromosomal locations and with similar efficiency in a multiplex reaction. The sequences for three primer pairs were taken from Kamimura *et al.* (2001) and the sequences for the other primer pairs were designed for this study. All five PCR products could be successfully amplified in a multiplex reaction, as shown by the whole cell extract (WCE) lanes in Figures 3.2-3.5.

The next step in setting up the ChIP assay was to test that the anti-HA and anti-MYC antibodies worked for the ChIP procedure. A subunit of the ORC complex was chosen to test this as *S. cerevisiae* ORC binds specifically to replication origins throughout the cell cycle (Liang & Stillman, 1997). In this ChIP assay a PCR fragment corresponding to the *ARS305* location should be specifically generated after immunoprecipitation of a tagged ORC subunit cross-linked to DNA. To test this, a wild type strain (RCY2459) and a strain expressing Orc1-HA (CEY8) were grown to mid-log phase in YPD at 30°C.

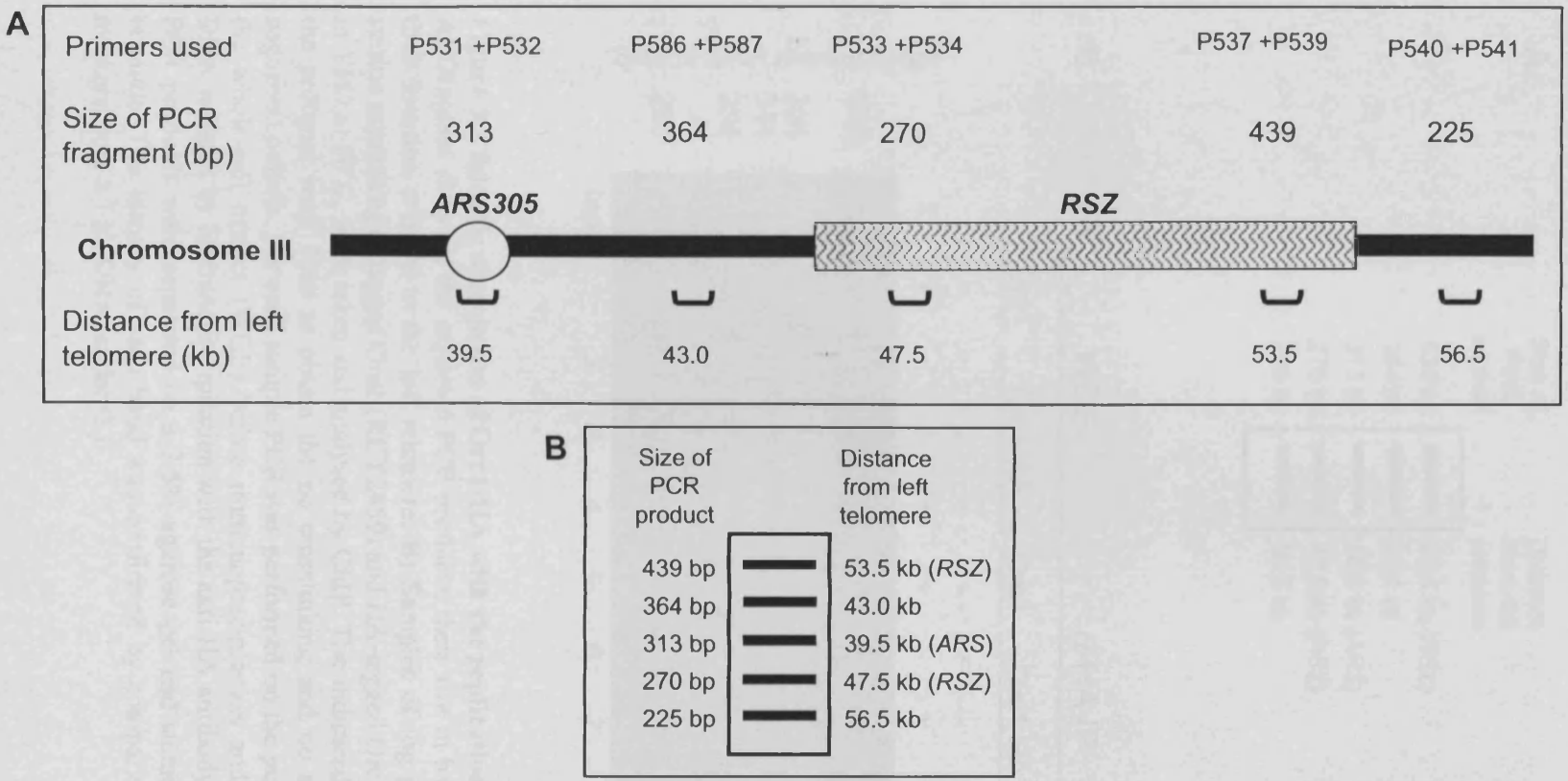

Figure 3.1 Schematic of a section of chromosome III showing the location of the PCR fragments used in the ChIP assay. **A)** Five sets of primers were used to scan a region spanning 17 kb from the early firing replication origin *ARS305* through the downstream *RSZ*. The distance from the left telomere, the size of the PCR fragment amplified at each location and the name of the primers used are shown. **B)** Diagram of the expected PCR products, amplified from genomic DNA using the primers specified, anaylsed on a 2.5% agarose gel.

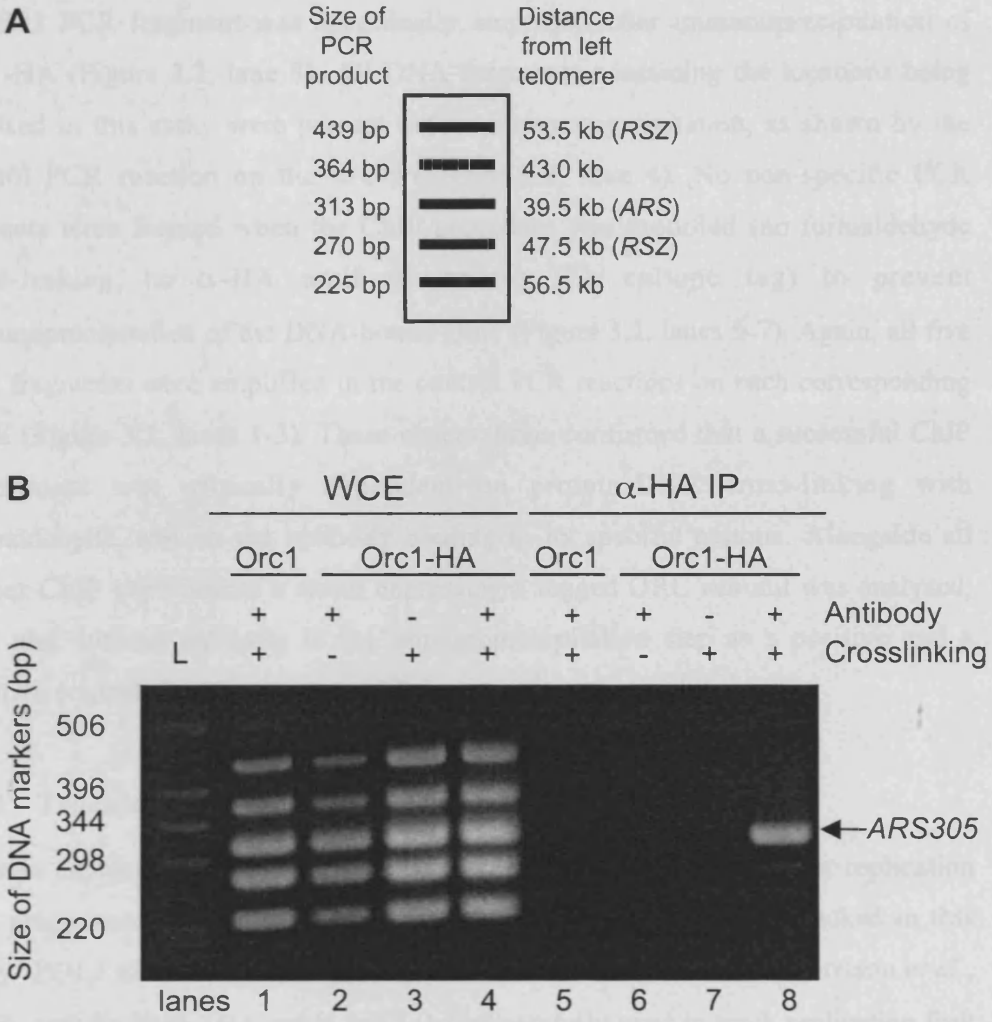

Figure 3.2 Specific association of Orc1-HA with the replication origin *ARS305*. **A)** Diagram showing the expected PCR products, their size in base pairs (bp) and their location relative to the left telomere. **B)** Samples of log phase cultures of strains expressing untagged Orc1 (RCY2459) and HA-tagged Orc1 (CEY8), grown in YPD at 30°C, were taken and analysed by ChIP. The indicated modifications to the protocol were done to obtain the no crosslinking and no anti-HA antibody negative controls. For each sample PCR was performed on the purified DNA from the whole-cell extract (WCE) before immunoprecipitation and on the purified DNA isolated by immunoprecipitation with the anti-HA antibody (α-HA IP). The PCR products were separated on a 2.5% agarose gel and stained with ethidium bromide. The identity of each band was confirmed by comparison to DNA size markers from a 1 kb DNA ladder (L).

Samples of these cultures were analysed by ChIP (Section 2.7). As expected, the *ARS305* PCR fragment was specifically amplified after immunoprecipitation of Orc1-HA (Figure 3.2, lane 8). All DNA fragments containing the locations being assessed in this assay were present before immunoprecipitation, as shown by the control PCR reaction on the WCE (Figure 3.2, lane 4). No non-specific PCR products were formed when the ChIP procedure was modified (no formaldehyde cross-linking, no α-HA antibody or no HA epitope tag) to prevent immunoprecipitation of the DNA-bound Orc1 (Figure 3.2, lanes 5-7). Again, all five PCR fragments were amplified in the control PCR reactions on each corresponding WCE (Figure 3.2, lanes 1-3). These observations confirmed that a successful ChIP experiment was critically dependent on protein-DNA cross-linking with formaldehyde, and on the antibody binding to its specific epitope. Alongside all further ChIP experiments a strain expressing a tagged ORC subunit was analysed, with and without antibody in the immunoprecipitation step as a positive and a negative control respectively.

3.2.2 Tracking replication fork progression in wild type cells

A strain expressing HA-tagged Pol2 (CY5677) was used to test whether replication fork progression from *ARS305* into the downstream *RSZ* could be tracked in this assay. *POL2* encodes the catalytic subunit of DNA polymerase ε (Morrison *et al.*, 1990), and the Pol2-3HA strain has been successfully used to track replication fork progression previously in a ChIP assay (Lucca *et al.*, 2004). The *POL2-3HA* strain was grown to mid-log phase in YPD at 30°C and arrested in G1 with α-factor for two and a half hours. The culture was then shifted to 18°C for a further hour, before the cells were released into either fresh YPD or 100 mM HU at 18°C (Figure 3.3A). This experiment was done at the lower temperature of 18°C to slow down replication fork progression and therefore improve the temporal resolution of the assay. Half of the culture was released from α-factor into fresh YPD to track replication fork progression under normal replication conditions. The other half was released from α-factor into 100 mM HU as a control to track replication fork progression under a condition where replication forks are expected to stall close to replication origins

(Koc *et al.*, 2004). Samples for ChIP analysis were taken periodically (as shown in Figure 3.3C) as cells progressed through a synchronous S-phase.

The positive and negative controls using the Orc1-HA strain were successful (Figure 3.3C, lanes 11 and 12), and all five PCR products were amplified from the WCE control of each sample (Figure 3.3C, lanes 3-10). The association of Pol2-3HA with the replication origin *ARS305* was detected 40 minutes after release from α-factor into both YPD and HU (Figure 3.3C, lanes 14 and 18). This is expected, as HU should not disrupt the firing of an early origin such as *ARS305* (Santocanale & Diffley, 1998). Under normal replication conditions association of Pol2-3HA with all downstream regions was seen by 60 minutes after release from α-factor (Figure 3.3C, lane 15). However, the temporal resolution of the assay was not good enough to track the sequential progression of the replication fork through each fragment. In the presence of 100 mM HU, Pol2-3HA could still only be detected at the replication origin and at the region 3.5 kb downstream by 80 minutes after release from α-factor (Figure 3.3C, lane 20). This observation is in accordance with a previous study that analysed DNA replication intermediates formed in the presence of 200 mM HU; at 90 minutes after release from α-factor at 25°C replication forks from early origins had progressed to form a bubbles of about 2-7 kb in length around the replication origin (Santocanale & Diffley, 1998)

3.2.3 Tracking replication fork progression in *arg4::mec1-4* cells

The results presented in the previous section showed that HU-induced replication fork stalling could be detected by this ChIP assay at 18°C (Figure 3.3). However, to test the hypothesis that Mec1 controls local dNTP synthesis specifically required for progression through *RSZs*, more subtle differences in replication fork progression than those caused by HU would need to be detected. For example it would be useful to be able detect the accumulation of replication forks in *RSZs* in the *arg4::mec1-4* strain at the restrictive temperature.

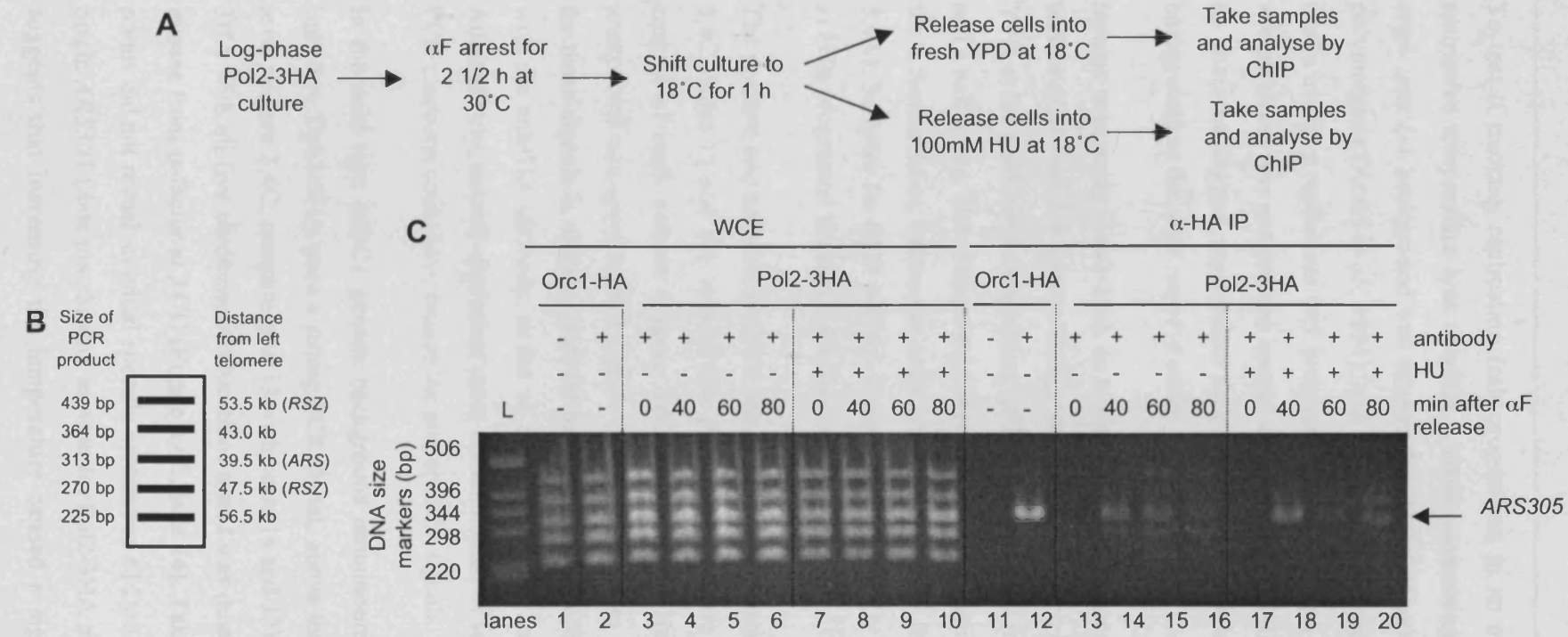

Figure 3.3 Movement of the polymerase ε subunit Pol2 with the replication fork. A) Outline of the experimental procedure. **B)** Diagram showing the expected PCR products, their size in base pairs (bp) and their location relative to the left telomere. **C)** Strains expressing HA-tagged Pol2 (CY5677) and HA-tagged Orc1 (CEY8) were grown in YPD at 30°C. Samples were taken from the log-phase Orc1-HA culture and analysed by ChIP for the positive and negative (no antibody) controls. Samples were taken from the synchronous Pol2-3HA culture at the indicated time points and analysed by ChIP. For each sample PCR was performed on the purified DNA from the whole cell extract (WCE) before immunoprecipitation and on the purified DNA isolated by immunoprecipitation with the anti-HA antibody (α-HA IP). The PCR products were separated on a 2.5% agarose gel and stained with ethidium bromide. The identity of each band was confirmed by comparison to DNA size markers from a 1 kb DNA ladder (L).

To test if tracking replication fork progression in an *arg4::mec1-4* strain at the restrictive temperature was feasible, a strain expressing HA-tagged Dpb3 in the *arg4::mec1-4* background was constructed. Dpb3 encodes the smallest subunit of polymerase ε (Araki *et al.*, 1991), and had been recommended as a good protein to use in tracking replication fork progression (K. Shirahige, personal communication). A new strain was constructed instead of using the Pol2-3HA strain used previously so that the tagged replication fork component would be in the same strain background as the *arg4::mec1-4* strain.

Strains expressing Dpb3-3HA in a wild type *MEC1* genetic background (CEY18) and an *arg4::mec1-4* genetic background (CEY81) were grown to mid-log phase in YPD at the permissive temperature of 23°C and arrested in G1 with α-factor for two and a half hours. The cultures were then shifted to the restrictive temperature of 34°C for a further hour, before the cells were released into fresh YPD at 34°C (Figure 3.4A). Samples for ChIP analysis were taken periodically (as shown in Figure 3.4C) as cells progressed through a synchronous S-phase.

The positive and negative controls using the Orc1-HA strain were successful (Figure 3.4C, lanes 11 and 12), and all five PCR products were amplified from the WCE control of each sample (Figure 3.4C, lanes 3-10). However, there were some unexpected non-specific PCR signals (Figure 3.4C, lanes 12,13 and 17). The reason for these signals is unclear. It could be due to non-specific DNA being precipitated with the anti-HA antibody, as the no antibody control had no non-specific signals. Alternatively, aerosol-dependent cross-contamination of samples when setting up the PCR reactions could have caused the non-specific signals.

In the wild type *MEC1* genetic background immunoprecipitation of DNA cross-linked to Dpb3-3HA gave a strong PCR signal, above the non-specific background level (Figure 3.4C; compare lane 13 with lanes 14 and 15). The association of Dpb3-3HA with all five chromosomal locations tested was detected only 15 minutes after release from α-factor at 34°C (Figure 3.4C, lane 14). Taking samples at earlier time points did not reveal an initial specific association of Dpb3-3HA with the replication origin *ARS305* (data not shown), as seen for Pol2-3HA at 18°C (Figure 3.3C). This suggests that increasing the temperature caused a significant reduction in the

temporal resolution of the assay. Also, the PCR signal from the DNA immunoprecipitated with Dpb3-3HA in the *arg4::mec1-4* cells was much weaker (barely above the non-specific background level) than that from the wild type *MEC1* cells (Figure 3.4C, compare lanes 13-16 with 17-20). This was despite the DNA having been isolated from a similar number of cells, as shown by the PCR signal from each WCE (Figure 3.4C, lanes 3-10). The reasons for this are unclear, but the weak signal could indicate a reduced stability of the replication fork in the absence of Mec1 function. Alternatively *ARS305* might fire with reduced efficiency in *arg4::mec1-4* cells at the restrictive temperature, although there are no published data to suggest that the firing efficiency of *ARS305* is affected in the absence of Mec1 function.

3.2.4 The chromatin association of Mec1

Mec1 is recruited to sites of DNA replication stress and this has been shown previously by ChIP (Osborn & Elledge, 2003). Whether Mec1 associates with the replication fork during unchallenged replication remains unclear (Lambert & Carr, 2005). One prediction from the hypothesis that Mec1 is important for fine-tuning dNTP availability with replication fork progression through *RSZs* is that Mec1 should associate with the replication fork, either throughout S-phase or specifically at *RSZs*.

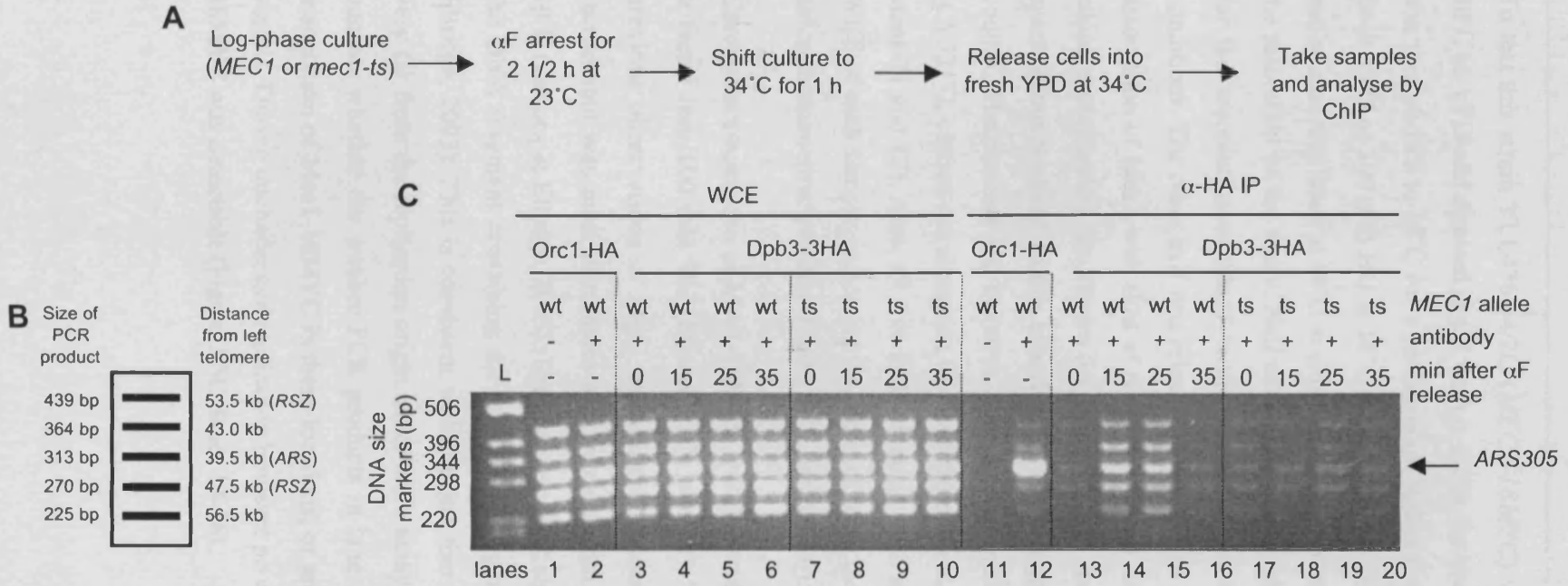

Figure 3.4 Movement of the polymerase ε subunit Dpb3 with the replication fork . A) Outline of the experimental procedure. **B)** Diagram showing the expected PCR products, their size in base pairs (bp) and their location relative to the left telomere. **C)** Strains expressing HA-tagged Orc1 (CEY8) and HA-tagged Dpb3 with either the wild-type (wt) (CEY18) or the temperature sensitive (ts) (CEY81) *MEC1* allele were grown in YPD at 23°C. Samples were taken from the log phase Orc1-HA culture and analysed by ChIP for the positive and negative (no antibody) controls. Samples were taken from the synchronous Dpb3-3HA cultures at the indicatated time points and analysed by ChIP. For each sample PCR was performed on the purified DNA from the whole cell extract (WCE) before immunoprecipitation and on the purified DNA isolated by immunoprecipitation with the anti-myc antibody (α-HA IP). The PCR products were separated on a 2.5% agarose gel and stained with ethidium bromide. The identity of each band was confirmed by comparison to DNA size markers from a 1 kb DNA ladder (L).

To test this strain YLL476.34/2C (*MEC1-18MYC*) was grown to mid-log phase at 30°C in YPD and arrested in G1 with α-factor for two and a half hours. The culture was then shifted to 18°C for a further hour, before the cells were released into either fresh YPD or 100 mM HU at 18°C (Figure 3.5A). As previously, the α-factor arrest and release was done at 18°C to slow down replication fork progression and improve the resolution of the assay. Half of the culture was released into fresh YPD to look for the association of Mec1 with the replication fork under normal replication conditions. The other half was released into 100 mM HU as a control to monitor the association of Mec1 with sites of replication stress. Samples for ChIP analysis were taken periodically (as shown in Figure 3.5C) as cells progressed through a synchronous S-phase. In this experiment a MYC-tagged Orc2 subunit was used as a control. The positive and negative control experiments with the Orc2-9MYC strain (CY3217), carried out alongside the main experiment, were successful (Figure 3.5C, lanes 11 and 12). Also, all five PCR products were successfully amplified from the WCE of each sample, indicating the presence of all the DNA fragments in the sample before immunoprecipitation (Figure 3.5C, lanes 1-10).

Chromatin association of Mec1-18MYC was detected 80 minutes after release from α-factor into 100 mM HU (Figure 3.5C, lane 20). This timing is consistent with previous observations of Mec1 recruitment to sites of replication stress, where recruitment was seen 60 minutes after release from α-factor into 200 mM HU at 19°C (Osborn & Elledge, 2003). The strongest PCR signal in lane 20 corresponded to the DNA fragment containing the replication origin (as also seen by Osborn and Elledge, 2003). This is consistent with the fact that replication forks do not move very far from the replication origin under these assay conditions (Figure 3.3C). It is unclear whether the weaker PCR products in lane 20 represent a real chromatin association of Mec1-18MYC in these locations, or are just non-specific background signals. During unchallenged replication however no chromatin association of Mec1-18MYC was detectable (Figure 3.5C, lanes 13-16).

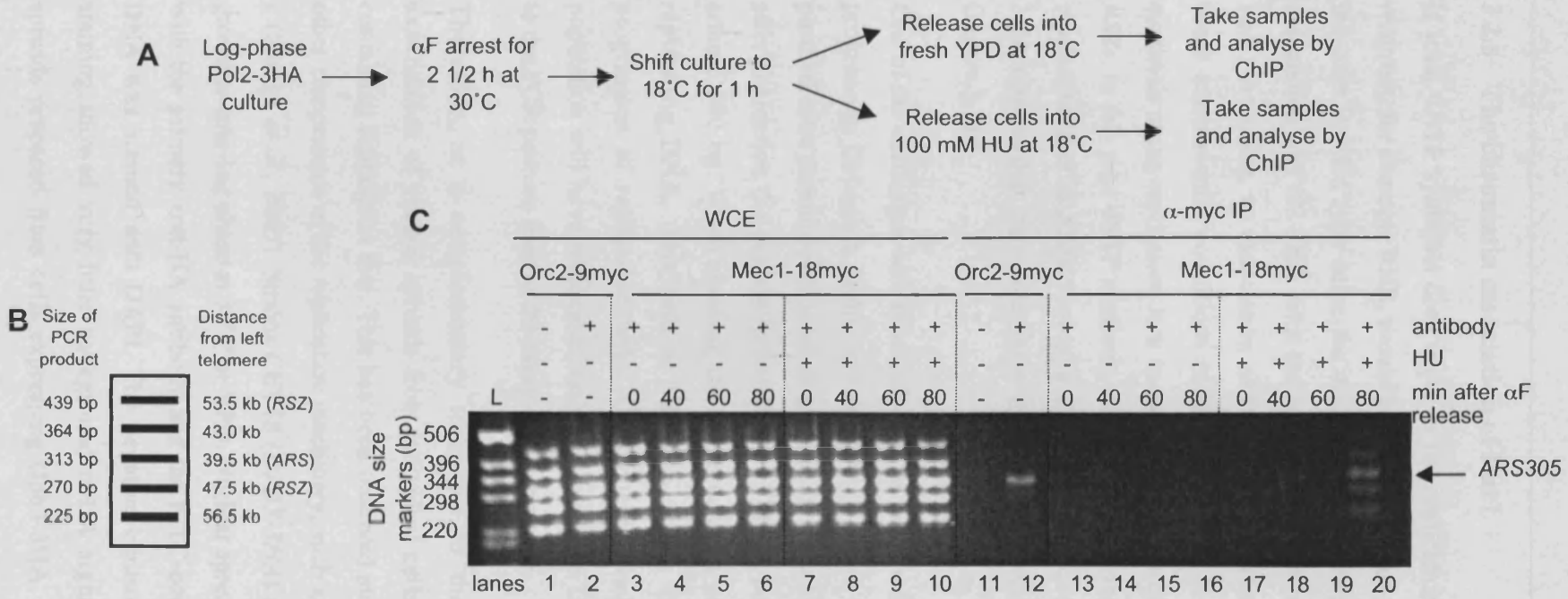

Figure 3.5 HU-induced recruitment of Mec1 to the replication fork. A) Outline of the experimental procedure. **B)** Diagram showing the expected PCR products, their size in base pairs (bp) and their location relative to the left telomere. **C)** Strains expressing myc-tagged Orc2 (CY3217) and myc-tagged Mec1 (YLL476.34/2C) were grown in YPD at 30°C. Samples were taken from the log phase Orc2-9myc culture and analysed by ChIP for the positive and negative (no antibody) controls. Samples were taken from the synchronous Mec1-18myc culture at the indicated time points and analysed by ChIP. For each sample PCR was performed on the purified DNA from the wholecell extract (WCE) before immunoprecipitation and on the purified DNA isolated by immunoprecipitation with the anti-myc antibody (α-myc IP). The PCR products were separated on a 2.5% agarose gel and stained with ethidium bromide. The identity of each band was confirmed by comparison to DNA size markers from a 1 kb DNA ladder (L).

3.2.5 The chromatin association of Rnr1

If local dNTP synthesis does occur at the replication fork, then the key synthetic enzymes, for example RNR, should be associated with the replisome. To test if this is the case in wild type cells, the equivalent ChIP experiment used to observe the association of Pol2-3HA with the replicating DNA was repeated with HA-tagged Rnr1. However, no association of HA-Rnr1 with the replication fork was seen in these experimental conditions (data not shown). It is possible that local dNTP synthesis at the replication fork is specifically required for fork progression through *RSZs*. In this case dNTP synthetic enzymes might only associate transiently with the replication fork at *RSZs*. However tracking replication fork progression with Pol2-3HA showed that the resolution of the ChIP assay was not good enough to test this (Figure 3.3).

One of the challenges with this ChIP assay is that it relies on the cells in a population progressing through a highly synchronous S-phase so that enough DNA can be purified after immunoprecipitation to generate a specific PCR signal. For example, after sonication the protein-linked DNA will have been sheared into fragments of around 500 bp. When assaying for the association of replisome proteins with the replicating DNA, there will be variation across the population in the rate of progression of replication forks. Consequently, only a fraction of cells in the population will have replisomes associated with the DNA fragments corresponding to the PCR primers used in the assay at any one time.

Therefore, as a complementary technique to the ChIP assay, microscopic examination of nuclear spreads from individual cells was used to look for Rnr1-containing replication foci. This has been observed successfully in *S. cerevisiae* for other components of the replication machinery, such as DNA polymerases α, δ, and ε (Hiraga *et al.*, 2005). Strains CEY18 (*DPB3-3HA*) and CEY21 (*HA-RNR1*) were grown to mid-log phase at 30°C in YPD. Nuclear spreads were prepared and stained with the primary anti-HA antibody and the FITC-conjugated secondary antibody. DNA was stained with DAPI. The negative control with no anti-HA antibody staining showed very little background α-HA signal (Figure 3.6A). In nuclear spreads prepared from cells expressing Dpb3-3HA, the α-HA signal mostly co-

localised with the DAPI signal consistent with the polymerase ε subunit being a chromatin-associated protein (Figure 3.6B). However, in spreads prepared from cells expressing HA-Rnr1, the α-HA signal does not co-localise with the DAPI signal suggesting that Rnr1 is not strongly associated with the chromatin (Figure 3.6C). This observation is consistent with published data that show that Rnr1 is mostly localised in the cytoplasm (Yao *et al.*, 2003)

3.3 Discussion

3.3.1 Technical limitations of the ChIP assay

The experiments presented in this chapter showed no evidence for the association of Mec1 and Rnr1 with the replication fork under normal replication conditions. Although this might be because the association does not happen, it is also possible that the ChIP assay is not sensitive enough to detect it. For example it might be unfeasible to generate a PCR signal from DNA immunoprecipitated with replisome proteins that are present in small quantities, or that only associate transiently or loosely. The ability of an antibody to bind to its epitope when assembled differently within a large protein complex could also affect the efficiency of the immunoprecipitation step. Similar problems (detecting small quantities of proteins and detecting proteins only transiently or loosely associated with the chromatin) will also affect the immunofluorescence technique, tried as an alternative to the ChIP assay.

Other technical limitations of the ChIP assay, such as the reduced temporal resolution at higher temperatures and the weak PCR signal from polymerase-linked DNA in *arg4::mec1-4* cells, were described in the results section. Together, these technical limitations meant that it was not feasible to continue with this investigation.

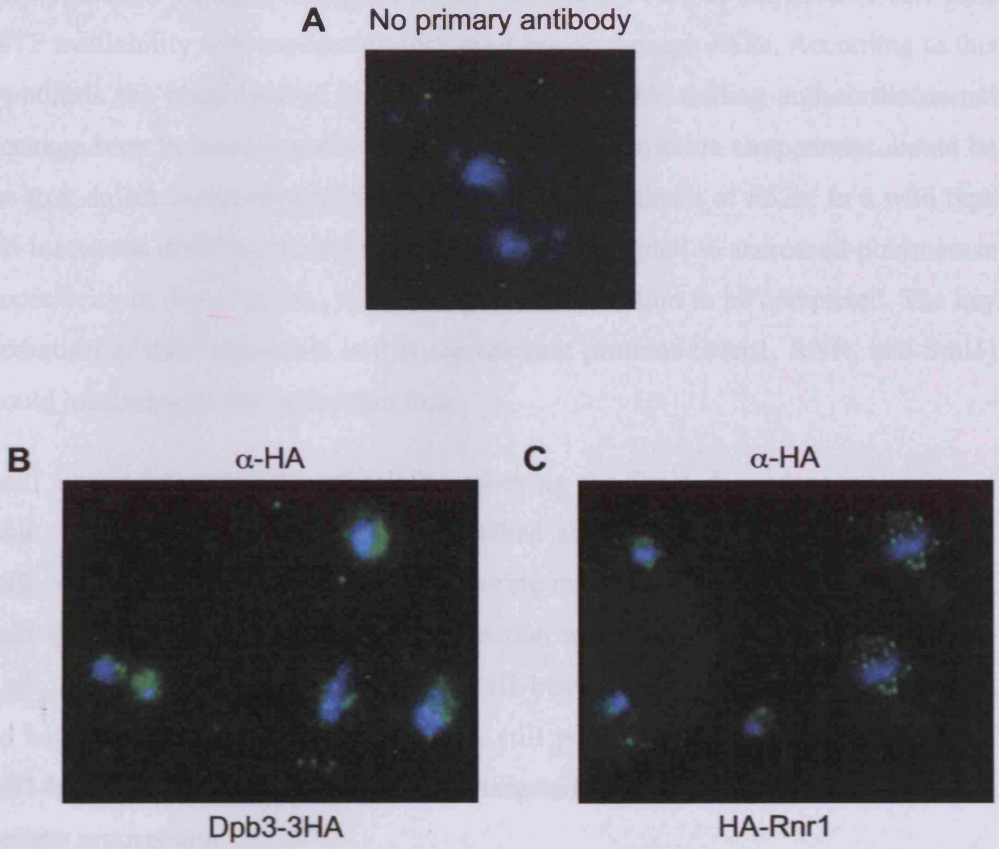

Figure 3.6 Immunostained nuclear spreads of cells expressing Dpb3-3HA or HA-Rnr1. The indicated strains were grown to mid-log phase in YPD at 30°C. Nuclear spreads were prepared and stained with the primary α-HA antibody and the FITC-conjugated secondary antibody. DNA was stained with DAPI. The images shown are an overlay of the DAPI (blue) signal and the FITC (green) signal. **A)** Nuclear spreads from cells expressing Dpb3-3HA (CEY18) without primary α-HA antibody staining. **B)** Nuclear spreads from cells expressing Dpb3-3HA (CEY18) with primary α-HA antibody staining. **C)** Nuclear spreads from cells expressing HA-Rnr1 (CEY21) with primary α-HA antibody staining.

3.3.2 The role of Mec1 in regulating dNTP availability during DNA replication

The hypothesis being investigated stated that Mec1 could be required to fine-tune dNTP availability with replication fork progression through *RSZs*. According to this hypothesis the phenotype of prolonged replication fork stalling and chromosomal breakage seen in *mec1-4* and *mec1-40* cells at the restrictive temperature would be due to a defect in the upregulation of local dNTP synthesis at *RSZs*. In a wild type cell increased dNTP synthesis at *RSZs* would be coupled to increased polymerase processivity in these regions, so enabling DNA replication to be completed. The key prediction of this hypothesis is that the relevant proteins (Mec1, RNR, and Sml1) should localise with the replication fork.

Mec1 upregulates dNTP synthesis by relieving the Sml1-dependent inhibition of RNR. According to the hypothesis described above a population of Sml1-bound RNR, which could be targeted by Mec1 during replication of *RSZs*, must exist. Bulk Sml1 degradation occurs at the G1/S transition in a Mec1-dependent manner (Zhao *et al.*, 2001). Therefore the amount of Sml1-bound RNR significantly decreases at the beginning of S-phase. However it is still possible that a small population of Sml1-bound RNR remains, which can be targeted by Mec1 more specifically during S-phase progression

Studies on the sub-cellular localisation of RNR suggest that bulk dNTP synthesis takes place in the cytoplasm in both *S. cerevisiae* (Yao *et al.*, 2003) and mammalian cells (Engstrom *et al.*, 1984; Engstrom & Rozell, 1988). The existence in eukaryotes of a pool of nucleotides that is channelled directly to the replication fork has been much debated (Mathews & Slabaugh, 1986; Mathews, 1993; Muller, 1994; Prem veer Reddy & Pardee, 1980). The consensus opinion is that any channelling that might occur in eukaryotes is non-essential and does not provide the majority of dNTPs for DNA replication. However, the possibility that there is a small population of RNR that synthesises dNTPs at the site of replication still exists.

The basis for suspecting that *S. cerevisiae* Mec1 might be associated with the replisome is stronger. The metazoan homologue of Mec1, ATR, associates with chromatin in an unperturbed S-phase (Dart *et al.*, 2004; Hekmat-Nejad *et al.*, 2000)

and the *S. pombe* Mec1 homolog, Rad3, has been suggested to be part of the replisome (Furuya *et al.*, 2004; Lambert & Carr, 2005). ATR is important for maintaining genomic stability at fragile sites (Casper *et al.*, 2002), which are regions of the genome that are particularly difficult to replicate and are analogous to *RSZs* (Section 1.2.3). It is interesting to note that Dart *et al.* (2004) suggest that ATR might be recruited to the replicating DNA specifically in areas such as fragile sites that are difficult to replicate. There is no known mammalian equivalent of Sml1, and currently it is not known if ATR can regulate dNTP synthesis in a similar way to Mec1. Despite this, the described behaviour of the ATR protein is similar to that proposed for Mec1 in the hypothesis tested here.

Chapter 4

GIS2 is a multicopy suppressor of the lethality of *mec1* temperature sensitive alleles

4.1 Introduction

GIS2 had been previously isolated in our lab as a multicopy suppressor of the lethality of the temperature sensitive *mec1-40* allele. The genetic screen in which *GIS2* was isolated used a YEp24 (2μm, *URA3*) plasmid-based library to search for multicopy suppressors of the temperature sensitivity of a *mec1-40* diploid strain. Of the suppressors isolated and sequenced *GIS2* appeared five independent times on three different library plasmid clones. *RNR1* was isolated four times and *MEC1* once. The name *GIS* comes from *gig* suppressor, where *gig* stands for glucose inhibition of gluconeogenic growth. *GIS2* was initially isolated as a suppressor of the inability of *snf1Δ mig1Δ gig1/2/3* mutants to grow on galactose (Balciunas & Ronne, 1999). The *snf1Δ mig1Δ gig1/2/3* mutant has a defect in the transcription of genes required to metabolise galactose. The DNA sequence shows that *GIS2* encodes a zinc finger protein, which is conserved in higher eukaryotes. The higher eukaryotic homolog, cellular nucleic acid binding protein (CNBP), is an essential gene required for correct forebrain development (Abe *et al.*, 2006; Chen *et al.*, 2003; Weiner *et al.*, 2007). The molecular function of *GIS2* in yeast remains unknown and there are no published links between *GIS2* and the DNA damage response pathway. Therefore, the new focus in investigating the essential role of *MEC1* was on understanding the mechanism of this suppression.

4.2 Results

4.2.1 *GIS2* is a multicopy suppressor of the lethality of *mec1* temperature sensitive alleles

The first step in understanding the basis for suppression was to investigate in more detail the genetic interaction between the suppressor *GIS2* and the original gene *MEC1*. There are two different temperature sensitive alleles of *mec1*, *mec1-4* and *mec1-40*, routinely used in our lab. The *mec1-4* allele is used in either the endogenous *MEC1* locus, where it replaces the wild type copy of *MEC1*, or the exogenous *arg4* locus, denoted *mec1-4* and *arg4::mec1-4* respectively. The *mec1-40* allele is used in just the exogenous *arg4* locus and is denoted *arg4::mec1-40*. Strains with the *mec1-4* or *mec1-40* alleles in the *arg4* locus have the wild type copy of *MEC1* deleted. To assess the ability of multicopy *GIS2* to suppress the lethality of these *mec1* temperature sensitive alleles, the multicopy *GIS2* plasmid was transformed into strains expressing *arg4::mec1-4* (RCY415), *arg4::mec1-40* (RCY426) and *mec1-4* (RCY620). As controls, the corresponding empty vector (YEp24) and a multicopy *MEC1* plasmid (pCLE5) were also transformed into these strains. The resulting strains were grown overnight at 23°C in SD-URA media, diluted to an OD_{600} of 0.5, and 10-fold serial dilutions were spotted onto SD-URA agar. The agar plates were incubated at the indicated temperatures for two days (Figure 4.1).

As has been previously characterised, the restrictive temperature of each *mec1* temperature sensitive strain was different (Cha & Kleckner, 2002). The restrictive temperature for the *arg4::mec1-4* strain (CEY155) was 30°C (Figure 4.1A), whereas for the *mec1-4* strain (CEY167) it was 34°C (Figure 4.1B). It is not clear why placing the same allele at two different loci confers a different phenotype, but it could be due to different levels of gene expression from the native promoter when placed in different chromosomal locations. The restrictive temperature for the different allele, *arg4::mec1-40* (CEY131), was 37°C (Figure 4.1C).

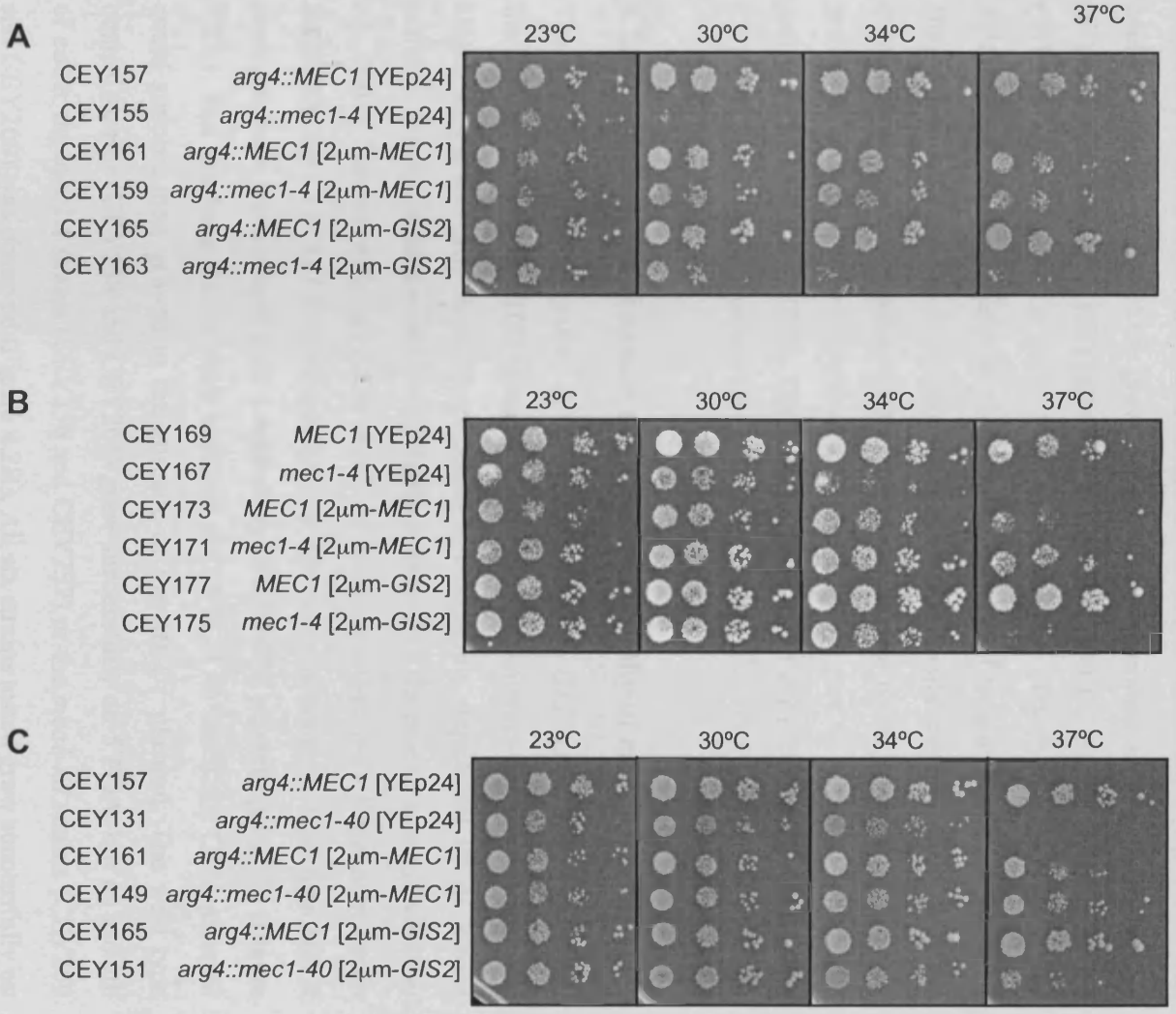

Figure 4.1 Multicopy *GIS2* suppresses the lethality of *mec1* temperature sensitive alleles. The indicated strains were grown overnight at 23°C in SD-URA. The following morning each culture was diluted to OD_{600} of 0.5, and 10-fold serial dilutions were spotted onto SD-URA agar. Agar plates were incubated at the indicated temperature for two days. The plasmids used were YEp24 (empty vector), pCLE5 (2µm-*MEC1*) and pCLE8 (2µm-*GIS2*).

Multicopy *GIS2* improved the growth of all three temperature sensitive *mec1* strains (Figure 4.1A compare CEY163 with CEY155 at 30°C; Figure 4.1B compare CEY175 with CEY167 at 34°C; Figure 4.1C compare CEY151 with CEY131 at 37°C). This effect of multicopy *GIS2* on the growth of temperature sensitive *mec1* strains was reproducibly observed in several experimental repeats, using multiple independent clones for each strain. However, whereas multicopy *MEC1* restored growth to wild type levels, multicopy *GIS2* did not (Figure 4.1A compare CEY163 and CEY159 with CEY157; Figure 4.1B compare CEY175 and CEY171 with CEY169; Figure 4.1C compare CEY151 and CEY149 with CEY157).

4.2.2 Multicopy *GIS2* cannot suppress the lethality of *mec1Δ* or *mec1-kd*

The next step in understanding the interaction between *GIS2* and *MEC1* was to test the ability of multicopy *GIS2* to suppress the complete deletion and kinase-dead (kd) alleles of *MEC1*. The function of Mec1 is completely dependent on its kinase activity, and so the kinase-dead *mec1* allele is lethal like the *mec1Δ* allele (Paciotti *et al.*, 2001). Strains with *mec1Δ* or *mec1-kd* mutations that were dependent on an *ARS/CEN-MEC1-URA3* plasmid (pMK9) for survival, and congenic wild type *MEC1* controls, were transformed with a multicopy *GIS2-TRP1* plasmid (pCLE9) (Figure 4.2A). The resulting strains were streaked onto 5'FOA to see if the *GIS2* plasmid could support their growth in the absence of the *MEC1* plasmid. The wild type control strains (CEY258 and CEY261) grew successfully on 5'FOA, but no growth of either the *mec1Δ* strains (CEY256 and CEY257) or the *mec1-kd* strains (CEY259 and CEY260) was observed (Figure 4.2B). All six strains tested grew successfully on the equivalent media without 5'FOA (Figure 4.2B). The fact that multicopy *GIS2* has no detectable effect on the viability of *mec1Δ* or *mec1-kd* strains, suggests that some hypomorphic Mec1 activity is required for the *GIS2*-dependent improvement of the viability of the temperature sensitive *mec1* strains.

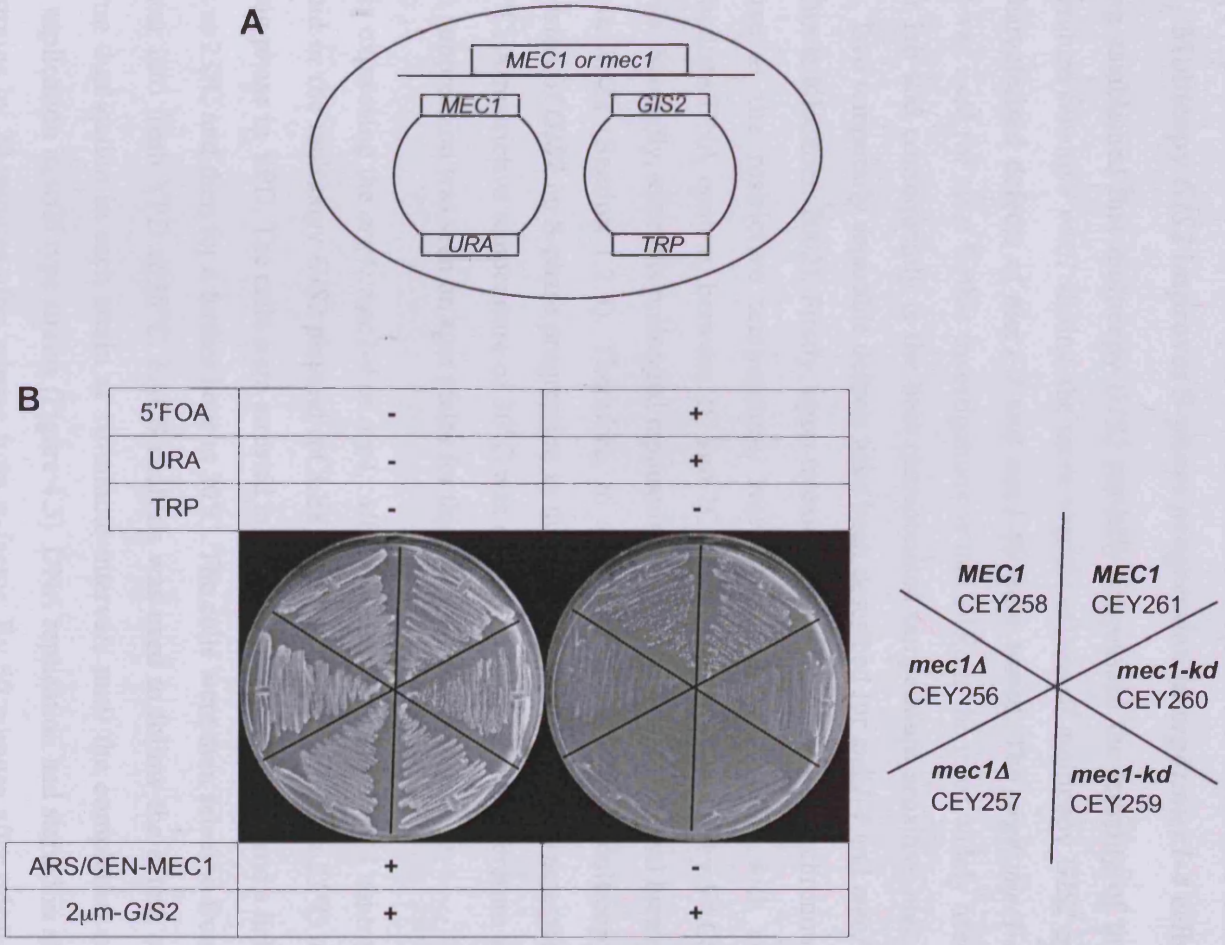

Figure 4.2 Multicopy *GIS2* does not rescue *mec1Δ* or *mec1-kd* lethality. A) Plasmids pMK9 (*ARS/CEN-MEC1-URA3*) and pCLE9 (2μm-*GIS2-TRP1*) were transformed into *MEC1*, *mec1-kd* or *mec1Δ* strains. **B)** The resulting strains were streaked onto minimal agar media supplemented with lysine, leucine, arginine and histidine. Uracil and 5'FOA were added as indicated. The *MEC1* genotype and strain number of the strain in each section of the plates is indicated in the right hand panel.

4.2.3 Multicopy *GIS2* improves S-phase progression in *arg4::mec1-4* cells

Having established that multicopy *GIS2* partially suppressed the lethality of the temperature sensitive *mec1* strains, the more specific effects of multicopy *GIS2* on the characterised defects of *mec1-4* and *mec1-40* were tested. The *arg4::mec1-4* allele was used for most further investigations as this allele is the most widely used in our lab and consequently is the best characterised temperature sensitive *mec1* allele. Two temporally separable defects have been described for *mec1-4* and *mec1-40* (Cha & Kleckner, 2002). Firstly, upon release from α-factor into a synchronous S-phase at the restrictive temperature, *mec1-4* and *mec1-40* cells with an intermediate DNA content, between 1C and 2C, accumulate as assessed by FACS analysis. Secondly, after this prolonged replication fork stalling, chromosomal breaks form in *RSZs* (Section 1.2.3). Therefore, to start with the effect of multicopy expression of *GIS2* on S-phase progression in the *arg4::mec1-4* strain was assessed at 30°C. A restrictive temperature of 30°C was chosen as it was the temperature at which suppression was seen on agar plates for this allele (Figure 4.1A).

Strains expressing the *arg4::mec1-4* or *arg4::MEC1* alleles, with the YEp24 control plasmid or the multicopy *GIS2* plasmid (pCLE8), were grown overnight at 23°C to mid-log phase in YPD. The cells were arrested in G1 with α-factor for two and a half hours at 23°C and then for a further hour at 30°C. The cells were then released from α-factor into fresh YPD at 30°C. FACS analysis was used to follow the extent of genome duplication in each strain at 10-minute intervals until the completion of DNA replication in wild type strains (Figure 4.3). DNA replication had started in all four strains by 20 minutes after release from α-factor. By 50 minutes after release from α-factor most *arg4::MEC1* cells (CEY157 and CEY165) had a 2C DNA content. The fraction of *arg4::mec1-4* cells (CEY155 and CEY163) with an intermediate DNA content between 1C and 2C at 50 minutes after release from α-factor was notably higher than that in the *arg4::MEC1* cells (CEY157 and CEY165).

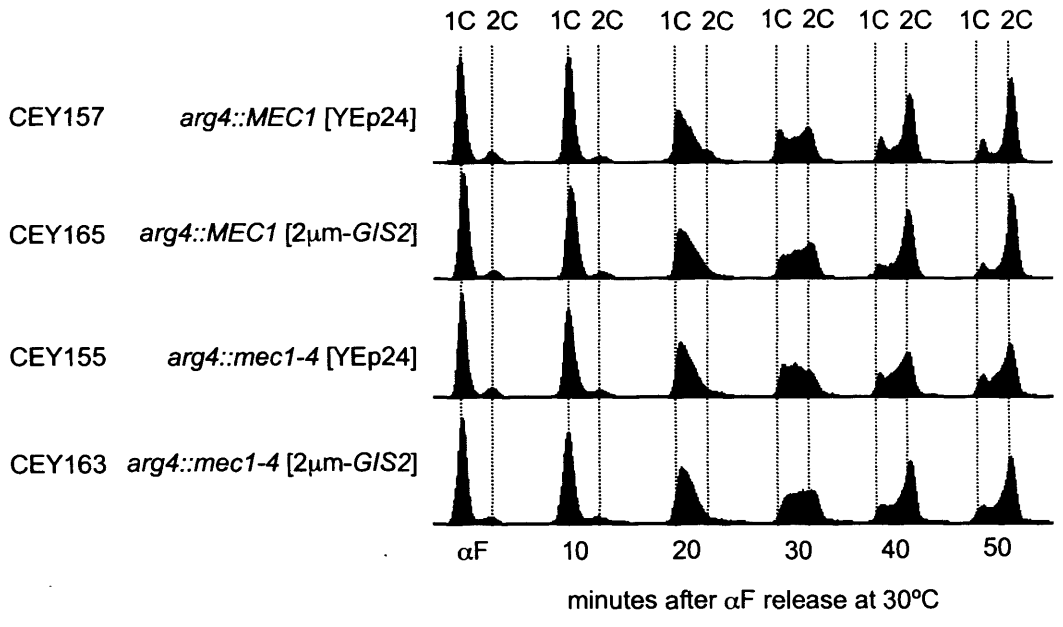

Figure 4.3 Multicopy *GIS2* improves S-phase progression in *arg4::mec1-4* cells. Log phase cultures of the indicated strains, grown at 23°C in YPD, were arrested in G1 with α-factor for two and a half hours at 23°C and a further one hour at 30°C . Cells were released into fresh YPD at 30°C and samples were taken every 10 minutes for FACS analysis. The 1C and 2C DNA content is as indicated. Each FACS profile represents 50,000 counts.

However, the fraction of cells with an intermediate DNA content between 1C and 2C at 50 minutes after release from α-factor was lower in the *arg4::mec1-4* strain expressing multicopy *GIS2* (CEY163) than in the *arg4::mec1-4* strain with the YEp24 control plasmid (CEY155). Therefore, the presence of the multicopy *GIS2* plasmid in the *arg4::mec1-4* cells improved progression through S-phase, as assessed by bulk DNA replication. This effect of multicopy *GIS2* on S-phase progression in the *arg4::mec1-4* cells was reproducibly observed in several experimental repeats, using multiple independent clones for each strain. However, bulk DNA replication still did not proceed as efficiently as in wild type cells. This is consistent with the observation that multicopy *GIS2* does not restore growth of temperature sensitive *mec1* strains to wild type levels on agar plates (Figure 4.1).

4.2.4 Multicopy *GIS2* reduces chromosomal break formation in *arg4::mec1-4* cells

Figure 4.3 showed that, of the two defects described for *mec1-4* and *mec1-40* cells, multicopy *GIS2* reduced the accumulation of *arg4::mec1-4* cells with an intermediate DNA content. Therefore, the next stage was to assess the effect of multicopy *GIS2* on chromosomal break formation in *arg4::mec1-4* cells. Strains expressing the *arg4::mec1-4* or *arg4::MEC1* alleles, with the YEp24 control plasmid or the multicopy *GIS2* plasmid, were grown overnight at 23°C to mid-log phase in YPD. The cells were arrested in G1 with α-factor for two and a half hours at 23°C and then for a further hour at 30°C. The cells were then released from α-factor into fresh YPD at 30°C. A sample from each culture was taken five hours after release from α-factor to assess the level of chromosomal fragmentation by pulsed-field gel electrophoresis and Southern blot analysis (Figure 4.5). Additionally samples from the *arg4::mec1-4* [YEp24] (CEY155) and *arg4::mec1-4* [2μm-*GIS2*] (CEY163) cultures were plated out, onto both YPD and SD-URA, every hour. The agar plates were incubated at the permissive temperature of 23°C firstly to assess the effect multicopy *GIS2* has on the viability of the *arg4::mec1-4* strain under these experimental conditions (Figure 4.4), and secondly to assess the stability of the 2μm plasmids. The average percentage of cells, taken over all time points (0-8 hours) for one experiment, that maintained the 2μm YEp24 plasmid was 85% and the 2μm

GIS2 plasmid was 87%. The fraction of *arg4::mec1-4* cells that was viable when returned to growth at 23°C after incubation in α-factor at 30°C was set to 100%. The *mec1-4* and *mec1-40* cells lose viability after attempting DNA replication in the absence of Mec1 function (Cha & Kleckner, 2002). Therefore *arg4::mec1-4* cells held in G1 should remain viable, even with the Mec1-4 protein inactivated.

The percentage of viable *arg4::mec1-4* [YEp24] cells (CEY155) remained fairly constant, at around 100%, up to five hours after release from α-factor (Figure 4.4). The fraction of viable *arg4::mec1-4* [YEp24] cells then started to decrease at later time points. This is consistent with that fact that *mec1-4 and mec1-40* cells do not lose viability until chromosomal breaks form, after a period of prolonged replication fork stalling (Cha & Kleckner, 2002). On the other hand, the percentage of viable *arg4::mec1-4* [2μm-*GIS2*] cells (CEY163) steadily increased after release from α-factor, and by six hours had almost doubled (Figure 4.4). This shows that a fraction of the *arg4::mec1-4* [2μm-*GIS2*] cells were proliferating successfully. However, the percentage of viable cells after six hours is significantly less than that expected from a wild type strain, which has a doubling time of less than two hours at 30°C. This level of growth is consistent with the effect of multicopy *GIS2* seen on the growth of temperature sensitive *mec1* strains on agar plates (Figure 4.1) and on S-phase progression in the *arg4::mec1-4* strain (Figure 4.3).

The effect of multicopy *GIS2* on the level of chromosomal fragmentation in the *arg4::mec1-4* strain was assessed by probing for chromosome III fragments in a Southern blot, as done previously in Cha and Kleckner (2002). DNA fragments from each strain were separated by pulsed-field gel electrophoresis and analysed by Southern blot. The probe used, *CHA1*, was located approximately 16 kb from the end of chromosome III. So, in addition to the full-length chromosome, it detected DNA fragments of different sizes formed upon chromosomal break formation in *RSZs* (Figure 4.5A). The full-length chromosome III was successfully detected in each strain using the *CHA1* probe (Figure 4.5B). Also in each strain a significant fraction of chromosome III remained in the wells of the gel. This fraction represents any non-linear form of chromosome III, such as replication intermediates.

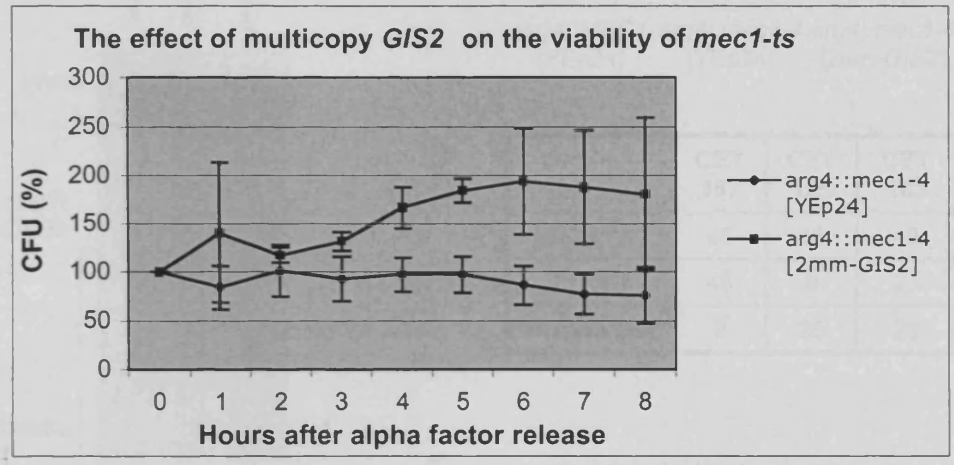

Figure 4.4 The effect of multicopy *GIS2* on the viability of *arg4::mec1-4* cells. Log phase cultures of strains CEY155 (*arg4::mec1-4* [YEp24]) and CEY163 (*arg4::mec1-4* [2μm-*GIS2*]), grown at 23˚C in YPD, were arrested in G1 with α-factor for two and a half hours at 23˚C and a further one hour at 30˚C . Cells were released into fresh YPD at 30˚C and samples were plated out onto YPD agar every hour. The agar plates were incubated at the permissive temperature of 23˚C for four days. The number of colonies at each time point for each strain were then counted (CFU; colony forming units). The number of colonies formed in each strain from the sample taken immediately after release from α-factor (0 h) was set to 100%. The number of colonies formed in each strain from the samples taken at subsequent time points were expressed as a percentage of the 0 h time point. The graph shows the average CFU from three independent experiments. The error bars show ± one standard deviation for each time point.

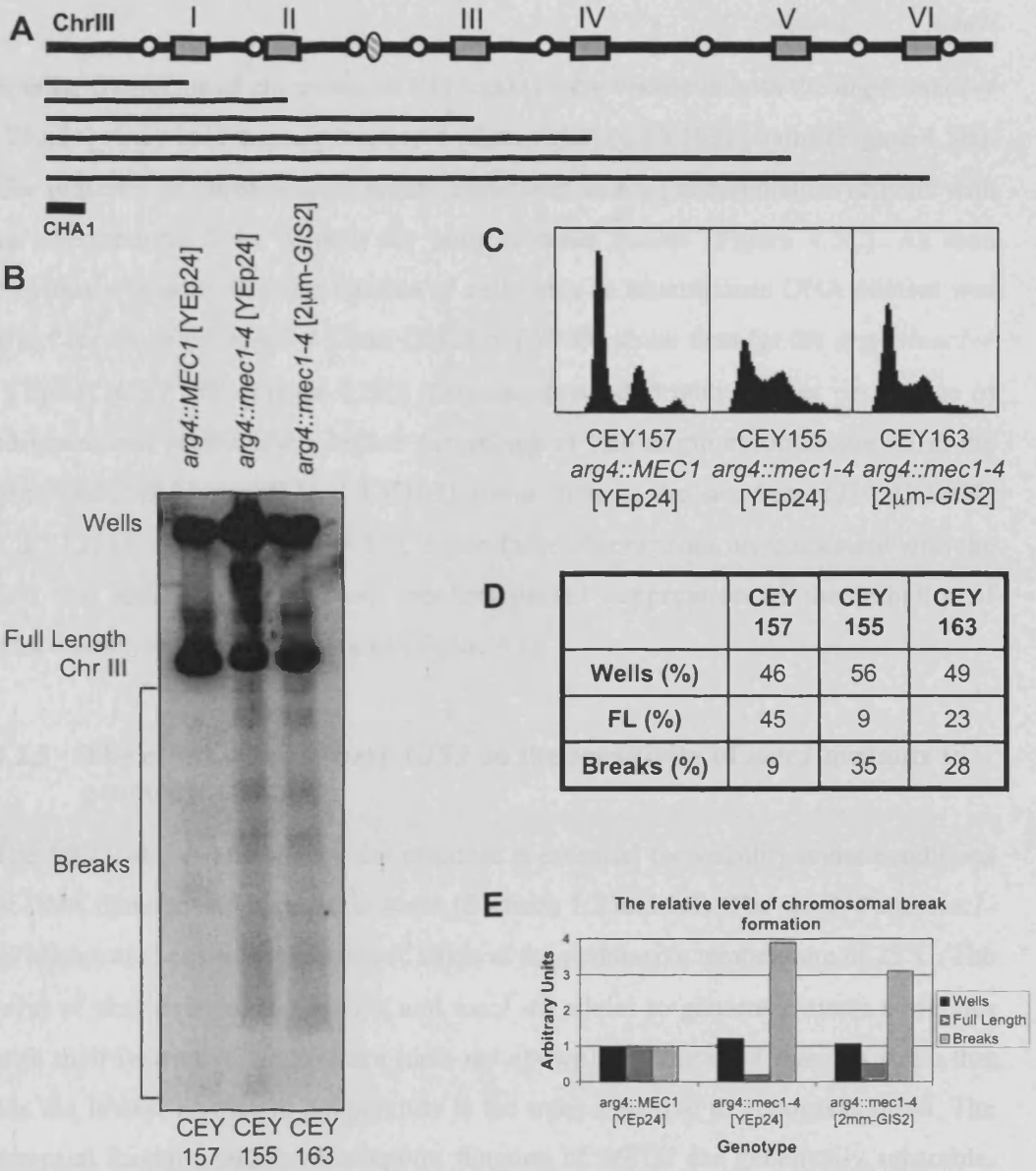

	CEY 157	CEY 155	CEY 163
Wells (%)	46	56	49
FL (%)	45	9	23
Breaks (%)	9	35	28

Figure 4.5 The effect of multicopy *GIS2* on chromosomal break formation in *arg4::mec1-4* cells. Log phase cultures of the indicated strains, grown at 23°C in YPD, were arrested in G1 with α-factor for two and a half hours at 23°C and a further one hour at 30°C. Cells were released into fresh YPD at 30°C and samples were taken for PFGE and FACS analysis five hours later. **A)** Diagram of chromosome III showing the positions of the six *RSZs* (grey boxes), the centromere (striped oval) and the efficient replication origins (white circles). The chromosomal fragments, detected by Southern blot analysis using the *CHA1* probe, upon break formation in any one *RSZ* are also shown. **B)** DNA fragments from each strain were separated by pulsed-field gel electrophoresis and analysed by Southern blot using the *CHA1* probe. **C)** The FACS profiles from the samples analysed in (B). Each FACS profile represents 50,000 counts. **D)** The chromosome III (*CHA1*) signals from the wells, the full length chromosome and the break fragments were quantified for each strain using ImageJ software. The percentage of the total signal for each is shown in the table. **E)** A graphical representation of the data in (D), with the signal from each gel section expressed relative to wild type.

Smaller fragments of chromosome III (breaks) were visible in both the *arg4::mec1-4* [YEp24] (CEY155) and *arg4::mec1-4* [2μm-*GIS2*] (CEY163) strains (Figure 4.5B). The presence of chromosomal breaks correlated with an accumulation of cells with an intermediate DNA content for both of these strains (Figure 4.5C). As seen previously (Figure 4.3), the fraction of cells with an intermediate DNA content was lower for the *arg4::mec1-4* [2μm-*GIS2*] (CEY163) strain than for the *arg4::mec1-4* [YEp24] (CEY155) (Figure 4.5C). This also correlated with a lower percentage of chromosomal breaks and a higher percentage of full-length chromosome III in the *arg4::mec1-4* [2μm-*GIS2*] (CEY163) strain than in the *arg4::mec1-4* [YEp24] (CEY155) (Figure 4.5D and 4.5E). Again these observations are consistent with the fact that multicopy *GIS2* only confers partial suppression of the lethality of temperature sensitive *mec1* strains (Figure 4.1).

4.2.5 The effect of multicopy *GIS2* on the sensitivity of *mec1* mutants to genotoxic stress

The *MEC1*-dependent checkpoint response is essential for viability under conditions of DNA damage and replication stress (Sections 1.3 and 1.4). The *mec1-4* and *mec1-40* alleles are sensitive to genotoxic stress at the permissive temperature of 23°C. The level of sensitivity of the *mec1-4* and *mec1-40* alleles to genotoxic stress correlates with their restrictive temperature (data not shown). So, the *arg4::mec1-4* strain that has the lowest restrictive temperature is the most sensitive to genotoxic stress. The essential function and the checkpoint function of *MEC1* are genetically separable. So, increasing dNTP levels rescues the inviability of *mec1Δ* but does not restore checkpoint function (Desany *et al.*, 1998; Zhao *et al.*, 1998). *GIS2* could be acting in a similar way and restoring viability by bypassing the essential requirement for *MEC1*, but without affecting checkpoint function. Alternatively, *GIS2* could be improving Mec1 function, for example by increasing the expression of *arg4::mec1-4*. In the latter scenario it is expected that both the essential growth function and the DNA damage or replication stress response would be improved. Therefore, the effect of multicopy *GIS2* on the ability of the *arg4::mec1-4* strain to grow in the presence of genotoxic stress was tested (Figure 4.6). The *arg4::mec1-4* strain (RCY415), a *mec1Δ sml1Δ* strain (RCY308) and wild type control strains (RCY483 and CEY461)

were transformed with the YEp24 control plasmid, a multicopy *MEC1* plasmid (pCLE5), a multicopy *GIS2* plasmid (pCLE8) or a multicopy *RNR1* plasmid (pCLE11). The resulting strains were grown overnight in SD-URA media at 23°C or 30°C as described in the figure legend (Figure 4.6). The following morning each culture was diluted to an OD_{600} of 0.5, and 10-fold serial dilutions were spotted onto SD-URA agar supplemented with HU or MMS at the indicated concentrations (Figure 4.6). Agar plates with the *arg4::mec1-4* strains were incubated at 23°C for three days and agar plates with the *mec1Δ sml1Δ* strains were incubated at 30°C for two days (Figure 4.6).

At the permissive temperature of 23°C the *arg4::mec1-4* strain was more resistant to HU and MMS than the *mec1Δ sml1Δ* strain (compare the growth of CEY155 in Figure 4.6A and CEY542 in Figure 4.6B on 1 mM HU and on 0.002% MMS). However, as expected the *arg4::mec1-4* strain (CEY155) was more sensitive to HU and MMS than the *arg4::MEC1* strain (CEY157). Increasing dNTP levels can improve resistance to DNA damage in checkpoint proficient strains (Chabes *et al.*, 2003a). Multicopy expression of *RNR1* in the *arg4::mec1-4* strain improved growth slightly in the presence of 0.002% MMS, but not at higher MMS concentrations (Figure 4.6A; compare CEY482 and CEY155). No equivalent effect of multicopy *RNR1* was seen on the growth of the *arg4::mec1-4* strain in the presence of HU, probably because HU is an inhibitor of RNR. Multicopy *RNR1* had no effect on the growth of the *mec1Δsml1Δ*strain in the presence of genotoxic stress at the concentrations tested (Figure 4.6B; compare CEY547 and CEY542). This is probably because checkpoint function is completely lost in the *mec1Δ* strain, whereas the *arg4::mec1-4* strain retains some residual checkpoint function at 23°C. The expression of multicopy *GIS2* had no effect on the growth of either the *arg4::mec1-4* or *mec1Δ sml1Δ* strains in the presence of MMS, but did appear to improve growth of the *arg4::mec1-4* strain in the presence of HU (Figure 4.6A compare CEY163 with CEY155; Figure 4.6B compare CEY545 with CEY542). However, this effect of multicopy *GIS2* in improving the ability of the *arg4::mec1-4* strain to grow in the presence of HU was not seen in the other experimental repeat. Therefore it remains unclear what the precise effect of multicopy *GIS2* is on the ability of the *arg4::mec1-4* strain to grow in the presence of genotoxic stress.

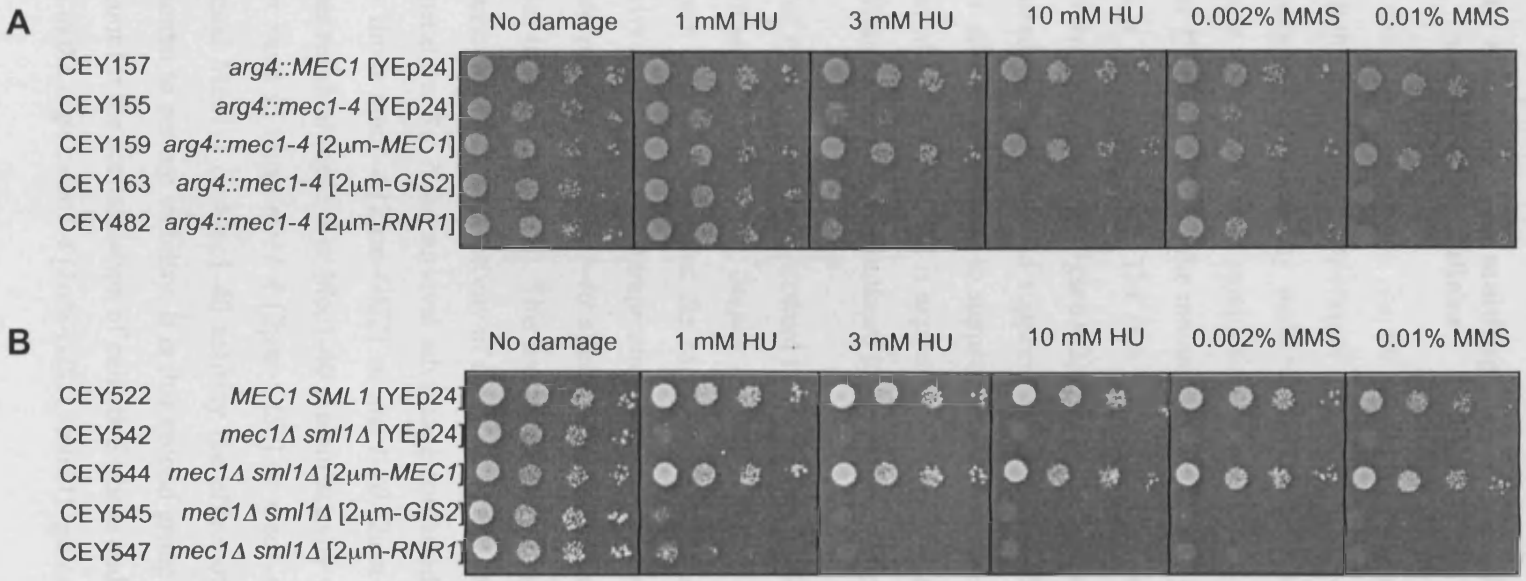

Figure 4.6 Multicopy *GIS2* does not rescue the sensitivity of *mec1* mutants to genotoxoic stress. A) The indicated strains were grown at overnight at 23°C in SD-URA. The following morning each culture was diluted to an OD_{600} of 0.5, and 10-fold serial dilutions were spotted onto SD-URA agar. Agar plates were incubated at 23°C for three days. **B)** The indicated strains were grown overnight at 30°C in SD-URA. The following morning each culture was diluted to an OD_{600} of 0.5, and 10-fold serial dilutions were spotted onto SD-URA agar. Agar plates were incubated at 30°C for two days. In (A) and (B) the indicated concentration of HU or MMS was added to the SD-URA agar. The plasmids used were YEp24 (empty vector), pCLE5 (2μm-*MEC1*), pCLE8 (2μm-*GIS2*) and pCLE11 (2μm-*RNR1*).

4.3 Discussion

4.3.1 *GIS2* is a weak multicopy suppressor of the lethality of temperature sensitive *mec1* alleles

The data presented in this chapter confirmed that multicopy *GIS2* is a suppressor of the lethality of the temperature sensitive *mec1* alleles. However, the level of suppression conferred by multicopy *GIS2*, as assessed by growth on agar plates (Figure 4.1), the timely completion of bulk DNA replication in a synchronous S-phase (Figure 4.3), and the maintenance of viability during growth at 30°C (Figure 4.5), is relatively weak. The fact that no *GIS2*-dependent suppression of *mec1Δ* or *mec1-kd* was detected (Figure 4.2) suggests that some hypomorphic Mec1 activity is required for the observed suppression of the lethality of the temperature sensitive *mec1* alleles. Therefore, to suppress *mec1-4* or *mec1-40* temperature sensitivity the effect of multicopy *GIS2* is expected to, somehow, add to residual Mec1-4 or Mec1-40 function. This idea is outlined in the model in Figure 4.7.

In this model, as the temperature is increased the Mec1-4 or Mec1-40 protein would retain some functionality, despite its activity falling below the threshold for viability (Figure 4.7). The idea that the Mec1-4 and Mec1-40 proteins retain some residual activity at the restrictive temperature is supported by previous observations in our lab where *mec1-4* and *mec1-40* alleles show different genetic interactions to *mec1Δ* alleles (unpublished data). This model also assumes that there is natural variation in the amount of residual activity of the Mec1-4 and Mec1-40 proteins at the restrictive temperature. So, if the survival advantage conferred by multicopy *GIS2* is marginal, only those *mec1-4* [2μm-*GIS2*] or *mec1-40* [2μm-*GIS2*] cells that naturally have higher residual Mec1-4 or Mec1-40 protein activity will be able to proliferate. On the other hand in those *mec1-4* [2μm-*GIS2*] or *mec1-40* [2μm-*GIS2*] cells with lower residual Mec1-4 or Mec1-40 activity the effect of multicopy *GIS2* would not be sufficient to restore viability. It is this second group of cells that would, presumably, account for the accumulation of cells in S-phase and the chromosomal fragmentation seen in the *arg4::mec1-4* [2μm-*GIS2*] strain (Figures 4.3 and 4.5).

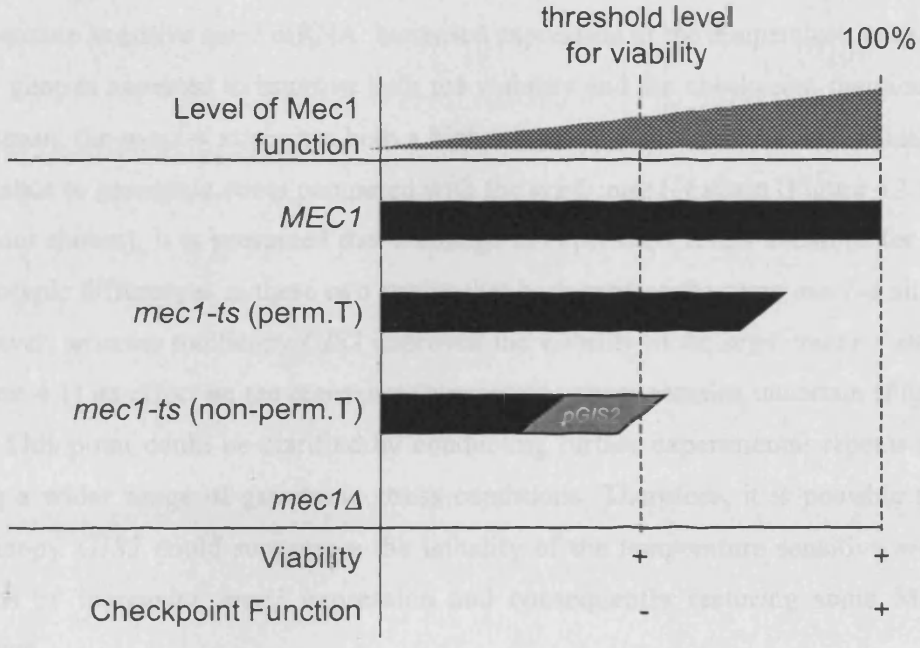

Figure 4.7 A model to illustrate the weak suppression of the lethality of temperature sensitive *mec1* alleles by multicopy *GIS2*. A *MEC1* wild type strain has 100% activity and is therefore fully proficient in both its essential role and its checkpoint function. The temperature sensitive *mec1* allele (*mec1-ts*) at its permissive temperature (perm.T) is viable, but has a reduced level of activity compared with the wild type allele. As the temperature is increased, in temperature sensitive *mec1* alleles the level of Mec1 activity falls below the viability threshold (black bar, non-perm.T). There will be natural variation in the level of activity of the temperature sensitive Mec1 protein within a population (shown here by the sloping end on the bar). The proposed contribution of multicopy *GIS2 (pGIS2)*, on top of the residual activity of the temperature sensitive Mec1 protein, is shown (grey bar).

4.3.2 What is the underlying mechanism of suppression?

Several scenarios whereby the effect of multicopy *GIS2* expression could add to the residual function of the temperature sensitive Mec1 protein to restore viability can be imagined. For example, increased *GIS2* expression could lead to increased transcription of the temperature sensitive *mec1* gene or increased translation of the temperature sensitive *mec1* mRNA. Increased expression of the temperature sensitive *mec1* gene is expected to improve both the viability and the checkpoint function of that strain: the *mec1-4* strain has both a higher restrictive temperature and increased resistance to genotoxic stress compared with the *arg4::mec1-4* strain (Figure 4.1 and data not shown). It is presumed that a change in expression levels accounts for the phenotypic differences in these two strains that both express the same *mec1-4* allele. However, whereas multicopy *GIS2* improved the viability of the *arg4::mec1-4* strain (Figure 4.1) its effect on the resistance to genotoxic stress remains uncertain (Figure 4.6). This point could be clarified by conducting further experimental repeats and using a wider range of genotoxic stress conditions. Therefore, it is possible that multicopy *GIS2* could suppresses the lethality of the temperature sensitive *mec1* strains by increasing *mec1* expression and consequently restoring some Mec1 function.

Another possibility is that multicopy *GIS2* could somehow promote the association of Mec1 kinase substrates with the hypomorphic temperature sensitive Mec1 protein. The role of *MEC1* in promoting the cell cycle-dependent fluctuation in Sml1 protein levels is presumed to be its essential function. This fluctuation in Sml1 protein levels, although completely dependent on *MEC1*, is only partially dependent on *RAD53* and *DUN1* (Zhao *et al.*, 2001; Zhao & Rothstein, 2002). The Mec1-Rad53-Dun1 signalling cascade is important for both the essential and the checkpoint function of *MEC1*. Thus, if the molecular effect of increased *GIS2* expression were to promote increased association of Rad53 with the hypomorphic temperature sensitive Mec1 protein, then an increase in the ability of the temperature sensitive *mec1* [2μm-*GIS2*] strain to respond to all types of genotoxic stress would be expected. However, as described above, this was not seen. Therefore an increase in the association of known Mec1 kinase substrates, such as Rad53, with the hypomorphic temperature sensitive Mec1 protein is unlikely to account for the observed suppression. But, an increase in

the association of, as yet uncharacterised, Mec1 kinase substrates with the hypomorphic temperature sensitive Mec1 protein could. For example, components of the replisome could be targets of the Mec1 kinase during normal DNA replication, which might help promote replication fork stability.

Lastly, multicopy *GIS2* could cause molecular changes in the cell that bypass the essential requirement for Mec1 function. This is the mechanism of suppression by which increasing dNTP levels, for example deleting *SML1* or over-expressing *RNR1*, can restore viability in a *mec1Δ* strain. The effect on the viability of *mec1-4* and *mec1-40* alleles of either deleting *SML1* or over-expressing *RNR1* is much greater than that of multicopy *GIS2*. So, whereas multicopy *GIS2* only causes a slight increase in the restrictive temperature of temperature sensitive *mec1* strains (Figure 4.1), growth is restored to wild type levels in temperature sensitive *mec1 sml1Δ* or *mec1* [p*RNR1*] strains at 37°C (data not shown). Therefore, multicopy *GIS2* could work by a similar mechanism and suppresses the lethality of temperature sensitive *mec1* strains by somehow increasing dNTP levels. However, to explain the weak level of suppression, the magnitude of this proposed dNTP level increase must be relatively modest.

A modest *GIS2*-dependent increase in dNTP levels could explain the observed effects of multicopy *GIS2* on the phenotype of temperature sensitive *mec1* cells. FACS analysis of *arg4::mec1-4* cells undergoing synchronous DNA replication at the restrictive temperature showed that a significant fraction of these cells accumulated with an intermediate DNA content, between 1C and 2C, after the first cell cycle (Figure 4.3). Expression of multicopy *GIS2* reduced the fraction of these cells that had an intermediate DNA content (Figure 4.3). This suggests that increasing *GIS2* expression helps the *arg4::mec1-4* cells to complete DNA replication. Increasing *GIS2* expression also reduced the formation of breaks in *RSZs* on chromosome III in *arg4::mec1-4* cells (Figure 4.5). Currently it is not known why chromosomal breaks form in *RSZs* in *mec1-4* and *mec1-40* cells. However break formation is suppressed by deleting *SML1* (Cha & Kleckner, 2002), suggesting that an insufficient level of dNTPs is a contributory factor. It is reasonable to propose that the increased fraction of cells in the *arg4::mec1-4* [2μm-*GIS2*] strain that complete

replication corresponds to the decreased fraction of cells in the *arg4::mec1-4* [2μm-*GIS2*] strain that form chromosomal breaks. It is also reasonable to propose that this fraction of cells represents those that can form colonies when assessing growth on agar plates. However it should be noted that the precise causal relationship between prolonged replication fork stalling, chromosomal break formation and cell viability is not fully understood.

Overall a *GIS2*-dependent, modest increase in dNTP levels is a reasonable explanation to account for the data presented in this Chapter. However, it is also possible that multicopy *GIS2* could suppress the lethality of temperature sensitive *mec1* strains by a different mechanism. In an attempt to learn more about the essential function of *MEC1* I aimed to elucidate the molecular mechanism of *GIS2*-dependent suppression of the lethality of temperature sensitive *mec1* strains. Initially, I investigated the effect of multicopy *GIS2* on known mechanisms of suppressing *mec1Δ* lethality. Then I looked at the role of *GIS2* itself. Finally I examined the effects of other conditions that were linked to *GIS2* function on the viability of temperature sensitive *mec1* strains. The results of these investigations are presented in the following Chapters.

Chapter 5

The effect of multicopy *GIS2* on the regulation of dNTP synthesis

5.1 Introduction

Most known suppressors of the lethality of *mec1Δ* have been linked to either an increase in dNTP synthesis or a reduction in the rate of dNTP consumption (Table 5.1). As there is no other known mechanism for restoring viability in a *mec1Δ* strain, it is reasonable to suggest that increasing *GIS2* expression, somehow, causes a modest increase in dNTP levels to partially suppress the lethality of temperature sensitive *mec1* strains. This idea was investigated further by assessing the effects of multicopy *GIS2* expression on the key mechanisms known to be involved in regulating dNTP availability.

Table 5.1 Known mechanisms of suppression of *mec1Δ* lethality

Suppressor	Description	Reference
sml1Δ	Sml1 inhibits RNR enzymatic activity.	(Zhao *et al.*, 1998)
RNR1	*RNR1* encodes a large subunit of RNR.	(Desany *et al.*, 1998)
RNR3	*RNR3* encodes a large subunit of RNR, which is expressed under DNA damage conditions.	(Desany *et al.*, 1998)
RAD53	Rad53 is a kinase that functions downstream of Mec1.	(Sanchez *et al.*, 1996)
TEL1	Tel1 is a kinase that shows partial functionally redundancy with Mec1.	(Morrow *et al.*, 1995)
DUN1	Dun1 is a kinase that functions downstream of Mec1.	(Sanchez *et al.*, 1996)
crt1Δ	Crt1 is a transcriptional inhibitor of the *RNR2,3,4* genes.	(Huang *et al.*, 1998)
dbf4-1/cdc7-1	Mutant alleles of *DBF4* or *CDC7* prevent the Dbf4/Cdc7 kinase activating replication origin firing at the restrictive temperature. The cell therefore consumes dNTPs more slowly.	(Desany *et al.*, 1998)
cln1Δ cln2Δ	Deletion of *CLN1* and *CLN2* delay the G1/S transition and therefore prolong the period of *RNR1* gene transcription before the onset of DNA replication.	(Vallen & Cross, 1999)

Suppressor	Description	Reference
yku70Δ/ yku80Δ	YKU70/80 are part of the NHEJ machinery. These deletions lead to an increase in *TEL1* mRNA and a reduction in Sml1 protein levels.	(Corda *et al.*, 2005)
hug1Δ	Mechanism unknown. Function unknown. *HUG1* transcription is upregulated in response to DNA damage.	(Basrai *et al.*, 1999)
WTM2	Wtm2 is a WD40 repeat protein. Over-expression of *WTM2* leads to cytoplasmic relocalisation of the small RNR subunits.	(Lee & Elledge, 2006)
nrm1Δ	Nrm1 is a transcriptional repressor that represses MBF. MBF regulates *RNR1* transcription at G1/S	(de Bruin *et al.*, 2006)
ptc2Δ	Ptc2 is a phosphatase that negatively regulates the DNA damage checkpoint.	(Marsolier *et al.*, 2000)
chd1Δ	Mechanism unknown. Chd1 is an ATP-dependent chromatin remodeler that negatively regulates DNA replication.	(Biswas *et al.*, 2008)

5.2 Results

5.2.1 The effect of multicopy *GIS2* on Sml1 protein levels

Cells lacking *MEC1* function lose the ability to degrade the Sml1 protein at the onset of DNA replication (Zhao *et al.*, 2001). It is generally believed that it is this inability to degrade Sml1 that causes cell death, due to insufficient dNTPs being available for DNA replication. Therefore, the possibility that multicopy expression of *GIS2* might, somehow, decrease Sml1 protein levels was tested. The Sml1 protein levels were assessed in both log phase and α-factor arrested cells. Cells arrested in G1 with α-factor were used so that any differences observed could be attributed to the effects of multicopy *GIS2*, and not to variations in the cell cycle fluctuation of Sml1 protein levels.

Strains expressing *SML1* with an N-terminal 3MYC tag (Section 2.10.4) and the *arg4::mec1-4* or *arg4::MEC1* alleles with either the YEp24 control plasmid or the multicopy *GIS2* plasmid were constructed. These strains were grown overnight to mid-log phase at 23°C in YPD. Half of each culture was shifted to 30°C for four hours to assess Sml1 protein levels in a log phase culture with the Mec1-4 protein inactivated. The other half was arrested in G1 with α-factor for two and a half hours at 23°C and for a further one hour at 30°C to assess Sml1 protein levels in a G1

culture with the Mec1-4 protein inactivated. Samples were then taken from these cultures for protein extraction and FACS analysis. Proteins were separated on a 15% polyacrylamide gel by SDS-PAGE and analysed by Western blot using an anti-MYC antibody. The signals from the 3MYC-Sml1 protein and the non-specific band were quantified from scanned images of the Western blot. The amount of 3MYC-Sml1 for each condition, relative to the non-specific band was calculated. The average values from 5 independent experiments are shown in Figure 5.1.

The FACS profiles of each culture showed that there was a difference between the different strain genotypes in the distribution of log phase cells at 30°C in different cell cycle phases (Figure 5.1A). Most notably, the *arg4::mec1-4* [YEp24] strain had a greater proportion of cells with a 1C DNA content than the other genotypes and the *arg4::mec1-4* [2μm-*GIS2*] strain a greater proportion of cells with an intermediate DNA content than the other genotypes. This therefore validated the decision to additionally assess the Sml1 protein levels in G1 arrested cells, to avoid the possibility that variations in Sml1 protein levels could be due to cells being in different in cell cycle phases.

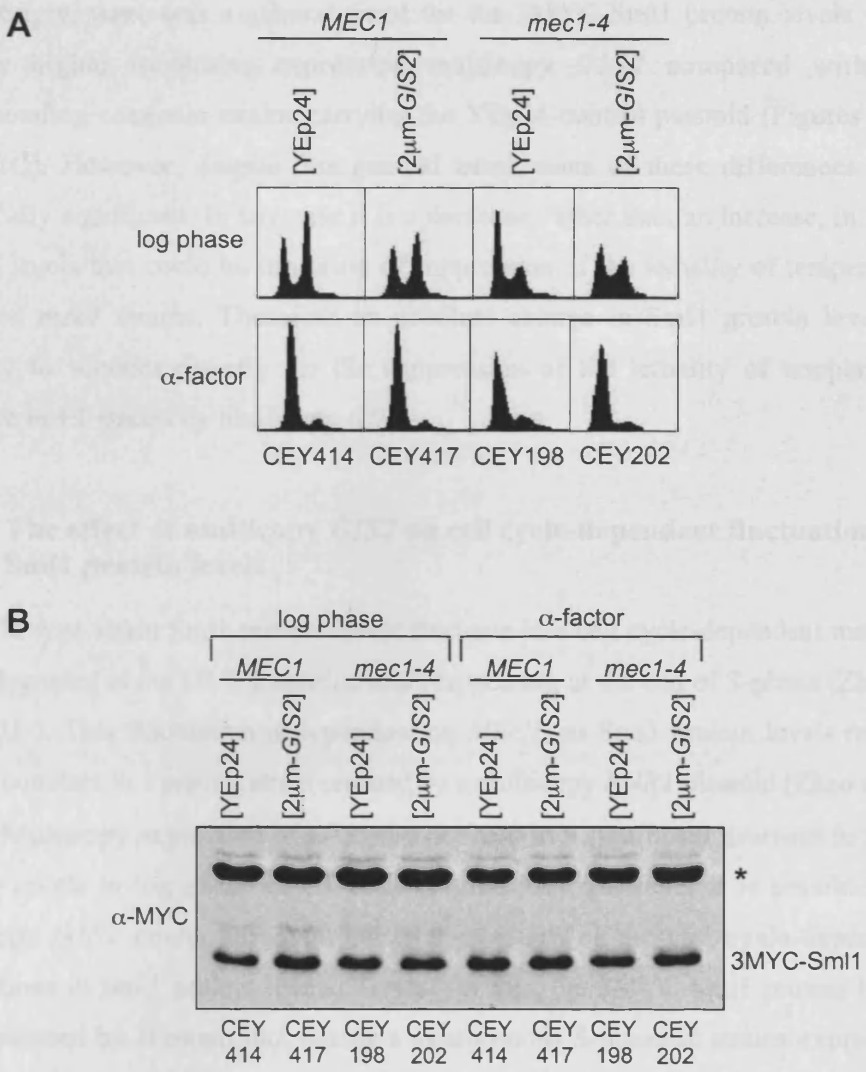
A
MEC1
mec1-4
[YEp24]
[2μm-GIS2]
[YEp24]
[2μm-GIS2]
log phase
α-factor
CEY414 CEY417 CEY198 CEY202
B
log phase
α-factor
MEC1
mec1-4
MEC1
mec1-4
[YEp24]
[2μm-GIS2]
[YEp24]
[2μm-GIS2]
[YEp24]
[2μm-GIS2]
[YEp24]
[2μm-GIS2]
α-MYC
*
3MYC-Sml1
CEY 414
CEY 417
CEY 198
CEY 202
CEY 414
CEY 417
CEY 198
CEY 202
C
The effect of multicopy GIS2 on Sml1 protein levels
Arbitrary Units
3.0
2.5
2.0
1.5
1.0
0.5
0.0
CEY414
CEY417
CEY198
CEY202
CEY414
CEY417
CEY198
CEY202
log phase
alpha factor

Interestingly, there was a general trend for the 3MYC-Sml1 protein levels to be slightly higher in strains expressing multicopy *GIS2* compared with the corresponding congenic strains carrying the YEp24 control plasmid (Figures 5.1B and 5.1C). However, despite this general trend, none of these differences were statistically significant. In any case it is a decrease, rather than an increase, in Sml1 protein levels that could be the cause of suppression of the lethality of temperature sensitive *mec1* strains. Therefore an absolute change in Sml1 protein levels is unlikely to account directly for the suppression of the lethality of temperature sensitive *mec1* strains by multicopy *GIS2*.

5.2.2 The effect of multicopy *GIS2* on cell cycle-dependent fluctuations in Sml1 protein levels

In a wild type strain Sml1 protein levels fluctuate in a cell cycle-dependent manner, being degraded at the G1/S transition and reappearing at the end of S-phase (Zhao *et al.*, 2001). This fluctuation is dependent on *MEC1,* as Sml1 protein levels remain mostly constant in a *mec1Δ* strain rescued by a multicopy *RNR1* plasmid (Zhao *et al.*, 2001). Multicopy expression of *GIS2* did not lead to a significant decrease in Sml1 protein levels in log phase or G1 cells (Figure 5.1). However it is possible that multicopy *GIS2* could, somehow, alter the pattern of the cell cycle-dependent fluctuations in Sml1 protein levels. To test for this, the 3MYC-Sml1 protein levels were assessed by Western blot during a synchronous S-phase in strains expressing *3MYC-SML1* and the *arg4::mec1-4* allele with the YEp24 control plasmid (CEY198) or the multicopy *GIS2* plasmid (CEY202), and the congenic wild type *arg4::MEC1* allele with the YEp24 control plasmid (CEY414).

Strains were grown overnight to mid-log phase in YPD at 23°C for the *arg4::mec1-4* allele and at 30°C for the *arg4::MEC1* strain. The following morning cells were arrested in G1 with α-factor, as described in the figure legends. Cells were then released into fresh YPD at the indicated temperature, and samples were taken every 10 minutes for protein extraction and FACS analysis. Proteins were separated on 15% polyacrylamide gels by SDS-PAGE and analysed by Western blot using an anti-MYC antibody. The signals from the 3MYC-Sml1 protein and the non-specific band were quantified from scanned images of the Western blots using ImageJ software.

The graphs show the levels of 3MYC-Sml1 in the Western blots, normalised to the non-specific band, and expressed relative to the α-factor sample which was set to 1.00.

As expected, the wild type *arg4::MEC1 3MYC-SML1* [YEp24] control strain (CEY414) showed a decrease in Sml1 protein levels as cells entered S-phase (Figure 5.2A). This decrease was not as large as that observed for the *MEC1 3MYC-SML1* strain (CEY96), which was probably due to differences in how synchronously the cells entered S-phase (compare the 20 minute time point in the FACS profiles in Figure 2.3B and Figure 5.2A). The *arg4::mec1-4 3MYC-SML1* [YEp24] strain (CEY198) also showed a decrease in Sml1 protein levels as cells entered S-phase at the permissive temperature of 23°C (Figure 5.2B). The magnitude of this decrease was similar to that seen for the *arg4::MEC1* strain in Figure 5.2A, although the timing was different, probably due to the fact that DNA replication is slower at 23°C than at 30°C. Therefore at the permissive temperature, when cells are viable, the *arg4::mec1-4* strain can downregulate Sml1 protein levels as expected.

The 3MYC-Sml1 protein levels were assessed during a synchronous S-phase in two independent experiments for strains *arg4::mec1-4 3MYC-SML1* [YEp24] strain (CEY198) and *arg4::mec1-4 3MYC-SML1* [2μm-*GIS2*] strain (CEY202) (Figures 5.3 and 5.4). The *arg4::mec1-4 3MYC-SML1* [YEp24] strain did not show a decrease in Sml1 protein levels as cells entered S-phase at the restrictive temperature of 30°C (Figure 5.3). Quantification of the 3MYC-Sml1 protein levels in both Western blots showed that by one hour after release from α-factor, the level of 3MYC-Sml1 had doubled (Figure 5.3). So, in cells undergoing DNA replication in the absence of Mec1 function, there was an accumulation of Sml1. However, the extent of Sml1 accumulation at later time points was different between the two repeats. The reasons for this are not clear.

In Figure 5.3A, as expected, the absence of a decrease in Sml1 after release from α-factor correlated with the accumulation of cells with an intermediate (between 1C and 2C) DNA content shown in the FACS profiles. In Figure 5.3B, however, the absence of a decrease in Sml1 after release from α-factor did not correlate with an accumulation of cells with an intermediate DNA content. The difference between the

FACS profiles in Figures 5.3A and 5.3B can be accounted for by day-to-day variation in the behaviour of the *arg4::mec1-4* strain. In the majority of cases, *arg4::mec1-4* cells with an intermediate DNA content accumulate in the first cell cycle after synchronous release from α-factor. However, occasionally these cells do complete successfully this first S-phase. In other *mec1* strains, *mec1-4* and *arg4::mec1-40*, cells do not reproducibly accumulate in S-phase in the first cell cycle after synchronous release from α-factor.

The absence of a decrease in Sml1 in both cases is consistent with the Mec1-4 protein having been inactivated by the temperature shift to 30°C. More significantly however, in Figure 5.3B the cells appear to successfully complete S-phase without degrading Sml1. This could be because these cells have sufficient remaining dNTP levels from their period of log phase growth before the α-factor arrest. Alternatively, this observation could suggest that there is residual activity of the Mec1-4 protein at 30°C that helps the cells progress through DNA replication, but without increasing dNTP levels.

In contrast, the *arg4::mec1-4 3MYC-SML1* [2μm-*GIS2*] strain (CEY202), did not show the same accumulation of 3MYC-Sml1 after release from α-factor as the *arg4::mec1-4 3MYC-SML1* [YEp24] strain (compare the graphs in Figures 5.3 and 5.4). Instead, the *arg4::mec1-4 3MYC-SML1* [2μm-*GIS2*] strain (CEY202) showed a slight decrease in Sml1 protein levels as cells entered S-phase (Figure 5.4). However, the magnitude of this decrease was less than that seen in wild type cells: at maximum a 35% drop in strain CEY202 compared with almost a 50% drop in strain CEY414 (compare the graphs in Figure 5.3A and Figure 5.4B). This difference is more significant if compared with the 3MYC-Sml1 fluctuations in the wild type strain shown in Figure 2.3, where the 3MYC-Sml1 protein levels drop to almost nothing. This strain (CEY96), shown in Figure 2.3, entered S-phase more synchronously than the wild type strain (CEY414) shown in Figure 5.3A, making this a better estimate of the magnitude of the cell cycle-dependent fluctuations in Sml1 protein levels in a wild type cell.

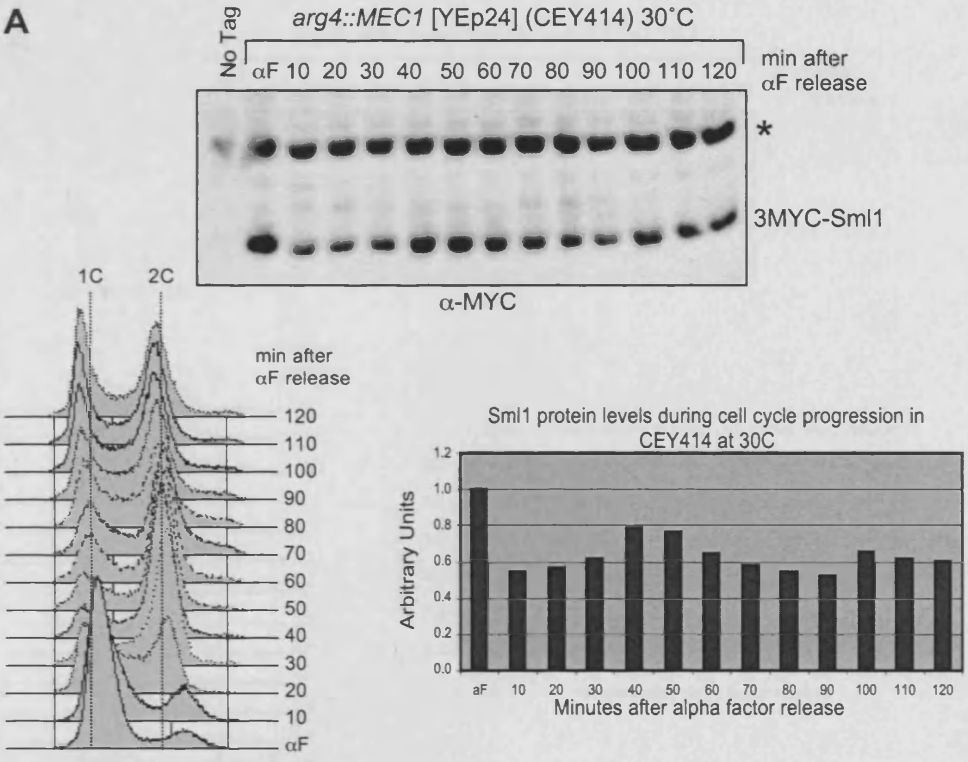
A
arg4::MEC1 [YEp24] (CEY414) 30˚C
No Tag
αF 10 20 30 40 50 60 70 80 90 100 110 120
min after αF release
*
3MYC-Sml1
α-MYC
1C
2C
min after αF release
120
110
100
90
80
70
60
50
40
30
20
10
αF
Sml1 protein levels during cell cycle progression in CEY414 at 30C
Arbitrary Units
1.2
1.0
0.8
0.6
0.4
0.2
0.0
aF 10 20 30 40 50 60 70 80 90 100 110 120
Minutes after alpha factor release

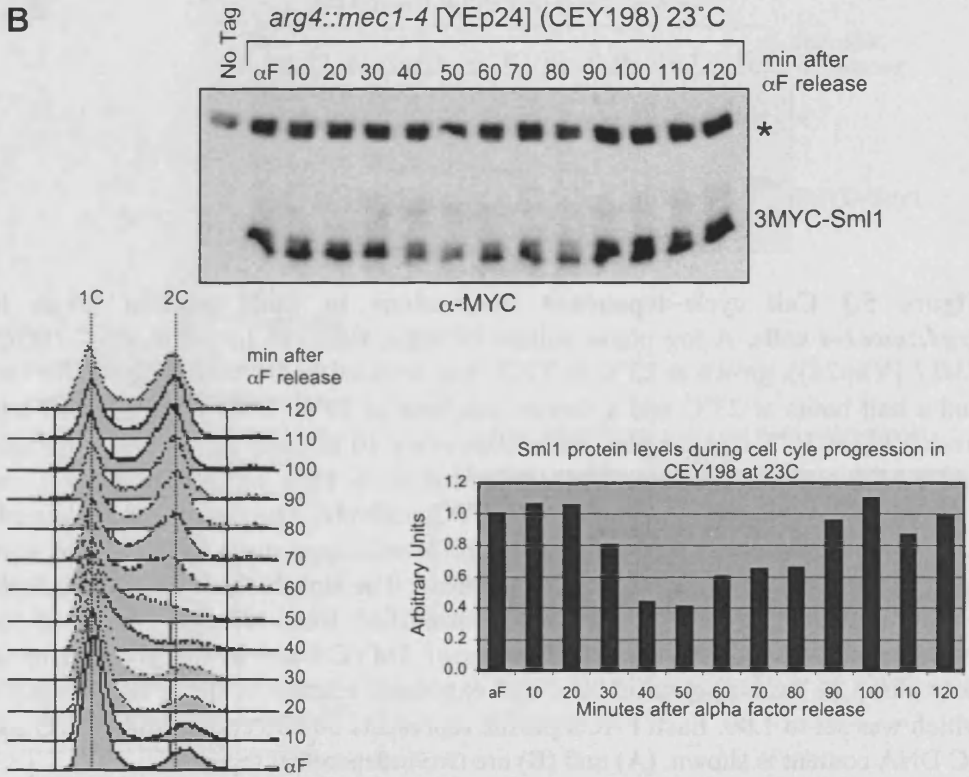
B
arg4::mec1-4 [YEp24] (CEY198) 23˚C
No Tag
αF 10 20 30 40 50 60 70 80 90 100 110 120
min after αF release
*
3MYC-Sml1
α-MYC
1C
2C
min after αF release
120
110
100
90
80
70
60
50
40
30
20
10
αF
Sml1 protein levels during cell cyle progression in CEY198 at 23C
Arbitrary Units
1.2
1.0
0.8
0.6
0.4
0.2
0.0
aF 10 20 30 40 50 60 70 80 90 100 110 120
Minutes after alpha factor release

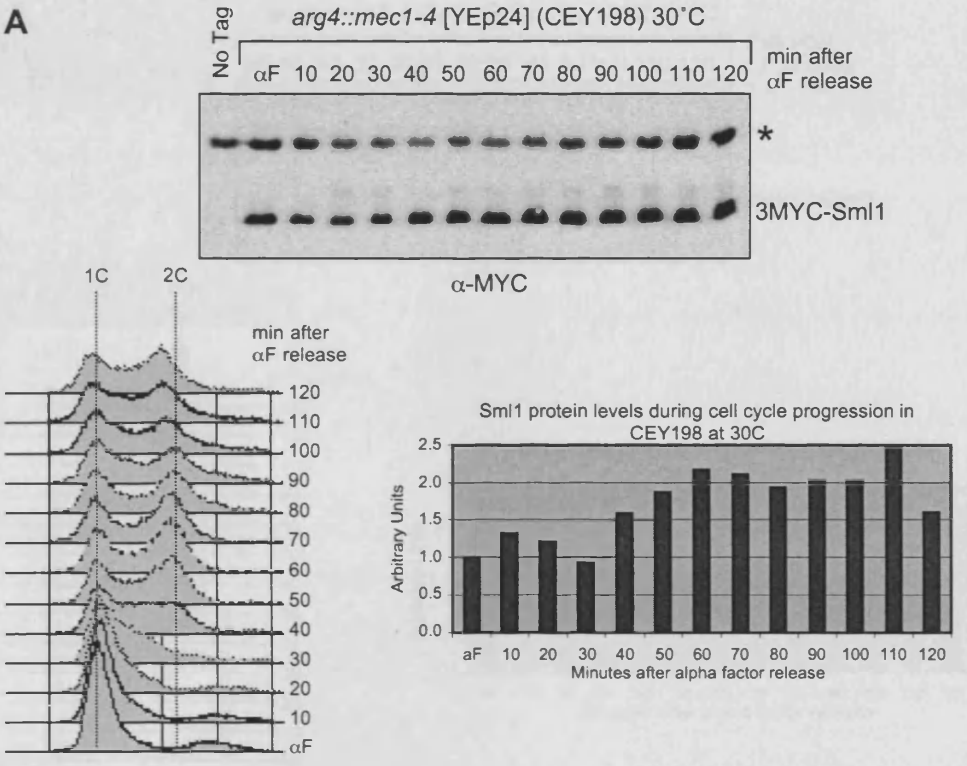
A
arg4::mec1-4 [YEp24] (CEY198) 30°C
No Tag
αF 10 20 30 40 50 60 70 80 90 100 110 120
min after αF release
*
3MYC-Sml1
α-MYC
1C
2C
min after αF release
120
110
100
90
80
70
60
50
40
30
20
10
αF
Sml1 protein levels during cell cycle progression in CEY198 at 30C
Arbitrary Units
2.5
2.0
1.5
1.0
0.5
0.0
aF 10 20 30 40 50 60 70 80 90 100 110 120
Minutes after alpha factor release

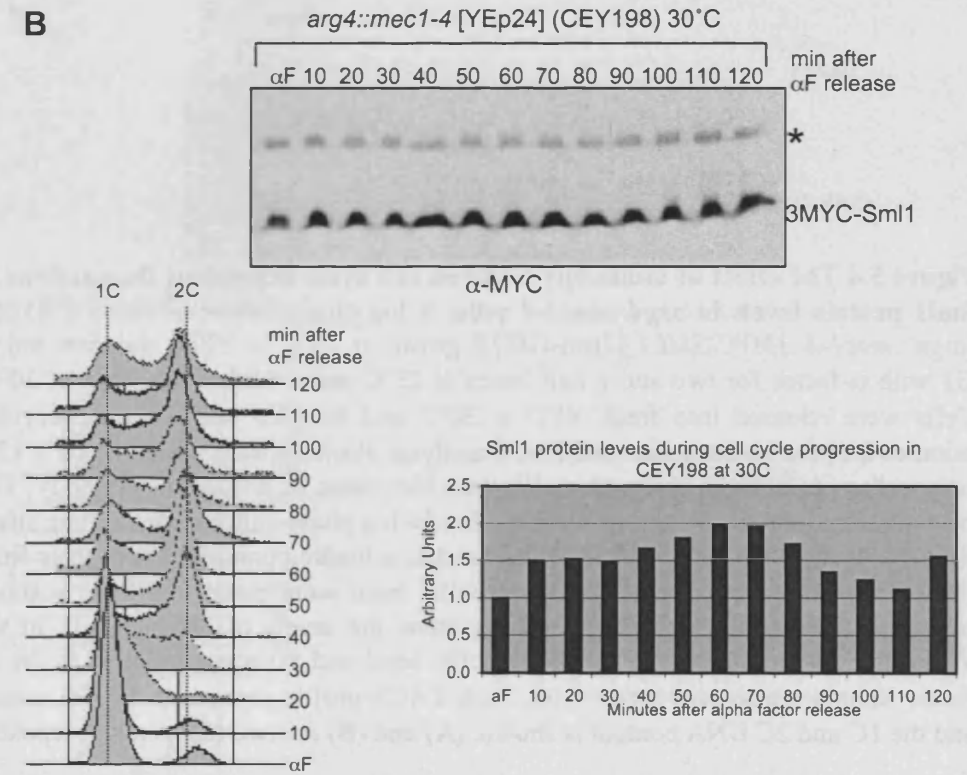
B
arg4::mec1-4 [YEp24] (CEY198) 30°C
αF 10 20 30 40 50 60 70 80 90 100 110 120
min after αF release
*
3MYC-Sml1
α-MYC
1C
2C
min after αF release
120
110
100
90
80
70
60
50
40
30
20
10
αF
Sml1 protein levels during cell cycle progression in CEY198 at 30C
Arbitrary Units
2.5
2.0
1.5
1.0
0.5
0.0
aF 10 20 30 40 50 60 70 80 90 100 110 120
Minutes after alpha factor release

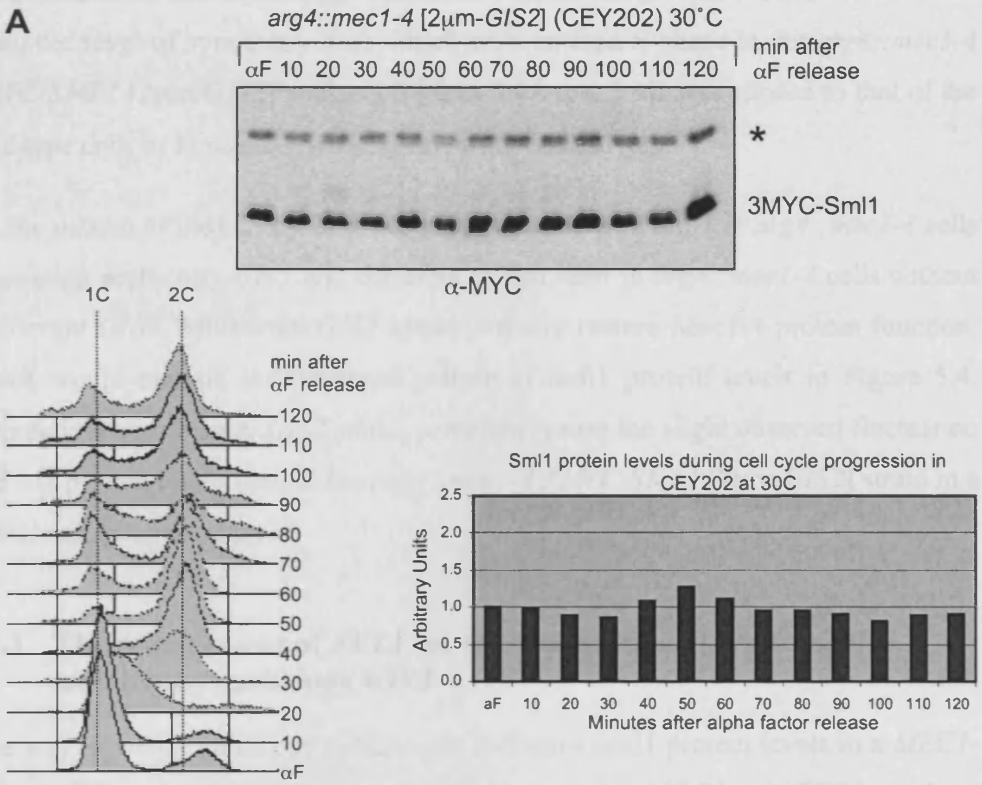
A
arg4::mec1-4 [2μm-GIS2] (CEY202) 30˚C
αF 10 20 30 40 50 60 70 80 90 100 110 120
min after αF release
*
3MYC-Sml1
α-MYC
1C
2C
min after αF release
120
110
100
90
80
70
60
50
40
30
20
10
αF
Sml1 protein levels during cell cycle progression in CEY202 at 30C
Arbitrary Units
2.5
2.0
1.5
1.0
0.5
0.0
aF 10 20 30 40 50 60 70 80 90 100 110 120
Minutes after alpha factor release

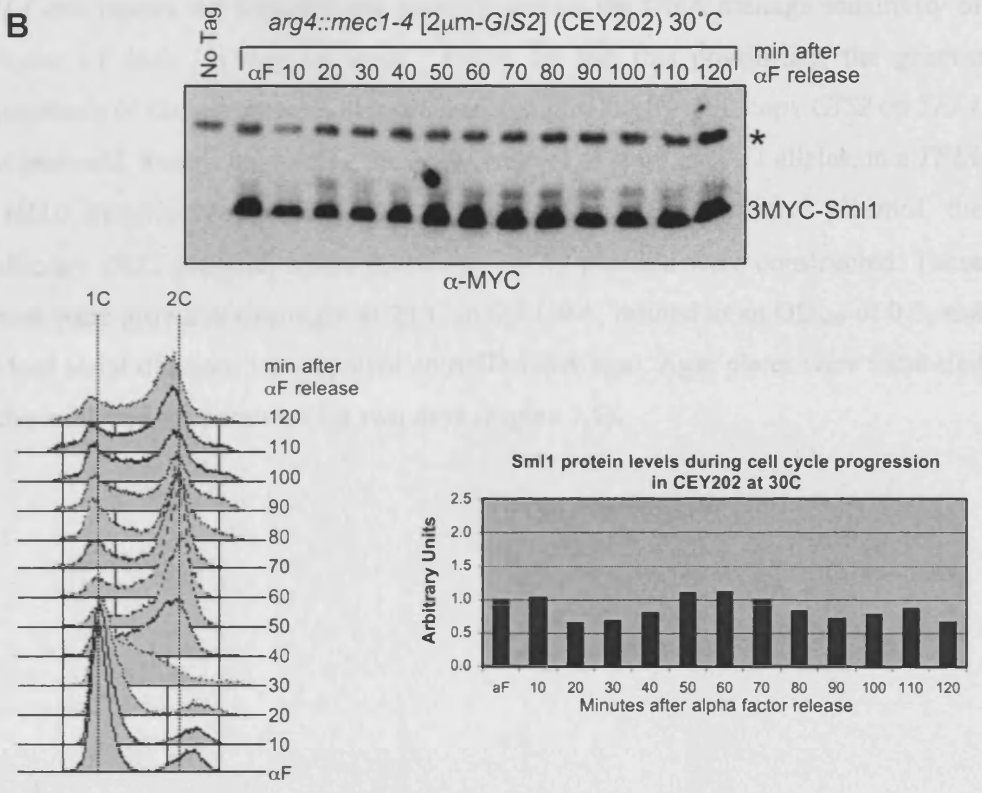
B
No Tag
arg4::mec1-4 [2μm-GIS2] (CEY202) 30˚C
αF 10 20 30 40 50 60 70 80 90 100 110 120
min after αF release
*
3MYC-Sml1
α-MYC
1C
2C
min after αF release
120
110
100
90
80
70
60
50
40
30
20
10
αF
Sml1 protein levels during cell cycle progression in CEY202 at 30C
Arbitrary Units
2.5
2.0
1.5
1.0
0.5
0.0
aF 10 20 30 40 50 60 70 80 90 100 110 120
Minutes after alpha factor release

Also, the level of synchrony with which cells entered S-phase in the *arg4::mec1-4 3MYC-SML1* [2μm-*GIS2*] strain in Figures 5.4A and 5.4B was similar to that of the wild type cells in Figure 2.3, making this a fair comparison.

So, the pattern of the cell cycle-dependent fluctuations in Sml1 in *arg4::mec1-4* cells expressing multicopy *GIS2* was different to that seen in *arg4::mec1-4* cells without multicopy *GIS2*. Multicopy *GIS2* could partially restore Mec1-4 protein function, which would explain the observed pattern of Sml1 protein levels in Figure 5.4. Alternatively, multicopy *GIS2* could, somehow, cause the slight observed fluctuation in Sml1 protein levels seen in the *arg4::mec1-4 3MYC-SML1* [2μm-*GIS2*] strain in a *MEC1*-independent manner.

5.2.3 The requirement of *TEL1* for the suppression of *arg4::mec1-4* lethality by multicopy *GIS2*

One way in which multicopy *GIS2* might influence Sml1 protein levels in a *MEC1*-independent manner is by increasing Tel1 activity. *MEC1* and *TEL1* perform partially redundant roles in the response to genotoxic stress. So, over-expression of *TEL1* can rescue the lethality and partially rescue the DNA damage sensitivity of deletion of *MEC1* (Morrow *et al.*, 1995). To test this possibility, the genetic dependence of the suppression of *arg4::mec1-4* lethality by multicopy *GIS2* on *TEL1* was assessed. Strains expressing the *arg4::mec1-4* or *arg4::MEC1* alleles, in a *TEL1* or *tel1Δ* genetic background, and with either the YEp24 control plasmid, the multicopy *GIS2* plasmid, or the multicopy *RNR1* plasmid were constructed. These strains were grown at overnight at 23°C in SD-URA, diluted to an OD_{600} of 0.5, and 10-fold serial dilutions were spotted onto SD-URA agar. Agar plates were incubated at the indicated temperatures for two days (Figure 5.5).

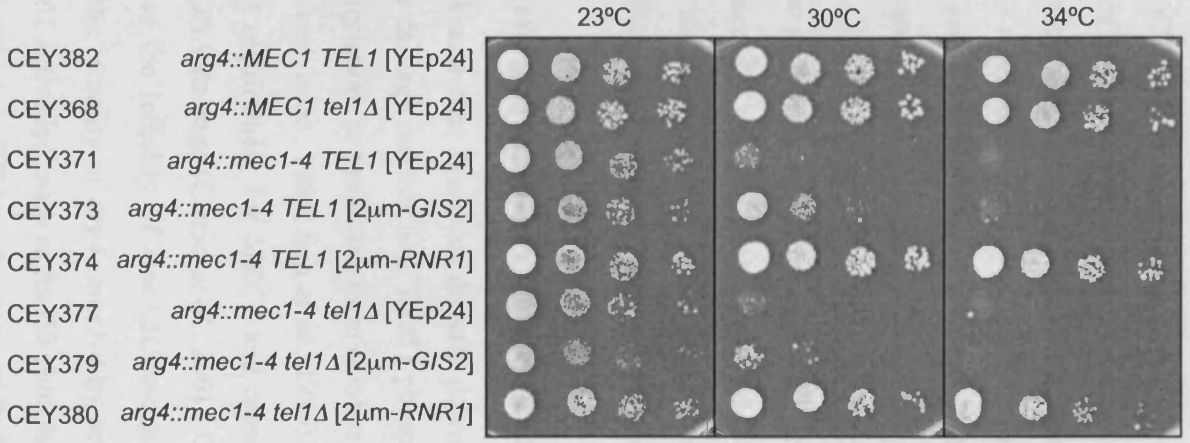

Figure 5.5 The requirement of *TEL1* for the suppression of *arg4::mec1-4* lethality by multicopy *GIS2*. The indicated strains were grown overnight at 23˚C in SD-URA. The following morning each culture was diluted to OD_{600} of 0.5, and 10-fold serial dilutions were spotted onto SD-URA agar. Agar plates were incubated at the indicated temperature for two days. The plasmids used were YEp24 (empty vector), pCLE8 (2μm-*GIS2*) and pCLE11 (2μm-*RNR1*).

Multicopy *GIS2* improved the viability of the *arg4::mec1-4 TEL1* strain at 30°C as expected (Figure 5.5; compare CEY371 and CEY373). However, multicopy *GIS2* had less of an effect on the viability of the *arg4::mec1-4 tel1Δ* strain (Figure 5.5; compare CEY373 and CEY379). Multicopy *RNR1* restored growth to wild type levels in the *arg4::mec1-4* strain, irrespective of the presence of *TEL1* (Figure 5.5; compare CEY371 with CEY374, and CEY377 with CEY380). Therefore, the partial suppression of *arg4::mec1-4* lethality by multicopy *GIS2* is weaker in the absence of *TEL1*. One explanation for this observation is that the effect of multicopy *GIS2* on *arg4::mec1-4* requires the activity of the Tel1 protein. Alternatively, it could be that the effect of multicopy *GIS2* is too weak to overcome the loss of both Mec1 and Tel1 function. A *mec1Δ tel1Δ sml1Δ* strain is more sensitive to genotoxic stress than a *mec1Δ TEL1 sml1Δ* strain (Morrow *et al.*, 1995). The hypomorphic *mec1* mutant, *mec1-21*, also shows a greater decrease in telomere length when combined with *tel1Δ* than either *mec1-21* or *tel1Δ* strains do alone (Ritchie *et al.*, 1999). Investigation of the effect of multicopy *GIS2* on the expected downstream effects of *TEL1* activation should help distinguish between these two possibilities.

5.2.4 The effect of multicopy *GIS2* on Rad53 activation

Rad53 is a kinase that functions directly downstream of Mec1 and Tel1 (Section 1.3.3). DNA damage induces both Rad53 phosphorylation by Mec/Tel1 and Rad53 autophosphorylation, so the active form exhibits a mobility shift detectable by SDS-PAGE (Pellicioli *et al.*, 1999; Sun *et al.*, 1996). Over-expression of *TEL1* bypasses the essential requirement for *MEC1* and causes activation of Rad53 even in the absence of DNA damage (Clerici *et al.*, 2001). Over-expression of *RAD53* itself can also suppress the lethality of *mec1Δ*(Sanchez *et al.*, 1996). If multicopy *GIS2* suppresses the lethality of *arg4::mec1-4* by activating Tel1 then the downstream effects of Tel1 activation, such as Rad53 phosphorylation, should be seen. Therefore, the effect of multicopy *GIS2* on the status of Rad53 phosphorylation was assessed.

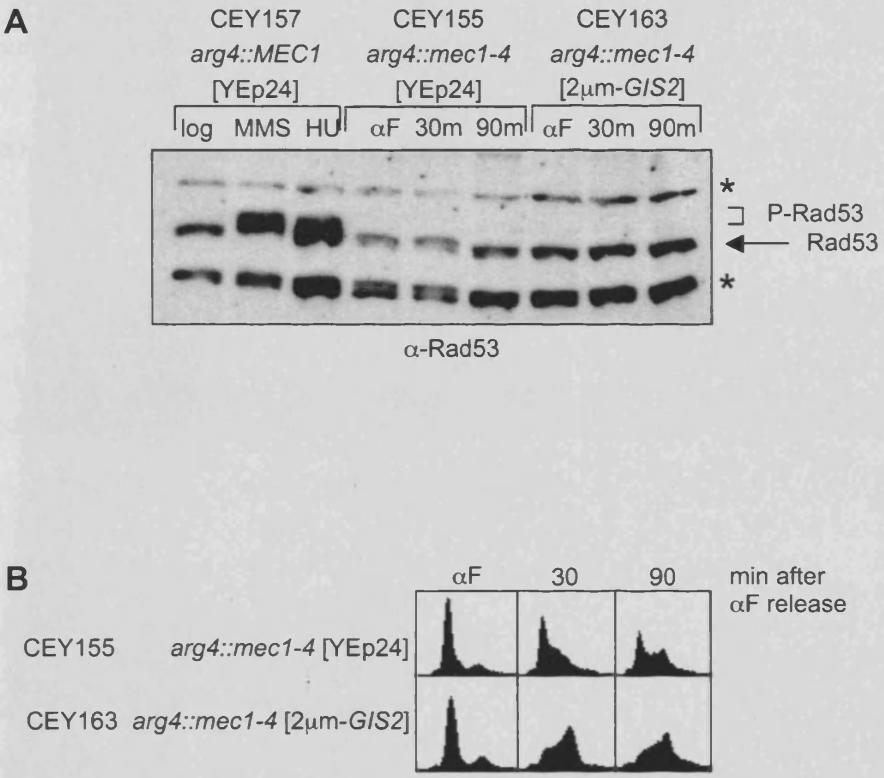

Figure 5.6 Multicopy *GIS2* does not lead to detectable Rad53 activation. Log phase cultures of strains CEY155 (*arg4::mec1-4* [YEp24]) and CEY163 (*arg4::mec1-4* [2μm-*GIS2*]), grown at 23°C in YPD, were arrested in G1 with α-factor for two and a half hours at 23°C and a further one hour at 30°C. Cells were released into fresh YPD at 30°C and samples were taken for protein extraction and FACS analysis at the indicated time points. Protein extracts were also made from control samples from log phase cultures of strain CEY157 (*arg4::MEC1* [YEp24]), treated with 0.03% MMS or 50 mM HU for three hours at 30°C. **A)** Proteins were separated on a 8% polyacrilamide gel and analysed by Western blot using an anti-Rad53 antibody. * denotes two non-specific bands. The band corresponding to the Rad53 protein and the slower migrating bands corresponding to the phosphorylated Rad53 protein (P-Rad53) are indicated. **B)** The FACS profiles corresponding to the protein extracts from CEY155 and CEY163 analysed in (A). Each FACS profile represents 50,000 counts.

Strains expressing the *arg4::mec1-4* allele with either the YEp24 control plasmid (CEY155) or the multicopy *GIS2* plasmid (CEY163) were grown overnight to mid-log phase at 23°C in YPD. Cells were then arrested in G1 with α-factor for two and a half hours at 23°C and a further one hour at 30°C. Cells were released into fresh YPD at 30°C and samples were taken for protein extraction and FACS analysis at the indicated time points (Figure 5.6). Control samples were also made from log phase cultures of strain CEY157 (*arg4::MEC1* [YEp24]), treated with 0.03% MMS or 50 mM HU as indicated.

Although a significant Rad53 mobility shift was seen in the damage treated controls (CEY157), no Rad53 mobility shift was seen in the *arg4::mec1-4* [YEp24] (CEY155) or the *arg4::mec1-4* [2μm-*GIS2*] (CEY163) strains in either G1 (αF lanes) or S-phase (30m, 90m lanes) (Figure 5.6A). The FACS profiles confirmed that the protein extracts analysed in Figure 5.6A were made from cells that were in either G1 or S-phase (Figure 5.6B). Therefore, the suppression of *arg4::mec1-4* by multicopy *GIS2* is unlikely to be via *TEL1*-dependent Rad53 activation.

5.2.5 The requirement of *DUN1* for the suppression of *mec1-4* lethality by multicopy *GIS2*

It is possible that *GIS2*-dependent activation of Tel1 could influence Sml1 protein levels, but without inducing detectable Rad53 activation. Sml1 degradation is dependent on a kinase cascade, normally initiated by Mec1: Mec1 activates Rad53, which in turn activates Dun1, and Dun1 phosphorylates Sml1 (Uchiki *et al.*, 2004; Zhao & Rothstein, 2002). The phosphorylated form of Sml1 is then targeted for degradation. If *GIS2*-dependent suppression of the lethality of the temperature sensitivity of *mec1* strains depends on a reduction of Sml1 protein levels through its normal regulatory pathways then the suppression should be genetically dependent on *DUN1*. To test for this a *mec1-4 dun1Δ* double mutant needed to be constructed. Deletion of *DUN1* shows synthetic growth defects with hypomorphic *mec1* mutants (Zhao & Rothstein, 2002), and Mec1 function is compromised in *mec1-4* and *mec1-40* strains even at the permissive temperature (Figure 4.6). Therefore, it was not clear whether the *arg4::mec1-4 dun1Δ* double mutant would be viable. To ensure this could be accurately assessed, the double mutant was constructed using the *mec1-4*

allele in the endogenous locus. This allele does not carry the *mec1Δ* mutation and so, assuming no synthetic lethality, dissection of tetrads from the *MEC1/mec1-4 dun1Δ/DUN1* heterozygous diploid should give four viable spores at 23°C. Indeed, this is what was observed (data not shown) indicating that the *mec1-4 dun1Δ* strain was viable at 23°C.

To assess the genetic dependence of the suppression of *mec1-4* lethality by multicopy *GIS2* on *DUN1*, strains expressing *MEC1* or *mec1-4*, in a *DUN1* or *dun1Δ* genetic background, and with either the YEp24 control plasmid or the multicopy *GIS2* plasmid were constructed. These strains were grown overnight at 23°C in SD-URA, diluted to an OD_{600} of 0.5, and 10-fold serial dilutions were spotted onto SD-URA agar. Agar plates were incubated at the indicated temperatures for two days (Figure 5.7). Although the *mec1-4 dun1Δ* double mutant was viable at 23°C it had a lower restrictive temperature compared with the *mec1-4* single mutant (Figure 5.7; compare CEY689 and CEY693). The presence of the multicopy *GIS2* plasmid partially suppressed the lethality of *mec1-4 DUN1* at 34°C as expected (Figure 5.7; compare CEY691 and CEY689). The presence of the multicopy *GIS2* plasmid also suppressed the lethality of *mec1-4 dun1Δ*, but only at 30°C and not at 34°C (Figure 5.7; compare CEY695 and CEY693). Given the weak suppression of the lethality of temperature sensitive *mec1* strains conferred by multicopy *GIS2* and the effect of *dun1Δ* in lowering the restrictive temperature of *mec1-4*, these data show that suppression of *mec1-4* lethality by multicopy *GIS2* does not depend on *DUN1*.

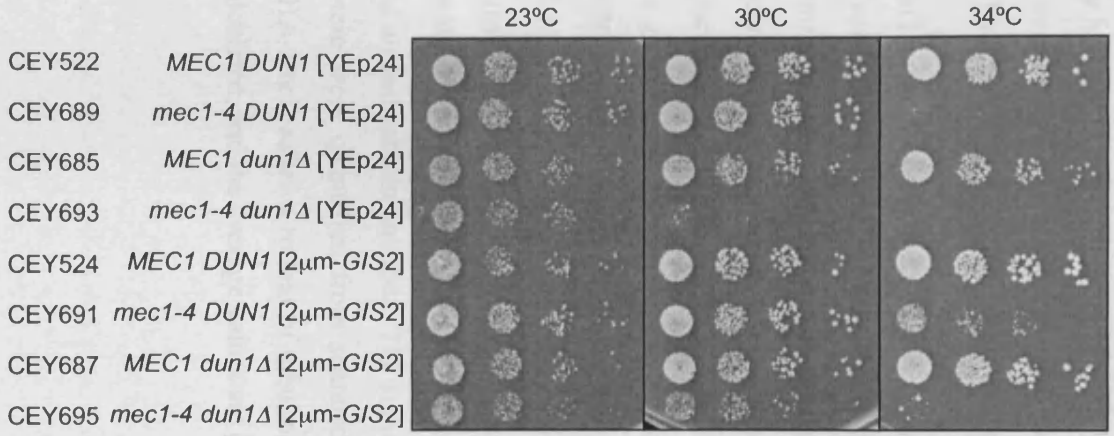

Figure 5.7 The requirement of *DUN1* for the suppression of *arg4::mec1-4* lethality by multicopy *GIS2*. The indicated strains were grown overnight at 23˚C in SD-URA. The following morning each culture was diluted to OD_{600} of 0.5, and 10-fold serial dilutions were spotted onto SD-URA agar. Agar plates were incubated at the indicated temperature for two days. The plasmids used were YEp24 (empty vector) and pCLE8 (2μm-*GIS2*).

5.2.6 The effect of multicopy *GIS2* on Rnr1 protein levels

Increased *RNR1* expression is a well-known mechanism of suppressing *mec1Δ* lethality (Desany *et al.*, 1998). Therefore, multicopy expression of *GIS2* could suppress the lethality of temperature sensitive *mec1* strains by somehow increasing Rnr1 protein levels. Additionally, the Sml1 protein has a short half-life and is stabilised by binding to Rnr1 (Zhao *et al.*, 2001). Therefore the observation that cells expressing multicopy *GIS2* tended to have higher Sml1 proteins levels could be indicative of increased levels of the large RNR subunit (Rnr1 or Rnr3).

The HA-Rnr1 protein levels were assessed just in log phase cells, as there is no detectable variation in Rnr1 protein levels during the cell cycle (L. Johnston, personal communication). To do this, strains expressing *RNR1* with an N-terminal HA tag (Section 2.10.3) and the *arg4::mec1-4* or *arg4::MEC1* alleles, with either the YEp24 control plasmid or the multicopy *GIS2* plasmid were constructed. These strains were grown overnight to mid-log phase at 23°C in YPD. Each culture was shifted to 30°C for four hours to assess HA-Rnr1 protein levels in a log phase culture with the Mec1-4 protein inactivated. Samples were taken from these cultures for protein extraction and FACS analysis. Proteins were separated on a 10% polyacrylamide gel by SDS-PAGE and analysed by Western blot using an anti-HA antibody and an anti-tubulin antibody. The signals from the HA-Rnr1 protein and the tubulin protein were quantified from scanned images of the Western blots. The amount of HA-Rnr1, relative to that of tubulin, from four independent experiments was then calculated, and the average values are presented in Figure 5.8.

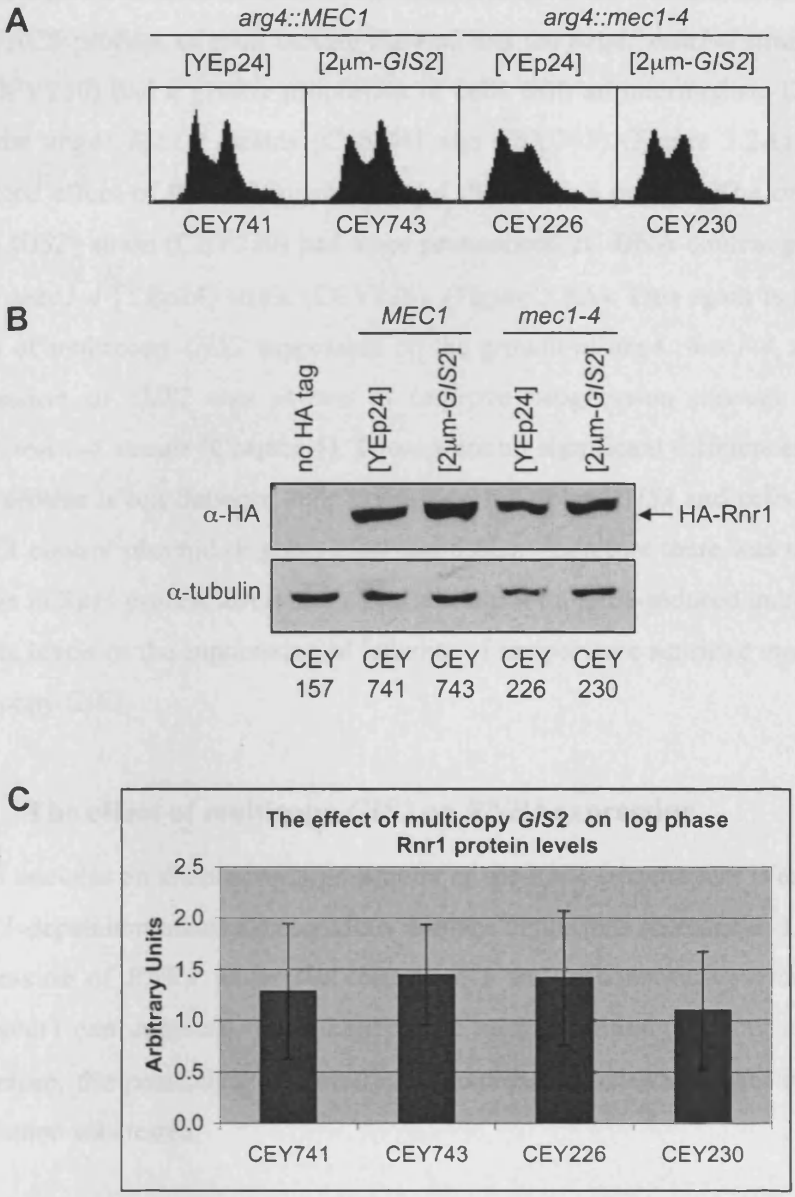

Figure 5.8 Multicopy *GIS2* does not lead to an increase in Rnr1 protein levels. The indicated strains were grown overnight to mid-log phase at 23°C in YPD. Each culture was shifted to 30°C for four hours, before samples were taken for protein extraction and FACS analysis. **A)** The FACS profiles that correspond to the protein samples analysed in (B). Each FACS profile represents 50,000 counts. **B)** Proteins were separated on a 10% polyacrilamide gel and analysed by Western blot. The blot was probed sequentially using an anti-HA antibody and an anti-tubulin antibody. **C)** The signals from the HA-Rnr1 protein and the α-tubulin protein were quantified from scanned images of the Western blots. The graph shows the average levels of the HA-Rnr1 protein, normalised to the tubulin loading control and calculated from four independent experiments. The error bars show ± one standard error of the mean.

The FACS profiles of each culture showed that the *arg4::mec1-4* strains (CEY226 and CEY230) had a greater proportion of cells with an intermediate DNA content than the *arg4::MEC1* strains (CEY741 and CEY743) (Figure 5.2A). This is the expected effect of thermal inactivation of the Mec1-4 protein. The *arg4::mec1-4* [2μm-*GIS2*] strain (CEY230) had more pronounced 2C DNA content peak than the *arg4::mec1-4* [YEp24] strain (CEY226), (Figure 5.8A). This again is the expected effect of multicopy *GIS2* expression on the growth of *arg4::mec1-4*, as multicopy expression of *GIS2* was shown to improve progression through S-phase in *arg4::mec1-4* strains (Chapter 4). There were no significant differences in the HA-Rnr1 protein levels between cells expressing multicopy *GIS2* and cells carrying the YEp24 control plasmid (Figures 5.8B and 5.8C). Therefore there was no detectable change in Rnr1 protein levels that could account for a *GIS2*-induced increase in Sml1 protein levels or the suppression of lethality of temperature sensitive *mec1* strains by multicopy *GIS2*.

5.2.7 The effect of multicopy *GIS2* on *RNR3* expression

RNR3 encodes an alternative large subunit of the RNR enzyme that is expressed in a *MEC1*-dependent manner under DNA damage conditions (Elledge & Davis, 1990). Expression of *RNR3* under the control of a strong constitutive promoter (GAP promoter) can suppress the lethality of a *mec1Δ* strain (Desany *et al.*, 1998). Therefore, the possibility that multicopy expression of *GIS2* might induce *RNR3* expression was tested.

Strains expressing the *arg4::mec1-4* or *arg4::MEC1* alleles, with either the YEp24 control plasmid or the multicopy *GIS2* plasmid were grown overnight at 23°C to mid-log phase in YPD. Half of each culture was shifted to 30°C for four hours to assess *RNR3* mRNA levels in a mid-log phase culture with the Mec1-4 protein inactivated. As a control, the other half of each culture was shifted to 30°C for 1 hour to inactivate the temperature sensitive Mec1 protein, before 50 mM HU (a condition expected to induce *RNR3* expression) was added for a further 3 hours. Samples were taken from these cultures for RNA extraction. RNA samples were separated on a 1.2% agarose gel and analysed by Northern blot. The blots were probed sequentially

for *RNR3* (2610 bases) and *RPB4* (RNA polymerase II subunit loading control; 666 bases).

RNR3 expression is induced by HU treatment in both *arg4::MEC1* and *arg4::mec1-4* strains (Figure 5.9A). Quantification of the *RNR3* signal, normalised to the *RPB4* signal, showed roughly a 3.5 fold induction of *RNR3* mRNA in all four cultures. This increase is considerably less than expected, as a 100-fold induction in *RNR3* expression has been shown previously upon treatment with the UV-mimetic 4-nitroquinoline (4-NQO) (Elledge & Davis, 1990).

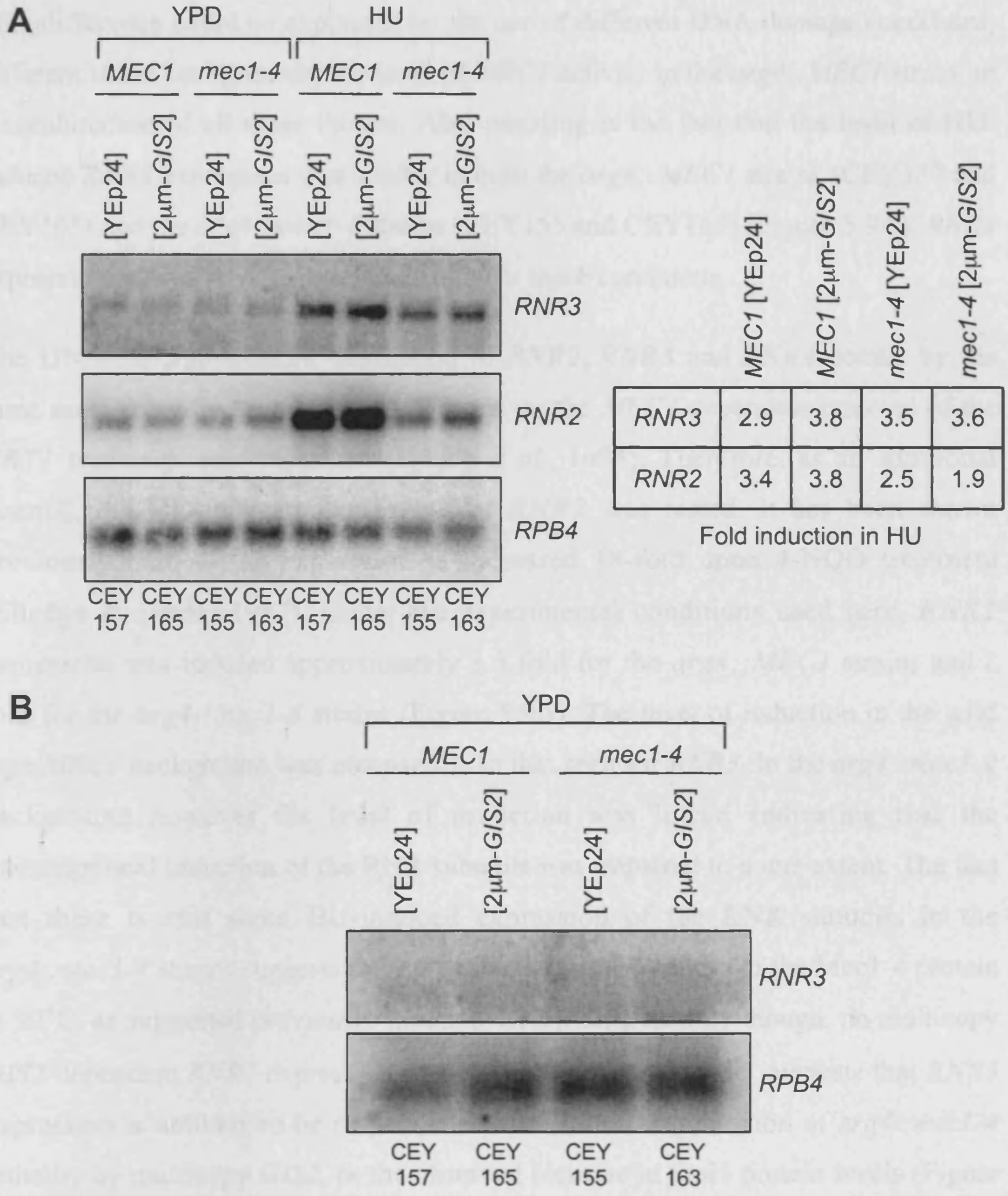

Figure 5.9 Multicopy *GIS2* does not lead to detectable expression of *RNR3*. The indicated strains were grown overnight to mid-log phase at 23°C in YPD. Half of each culture was shifted to 30°C for four hours. The other half was shifted to 30°C for one hour, and then 50 mM HU was added for a further three hours. Samples were taken from these cultures for RNA extraction. RNA samples were separated on 1.2% agarose gels and analysed by Northern blot. **A)** Northern blot of the RNA samples from the HU and YPD cultures. The same blot was probed sequentially for *RNR3* (2610 bases), *RNR2* (1200 bases) and *RPB4* (RNA polymerase II subunit loading control; 666 bases). The fold induction of *RNR3* and *RNR2* expression in HU, after normalisation to the RPB4 loading control, for each strain is shown in the table. **B)** Northern blot with the RNA samples from just the YPD cultures to get a longer exposure of the *RNR3* signal. The same blot was probed sequentially for *RNR3* and *RPB4*.

This difference could be explained by the use of different DNA damage conditions, different strain backgrounds, the level of *MEC1* activity in the *arg4::MEC1* strain, or a combination of all these factors. Also puzzling is the fact that the level of HU-induced *RNR3* expression was similar in both the *arg4::MEC1* strains (CEY157 and CEY165) and the *arg4::mec1-4* strains (CEY155 and CEY163) (Figure 5.9A): *RNR3* expression should be *MEC1*-dependent under these conditions.

The DNA-damage-induced expression of *RNR2*, *RNR3* and *RNR4* occurs by the same mechanism in each case and depends on the *MEC1*-dependent removal of the *CRT1* transcriptional repressor (Huang *et al.*, 1998). Therefore, as an additional control, the HU-induced expression of *RNR2* was tested. It has been shown previously that *RNR2* expression is increased 18-fold upon 4-NQO treatment (Elledge & Davis, 1987). Under the experimental conditions used here, *RNR2* expression was induced approximately 3.5 fold for the *arg4::MEC1* strains and 2 fold for the *arg4::mec1-4* strains (Figure 5.9A). The level of induction in the wild type *MEC1* background was comparable to that seen for *RNR3*. In the *arg4::mec1-4* background however the level of induction was lower, indicating that the transcriptional induction of the RNR subunits was impaired to some extent. The fact that there is still some HU-induced expression of the RNR subunits in the *arg4::mec1-4* strains suggests there was some residual activity of the Mec1-4 protein at 30°C, as suggested previously (Section 4.3.1). Significantly though, no multicopy *GIS2*-dependent *RNR3* expression was seen (Figure 5.9B). This suggests that *RNR3* expression is unlikely to be responsible either for the suppression of *arg4::mec1-4* lethality by multicopy *GIS2*, or the observed increase in Sml1 protein levels (Figure 5.1).

5.2.8 The effect of multicopy *GIS2* on *RNR1* expression

Another key mechanism known to be involved in regulating dNTP availability is the induction of *RNR1* transcription at the G1/S transition (Section 1.5.2). Delaying the initiation of origin firing relative to *RNR1* induction allows for a prolonged period of increased dNTP synthesis before DNA replication starts. For example, holding a *dbf4-ts* mutant at the restrictive temperature after release from α-factor allows *RNR1* transcription but prevents origin firing. When replication is then allowed to proceed

in HU at the permissive temperature, cells that were held at the restrictive temperature show an extended period of DNA synthesis compared with those that progress directly from α-factor to HU (Koc *et al.*, 2004). Such a period of increased dNTP synthesis before the onset of DNA replication has been shown to bypass the essential function of *mec1Δ*. So *cln1Δ cln2Δ*, which delays the transition into S-phase, can rescue the lethality of *mec1Δ* (Vallen & Cross, 1999). So, multicopy expression of *GIS2* could alter the pattern, in either the level or the timing, of *RNR1* induction at the G1/S transition. To test for this, the level and timing of *RNR1* mRNA induction after synchronous release from α-factor was measured by Northern blot (Figure 5.10).

Strains expressing the *arg4::mec1-4* or the *arg4::MEC1* alleles, with either the YEp24 control plasmid or the multicopy *GIS2* plasmid were grown overnight to mid-log phase at 23°C in YPD. The cells were arrested in G1 with α-factor for two and a half hours at 23°C and then for a further hour at 30°C. The cells were then released from α-factor into fresh YPD at 30°C, and samples were taken every 10 minutes for RNA extraction and FACS analysis. RNA samples were separated on a 1.2% agarose gel and analysed by Northern blot. The same blot was probed sequentially for *ACT1* (actin loading control) and *RNR1*, and these signals were quantified using ImageJ software. The graph shows the level of *RNR1* mRNA, normalised to the *ACT1* loading control and expressed relative to the α-factor sample which was set to 1.00.

The FACS profiles showed the expected accumulation of cells with an intermediate DNA content in the *arg4::mec1-4* [YEp24] strain (CEY155), and also the improvement of S-phase progression in the *arg4::mec1-4* [2μm-*GIS2*] strain (CEY163) (Figure 5.10A). There was a delay in start of bulk DNA replication in the *arg4::mec1-4* [YEp24] strain (CEY155) compared with the other three strains (Figure 5.10A; profiles at 20 minutes). Although this is sometimes observed in the temperature sensitive *mec1* strains, it is not reproducible and probably represents day-to-day variation in the behaviour of these strains.

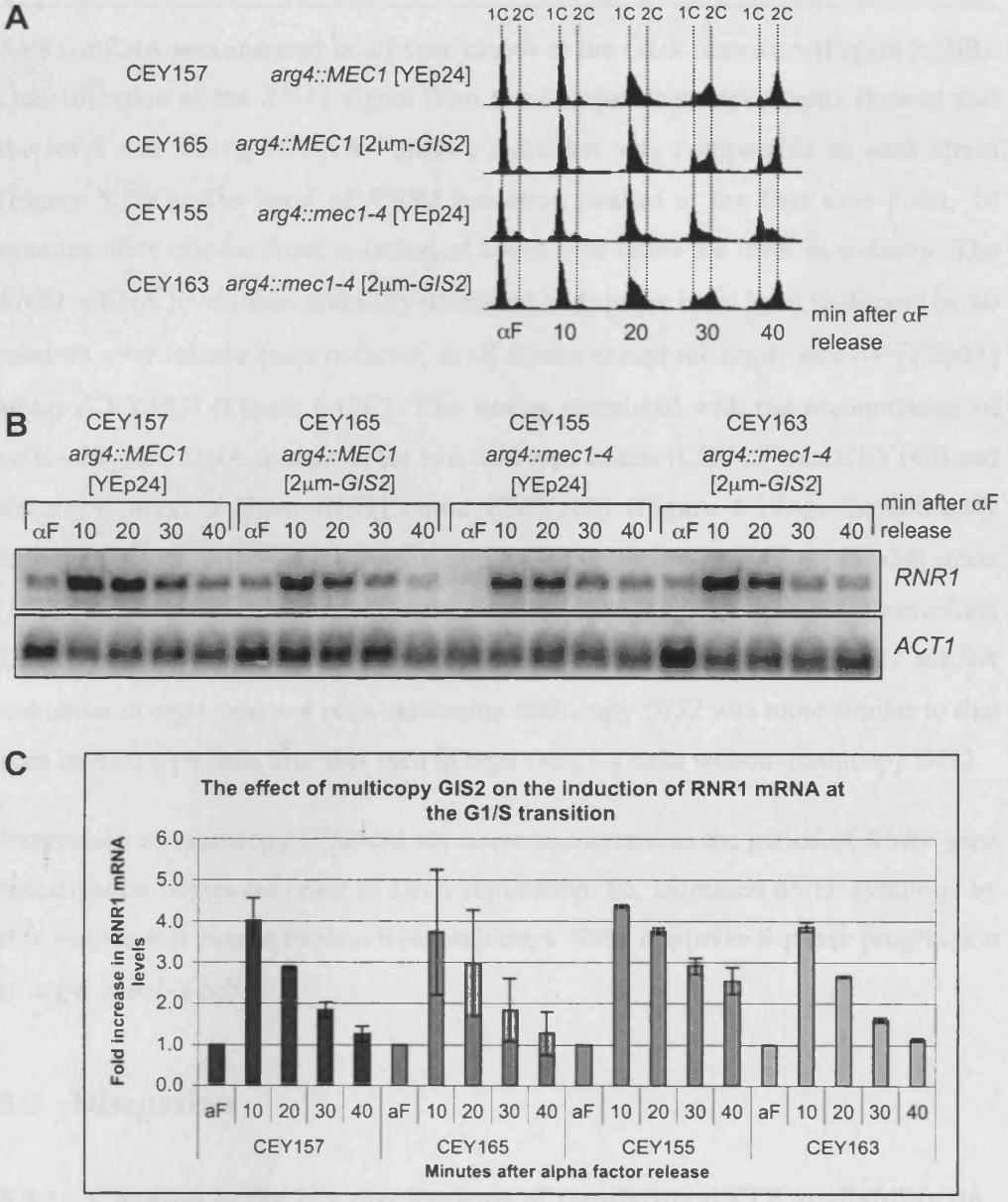

Figure 5.10 Multicopy *GIS2* does not lead to a change in the level or timing of *RNR1* mRNA induction at G1/S. Log phase culture of the indicated strains, grown at 23°C in YPD, were arrested in G1 with α-factor for two and a half hours at 23°C and a further one hour at 30°C. Cells were released into fresh YPD at 30°C and samples were taken every 10 minutes for RNA extraction and FACS analysis. **A)** The FACS profiles corresponding to the RNA samples analysed in (B). The 1C and 2C DNA content is indicted. Each FACS profile represents 50,000 counts. **B)** RNA samples were separated on a 1.2% agarose gel and analysed by Northern blot. The same blot was probed sequentially for *ACT1* (actin loading control; 1138 bases) and *RNR1* (2667 bases). **C)** The *RNR1* and *ACT1* signals were quantified. The graph shows the levels of *RNR1* mRNA, normalised to the *ACT1* signal and for each strain expressed relative to the α-factor sample which was set to 1.00. The average of two independent experiments is shown and the error bars represent the range of the fold induction values obtained.

RNR1 mRNA was induced in all four strains at the G1/S transition (Figure 5.10B). Quantification of the *RNR1* signal from two independent experiments showed that the level and timing of *RNR1* mRNA induction was comparable in each strain (Figure 5.10C). The level of *RNR1* induction peaked at the first time point, 10 minutes after release from α-factor, at about four times the level in α-factor. The *RNR1* mRNA levels then gradually decreased back to the basal level (α-factor) by 40 minutes after release from α-factor, in all strains except the *arg4::mec1-4* [YEp24] strain (CEY155) (Figure 5.10C). This timing correlated with the accumulation of cells with a 2C DNA content in the two wild type strains (CEY157 and CEY165) and the *arg4::mec1-4* [2μm-*GIS2*] strain (CEY163) (Figure 5.10A). Significantly however, *RNR1* mRNA levels remained elevated in the *arg4::mec1-4* [YEp24] strain (CEY155), which correlated with the accumulation of cells with an intermediate DNA content (Figures 5.10A and 5.10C). Overall, the pattern of *RNR1* mRNA induction in *arg4::mec1-4* cells expressing multicopy *GIS2* was more similar to that seen in wild type cells than that seen in *arg4::mec1-4* cells without multicopy *GIS2*.

Expression of multicopy *GIS2* did not cause an increase in the period of *RNR1* gene transcription before the onset of DNA replication. So, increased dNTP synthesis by this mechanism cannot explain how multicopy *GIS2* improves S-phase progression in *arg4::mec1-4* cells.

5.3 Discussion

5.3.1 Changes in the key mechanisms of regulating dNTP availability do not explain the suppression of the lethality of temperature sensitive *mec1* alleles by multicopy *GIS2*

There are two situations in which a cell needs to dramatically increase dNTP production: during DNA replication and in response to DNA damage. In both cases this is achieved by increasing the activity of the RNR enzyme, which catalyses the rate limiting step in dNTP synthesis (Section 1.5). The data presented in this chapter show the effect of multicopy *GIS2* expression on the key mechanisms involved in increasing RNR activity.

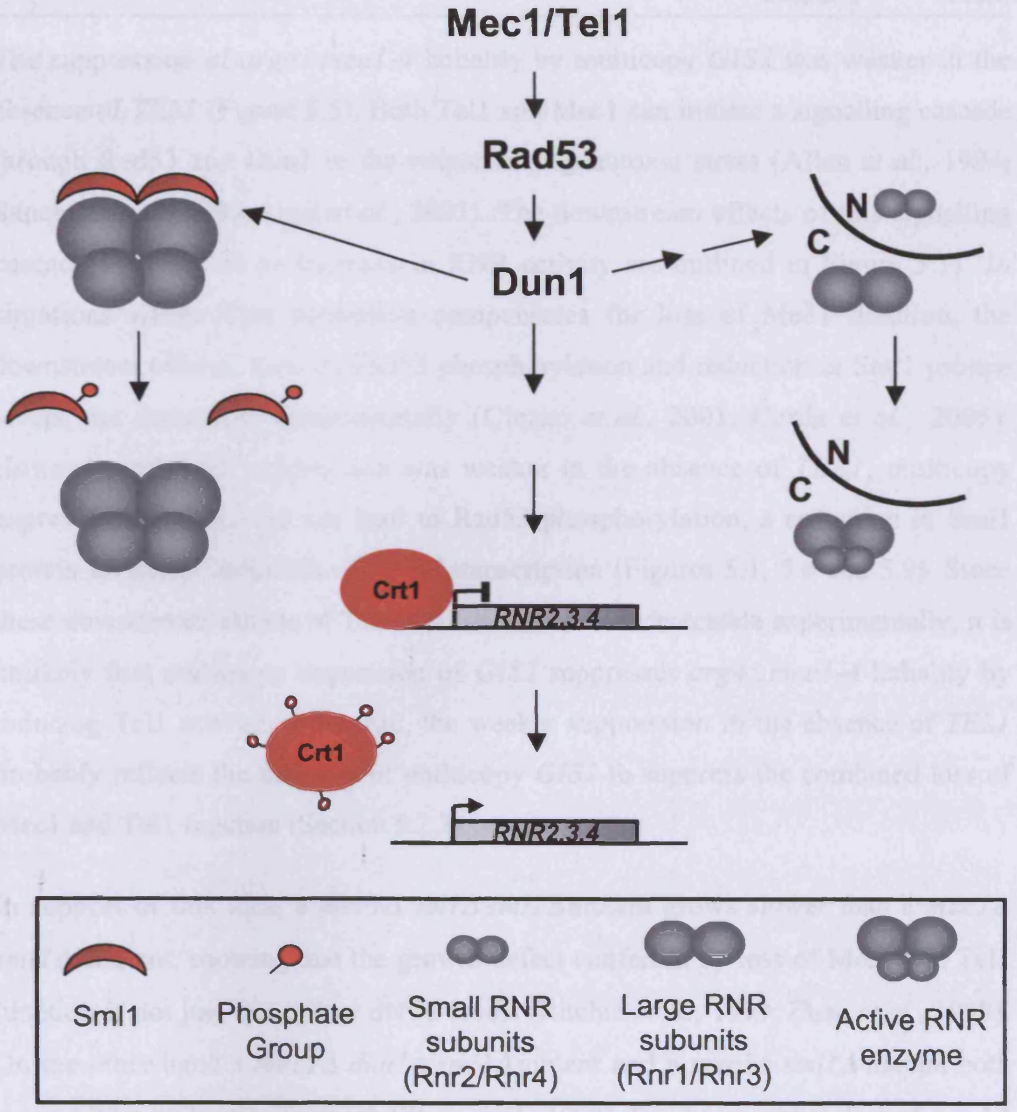

Figure 5.11 *MEC1-/TEL1*-dependent mechanisms of upregulating dNTP synthesis in response to genotoxic stress. Upon detection of genotoxic stress a *MEC1-/TEL1*-dependent signaling cascade is activated. This results in the activation of the downstream kinases Rad53 and Dun1. Dun1 directly phosphorylates Sml1, which is an inhibitor of the enzymatic activity of RNR. The phosphoylated form of Sml1 dissociates from RNR and is degraded. Crt1, a transcriptional inhibitor of *RNR2*, *RNR3* and *RNR4*, is phosphorylated in a *DUN1*-dependent manner. The hyperphosphorylated form of Crt1 dissociates from the DNA, so that expression of *RNR2, RNR3* and *RNR4* are increased. In response to genotoxic stress the small RNR subunits relocate from the nucleus (N) to the cytoplasm (C), where the large RNR subunits are located. This relocalisation is dependent on the Mec1/Rad53/Dun1 signaling cascade.

The suppression of *arg4::mec1-4* lethality by multicopy *GIS2* was weaker in the absence of *TEL1* (Figure 5.5). Both Tel1 and Mec1 can initiate a signalling cascade through Rad53 and Dun1 in the response to genotoxic stress (Allen *et al.*, 1994; Sanchez *et al.*, 1996; Usui *et al.*, 2001). The downstream effects of this signalling cascade that lead to an increase in RNR activity are outlined in Figure 5.11. In situations where Tel1 activation compensates for loss of Mec1 function, the downstream effects, such as Rad53 phosphorylation and reduction in Sml1 protein levels, are detectable experimentally (Clerici *et al.*, 2001; Corda *et al.*, 2005). However, although suppression was weaker in the absence of *TEL1*, multicopy expression of *GIS2* did not lead to Rad53 phosphorylation, a reduction in Sml1 protein levels, or induction of *RNR3* transcription (Figures 5.1, 5.6 and 5.9). Since these downstream effects of Tel1 activation were not detectable experimentally, it is unlikely that multicopy expression of *GIS2* suppresses *arg4::mec1-4* lethality by inducing Tel1 activation. Instead, the weaker suppression in the absence of *TEL1* probably reflects the inability of multicopy *GIS2* to suppress the combined loss of Mec1 and Tel1 function (Section 5.2.3).

In support of this idea, a *mec1Δ tel1Δ sml1Δ*mutant grows slower than a *mec1Δ sml1Δ* mutant, showing that the growth defect conferred by loss of Mec1 and Tel1 function is not just due to low dNTP levels (Ritchie *et al.*, 1999; Zhao *et al.*, 1998). On the other hand a *mec1Δ dun1Δ sml1Δ*mutant and a *mec1Δ sml1Δ* mutant both show wild type levels of growth (Zhao *et al.*, 1998). So, the growth defect of *mec1Δ* and *mec1Δ dun1Δ* can be fully suppressed by increasing dNTP levels. The Dun1 kinase acts downstream of Mec1 and is required for the efficient phosphorylation and degradation of Sml1 in S-phase (Zhao & Rothstein, 2002). However, some residual Sml1 phosphorylation and cell cycle-dependent fluctuation in protein levels do occur in *dun1Δ*, but not in *mec1Δ*p*RNR1*, which might account for why *dun1Δ* is viable (Zhao *et al.*, 2001; Zhao & Rothstein, 2002).

Deletion of *DUN1* shows synthetic growth defects with hypomorphic *mec1* alleles (Zhao & Rothstein, 2002). Presumably this is because the Mec1-dependent checkpoint is required to deal with the problems that arise from undergoing DNA replication with limiting dNTPs (caused by *dun1Δ*). Accordingly, a synthetic growth

defect was observed between *dun1Δ* and *mec1-4* (Figure 5.7). Despite this, suppression of *mec1-4* lethality by multicopy *GIS2* was not dependent on *DUN1* (Figure 5.7). As the Dun1 kinase transduces the downstream signals required for *TEL1*-dependent suppression of loss of Mec1 function via activation of the genotoxic stress response (Figure 5.11), this also suggests that suppression does not require Tel1 activation. Additionally, deletion of *TEL1* did not completely eliminate *GIS2*-dependent suppression (Figure 5.5), which would be expected were Tel1 activity required for the suppression. These observations therefore add weight to the above argument that, rather than suppression being caused by *GIS2*-dependent Tel1 activation, multicopy *GIS2* cannot suppress the combined loss of Mec1 and Tel1 function.

Increasing the expression of *RNR1* is one of the best-known mechanisms for suppressing *mec1Δ* lethality. Therefore, the possibility that multicopy *GIS2* affected *RNR1* transcription was tested (Figure 5.10). However, no change in the timing or level of *RNR1* mRNA induction, which would account for the *GIS2*-dependent suppression of *arg4::mec1-4*, was observed.

Taken together there is strong evidence that an increase in RNR activity, via alteration or activation of the normal physiological signalling pathways, does not account for the suppression of *arg4::mec1-4* lethality by multicopy *GIS2*. If a significant *GIS2*-dependent effect that promoted RNR activation was detected, it would be difficult to explain why multicopy *GIS2* cannot suppress the lethality of *mec1Δ* and can only partially suppress the lethality of temperature sensitive *mec1* alleles. Therefore, these data are consistent with the data from Chapter 4 that describe *GIS2* as a weak multicopy suppressor of the lethality of temperature sensitive *mec1* alleles. These data do not however rule out the possibility of small changes in the pathways tested that can increase RNR activity, but that are undetectable experimentally. However, if the *GIS2*-dependent suppression of the lethality of temperature sensitive *mec1* alleles is via an increase in dNTP levels, the possibility that it occurs by a more indirect route is favoured.

5.3.2 The effect of multicopy *GIS2* on Sml1 protein levels

Sml1 protein levels were initially assessed to see if *GIS2*-dependent suppression of the lethality of temperature sensitive *mec1* alleles could be explained by a decrease in Sml1. However, when the levels of 3MYC-Sml1 were compared in strains with and without multicopy *GIS2*, no *GIS2*-dependent decrease in Sml1 protein levels was seen (Figure 5.1). In fact, strains expressing multicopy *GIS2* tended to have slightly increased levels of Sml1. As Sml1 is an inhibitor of the RNR enzyme an increase in Sml1 protein levels could not directly explain the *GIS2*-dependent suppression of the lethality of temperature sensitive *mec1* alleles. The possibility that the increased Sml1 protein levels were caused by an increase in Rnr1 protein levels, which could directly explain the *GIS2*-dependent suppression of the lethality of temperature sensitive *mec1* alleles, was tested experimentally. However, no increase in HA-Rnr1 protein levels was seen (Figure 5.8). Another possibility is that an increase in Sml1 protein levels could be caused by multicopy *GIS2* expression altering the balance of protein synthesis and protein degradation.

A change in the pattern of the cell cycle-dependent fluctuations in Sml1 protein levels was also seen between *arg4::mec1-4* strains with and without multicopy *GIS2* (Figures 5.3 and 5.4). In the *arg4::mec1-4* [YEp24] strain the Sml1 protein accumulated after release from α-factor into a synchronous S-phase (Figure 5.3). This accumulation of Sml1 is probably a consequence of the absence of the degradation-promoting activity of Mec1. In the *arg4::mec1-4* [2μm-*GIS2*] strain there was no accumulation of Sml1, and additionally there was some restoration of the cell cycle-dependent fluctuation (Figure 5.4). Assuming that the accumulation of Sml1 in the *arg4::mec1-4* [YEp24] strain is due to the absence of the degradation-promoting activity of Mec1, Sml1 degradation must be somehow restored in the *arg4::mec1-4* [2μm-*GIS2*] strain.

Cell cycle-dependent Sml1 degradation in the *arg4::mec1-4* [2μm-*GIS2*] strain would be most simply explained by a *GIS2*-dependent restoration of Mec1-4 activity. However, suppression of *mec1-4* lethality by multicopy *GIS2* does not depend on *DUN1*. Dun1 is currently the only known kinase to phosphorylate Sml1 (Uchiki *et al.*, 2004). The main route by which *MEC1* promotes Sml1 degradation is via the

Dun1 kinase, which therefore suggests that the *GIS2*-induced cell cycle-dependent fluctuations in Sml1 protein levels are not due to restored Mec1-4 activity. However, this possibility cannot be ruled out completely as some residual cell cycle-dependent Sml1 degradation is seen in *dun1Δ* (Zhao & Rothstein, 2002).

Another possibility is that multicopy expression of *GIS2* enhances the function of the protein degradation machinery. In this model, a residually phosphorylated form of Sml1 (due to residual Mec1-4 activity at 30°C) would be more accessible to the protein degradation machinery, which would result in some cell cycle-dependent fluctuation in Sml1 protein levels. On the other hand, the idea that multicopy *GIS2* expression enhances the function of the protein degradation machinery is inconsistent with the previous observation that there is a trend for increased Sml1 in strains expressing multicopy *GIS2*. Alternatively, multicopy *GIS2* could lead to restoration of cell cycle-dependent fluctuations in Sml1 protein levels, independently of Mec1. This could be via a direct effect of multicopy *GIS2* on the protien degradation machinery, or it could be a consequence of the *GIS2*-dependent improvement of S-phase progression. In support of the idea of some Mec1-independent Sml1 degradation, in *S. pombe*, the cell cycle-dependent degradation of $Spd1^{(Sml1)}$ is independent of $Rad3^{Mec1}$ (Liu *et al.*, 2003). Instead, it is dependent on the COP9 signalosome, which activates the ubiquitin ligase that targets Spd1 for degradation.

The underlying cause for these two observations on Sml1 protein levels remains unknown. The more important question is: could either of them account for the *GIS2*-dependent suppression of the lethality of temperature sensitive *mec1* alleles? A general increase in Sml1 protein levels could not, as discussed previously (Section 5.2.1). A cell cycle-dependent decrease, in theory, could. However, assuming both of these observations are valid, cells expressing multicopy *GIS2* would start the cell cycle with increased Sml1 compared with wild type cells. So, the effect of any decrease in Sml1 on dNTP levels, from this starting point, is difficult to judge.

5.3.3 The improvement of S-phase progression in *arg4::mec1-4* by multicopy *GIS2*

The improvement of S-phase progression in *arg4::mec1-4* by multicopy *GIS2* was shown in Chapter 4. The restoration of Sml1 cell cycle-dependent fluctuations is a possible cause of this improved S-phase progression. A change in the cell cycle-dependent fluctuation of *RNR1* mRNA levels was also seen between *arg4::mec1-4* cells with and without multicopy *GIS2* (Figure 5.10). However, this is most likely to be a consequence, rather than a cause, of improved cell cycle progression.

In wild type strains, *RNR1* mRNA levels returned their basal level (level in α-factor), after approximately four-fold induction at the G1/S transition, as cells completed DNA replication. *RNR1* mRNA expression is induced in G1 after cells pass through START (Section 1.1.3). Another gene whose expression is induced at the same time, *NRM1*, acts as a repressor of MBF-regulated genes (de Bruin *et al.*, 2006). Therefore, as Nrm1 protein levels increase, MBF-regulated gene transcription is switched off. This confines MBF-regulated gene expression to G1/early S. In the *arg4::mec1-4* [YEp24] strain at 40 minutes after release from α-factor most cells were in G1 or S-phase, as judged from the FACS profile (Figure 5.10A). When quantified, the *RNR1* mRNA level had not returned to the basal level at this time point (Figure 5.10C). The reason for this is probably that there was a fraction of cells in this strain that remained in G1 where *RNR1* transcription had not been switched off. In the *arg4::mec1-4* [2μm-*GIS2*] strain at 40 minutes after release from α-factor most cells were in G2, as judged from the FACS profile, and *RNR1* mRNA levels had returned to their basal level. So, the pattern of *RNR1* mRNA induction correlated with the status of bulk DNA replication in both strains. Therefore, the fact that *RNR1* mRNA levels returned to their basal level in *arg4::mec1-4* [2μm-*GIS2*] cells, but not in *arg4::mec1-4* [YEp24] cells, is most likely to be a consequence of the fact that these cells passed through S-phase more efficiently than the *arg4::mec1-4* [YEp24] cells.

Overall the data presented in this Chapter show no detectable molecular changes that could clearly explain why multicopy *GIS2* suppresses the lethality of temperature sensitive *mec1* alleles. The issue of whether suppression depends on a modest increase in dNTP levels or not, along with other alternative mechanisms of suppression, are discussed further in the general discussion in Chapter 8.

Chapter 6

The role of *GIS2*

6.1 Introduction

To understand the effects of increasing *GIS2* expression on the growth of temperature sensitive *mec1* strains better, further investigation into the role of *GIS2* itself was conducted. Very little is known about *GIS2* and there is only one published research paper on *GIS2* in *S. cerevisiae* (Balciunas & Ronne, 1999). However, the homolog in higher eukaryotes, CNBP, has been more widely studied. These CNBP studies, and the data from Balciunas and Ronne (1999) were used as a basis to work from to improve current understanding of the role of *GIS2*.

6.2 Results

6.2.1 *GIS2*: a nucleic acid chaperone?

A nucleic acid chaperone is a nucleic acid binding protein that aids in the folding and rearrangement of nucleic acid structure. Thereby preventing the accumulation of kinetically-trapped, misfolded species and ensuring that the nucleic acid carries out its correct biological function (Herschlag, 1995). Certain features are expected in nucleic acid chaperones: i) nucleic acid binding activity and ii) the ability to remodel nucleic acid structure.

GIS2 encodes a protein with seven zinc fingers of the type $CX_2CX_4HX_4C$ (Figure 6.1), a motif typically found in nucleic acid binding proteins. The homolog of *GIS2* in higher eukaryotes is cellular nucleic acid binding protein (CNBP). CNBP is highly conserved between species: mouse, chick and *Xenopus* CNBPs have 100%, 99% and 94% identity at the amino acid level with human CNBP (hCNBP) respectively (Flink *et al.*, 1998; van Heumen *et al.*, 1997; Warden *et al.*, 1994). The name CNBP comes from the similarity of the zinc finger repeats in CNBP to those found in retroviral

nucleic acid binding proteins encoded by the *gag* genes (Rajavashisth *et al.*, 1989). These retroviral nucleic acid binding proteins bind to single-stranded DNA and RNA (Covey, 1986; Darlix & Spahr, 1982). Single-stranded nucleic acid binding activity has also been shown for *Homo sapiens* (Michelotti *et al.*, 1995; Rajavashisth *et al.*, 1989), *Rattus norvegicus* (Yasuda *et al.*, 1995), *Xenopus laevis* (Pellizzoni *et al.*, 1997), *Danio rerio* (Armas *et al.*, 2004) and *Bufo arenarum* (Armas *et al.*, 2008) CNBPs. Biochemical analysis of *Bufo arenarum* CNBP showed that it can promote the annealing and melting of nucleic acids *in vitro* (Armas *et al.*, 2008). Based on these observations, CNBP was suggested to be a nucleic acid chaperone.

CNBP has been proposed to have an important role in the control of gene expression, at both transcriptional and translational levels. Both positive (Konicek *et al.*, 1998; Shimizu *et al.*, 2003) and negative effects (Flink & Morkin, 1995; Rajavashisth *et al.*, 1989) on gene transcription have been described for CNBP. The best understood transcriptional target of CNBP is the *c-MYC* oncogene. Human CNBP binds to the purine-rich strand of the CT-element (CCCTCCCCA) in the *c-MYC* promoter (Michelotti *et al.*, 1995). Over-expression of mouse CNBP stimulates cell proliferation and *c-MYC* promoter activity (Shimizu *et al.*, 2003). Conversely the *cnbp*$^{-/-}$ mouse mutant is embryonic lethal, and areas of reduced cell proliferation in the *cnbp*$^{-/-}$ mouse embryo correspond to areas where *c-MYC* expression is absent (Chen *et al.*, 2003). Translational regulation by *Xenopus* CNBP has been described for a group of mRNAs that have a terminal oligopyrimidine (TOP) element in their 5'-untranslated region (5'UTR). These mRNAs encode proteins involved in the synthesis and function of the translational apparatus (Hamilton *et al.*, 2006). *Xenopus* CNBP binds the 5'UTR of ribosomal protein mRNAs (rp-mRNAs) (Pellizzoni *et al.*, 1997; Pellizzoni *et al.*, 1998). CNBP binding stabilises the secondary structure of the TOP element in the 5'UTR, and is predicted to cause translational repression (Crosio *et al.*, 2000).

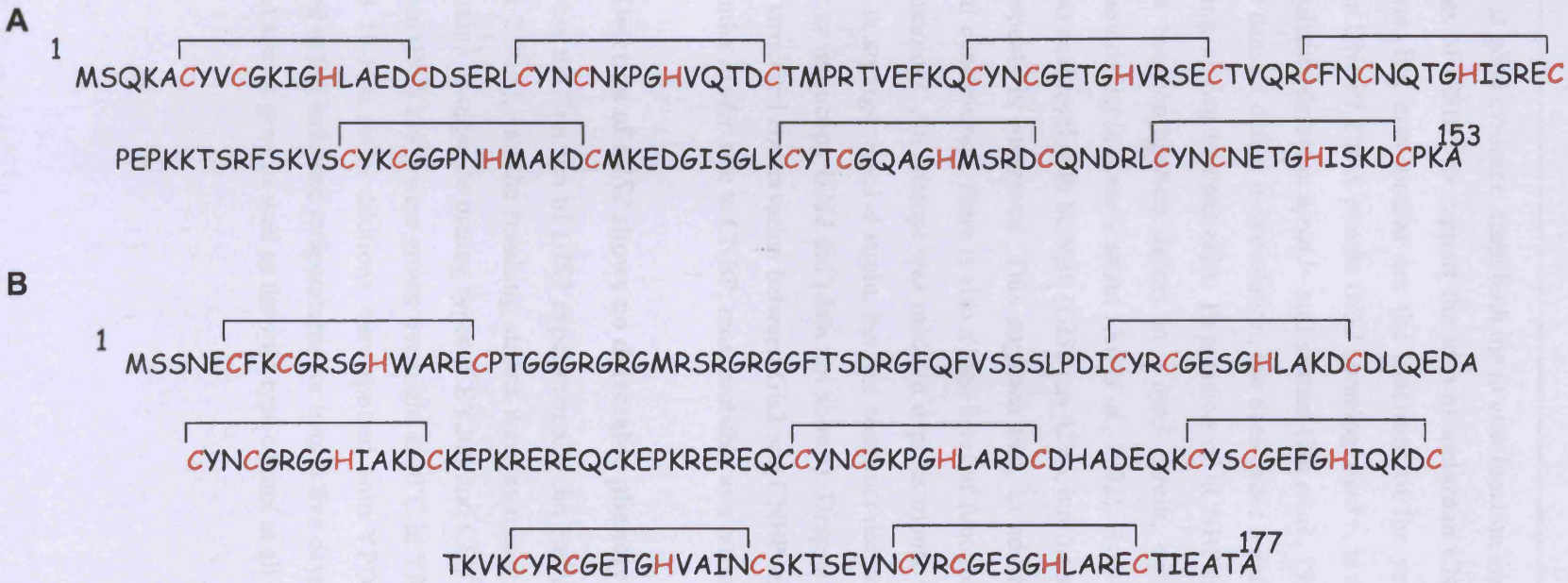

Figure 6.1 Gis2 and its homolog CNBP are small proteins with seven tandem zinc-finger motifs. The protein sequences of *S. cerevisiae* Gis2 **(A)** and human CNBP **(B)** are shown. The conserved residues that co-ordinate the Zn^{2+} ion are shown in red. The positions of the 7 tandem zinc-finger motifs ($CX_2CX_4HX_4C$) in each protein are shown by square brackets.

So there is good evidence, from both the *in vivo* function and the *in vitro* biochemical properties of CNBP, to support the idea of metazoan CNBP being a nucleic acid chaperone. But how similar are the functions of the yeast homologs to that of metazoan CNBP? The *S. pombe GIS2* homolog, *byr3+*, is a multicopy suppressor of the sporulation defect in a *ras1-* null mutant (Xu *et al.*, 1992). Loss of *byr3+* itself does not cause a defect in sporulation, but does cause a defect in conjugation during the mating of two haploid cells. Expression of hCNBP in *S. pombe* can partially suppress the conjugation defect in a *byr3-* strain, but it cannot suppress the sporulation defect in a *ras1-* strain (Xu *et al.*, 1992). Byr3 only has 36% identity at the amino acid level with hCNBP (*GIS2* has 42%), but the structure of the seven zinc finger repeats is conserved. This suggests that, in addition to the high level of structural conservation, there is also a high level of functional conservation between *GIS2* homologs. An attempt was made to express mouse CNBP from a multicopy plasmid in an arg4::*mec1-4* strain, but this construct did not suppress *arg4::mec1-4* lethality as multicopy *GIS2* did (data not shown). Despite this last observation, the level of structural conservation between Gis2 and CNBP strongly suggests that Gis2 has a similar *in vivo* role to CNBP, most probably as a nucleic acid chaperone.

6.2.2 Deletion of *GIS2* shows no detectable phenotype

To address the function of *GIS2* experimentally the entire *GIS2* ORF was deleted (Section 2.10.6), and the resulting strains were assessed for growth defects. Two *gis2Δ* strains of opposite mating types (CEY208 and CEY209) and a congenic wild type strain (RCY2447) were grown overnight at 30°C in YPD, diluted to an OD_{600} of 0.5, and 10-fold serial dilutions were spotted onto YPD agar. Agar plates were incubated at the indicated temperatures for two to five days. Figure 6.2A shows that the *gis2Δ* strains grew as well as the wild type control at all temperatures tested.

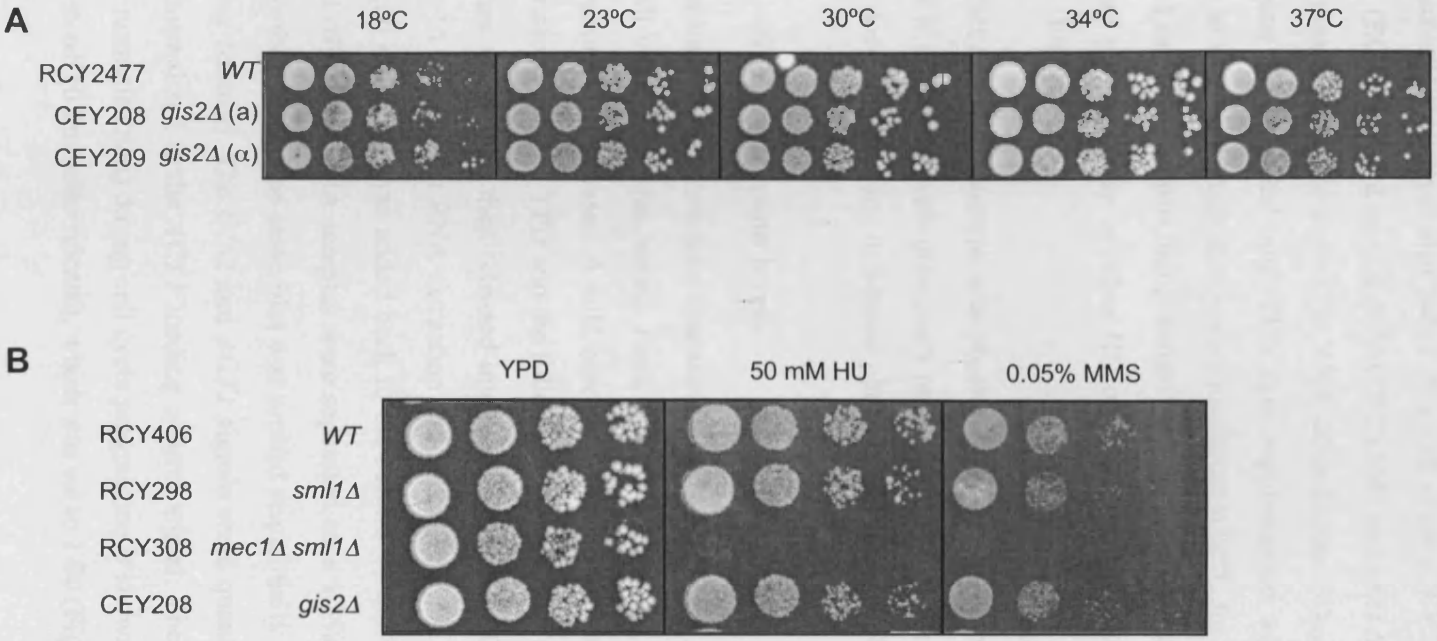

Figure 6.2 Deletion of *GIS2* shows no detectable phenotype. A) The indicated strains were grown overnight at 30˚C in YPD. The following morning each culture was diluted to an OD_{600} of 0.5, and 10-fold serial dilutions were spotted onto YPD agar. Agar plates were incubated at the indicated temperatures for two to five days. **B)** The indicated strains were grown overnight at 30˚C in YPD. The following morning each culture was diluted to OD_{600} of 0.5, and 10-fold serial dilutions were spotted onto YPD agar supplemented with 50 mM HU or 0.05% MMS as indicated. Agar plates were incubated at 30˚C for two days.

Since the focus of this investigation is the genetic interaction between multicopy *GIS2* and temperature sensitive *mec1* strains, the ability of a *gis2Δ* strain to respond to genotoxic stress was also tested. A *gis2Δ* strain (CEY208), a congenic wild type strain (RCY406), and *mec1Δ sml1Δ* (RCY308) and *sml1Δ* (RCY298) control strains were grown overnight at 30°C in YPD, diluted to an OD_{600} of 0.5, and 10-fold serial dilutions were spotted onto YPD agar supplemented with 50 mM HU or 0.05% MMS as indicated. Agar plates were incubated at 30°C for two days. As expected the *mec1Δ sml1Δ* strain was highly sensitive to genotoxic stress, whereas the *gis2Δ* strain showed no sensitivity to either HU or MMS compared with the wild type control strain (Figure 6.2B).

The fact that no phenotype was observed for the *gis2Δ* strains under the conditions tested is consistent with previously published data, which also state that deletion of *GIS2* does not show any detectable phenotype (Balciunas & Ronne, 1999).

6.2.3 *GIS2* expression levels

To continue the experimental characterisation of *GIS2*, its expression under different growth conditions was tested. First, the level of *GIS2* mRNA during cell cycle progression was assessed. A wild type strain (CEY354) was grown overnight to mid-log phase at 30°C in YPD and the following morning was arrested in G1 with αF for 3 hours. Cells were then released into fresh YPD at 30°C and samples were taken every 15 minutes for RNA extraction and FACS analysis. To restrict the analysis to one cell cycle, αF was added back to the culture 40 minutes after release from the initial αF block. RNA samples were separated on a 1.5% agarose gel and analysed by Northern blot. The same blot was probed sequentially for *GIS2* and *ACT1* (actin loading control). The *GIS2* and *ACT1* signals were quantified and the *GIS2* signal was normalised to the *ACT1* loading control signal. The level of *GIS2* expression (after normalisation) during cell cycle progression is shown relative to the expression level in αF (0 min after release), which was set to 1.00 (Figure 6.3A).

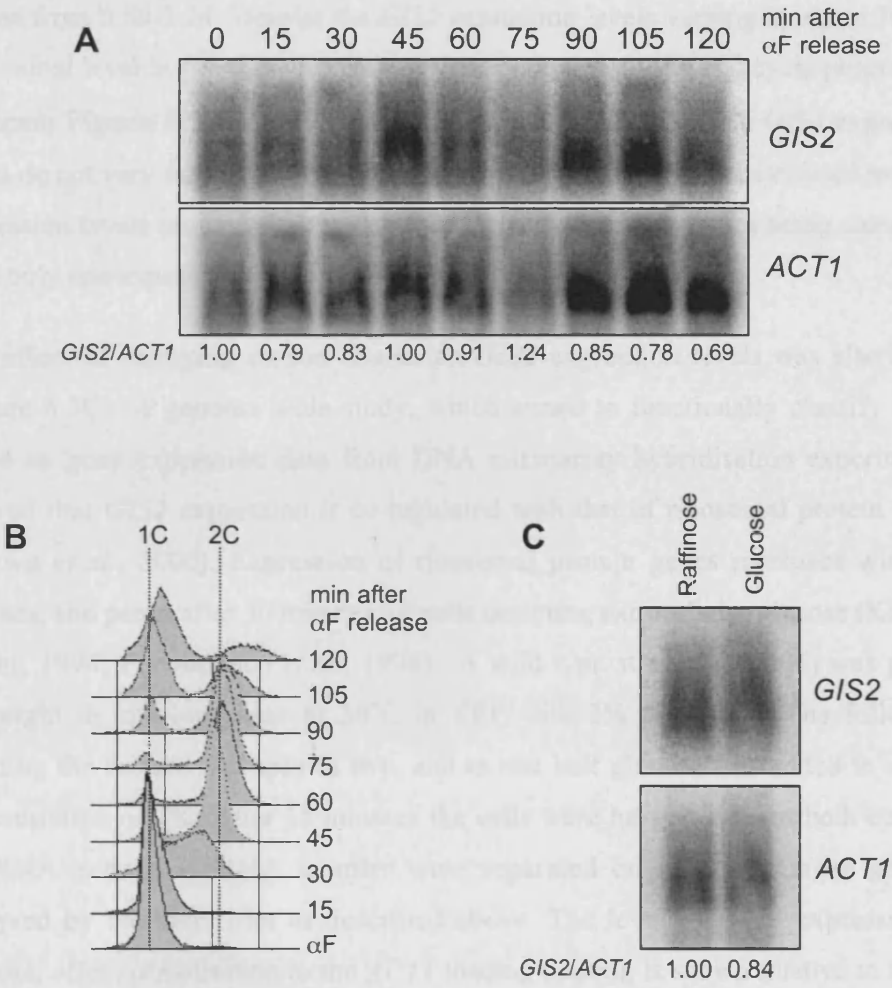

Figure 6.3 *GIS2* mRNA expression levels do not vary during cell cycle progression or upon carbon source change. A) A log phase culture of wild type strain CEY354, grown at 30°C in YPD, was arrested in G1 with αF for three hours. Cells were released into fresh YPD at 30°C and samples were taken every 15 minutes for RNA extraction and FACS analysis. Additional αF was added 40 minutes after release from αF to prevent entry into a second cell cycle. **B)** Each FACS profile represents 50,000 counts. The 1C and 2C DNA content is as indicated. **C)** A log phase culture of wild type strain CEY206, grown at 30°C in YEP with 2% raffinose, was split in two and glucose was added to a final concentration of 2% to one half. After 15 minutes the cells were harvested from both cultures for RNA extraction. **A&C)** RNA samples were separated on a 1.5% agarose gel and analysed by Northern blot. The same blot was probed sequentially for *GIS2* (462 bases) and *ACT1*(actin loading control; 1138 bases). The relative amounts of *GIS2* mRNA are shown, normalised to the *ACT1* loading control and expressed relative to the αF or raffinose sample which was set to 1.00.

The variation in the relative level of *GIS2* expression during cell cycle progression ranged from 0.69-1.24. Despite the *GIS2* expression levels varying by up to 30% of their initial level in αF, there was no trend that correlated with cell cycle progression (compare Figures 5.3A and 5.3B). Therefore it is most likely that *GIS2* expression levels do not vary during cell cycle progression. Consequently the calculated range in expression levels probably stems from the inaccuracy of the values being calculated from only one experiment.

The effect of changing carbon source on *GIS2* expression levels was also tested (Figure 6.3C). A genome wide study, which aimed to functionally classify genes based on gene expression data from DNA microarray hybridisation experiments, showed that *GIS2* expression is co-regulated with that of ribosomal protein genes (Brown *et al.*, 2000). Expression of ribosomal protein genes increases within 5 minutes, and peaks after 30 minutes, of cells detecting extracellular glucose (Klein & Struhl, 1994; Pernambuco *et al.*, 1996). A wild type strain (CEY206) was grown overnight to mid-log phase at 30°C in YEP with 2% raffinose. The following morning the culture was split in two, and to one half glucose was added to a final concentration of 2%. After 15 minutes the cells were harvested from both cultures for RNA extraction. RNA samples were separated on a 1.5% agarose gel and analysed by Northern blot as described above. The level of *GIS2* expression in glucose, after normalisation to the *ACT1* loading control, is shown relative to that in raffinose, which was set to 1.00 (Figure 6.3C). The *GIS2* expression level in glucose was calculated to be 16% lower than that in raffinose. However, this level of variation is less than that observed during cell cycle progression (Figure 6.3A), which is not likely to be significant. Based on these considerations it is concluded that no change in the *GIS2* expression level during the shift from raffinose to glucose as a carbon source was observed.

6.2.4 Gis2-GFP localises throughout the cell

Gis2 has been shown, by affinity-capture mass-spectrometry, to physically interact with five proteins (Krogan *et al.*, 2006). Three of these (Nop1, Pwp1, and Sbp1) have been linked to ribosome biogenesis and localise to the nucleolus (Clark *et al.*, 1990; Schimmang *et al.*, 1989; Suka *et al.*, 2006; Tollervey *et al.*, 1991; Zhang *et al.*,

2004). With this in mind, the localisation of the Gis2 protein was examined. A C-terminal GFP tag was introduced at the *GIS2* genomic locus (Section 2.10.7). This was done in the CG strain background to enable better microscopic examination of haploid cells (Figure 2.2). A strain expressing *GIS2-GFP* (CEY330) was grown to mid-log phase at 30°C. Cells were fixed with formaldehyde and the DNA was stained with DAPI before examination by fluorescence microscopy. Figure 6.4 shows that the GFP-tagged Gis2 localised throughout the cell. The strong signal also suggested that it was an abundant protein. However, these results should be interpreted with caution, as it has not been shown that the Gis2-GFP protein is functional.

6.2.5 Alteration of *GIS2* expression levels does not change wild type cell cycle progression

One mechanism of suppressing the lethality of a *mec1Δ* allele is to delay the start of DNA replication relative to the onset of transcription at the G1/S transition. This lengthens the period of increased *RNR1* transcription (and therefore presumably increased dNTP synthesis) before DNA replication starts, and can be achieved using a *cln1Δ cln2Δ* strain (Vallen & Cross, 1999). Therefore the potential effects of altering *GIS2* expression on cell cycle progression (budding patterns and bulk DNA synthesis) were assessed. Again, the CG strain background was used to enable better microscopic examination of haploid cells.

A strain expressing multicopy *GIS2* (CEY355), a strain with the *GIS2* ORF deleted (CEY473), and a congenic wild type control (CEY354) were grown overnight at 30°C in YPD to mid-log phase. Samples from each culture were taken for RNA extraction to confirm the status of *GIS2* expression. RNA samples were separated on a 1.5% agarose gel and analysed by Northern blot. The same blot was probed sequentially for *GIS2* and *ACT1* (actin loading control). As expected the *GIS2* signal from the cells expressing multicopy *GIS2* was considerably stronger than the *GIS2* signal from wild type cells, and no *GIS2* mRNA was detected in the *gis2Δ* strain (Figure 6.5A).

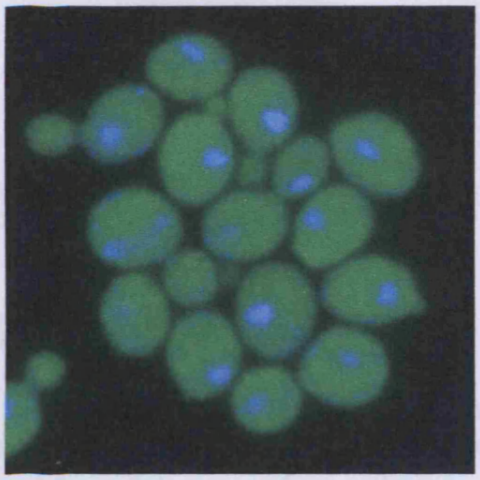

Figure 6.4 Gis2-GFP localises throughout the cell. Strain CEY330 (*GIS2-GFP*) was grown to mid-log phase at 30°C in YPD. Cells were fixed with formaldehyde and the DNA was stained with DAPI before examination by fluorescence microscopy. The image shows a merge of the DAPI (blue) and GFP (green) fluorescence signals.

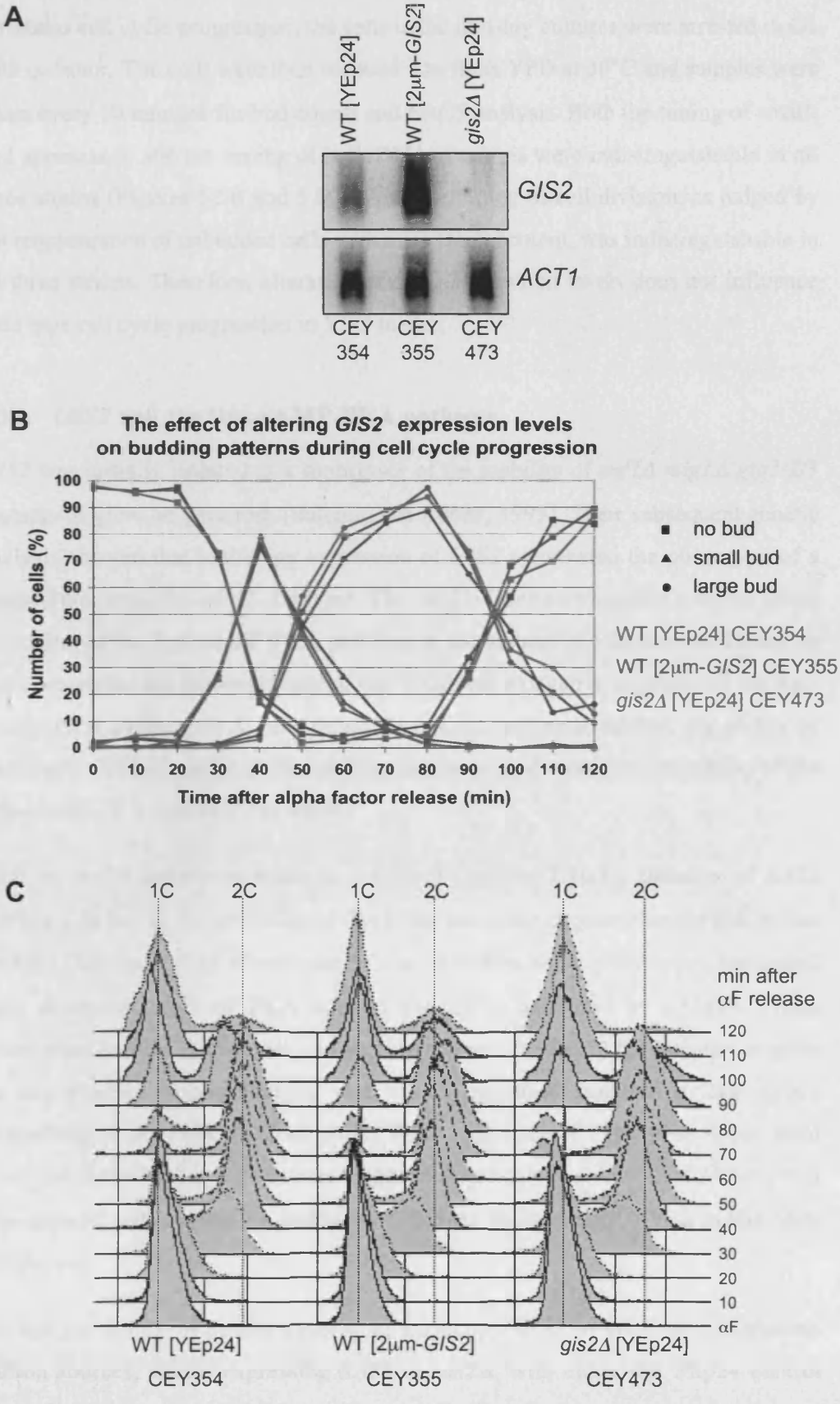
A
WT [YEp24]
WT [2μm-GIS2]
gis2Δ [YEp24]
GIS2
ACT1
CEY 354
CEY 355
CEY 473
B
The effect of altering GIS2 expression levels on budding patterns during cell cycle progression
Number of cells (%)
Time after alpha factor release (min)
no bud
small bud
large bud
WT [YEp24] CEY354
WT [2μm-GIS2] CEY355
gis2Δ [YEp24] CEY473
C
1C
2C
min after αF release
120
110
100
90
80
70
60
50
40
30
20
10
αF
WT [YEp24] CEY354
WT [2μm-GIS2] CEY355
gis2Δ [YEp24] CEY473

To assess cell cycle progression, the cells in the mid-log cultures were arrested in G1 with α-factor. The cells were then released into fresh YPD at 30°C and samples were taken every 10 minutes for bud counts and FACS analysis. Both the timing of small-bud appearance and the timing of bulk DNA synthesis were indistinguishable in all three strains (Figures 5.5B and 5.5C). Also the timing of cell division, as judged by the reappearance of unbudded cells with a 1C DNA content, was indistinguishable in all three strains. Therefore, alteration of *GIS2* expression levels does not influence wild type cell cycle progression in YPD media.

6.2.6 *GIS2* and the Ras-cAMP-PKA pathway

GIS2 was initially isolated as a suppressor of the inability of *snf1Δ mig1Δ gig1/2/3* mutants to grow on galactose (Balciunas & Ronne, 1999). Their subsequent genetic analysis showed that multicopy expression of *GIS2* aggravated the phenotype of a temperature sensitive *cdc25-5* mutant. The *cdc25-5* mutation confers a defect in the activation of the Ras-cAMP-PKA pathway at the restrictive temperature. Based on this observation the authors proposed that *GIS2* was a negative regulator of the Ras-cAMP-PKA pathway in *S. cerevisiae*. To test this proposal further, the ability of multicopy *GIS2* to confer known phenotypes associated with downregulation of the Ras-cAMP-PKA pathway was tested.

First, a *ras2Δ* strain was made as a control (Section 2.10.8). Deletion of *RAS2* confers a defect in the activation of Cyr1 (the adenylate cyclase enzyme that makes cAMP) (Section 1.6.1). Consequently, *ras2Δ* strains show phenotypes associated with downregulation of PKA activity (which is activated by cAMP). These phenotypes include i) a tendency to sporulate in rich media, ii) the inability to grow on non-glucose carbon sources, and iii) an increased resistant to heat shock (Engelberg *et al.*, 1994; Tatchell *et al.*, 1985). All three of these phenotypes were observed in the *ras2Δ* control strain (Figure 6.6 and data not shown). However, wild type diploid cells expressing multicopy *GIS2* did not sporulate in rich media (data not shown).

To test the ability of strains expressing multicopy *GIS2* to grow on non-glucose carbon sources, strains expressing *RAS2* or *ras2Δ*, with either the YEp24 control

plasmid or a multicopy *GIS2* plasmid were grown overnight at 30°C in SD-URA media. The following morning each culture was diluted to an OD_{600} of 0.5, and 10-fold serial dilutions were spotted onto minimal agar media lacking uracil with either 2% glucose, 2% galactose or 2% glycerol as a carbon source. Agar plates were incubated at 30°C for two days. Both of the *ras2Δ* strains (CEY595 and CEY663) failed to grow using galactose or glycerol as a carbon source, whereas the wild type *RAS2* strain expressing multicopy *GIS2* (CEY661) grew as well as the wild type control strain (CEY565) using all carbon sources (Figure 6.6). Therefore these observations suggest that, under these experimental conditions, the extent of any *GIS2*-dependent downregulation of *RAS* activity is mild.

The ability of multicopy *GIS2* to confer heat shock resistance was also tested. The *ras2Δ* strain reproducibly showed increased resistance to heat shock at 50°C compared with the wild type control strain. Expression of multicopy *GIS2* in a wild type strain did exhibit a heat shock resistant phenotype, to a similar extent as the *ras2Δ* strain, in some cases, but not reproducibly (data not shown). The cases where multicopy *GIS2* increased the heat shock resistance of a wild type strain could just have been an experimental artefact. Alternatively, multicopy expression of *GIS2* could confer heat shock resistance under specific, as yet unidentified, conditions. The type of media and the growth phase of the culture can significantly influence the ability of *S. cerevisiae* cells to withstand heat shock (Elliott & Futcher, 1993). For example stationary phase cells are more resistant to heat shock than log phase cells. It is possible that increased *GIS2* levels can only confer heat shock resistance when the cells are in a specific metabolic state, depending on their growth conditions.

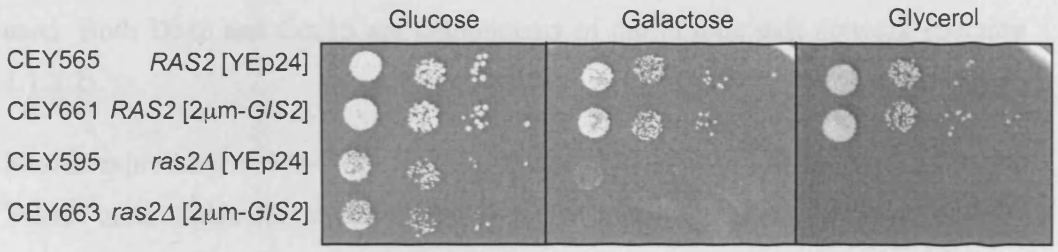

Figure 6.6 Multicopy *GIS2* does not prevent growth on non-glucose carbon sources. The indicated strains were grown overnight in SD-URA at 30°C. The following morning each culture was diluted to OD_{600} of 0.5 and 10-fold serial dilutions were spotted onto minimal agar media lacking uracil with the indicated carbon source at 2%. Agar plates were incubated at 30°C for 2 days. Plasmids used were YEp24 (empty vector) and pCLE8 (2μm-*GIS2*).

6.2.7 Multicopy *GIS2* suppresses *cdc15-2* temperature sensitivity

There are several published examples of how downregulating PKA activity, for example by deleting *RAS2*, can suppress the temperature sensitivity of some cell cycle mutants (Anghileri *et al.*, 1999; Bolte *et al.*, 2003; Heo *et al.*, 1999; Irniger *et al.*, 2000; Li *et al.*, 2005). Most of these mutations are in genes that are involved in anaphase or mitotic exit. The possibility that multicopy *GIS2* might also suppress some of these cell cycle mutants was tested. Two temperature sensitive mutant strains, *dbf2-2* and *cdc15-2*, that were readily available in our strain collection were used. Both Dbf2 and Cdc15 are components of the mitotic exit network (Section 1.1.5.2).

Strains expressing a *dbf2-2* or a *cdc15-2* temperature sensitive allele, with either the YEp24 control plasmid or a multicopy *GIS2* plasmid, were grown overnight at 23°C in SD-URA media. The following morning each culture was diluted to an OD_{600} of 0.5, and 10-fold serial dilutions were spotted onto SD-URA agar. Agar plates were incubated for two days at the indicated temperature. Multicopy expression of *GIS2* had a positive effect on the growth of the *cdc15-2* strain at 34°C, but not on the growth of the *dbf2-2* strain (Figure 6.7). The *dbf2-2* strain was slightly cold sensitive at 23°C and this effect was weakly enhanced by the expression of multicopy *GIS2*.

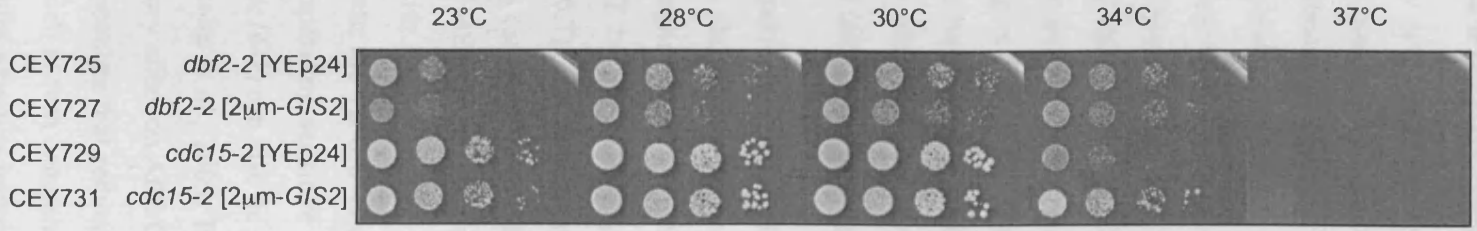

Figure 6.7 Multicopy *GIS2* suppresses *cdc15-2* temperature sensitivity. The indicated strains were grown overnight at 23°C in SD-URA. The following morning each culture was diluted to an OD_{600} of 0.5, and 10-fold serial dilutions were spotted onto SD-URA agar. Agar plates were incubated for two days at the indicated temperatures. Plasmids used were YEp24 (empty vector) and pCLE8 (2µm-*GIS2*).

6.3 Discussion

6.3.1 Is *GIS2* a negative regulator of the Ras-cAMP-PKA pathway?

The previously proposed role for *GIS2* as a negative regulator of the Ras-cAMP-PKA pathway was used as a model to investigate the role of *GIS2* further. No reproducible phenotypes that are commonly seen in mutants with decreased PKA activity were observed in strains expressing multicopy *GIS2* (Section 6.2.6). This suggests that increased *GIS2* expression does not have a dominant effect in reducing PKA activity. However, the fact that increased *GIS2* expression was achieved in all experiments by using multicopy *GIS2* under its own promoter should be considered. Although this system worked to increase *GIS2* expression during log phase growth in rich media (Figure 6.5A), it is possible that different growth conditions (for example non-glucose carbon sources) could affect *GIS2* expression levels, and consequently also affect the observed phenotype. Unfortunately attempts to make a strain that over-expressed *GIS2* from an exogenous promoter were unsuccessful.

The effect of multicopy *GIS2* on the growth of *dbf2-2* and *cdc15-2* strains was tested, as it has been shown that reduced PKA activity can suppress their temperature sensitivity (Anghileri *et al.*, 1999; Irniger *et al.*, 2000). It was interesting that multicopy *GIS2* did improve the growth of the *cdc15-2* strain, but not of the *dbf2-2* strain (Figure 6.7). The reasons why the temperature sensitivity of the *dbf2-2* and *cdc15-2* strains can be suppressed by downregulation of PKA activity are not clear. Inactivation of MEN genes, such as *DBF2* and *CDC15*, causes a cell cycle arrest in late mitosis with high levels of the mitotic cyclin Clb2 because of a failure to properly activate the APC/C (Jaspersen *et al.*, 1998; Surana *et al.*, 1993). The lethality of temperature sensitive mutants of APC/C subunits (*apc10-22*, *cdc27-1*, *cdc23-1* and *cdc16-1*) can also be suppressed by decreasing PKA activity (Anghileri *et al.*, 1999; Bolte *et al.*, 2003; Irniger *et al.*, 2000). Activated PKA is thought to have an inhibitory effect on APC/C function (Section 1.6.4). Therefore the authors of these studies speculate that reducing PKA activity removes this inhibitory effect on the APC/C, which in turn compensates for the APC/C defect caused by inactivation of the temperature sensitive mutant at the restrictive temperature. It is possible that the same model could account for the suppression of MEN mutants by decreasing

PKA activity. However, the genetic interactions between these APC/C and MEN mutants and the Ras-cAMP-PKA pathway or *GIS2* are complex, and are unlikely to be accounted for by a simple "one size fits all" model such as this. For example, the effect of multicopy *PDE2* (the phosphodiesterase enzyme that breaks down cAMP) is weaker than that of *ras2Δ* on the viability of a *dbf2-2* mutant (Irniger *et al.*, 2000). Also, multicopy *GIS2* increased the viability of a *cdc15-2* mutant, but not of a *dbf2-2* mutant (Figure 6.7).

The fact that both decreasing Ras-cAMP-PKA signalling and multicopy *GIS2* expression suppress the temperature sensitivity of a *cdc15-2* mutant could be a coincidence. More likely however is that decreasing Ras-cAMP-PKA signalling and increasing *GIS2* expression cause some overlapping downstream effects. Whether these shared downstream effects are a result of *GIS2* interacting directly with the Ras-cAMP-PKA pathway remains unclear. The strongest argument for *GIS2* interacting directly with the Ras-cAMP-PKA pathway is that the *S. pombe GIS2* homolog, *byr3+*, genetically interacts with *ras1-* (the only *RAS* gene in *S. pombe*) (Xu *et al.*, 1992). The downstream effectors of the *RAS* genes are different in *S. cerevisiae* and *S. pombe*. Therefore, according to this analogy, *GIS2* would interact directly with the *RAS* genes.

Overall there is evidence, discussed above, to suggest that *GIS2* function is somehow linked to Ras activity. However, it is likely that multicopy expression of *GIS2* only affects a subset of Ras-controlled processes. The main role of the Ras proteins is in regulating PKA activity, although Ras also controls other cellular processes independently of PKA (Section 1.6.1). Therefore, the proposed effects of multicopy *GIS2* on Ras activity may or may not depend on PKA activity. This is discussed further in the next Chapter.

6.3.2 What is the molecular role of *GIS2*?

The idea that *GIS2* is a nucleic acid chaperone was discussed in Section 6.2.1 and is based largely on published data about the metazoan homolog, CNBP. The observation that *GIS2* can be deleted without showing any detectable adverse phenotype, in the experimental conditions assayed, (Figure 6.2) contrasts with the

fact that CNBP is an essential gene for vertebrate embryogenesis (Abe *et al.*, 2006; Chen *et al.*, 2003). Two different roles have been shown for metazoan CNBP in different model organisms. One is a role in transcriptional regulation, which has been studied in most depth for the expression of *c-MYC* (Chen *et al.*, 2003; Michelotti *et al.*, 1995; Shimizu *et al.*, 2003). It is the failure in expression of the *c-MYC* transcription factor (and probably other unknown targets) in the *cnbp*$^{-/-}$ mouse that is thought to cause embryonic lethality. *GIS2* could be involved in non-essential transcriptional regulation in *S. cerevisiae*. *In vitro*, CNBP shows a preference for binding single-stranded guanosine-rich probes (Armas *et al.*, 2008; Yasuda *et al.*, 1995). Human CNBP binds to the purine-rich strand of the CT-element in the *c-MYC* promoter, which is 5 imperfect direct repeats of the "CCCTCCCCA" sequence (Michelotti *et al.*, 1995). In *S. cerevisiae* decreasing PKA activity activates transcription of genes with a STRE in their promoter (Smith *et al.*, 1998). Assuming increasing *GIS2* expression and decreasing PKA activity do share some downstream effects, it is interesting to note that the STRE (CCCCT) is a similar sequence to the CT-element. Although the main transcription factors that control STRE gene expression are known to be Msn2 and Msn4 (Martinez-Pastor *et al.*, 1996), it is possible that other factors, such as Gis2, could play a more minor role.

In support of this last idea, CNBP is phosphorylated by PKA in zebra fish embryonic extracts (Lombardo *et al.*, 2007). PKA-dependent phosphorylation of CNBP promoted, *in vitro*, the annealing of complementary oligonucleotides corresponding to the c-*MYC* promoter (i.e. its nucleic acid chaperone activity). The authors suggested that PKA-dependent phosphorylation of CNBP represented a conserved post-translational modification to fine-tune gene expression. This phosphorylation site is conserved in other higher eukaryotic CNBPs (T172 in hCNBP), but not in *S. cerevisiae* Gis2 (Figure 6.1). Thus, whereas a functional link between *GIS2* and PKA probably exists in *S. cerevisiae*, direct control of CNBP function by PKA would have arisen later on in evolution.

The other role described for metazoan CNBP is in translational regulation of mRNAs containing 5'TOP-elements, such as those that encode ribosomal proteins. This role is particularly intriguing when it comes to considering the role of *GIS2*. In a genome wide study, *GIS2* expression was shown to be co-regulated with that of ribosomal

proteins and co-regulation of gene expression often reflects a related function (Brown *et al.*, 2000). The level of ribosome biosynthesis is carefully balanced with growth rate (reviewed by Warner, 1999). Therefore, when growth conditions are good the expression of ribosomal proteins is induced via PKA activity (Klein & Struhl, 1994; Neuman-Silberberg *et al.*, 1995). An attempt was made to assess *GIS2* expression levels after switching from raffinose to glucose as a carbon source, but no change in *GIS2* expression was seen under these conditions (Figure 6.3C). It is possible those were not the right conditions in which to observe a change in expression levels. The upregulation of ribosomal protein gene expression is seen during the shift from a non-fermentable carbon source, such as glycerol or ethanol, to glucose (Pernambuco *et al.*, 1996). Raffinose is a trisaccharide of galactose, fructose, and glucose, which can be metabolised and used for fermentation. Therefore a better choice of carbon source in growing the culture before glucose addition would have been glycerol.

A potential link between *GIS2* and ribosome biogenesis is also suggested by the fact that Nop1, Sbp1, and Pwp1 (proteins that interact with *GIS2*) (Krogan *et al.*, 2006) have established links to ribosome biogenesis. These proteins are localised to the nucleolus and mutants confer defects in rRNA processing (Schimmang *et al.*, 1989; Tollervey *et al.*, 1991; Zhang *et al.*, 2004). The possibility that Gis2 was also a nucleolar protein was tested by looking at the localisation of Gis2-GFP. However, when tested, this protein localised throughout the cell (Figure 6.4). Unfortunately attempts to clone *GIS2-GFP* to test whether the fusion protein was functional or not were unsuccessful. However if the images do represent the functional localisation of Gis2, the nuclear and cytoplasmic localisation would be consistent with *GIS2* having a role in the transcriptional and translational regulation of gene expression, as suggested for CNBP. Reports on the cellular localisation of CNBP (nuclear or cytoplasmic) vary depending on the model organism, the tissue type, and the developmental stage (Armas *et al.*, 2004; Shimizu *et al.*, 2003; Warden *et al.*, 1994).

Overall, how the proposed nucleic acid chaperone activity of *GIS2* would contribute to its *in vivo* function remains unknown. CNBP is thought to play a role in fine-tuning the level of translation of TOP-element-containing mRNAs (Crosio *et al.*, 2000). This type of fine-tuning role would be consistent with the lack of detectable

phenotype in a *gis2Δ*. In view of the suspected links to Ras-cAMP-PKA signalling and ribosome biogenesis, it is tempting to speculate that *GIS2* could fine-tune gene expression to help cells balance their metabolic state with nutrient availability. Gis2 could do this by altering the stability of nucleic acid secondary structure in mRNAs or at gene promoter elements.

Chapter 7

Deletion of *RAS2* suppresses *arg4::mec1-4* lethality

7.1 Introduction

The links between *GIS2* and Ras activity were discussed in Chapter 6. Although the precise relationship between *GIS2* and Ras function remains unknown, multicopy expression of *GIS2* and downregulation of Ras activity seem to have some shared downstream effects. The focus of this thesis is on understanding the essential role of *MEC1*. Therefore, based on what has been learnt about *GIS2* (Chapter 6), potential genetic interactions between Ras activity and temperature sensitive *mec1* strains were investigated.

7.2 Results

7.2.1 Multicopy *GIS2* is not a general suppressor of temperature sensitive alleles

Decreasing Ras-cAMP-PKA signalling increases cellular resistance to heat shock (Iida, 1988). Interestingly, decreasing Ras-cAMP-PKA signalling does not significantly induce the expression of heat shock-induced protein chaperones (Boy-Marcotte *et al.*, 1999). It does however cause an increase in the levels of the storage carbohydrate trehalose (α,α-1,1-diglucose) (Tatchell *et al.*, 1985), and trehalose has been shown to increase the thermal stability of proteins (De Virgilio *et al.*, 1994; Hottiger *et al.*, 1994). So, it is possible that an increase in trehalose levels could stabilise the temperature sensitive Mec1-4 protein. This possibility is particularly relevant as there are other examples of temperature sensitive alleles that can be suppressed by decreasing Ras-cAMP-PKA signalling (Section 6.2.7). Therefore, the specificity of the effect of multicopy *GIS2* expression on the growth of temperature sensitive *mec1* strains was assessed. To do this, the ability of multicopy *GIS2*

expression to improve the viability of other temperature sensitive alleles readily available in the lab was tested.

Strains expressing a temperature sensitive alleles of a condensin subunit (*ycg1-2*), topoisomerase II (*top2-1*), separase (*esp1-1*), and *DBF4* (*dbf4-1*) with either the YEp24 control plasmid or the multicopy *GIS2* plasmid were grown overnight at 23°C in SD-URA. The following morning each culture was diluted to an OD_{600} of 0.5, and 10-fold serial dilutions were spotted onto SD-URA agar. The agar plates were incubated at the indicated temperature for two days. All four alleles tested showed the expected temperature sensitive growth, and this was not altered by the expression of multicopy *GIS2* (Figure 7.1). In addition, the temperature sensitivity of a *dbf2-2* allele, tested previously, was also not altered by increased *GIS2* expression (Figure 6.7). Therefore multicopy *GIS2* is not a general suppressor of temperature sensitive alleles, and the effect of multicopy *GIS2* that suppresses the lethality of temperature sensitive *mec1* strains is most likely to be something more specific to *MEC1* function or the temperature sensitive *mec1* alleles. Although trehalose is a thermoprotectant in wild type cells exposed to heat stress (De Virgilio *et al.*, 1994; Hottiger *et al.*, 1994), whether an increase in trehalose levels can act as a general suppressor of temperature sensitive alleles is not known.

7.2.2 Deletion of *RAS2* suppresses *arg4::mec1-4* lethality

Based on the proposed role of *GIS2* in regulating Ras function (Chapter 6), the effect of downregulating Ras activity on the viability of temperature sensitive *mec1* strains was investigated. A strain expressing the *arg4::mec1-4* allele with a deletion of *RAS2* was constructed, along with the congenic wild type controls. The resulting *arg4::MEC1 RAS2* (CEY480), *arg4::mec1-4 RAS2* (CEY477), *arg4::MEC1 ras2Δ* (CEY514) and *arg4::mec1-4 ras2Δ* (CEY511) strains were grown overnight at 23°C in YPD, diluted to an OD_{600} of 0.5, and 10-fold serial dilutions were spotted onto YPD agar. The agar plates were incubated at the indicated temperatures for two days. Deletion of *RAS2* did partially suppress the temperature sensitivity of the *arg4::mec1-4* strain (Figure 7.2).

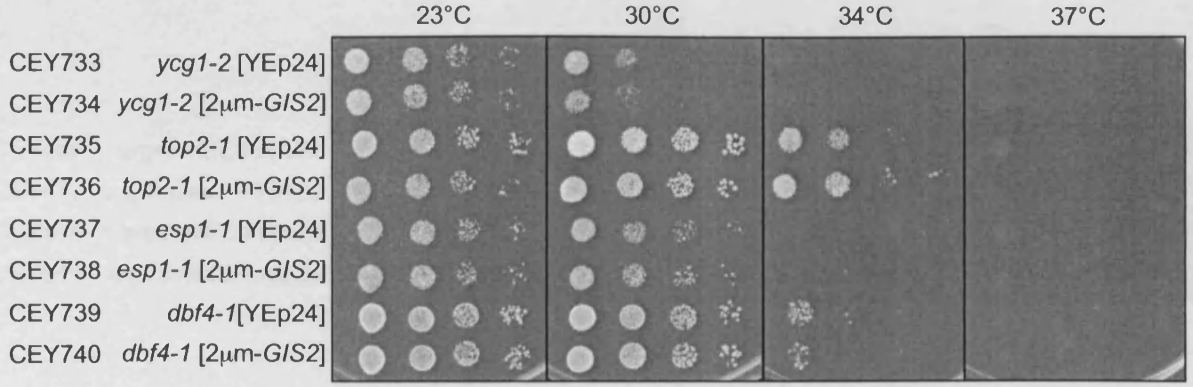

Figure 7.1 Multicopy *GIS2* is not a general suppressor of temperature sensitive alleles. The indicated strains were grown overnight at 23°C in SD-URA. The following morning each culture was diluted to OD_{600} of 0.5, and 10-fold serial dilutions were spotted onto SD-URA agar. The agar plates were incubated at the indicated temperatures for two days. The plasmids used were YEp24 (empty vector) and pCLE8 (2μm-*GIS2*).

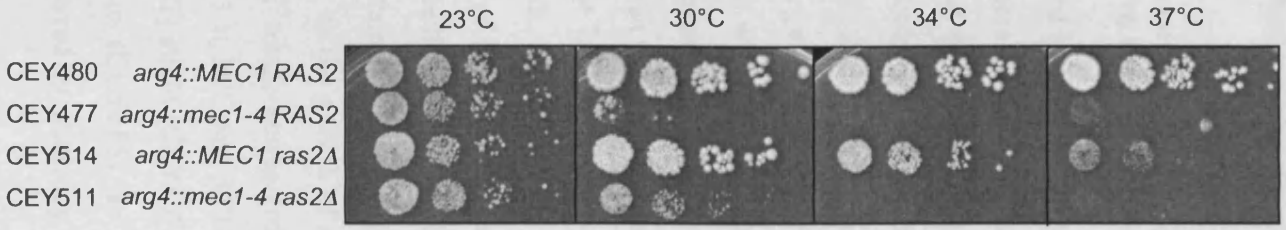

Figure 7.2 Deletion of *RAS2* suppresses *arg4::mec1-4* lethality. The indicated strains were grown overnight at 23°C in YPD. The following morning each culture was diluted to an OD_{600} of 0.5, and 10-fold serial dilutions were spotted onto YPD agar. The agar plates were incubated at the indicated temperatures for two days.

The *ras2Δ* strain itself was temperature sensitive at 37°C. This phenotype has been reported previously in the literature, and correlates with a defect in cytoskeletal polarity observed at high temperatures in a *ras2Δ* strain (Ho & Bretscher, 2001; Wigler *et al.*, 1988).

7.2.3 The effect of multicopy *GIS2* on the viability of *arg4::mec1-4* is epistatic to that of *ras2Δ*

The data presented so far show that *ras2Δ* and multicopy *GIS2* share the ability to suppress the temperature sensitivity of both the *cdc15-2* and the *arg4::mec1-4* strains (Figures 5.7 and 6.1). However, the mechanisms underlying these genetic interactions are not known. To investigate this further, the combined effect of *ras2Δ* and multicopy *GIS2* on the growth of the *arg4::mec1-4* strain was tested. Strains expressing the *arg4::mec1-4* or *arg4::MEC1* alleles, in *RAS2* or *ras2Δ* genetic backgrounds, and with either the YEp24 control plasmid or the multicopy *GIS2* plasmid were constructed. These strains were grown overnight at 23°C in SD-URA media, diluted to an OD_{600} of 0.5, and 10-fold serial dilutions were spotted onto SD-URA agar (Figure 7.3). The agar plates were incubated at the indicated temperature for two days. Both *ras2Δ* (CEY585) and multicopy *GIS2* (CEY665) suppressed the lethality of the *arg4::mec1-4* strain as expected (Figure 7.3). Multicopy *GIS2* seemed to have a marginally greater effect than *ras2Δ* in enhancing the growth of the *arg4::mec1-4* strain (compare CEY665 and CEY585 at 34°C). However this is difficult to judge as the growth of *ras2Δ* strains was slower than that of wild type strains at higher temperatures (compare colony size of CEY565/CEY661 and CEY595/CEY663 at 30°C and 34°C). The level of suppression in the *arg4::mec1-4 ras2Δ* [2μm-*GIS2*] strain (CEY667) was similar to that of the *arg4::mec1-4 RAS2* [2μm-*GIS2*] strain (CEY665), so deleting *RAS2* did not increase the level of suppression conferred by multicopy *GIS2*.

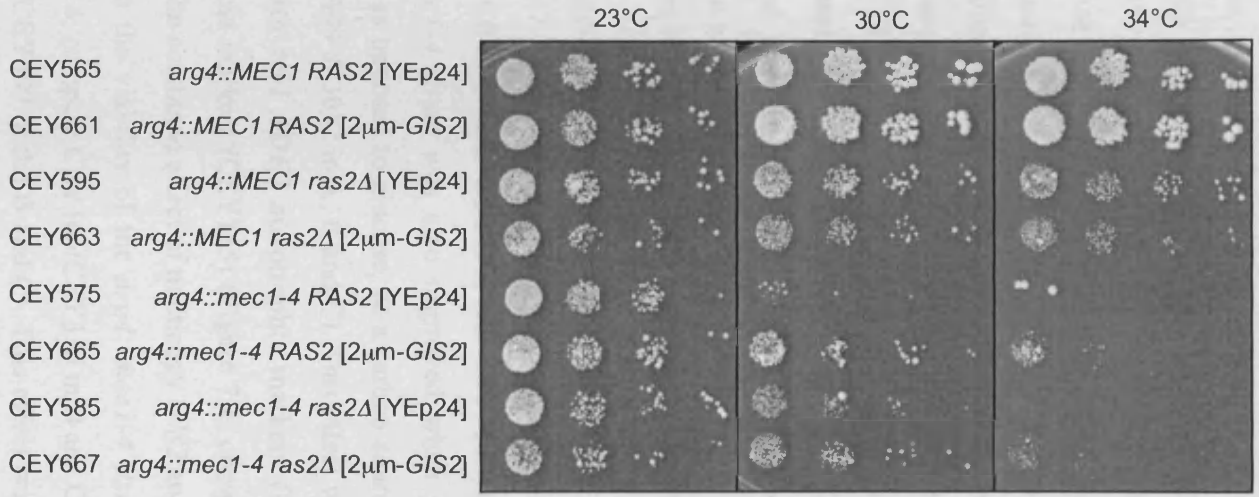

Figure 7.3 The effect of multicopy *GIS2* on the viability of *arg4::mec1-4* is epistatic to that of *ras2Δ*. The indicated strains were grown overnight at 23°C in SD-URA. The following morning each culture was diluted to an OD_{600} of 0.5, and 10-fold serial dilutions were spotted onto SD-URA agar. The agar plates were incubated at the indicated temperature for two days. The plasmids used were YEp24 (empty vector) and pCLE8 (2μm-*GIS2*).

7.2.4 Growth on non-glucose carbon sources suppresses *arg4::mec1-4* lethality

GIS2 was initially isolated as a suppressor of the inability of *snf1Δ mig1Δ gig1/2/3* mutants to grow on galactose (Balciunas & Ronne, 1999). The *snf1Δ mig1Δ gig1/2/3* mutant has a defect in the transcription of genes required to metabolise galactose. Also, some of the temperature sensitive APC/C and MEN mutants that can be suppressed by downregulating PKA activity can also be suppressed by growth on non-glucose carbon sources (Bolte *et al.*, 2003; Irniger *et al.*, 2000). Therefore, the ability of strains expressing the *arg4::mec1-4* or *arg4::MEC1* alleles, with either the YEp24 control plasmid or the multicopy *GIS2* plasmid, to grow on non-glucose carbon sources was assessed. As an additional control, two sets of strains were used: one with *TRP1* and *ade2* marker genes and the other with *trp1* and *ADE2* marker genes. These strains were grown overnight at 23°C in SD-URA, diluted to an OD_{600} of 0.5, and 10-fold serial dilutions were spotted on to minimal agar media lacking uracil with either 2% glucose, 2% galactose or 2% glycerol as a carbon source. Agar plates were then incubated at the indicated temperature for two days.

As expected, the expression of multicopy *GIS2* improved the viability of the *arg4::mec1-4* strain when grown with glucose as a carbon source (Figure 7.4A; compare CEY163 with CEY155, and CEY310 with CEY309). The viability of the *arg4::mec1-4* strain was also improved when grown with either galactose or glycerol, as opposed to glucose, as a carbon source (Figure 7.4; compare CEY155 and CEY309 at 30°C in A, B and C). This effect was stronger for the *arg4::mec1-4* strain with *trp1 ADE2* auxotrophic markers (CEY309) than with *TRP1 ade2* auxotrophic markers (CEY155) (Figure 7.4; compare CEY155 with CEY309 in B and C). The combined effect of multicopy *GIS2* and growth on a non-glucose carbon source on the viability of the *arg4::mec1-4* strain was greater than either alone (Figure 7.4; compare CEY163/CEY310 in B and C with CEY163/CEY310 in A and CEY155/CEY309 in the B and C). This effect was clearly observable for CEY163 (*TRP1 ade2*), but was not as noticeable for CEY310 (*trp1 ADE2*).

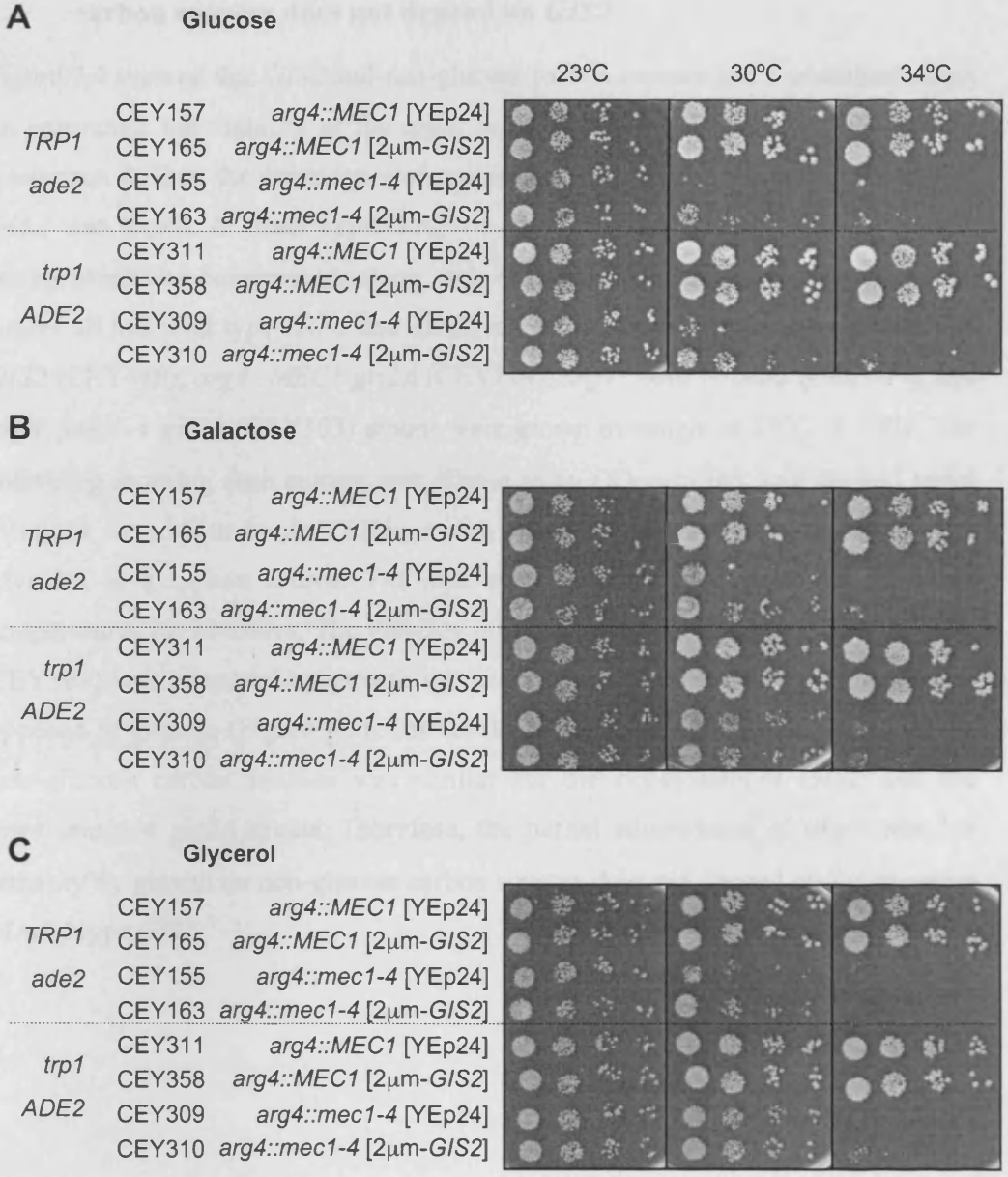

Figure 7.4 Growth on non-glucose carbon sources suppresses *arg4::mec1-4* lethality. The indicated strains were grown overnight at 23°C in SD-URA. The following morning each culture was diluted to an OD_{600} of 0.5, and 10-fold serial dilutions were spotted on to minimal agar media lacking uracil with the indicated carbon source at 2%. Agar plates were incubated at the indicated temperature for two days. Strains CEY157, CEY165, CEY155 and CEY163 are *TRP1 ade2::LK* and strains CEY311, CEY358, CEY309 and CEY310 are *trp1Δ::hisG ADE2*. The plasmids used were YEp24 (empty vector) and pCLE8 (2μm-*GIS2*).

7.2.5 Suppression of *arg4::mec1-4* lethality by growth on non-glucose carbon sources does not depend on *GIS2*

Figure 7.4 showed that *GIS2* and non-glucose carbon sources had a combined effect on enhancing the viability of the *arg4::mec1-4* strain. To investigate this genetic interaction further, the dependence of suppression by non-glucose carbon sources on *GIS2* was tested. A strain expressing the *arg4::mec1-4* allele in a *gis2Δ* genetic background was constructed, along with the congenic wild type controls. These strains all had wild type *TRP1* and *ADE2* marker genes. The resulting *arg4::MEC1 GIS2* (CEY480), *arg4::MEC1 gis2Δ* (CEY724), *arg4::mec1-4 GIS2* (CEY477), and *arg4::mec1-4 gis2Δ* (CEY303) strains were grown overnight at 23°C in YPD. The following morning each culture was diluted to an OD_{600} of 0.5, and 10-fold serial dilutions were spotted onto YEP agar with either 2% glucose, 2% galactose or 2% glycerol as a carbon source. The agar plates were incubated at the indicated temperatures for two days. The viability of the *arg4::mec1-4* strains (CEY477 and CEY303) was increased by growth on media containing galactose or glycerol, as opposed to glucose (Figure 7.5). The level of suppression conferred by growth on non-glucose carbon sources was similar for the *arg4::mec1-4 GIS2* and the *arg4::mec1-4 gis2Δ* strains. Therefore, the partial suppression of *arg4::mec1-4* lethality by growth on non-glucose carbon sources does not depend on the presence of wild type *GIS2*.

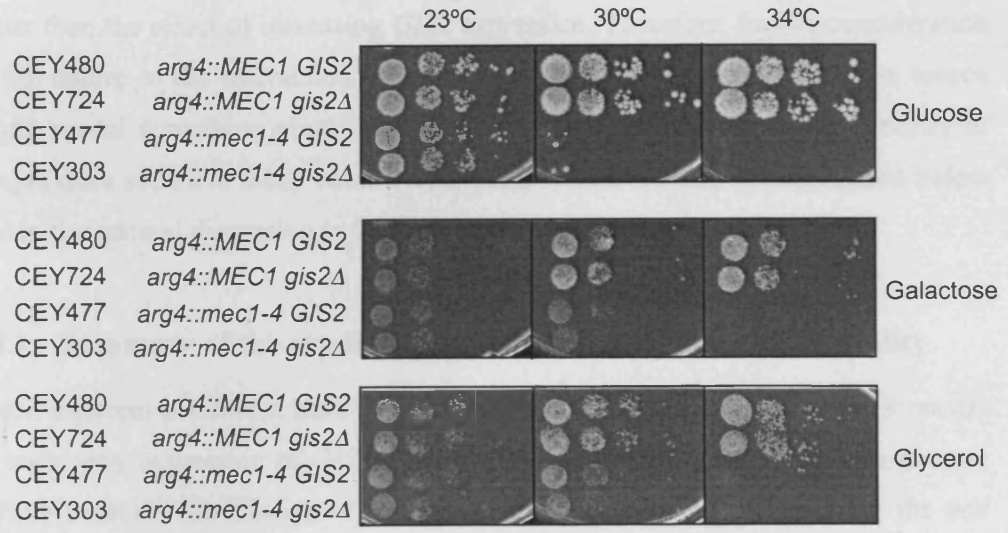

Figure 7.5 Suppression of *arg4::mec1-4* lethality by growth on non-glucose carbon sources does not depend on *GIS2*. The indicated strains were grown overnight at 23°C in YPD. The following morning each culture was diluted to an OD_{600} of 0.5, and 10-fold serial dilutions were spotted on to YEP agar with the indicated carbon source at 2%. Agar plates were incubated at the indicated temperature for two days.

7.3 Discussion

The initial motivation to investigate the potential effect of downregulating Ras activity on the viability of temperature sensitive *mec1* strains was based on the published genetic interaction between *GIS2* and *RAS* activity (Balciunas & Ronne, 1999). The data presented in this Chapter show that deletion of *RAS2* and growth on non-glucose carbon sources can suppress *arg4::mec1-4* lethality. Current understanding of the effect of these two conditions on cellular proliferation is much better than the effect of increasing *GIS2* expression. Therefore, further consideration of the nature of the interaction between *arg4::mec1-4* and *RAS2* or carbon source might reveal something about the *GIS2*-dependent suppression of the lethality of temperature sensitive *mec1* strains. This point is addressed in the discussion below and in the general discussion in Chapter 8.

7.3.1 Summary of the conditions that suppress *arg4::mec1-4* lethality

Three different conditions have been shown to suppress the lethality of *arg4::mec1-4*: multicopy expression of *GIS2*, deletion of *RAS2* and growth using non-glucose carbon sources. Modulation of PKA activity is important to ensure that the cell adapts its metabolism and growth rate to match the available nutrients (Section 1.6). All three of these conditions can be linked to the downregulation of PKA activity, although none of them in an exclusive manner (Figure 7.6). So, there are published data to suggest that the function of Gis2, and its homologs, is linked to Ras or PKA activity (Balciunas & Ronne, 1999; Lombardo *et al.*, 2007; Xu *et al.*, 1992). However, the role of Gis2 in the cell might be more general than an involvement with PKA activity. For example, in fine-tuning gene expression, which could be in a Ras/PKA-dependent and/or Ras/PKA-independent manner (Chapter 6).

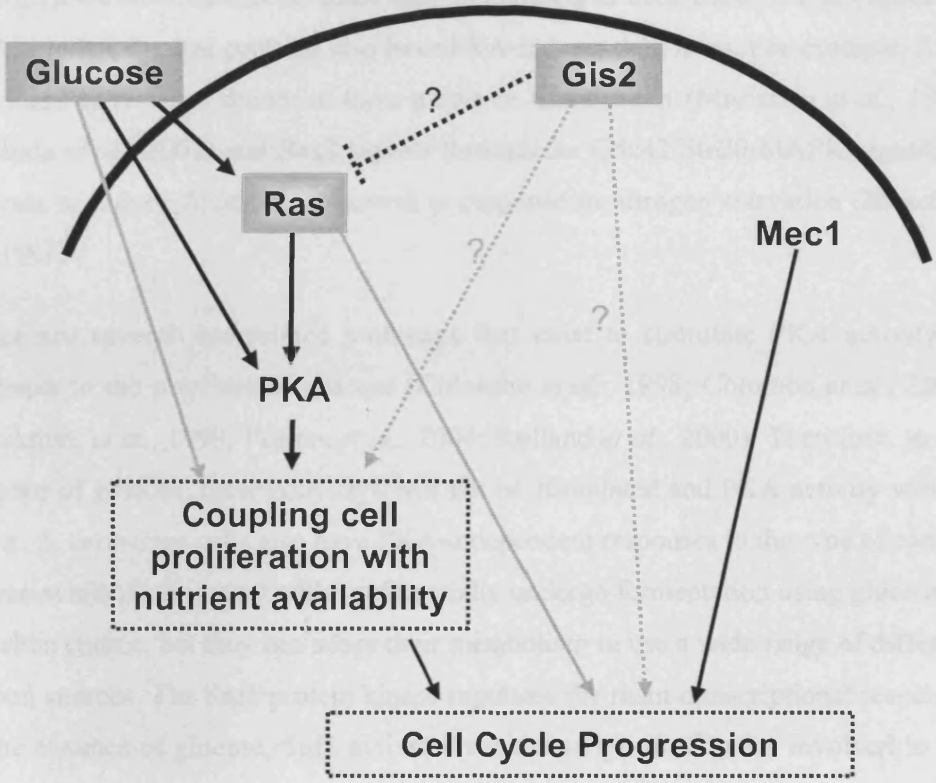

Figure 7.6 The regulation of PKA activity is a common theme in the three conditions that have been shown to suppress *arg4::mec1-4* lethality. The thick black line signifies the cell membrane. The dashed lines indicated possible roles for Gis2. The black arrows show how Gis2, the Ras proteins and carbon source can/could all influence PKA activity. The grey arrows represent PKA independent routes by which Gis2, the Ras proteins and carbon source can/could influence cell proliferation. Mec1 is known to be required for successful progression through the cell cycle. Progression through the cell cycle needs to be coupled with the available nutrients, and PKA activity is an important pathway to do this. Therefore, a change in PKA activity could, somehow, compensate for the defect in cell cycle progression in ***arg4::mec1-4*** at the non-permissive temperature. A decrease in PKA activity is a common route by which all three conditions that have been shown to suppress ***arg4::mec1-4*** lethality (grey boxes) could function.

Deletion of *RAS2* decreases PKA activity, but without inhibiting log phase growth, and consequently *ras2Δ* strains have been widely used in experimental studies of the Ras-cAMP-PKA pathway (Engelberg *et al.*, 1994; Tatchell *et al.*, 1985; Xue *et al.*, 1998). However it should be noted that, in addition to their main role in regulating PKA activity, the Ras proteins also have PKA-independent roles. For example, Ras1 and Ras2 have been shown to have a role in mitotic exit (Morishita *et al.*, 1995; Yoshida *et al.*, 2003) and Ras2 signals through the Cdc42/Ste20/MAPK signalling cascade to induce filamentous growth in response to nitrogen starvation (Mosch *et al.*, 1996).

There are several interrelated pathways that exist to stimulate PKA activity in response to the presence of glucose (Colombo *et al.*, 1998; Colombo *et al.*, 2004; Kraakman *et al.*, 1999; Peeters *et al.*, 2006; Rolland *et al.*, 2000). Therefore, in the absence of glucose, these pathways will not be stimulated and PKA activity will be lower. *S. cerevisiae* cells also have PKA-independent responses to the type of carbon source available. So, yeast cells preferentially undergo fermentation using glucose as a carbon source, but they can adapt their metabolism to use a wide range of different carbon sources. The Snf1 protein kinase regulates the main transcriptional response: in the absence of glucose, Snf1 activates the transcription of genes involved in the metabolism of alternative carbon sources, gluconeogenesis and respiration (Carlson, 1999). For example, upregulation of gluconeogenesis and respiration is essential for yeast cells to survive using non-fermentable carbon sources, such as glycerol (Schuller, 2003). Also, transcriptional activation of the *GAL* genes, which occurs in the presence of galactose and in the absence of glucose, is required to convert the hexose galactose into glucose-6-phosphate, which can then be used for fermentation (Johnston, 1987).

Since all three suppression conditions can be linked to the downregulation of PKA activity, the simplest explanation is that the viability of *arg4::mec1-4* is improved for the same reason in each case. Therefore, the prediction is that a downstream effect of decreasing PKA activity can, somehow, suppress the lethality of temperature sensitive *mec1* strains (Figure 7.6). Unfortunately this idea has not yet been tested directly as initial attempts to assess the effect of multicopy *BCY1* or *PDE2* on the growth of temperature sensitive *mec1* strains were not successful.

7.3.2 The relationship between the three conditions that suppress *arg4::mec1-4* lethality

The level of suppression of *arg4::mec1-4* lethality conferred by both *ras2Δ* and non-glucose carbon sources was similar to the level of suppression described for multicopy expression of *GIS2* (Section 4.2.1). Combining deletion of *RAS2* with increased expression of *GIS2* did not increase the level of suppression of *arg4::mec1-4* lethality further (Figure 7.3). This suggests that both these conditions influence the growth of *arg4::mec1-4* by the same mechanism. Multicopy expression of *GIS2* seemed to confer a marginally greater level of suppression of *arg4::mec1-4* lethality than deletion of *RAS2* did. Therefore, assuming a common mechanism of suppression, other *RAS*-independent effects of multicopy *GIS2* expression could also influence the growth of *arg4::mec1-4* strains.

Increased *GIS2* expression showed a combined effect with the absence of glucose on the level of suppression of *arg4::mec1-4* lethality (Figure 7.4). This is consistent with a model where *GIS2* acts by downregulating the Ras-cAMP-PKA signalling, and the absence of glucose can also independently downregulate PKA activity. In this model, suppression of *arg4::mec1-4* lethality by the absence of glucose should be independent of *GIS2*, and again this is what was seen (Figure 7.5).

One problem with this model however is that multicopy expression of *GIS2* does not have a dominant effect in decreasing PKA activity (Sections 5.2.6 and 5.3.1). For example, the combined effect of the absence of glucose and deleting *RAS2* on the growth of *arg4::mec1-4* could not be tested, because in this situation the level of PKA activity falls too low for cells to proliferate (Figure 6.7) (Tatchell *et al.*, 1985). However, the combined effect of the absence of glucose and increasing *GIS2* expression could be tested (Figure 7.4), which appears inconsistent with the fact that the effect of multicopy *GIS2* on the viability of *arg4::mec1-4* was epistatic to that of *ras2Δ* (Figure 7.3). Another possibility is that multicopy *GIS2* does not negatively regulate Ras activity, but instead independently causes some downstream effects that are shared by downregulation of PKA activity. Although this model still does not explain why multicopy *GIS2* showed a combined effect on the level of suppression of *arg4::mec1-4* lethality in the absence of glucose, but not with *ras2Δ*.

The observation that the effect of the absence of glucose on the growth of *arg4::mec1-4* varied depending on the auxotrophic markers genes of the strain is also puzzling (Figure 7.4). Downregulation of PKA activity causes significant changes to cellular metabolism (Thevelein & de Winde, 1999), and one of these changes may well account for the suppression of *arg4::mec1-4* lethality. It is possible that additional changes to cellular metabolism, depending on the auxotrophic requirements of a strain, can influence the level of suppression conferred.

A more detailed analysis of the relationship between *GIS2*, the Ras-cAMP-PKA pathway and the type of carbon source was beyond the scope of this thesis. But, despite the open questions described above, it remains a reasonable assumption that there is a common mechanism of suppression of *arg4::mec1-4* lethality for the three different conditions. This common mechanism of suppression is most likely to be downregulation of PKA activity.

Chapter 8

General Discussion

8.1 The role of *MEC1* in promoting replication fork progression through *RSZs*

The hypothesis investigated in Chapter 3 stated that Mec1 could be required to fine-tune dNTP availability with replication fork progression through *RSZs*. The key prediction of this hypothesis is that the relevant proteins (Mec1, RNR, and Sml1) should co-localise with the replication fork. Therefore, I tested this hypothesis by using ChIP and immunocytology to look for the association of Mec1 and Rnr1 with replicating DNA. However, no data were obtained that supported this hypothesis. Nevertheless, given the technical limitations of these assays (Section 3.3.1), the precise role of Mec1 in promoting continued replication fork progression through *RSZs*, and whether fork progression through *RSZs* depends on the role of Mec1 in regulating dNTP levels, remain open questions.

8.2 The mechanism of suppression of the lethality of temperature sensitive *mec1* alleles by multicopy *GIS2*

8.2.1 Elucidating the mechanism of suppression

Several possibilities were considered and tested experimentally to elucidate the nature of the interaction between the temperature sensitive *mec1* alleles and multicopy *GIS2*. The observation that multicopy *GIS2* could not detectably restore viability of *mec1Δ* or *mec1-kd* (Figure 4.2) suggested that the temperature sensitive Mec1 protein was required for suppression. Two further possibilities were then considered: i) that multicopy *GIS2* directly restored Mec1 activity or ii) that the effect of multicopy *GIS2* bypassed the essential function of Mec1, but still required some residual activity of the temperature sensitive Mec1 protein to increase viability. These models were initially presented in Section 4.3.1 and Figure 4.7.

Mec1 function could be restored by several different mechanisms. One would be to stabilise the temperature sensitive Mec1 protein at the restrictive temperature. This could be achieved by the Gis2 protein binding the temperature sensitive Mec1 protein directly. However, the structure of *GIS2* and the behaviour of its metazoan homolog, CNBP, suggested that Gis2 functions primarily through binding to nucleic acids (Section 6.2.1). The temperature sensitive Mec1 protein could also be stabilised by a change in cellular metabolism that generally increases the thermal stability of proteins. Multicopy *GIS2* did not have a general ability to suppress the lethality of temperature sensitive alleles of different genes (Figure 7.1). However, multicopy *GIS2*, and other related conditions such as *ras2Δ*, do have the ability to suppress the lethality of temperature sensitive alleles of several functionally distinct genes (Chapter 6).

Mec1 activity could also be restored by increasing the expression of the temperature sensitive *mec1* allele or by promoting the interaction of the temperature sensitive Mec1 protein with its kinase substrates (Section 4.3). Whatever the mechanism, if Mec1 function was being restored then this should be apparent phenotypically. For example, restoring Mec1 activity in temperature sensitive *mec1* strains should restore cell cycle-dependent fluctuations in Sml1 protein levels and would also be expected to increase the ability of cells to grow in the presence of genotoxic stress. The precise effect of multicopy *GIS2* on the ability of temperature sensitive *mec1* strains to grow in the presence of genotoxic stress remains unclear (Section 4.2.5). Some cell cycle-dependent fluctuation in Sml1 protein levels was seen in *arg4::mec1-4* cells expressing multicopy *GIS2* (Figure 5.4). This could be a direct effect of increased activity of the temperature sensitive Mec1 protein, it could be a Mec1-independent direct effect of multicopy *GIS2*, or it could be a consequence of the *GIS2*-dependent improvement in S-phase progression, as discussed in Section 5.3.2.

Overall, no experimental evidence is presented that strongly argues either way as to whether multicopy *GIS2* suppresses the lethality of temperature sensitive *mec1* alleles by directly restoring Mec1 function or by bypassing the essential function of *MEC1*.

8.2.2 Could changes in Sml1 protein levels account for the suppression?

Multicopy expression of *GIS2* lead to two different changes in Sml1 protein levels: a trend for a general increase in Sml1, but also a cell cycle-dependent decrease in Sml1 (Figures 5.1, 5.3 and 5.4). Although these two changes may appear inconsistent with each other, both could be accounted for by some change in the balance of protein synthesis and degradation. Decreasing Ras-cAMP-PKA signalling is known to have a significant effect on this balance. In a wild type cell, Ras-cAMP-PKA signalling is decreased in response to nutrient deprivation. The resultant effect is to shut down cellular metabolism as cells cease to proliferate. One effect of decreasing Ras-cAMP-PKA signalling activity is to decrease the transcription of ribosomal protein genes, so that protein synthesis rates are decreased (Klein & Struhl, 1994; Neuman-Silberberg *et al.*, 1995). Another effect is to promote autophagy, which is the pathway that targets proteins, and other cytoplasmic constituents, to the vaculolar compartment for degradation (Budovskaya *et al.*, 2004). The results presented in Chapter 7 suggest that suppression of the lethality of temperature sensitive *mec1* alleles by multicopy *GIS2* could be mediated by a downstream effect of decreasing PKA activity. If this downstream effect were a change in the balance of protein synthesis and degradation then the expected overall effect would be to decrease protein levels. This idea is therefore not consistent with the observed general increase in Sml1 protein levels (Figure 5.1).

A general alteration in the balance of protein synthesis and degradation is also difficult to reconcile with the increase in cell cycle-dependent degradation of Sml1 protein levels. For multicopy *GIS2* to restore cell cycle-dependent fluctuations in Sml1 protein levels it would need to specifically target the Sml1 degradation pathway during S-phase, rather than promote the general degradation of the autophagy pathway. The idea that *GIS2* could make Sml1 more accessible to the protein degradation machinery was suggested in Section 5.3.2. Sml1 is targeted for degradation by the 26S proteasome after ubiquitination by the SCF^{Cdc4} ubiquitin ligase (R. Rothstein, personal communication). Therefore, this idea could be tested further by assessing the phosphorylation status of Sml1 and the effect of mutations in the Sml1 degradation pathway on the suppression of the lethality of temperature sensitive *mec1* alleles by multicopy *GIS2*.

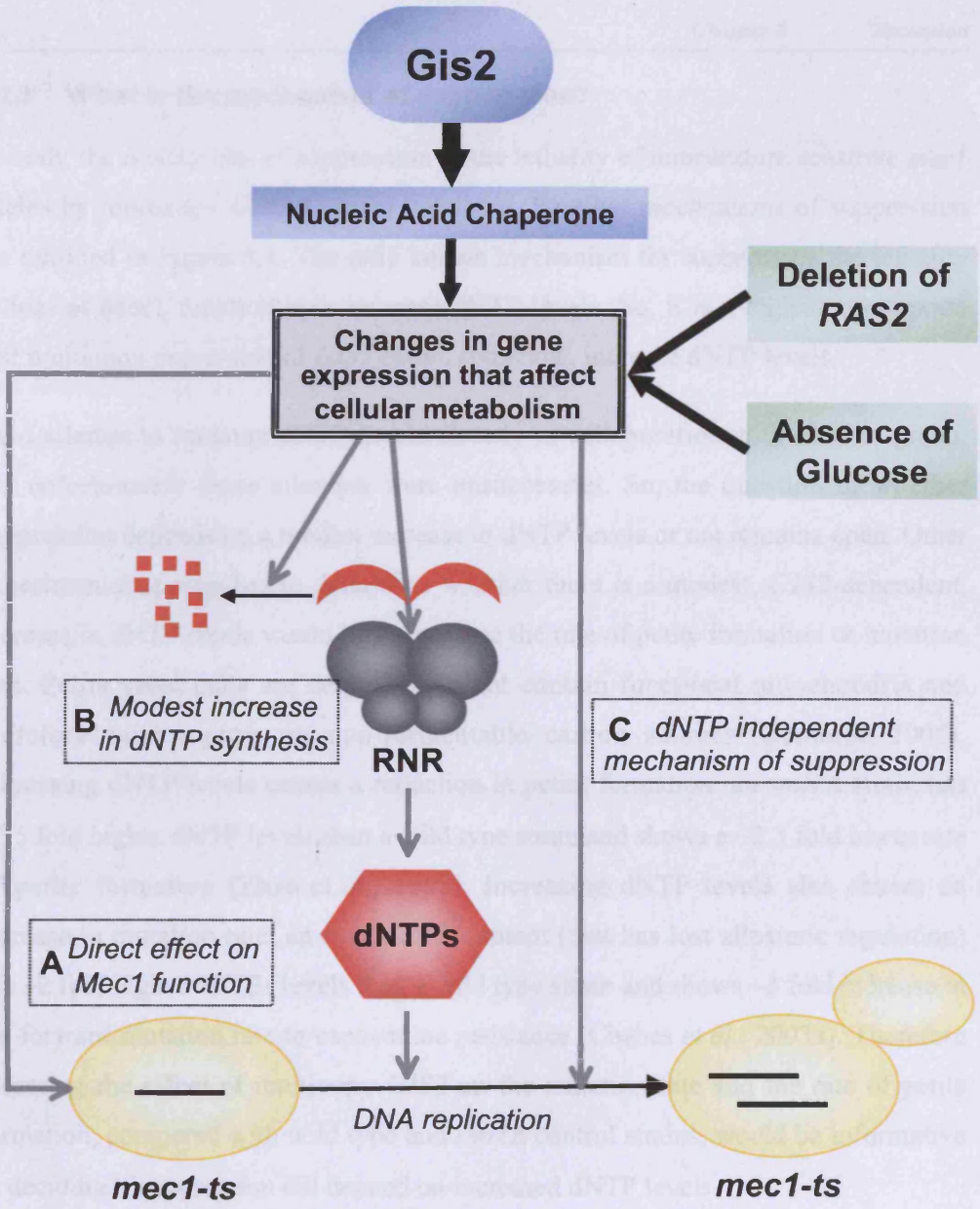

Figure 8.1 The nature of the genetic interaction between *GIS2* and temperature sensitive *mec1* alleles. A model outlining possible mechanisms of suppression of the lethality of temperature sensitive *mec1* alleles (*mec1-ts*) by multicopy *GIS2*, as discussed in Chapter 8. The molecular function of Gis2 is most likely to be as a nucleic acid chaperone. Multicopy *GIS2*, deletion of *RAS2*, and the absence of glucose have all been shown to independently suppress the lethality of *mec1-ts*. Assuming a common mechanism of suppression in each case, there are several possible mechanisms for how these conditions could influence the viability of a *mec1-ts* strain. **A)** There could be a direct effect to increase the activity of the Mec1-ts protein. **B)** There could be a modest increase in dNTP levels, for example by increasing the level of dNTP precursors, or by increasing Sml1 degradation. **C)** There could be a dNTP-independent mechanism of improving S-phase progression, for example by increasing the stability of the replisome.

8.2.3 What is the mechanism of suppression?

Overall, the mechanism of suppression of the lethality of temperature sensitive *mec1* alleles by multicopy *GIS2* remains unknown. Possible mechanisms of suppression are outlined in Figure 8.1. The only known mechanism for suppressing the lethality of loss of Mec1 function is to increase dNTP levels. So, it is a logical assumption that multicopy expression of *GIS2* could, somehow, increase dNTP levels.

I did attempt to measure dNTP levels directly in collaboration with another group, but unfortunately these attempts were unsuccessful. So, the question of whether suppression depends on a modest increase in dNTP levels or not remains open. Other experimental approaches to determine whether there is a modest, *GIS2*-dependent, increase in dNTP levels would be to measure the rate of petite formation or mutation rate. Petite yeast cells are cells that do not contain functional mitochondria and therefore cannot grow on non-fermentable carbon sources (Bernardi, 2005). Increasing dNTP levels causes a reduction in petite formation: an *sml1Δ* strain has ~2.5 fold higher dNTP levels than a wild type strain and shows a ~2.3 fold lower rate of petite formation (Zhao *et al.*, 1998). Increasing dNTP levels also causes an increase in mutation rate: an *rnr1-D57N* mutant (that has lost allosteric regulation) has ~2 fold higher dNTPs levels than a wild type strain and shows ~3 fold increase in the forward mutation rate to canavanine resistance (Chabes *et al.*, 2003a). Therefore assessing the effect of multicopy *GIS2* on the mutation rate and the rate of petite formation, compared with wild type and *sml1Δ* control strains, would be informative in deciding if suppression did depend on increased dNTP levels.

The available evidence suggests that *GIS2* encodes a nucleic acid chaperone that is somehow involved in gene expression (Section 6.2.1). With this in mind, multicopy expression of *GIS2* most likely causes some change in gene expression. Gis2 could bind to DNA, RNA, or both, and therefore could alter gene expression at different levels: for example transcription, RNA processing or mRNA translation. A detailed consideration of the proposed role of *GIS2* in regulating gene expression is beyond the scope of this thesis. So, assuming multicopy *GIS2* does cause some change in gene expression, independent of Mec1 function, how could this affect the lethality of temperature sensitive *mec1* alleles?

A significant possibility is that, via changes in gene expression, multicopy expression of *GIS2* somehow alters cellular metabolism. This effect would be consistent with a common mechanism of suppression of the lethality of temperature sensitive *mec1* alleles by multicopy *GIS2*, deletion of *RAS2* and growth on non-glucose carbon sources (Chapter 7; Figure 8.1). Assuming there is a common mechanism of suppression in these three situations, a resultant change in cellular metabolism could indirectly impact on dNTP metabolism to partially suppress the lethality of temperature sensitive *mec1* alleles. For example, a change in cellular metabolism could increase the level of dNTP precursors. This would then increase the flux through the RNR enzyme, and generate the predicted modest increase in dNTP levels that would cause partial suppression of the lethality of temperature sensitive *mec1* alleles (Chapter 4). Recently, it was shown that threonine biosynthesis contributes to a cells ability to maintain dNTP pools via its effect on *de novo* purine biosynthesis and consequent production of precursors for dNTP synthesis (Hartman, 2007). So, mutations in genes involved in threonine biosynthesis show a reduced ability to grow in the presence of HU. A reduction in Ras activity, or increased *GIS2* expression, or growth on non-glucose carbon sources could alter the balance of amino acid biosynthesis, with a consequent effect on dNTP synthesis. In support of this idea, genes involved in amino acid biosynthesis can be transcriptionally regulated by cAMP levels (Chen & Powers, 2006; Roosen *et al.*, 2005).

Another possibility is that changes in the redox balance of the cell could influence RNR activity (Carter *et al.*, 2006). To maintain its activity the RNR enzyme must be regenerated after each catalytic cycle. The oxidised form of RNR is reduced by thioredoxin (Camier *et al.*, 2007). One of the effects of downregulation of Ras activity is an increase in the expression of genes that protect against oxidative stress (Charizanis *et al.*, 1999). Therefore a reduction in Ras activity or increased *GIS2* expression could lead to an increase in the efficiency of the RNR catalytic cycle by making reduction of the oxidised form of RNR more favourable.

If suppression does not require an increase in dNTP levels, what could the mechanism be? One possibility is that multicopy *GIS2* could, somehow, increase the stability of the replisome. The prolonged replication fork stalling observed in *mec1-4* and *mec1-40* cells is presumably a result of suboptimal dNTP levels, as it can be

suppressed by deletion of *SML1* (Cha & Kleckner, 2002). If multicopy *GIS2* stabilises the replisome, this could allow replication to proceed more efficiently with a suboptimal level of dNTPs and would reduce the rate of replication fork stalling. An increase in trehalose levels, which is a known effect of decreasing PKA activity (Tatchell *et al.*, 1985), is a plausible mechanism for how multicopy *GIS2* could increase replisome stability. Additionally, as a nucleic acid chaperone, Gis2 could bind to stalled replication forks and contribute to replication fork stabilisation.

Alternatively, by altering some aspect of cellular metabolism, multicopy *GIS2* could be compensating for other, unknown, defects caused by loss of Mec1 function. The idea that the role of Mec1 is more wide ranging than currently understood is discussed in the next section.

8.3 Crosstalk between pathways that control nutrient availability and genomic integrity

The observation of a genetic interaction between *GIS2* and *MEC1* brings up the question of the importance of cross talk between different cellular signalling pathways. In fact there is increasing evidence, both in *S. cerevisiae* and in mammalian cells, that an efficient response to genotoxic stress requires an integrated response of different signalling pathways in the cell.

8.3.1 Examples of nutrient response pathways being used in the cellular response to genotoxic stress

PKA has been shown to contribute to the Mec1-dependent mitotic delay in response to DNA damage (Searle *et al.*, 2004). The Chk1 kinase functions downstream of Mec1 to execute this mitotic delay (Section 1.3.4.2). This study showed that, although deletion of *TPK1* (a PKA catalytic subunit) is not checkpoint defective on its own, co-deletion of *CHK1* and *TPK1* causes a greater mitotic checkpoint defect in response to DNA damage than deletion of *CHK1* alone. PKA negatively regulates APC/C activity by inhibitory phosphorylation of APC/C subunits in *S. pombe* and mammalian cells (Kotani *et al.*, 1998; Yamada *et al.*, 1997). Searle *et al.* (2004) showed that in *S. cerevisiae* Cdc20 is phosphorylated on PKA consensus sites in

response to DNA damage, in a Mec1- and PKA-dependent manner. The authors therefore suggest a model where Mec1 can control the activity of PKA to regulate the progression through mitosis, via Cdc20 phosphorylation, in the presence of DNA damage.

The TOR pathway is another nutrient sensing pathway that has been shown to be important for survival in the presence of genotoxic stress (Shen *et al.*, 2007). The TOR kinase (Tor1 and Tor2 in *S. cerevisiae*) is inhibited by the antibiotic rapamycin (Wullschleger *et al.*, 2006). Shen *et al.* (2007) showed that cells treated with rapamycin had a reduced ability to survive MMS-induced genotoxic stress. This reduced survival rate correlated with a defect in maintaining the MMS-induced transcriptional induction of *RNR1* and *RNR3*.

8.3.2 The role of Mec1

Recently a phosphoproteomics screen was conducted to identify novel kinase substrates of Mec1/Tel1 and Rad53 in *S. cerevisiae* (Smolka *et al.*, 2007). This approach identified many new targets in diverse nuclear processes, such as transcriptional regulation and RNA metabolism. A similar, more large-scale, analysis of mammalian proteins that are phosphorylated on ATM/ATR consensus sites in response to DNA damage also identified many new kinase substrates (Matsuoka *et al.*, 2007). In this screen, significant crosstalk between the DNA damage response pathway and insulin-AKT-TOR pathway was identified. One of the identified ATM/ATR kinase targets in this pathway was p70S6K (ribosomal protein S6 kinase). The functional homolog of p70S6K in *S. cerevisiae* is Sch9 (Urban *et al.*, 2007). Sch9 functions in a parallel pathway to Ras-cAMP-PKA in controlling the cellular response to nutrient availability (Toda *et al.*, 1988). Sch9 also contains a significant number of Mec1/Tel1 consensus phosphorylation sites (SQ/TQ motifs), suggesting it could be a target of the genotoxic stress response. Interestingly, deletion of *SCH9* can partially suppress the lethality of temperature sensitive *mec1* alleles (C. Wardlaw and R. Cha; unpublished data). Future work will focus on establishing whether Sch9 is a substrate of the Mec1 kinase and a possible role for crosstalk between Mec1 function and signalling through nutrient sensing pathways.

References

Abe, Y., Chen, W., Huang, W., Nishino, M. & Li, Y. P. (2006). CNBP regulates forebrain formation at organogenesis stage in chick embryos. *Dev Biol* **295**, 116-127.

Abraham, R. T. (2004). PI 3-kinase related kinases: 'big' players in stress-induced signaling pathways. *DNA Repair (Amst)* **3**, 883-887.

Admire, A., Shanks, L., Danzl, N., Wang, M., Weier, U., Stevens, W., Hunt, E. & Weinert, T. (2006). Cycles of chromosome instability are associated with a fragile site and are increased by defects in DNA replication and checkpoint controls in yeast. *Genes Dev* **20**, 159-173.

Agarwal, R., Tang, Z., Yu, H. & Cohen-Fix, O. (2003). Two distinct pathways for inhibiting pds1 ubiquitination in response to DNA damage. *J Biol Chem* **278**, 45027-45033.

Alcasabas, A. A., Osborn, A. J., Bachant, J. & other authors (2001). Mrc1 transduces signals of DNA replication stress to activate Rad53. *Nat Cell Biol* **3**, 958-965.

Alexandru, G., Uhlmann, F., Mechtler, K., Poupart, M. A. & Nasmyth, K. (2001). Phosphorylation of the cohesin subunit Scc1 by Polo/Cdc5 kinase regulates sister chromatid separation in yeast. *Cell* **105**, 459-472.

Allen, J. B., Zhou, Z., Siede, W., Friedberg, E. C. & Elledge, S. J. (1994). The SAD1/RAD53 protein kinase controls multiple checkpoints and DNA damage-induced transcription in yeast. *Genes Dev* **8**, 2401-2415.

Alvino, G. M., Collingwood, D., Murphy, J. M., Delrow, J., Brewer, B. J. & Raghuraman, M. K. (2007). Replication in hydroxyurea: it's a matter of time. *Mol Cell Biol* **27**, 6396-6406.

An, X., Zhang, Z., Yang, K. & Huang, M. (2006). Cotransport of the heterodimeric small subunit of the Saccharomyces cerevisiae ribonucleotide reductase between the nucleus and the cytoplasm. *Genetics* **173**, 63-73.

Anghileri, P., Branduardi, P., Sternieri, F., Monti, P., Visintin, R., Bevilacqua, A., Alberghina, L., Martegani, E. & Baroni, M. D. (1999). Chromosome separation and exit from mitosis in budding yeast: dependence on growth revealed by cAMP-mediated inhibition. *Exp Cell Res* **250**, 510-523.

Aparicio, O. M., Weinstein, D. M. & Bell, S. P. (1997). Components and dynamics of DNA replication complexes in S. cerevisiae: redistribution of MCM proteins and Cdc45p during S phase. *Cell* **91**, 59-69.

Araki, H., Hamatake, R. K., Morrison, A., Johnson, A. L., Johnston, L. H. & Sugino, A. (1991). Cloning DPB3, the gene encoding the third subunit of DNA polymerase II of Saccharomyces cerevisiae. *Nucleic Acids Res* **19**, 4867-4872.

Araki, H., Leem, S. H., Phongdara, A. & Sugino, A. (1995). Dpb11, which interacts with DNA polymerase II(epsilon) in Saccharomyces cerevisiae, has a dual role in S-phase progression and at a cell cycle checkpoint. *Proc Natl Acad Sci U S A* **92**, 11791-11795.

Armas, P., Cachero, S., Lombardo, V. A., Weiner, A., Allende, M. L. & Calcaterra, N. B. (2004). Zebrafish cellular nucleic acid-binding protein: gene structure and developmental behaviour. *Gene* **337**, 151-161.

Armas, P., Nasif, S. & Calcaterra, N. B. (2008). Cellular nucleic acid binding protein binds G-rich single-stranded nucleic acids and may function as a nucleic acid chaperone. *J Cell Biochem* **103**, 1013-1036.

Azvolinsky, A., Dunaway, S., Torres, J. Z., Bessler, J. B. & Zakian, V. A. (2006). The S. cerevisiae Rrm3p DNA helicase moves with the replication fork and affects replication of all yeast chromosomes. *Genes Dev* **20**, 3104-3116.

Bakkenist, C. J. & Kastan, M. B. (2003). DNA damage activates ATM through intermolecular autophosphorylation and dimer dissociation. *Nature* **421**, 499-506.

Balciunas, D. & Ronne, H. (1999). Yeast genes GIS1-4: multicopy suppressors of the Gal- phenotype of snf1 mig1 srb8/10/11 cells. *Mol Gen Genet* **262**, 589-599.

Baroni, M. D., Monti, P. & Alberghina, L. (1994). Repression of growth-regulated G1 cyclin expression by cyclic AMP in budding yeast. *Nature* **371**, 339-342.

Basrai, M. A., Velculescu, V. E., Kinzler, K. W. & Hieter, P. (1999). NORF5/HUG1 is a component of the MEC1-mediated checkpoint response to DNA damage and replication arrest in Saccharomyces cerevisiae. *Mol Cell Biol* **19**, 7041-7049.

Bassing, C. H., Chua, K. F., Sekiguchi, J. & other authors (2002). Increased ionizing radiation sensitivity and genomic instability in the absence of histone H2AX. *Proc Natl Acad Sci U S A* **99**, 8173-8178.

Bell, S. P. & Stillman, B. (1992). ATP-dependent recognition of eukaryotic origins of DNA replication by a multiprotein complex. *Nature* **357**, 128-134.

Bell, S. P. & Dutta, A. (2002). DNA replication in eukaryotic cells. *Annu Rev Biochem* **71**, 333-374.

Bentley, N. J., Holtzman, D. A., Flaggs, G., Keegan, K. S., DeMaggio, A., Ford, J. C., Hoekstra, M. & Carr, A. M. (1996). The Schizosaccharomyces pombe rad3 checkpoint gene. *Embo J* **15**, 6641-6651.

Bernardi, G. (2005). Lessons from a small, dispensable genome: the mitochondrial genome of yeast. *Gene* **354**, 189-200.

Biswas, D., Takahata, S., Xin, H., Dutta-Biswas, R., Yu, Y., Formosa, T. & Stillman, D. J. (2008). A Role for Chd1 and Set2 in Negatively Regulating DNA Replication in Saccharomyces cerevisiae. *Genetics* **178**, 649-659.

Bjorklund, S., Skog, S., Tribukait, B. & Thelander, L. (1990). S-phase-specific expression of mammalian ribonucleotide reductase R1 and R2 subunit mRNAs. *Biochemistry* **29**, 5452-5458.

Blagosklonny, M. V. & Pardee, A. B. (2002). The restriction point of the cell cycle. *Cell Cycle* **1**, 103-110.

Blankley, R. T. & Lydall, D. (2004). A domain of Rad9 specifically required for activation of Chk1 in budding yeast. *J Cell Sci* **117**, 601-608.

Bolte, M., Dieckhoff, P., Krause, C., Braus, G. H. & Irniger, S. (2003). Synergistic inhibition of APC/C by glucose and activated Ras proteins can be

mediated by each of the Tpk1-3 proteins in Saccharomyces cerevisiae. *Microbiology* **149**, 1205-1216.

Bomgarden, R. D., Yean, D., Yee, M. C. & Cimprich, K. A. (2004). A novel protein activity mediates DNA binding of an ATR-ATRIP complex. *J Biol Chem* **279**, 13346-13353.

Boorstein, W. R. & Craig, E. A. (1990). Regulation of a yeast HSP70 gene by a cAMP responsive transcriptional control element. *Embo J* **9**, 2543-2553.

Bos, J. L. (1989). ras oncogenes in human cancer: a review. *Cancer Res* **49**, 4682-4689.

Bourdon, A., Minai, L., Serre, V. & other authors (2007). Mutation of RRM2B, encoding p53-controlled ribonucleotide reductase (p53R2), causes severe mitochondrial DNA depletion. *Nat Genet* **39**, 776-780.

Boy-Marcotte, E., Lagniel, G., Perrot, M., Bussereau, F., Boudsocq, A., Jacquet, M. & Labarre, J. (1999). The heat shock response in yeast: differential regulations and contributions of the Msn2p/Msn4p and Hsf1p regulons. *Mol Microbiol* **33**, 274-283.

Brown, E. J. & Baltimore, D. (2000). ATR disruption leads to chromosomal fragmentation and early embryonic lethality. *Genes Dev* **14**, 397-402.

Brown, M. P., Grundy, W. N., Lin, D., Cristianini, N., Sugnet, C. W., Furey, T. S., Ares, M., Jr. & Haussler, D. (2000). Knowledge-based analysis of microarray gene expression data by using support vector machines. *Proc Natl Acad Sci U S A* **97**, 262-267.

Budovskaya, Y. V., Stephan, J. S., Reggiori, F., Klionsky, D. J. & Herman, P. K. (2004). The Ras/cAMP-dependent protein kinase signaling pathway regulates an early step of the autophagy process in Saccharomyces cerevisiae. *J Biol Chem* **279**, 20663-20671.

Byrne, S. M. & Hoffman, C. S. (1993). Six git genes encode a glucose-induced adenylate cyclase activation pathway in the fission yeast Schizosaccharomyces pombe. *J Cell Sci* **105 (Pt 4)**, 1095-1100.

Byun, T. S., Pacek, M., Yee, M. C., Walter, J. C. & Cimprich, K. A. (2005). Functional uncoupling of MCM helicase and DNA polymerase activities activates the ATR-dependent checkpoint. *Genes Dev* **19**, 1040-1052.

Callahan, J. L., Andrews, K. J., Zakian, V. A. & Freudenreich, C. H. (2003). Mutations in yeast replication proteins that increase CAG/CTG expansions also increase repeat fragility. *Mol Cell Biol* **23**, 7849-7860.

Calzada, A., Hodgson, B., Kanemaki, M., Bueno, A. & Labib, K. (2005). Molecular anatomy and regulation of a stable replisome at a paused eukaryotic DNA replication fork. *Genes Dev* **19**, 1905-1919.

Camier, S., Ma, E., Leroy, C., Pruvost, A., Toledano, M. & Marsolier-Kergoat, M. C. (2007). Visualization of ribonucleotide reductase catalytic oxidation establishes thioredoxins as its major reductants in yeast. *Free Radic Biol Med* **42**, 1008-1016.

Cannon, J. F. & Tatchell, K. (1987). Characterization of Saccharomyces cerevisiae genes encoding subunits of cyclic AMP-dependent protein kinase. *Mol Cell Biol* **7**, 2653-2663.

Carlson, M. (1999). Glucose repression in yeast. *Curr Opin Microbiol* **2**, 202-207.

Carter, G. W., Rupp, S., Fink, G. R. & Galitski, T. (2006). Disentangling information flow in the Ras-cAMP signaling network. *Genome Res* **16**, 520-526.

Casper, A. M., Nghiem, P., Arlt, M. F. & Glover, T. W. (2002). ATR regulates fragile site stability. *Cell* **111**, 779-789.

Casperson, G. F., Walker, N. & Bourne, H. R. (1985). Isolation of the gene encoding adenylate cyclase in Saccharomyces cerevisiae. *Proc Natl Acad Sci U S A* **82**, 5060-5063.

Celeste, A., Petersen, S., Romanienko, P. J. & other authors (2002). Genomic instability in mice lacking histone H2AX. *Science* **296**, 922-927.

Cha, R. S. & Kleckner, N. (2002). ATR homolog Mec1 promotes fork progression, thus averting breaks in replication slow zones. *Science* **297**, 602-606.

Chabes, A., Domkin, V. & Thelander, L. (1999). Yeast Sml1, a protein inhibitor of ribonucleotide reductase. *J Biol Chem* **274**, 36679-36683.

Chabes, A., Georgieva, B., Domkin, V., Zhao, X., Rothstein, R. & Thelander, L. (2003a). Survival of DNA damage in yeast directly depends on increased dNTP levels allowed by relaxed feedback inhibition of ribonucleotide reductase. *Cell* **112**, 391-401.

Chabes, A. L., Pfleger, C. M., Kirschner, M. W. & Thelander, L. (2003b). Mouse ribonucleotide reductase R2 protein: a new target for anaphase-promoting complex-Cdh1-mediated proteolysis. *Proc Natl Acad Sci U S A* **100**, 3925-3929.

Chang, E. C., Barr, M., Wang, Y., Jung, V., Xu, H. P. & Wigler, M. H. (1994). Cooperative interaction of S. pombe proteins required for mating and morphogenesis. *Cell* **79**, 131-141.

Charizanis, C., Juhnke, H., Krems, B. & Entian, K. D. (1999). The oxidative stress response mediated via Pos9/Skn7 is negatively regulated by the Ras/PKA pathway in Saccharomyces cerevisiae. *Mol Gen Genet* **261**, 740-752.

Chen, J. C. & Powers, T. (2006). Coordinate regulation of multiple and distinct biosynthetic pathways by TOR and PKA kinases in S. cerevisiae. *Curr Genet* **49**, 281-293.

Chen, W., Liang, Y., Deng, W., Shimizu, K., Ashique, A. M., Li, E. & Li, Y. P. (2003). The zinc-finger protein CNBP is required for forebrain formation in the mouse. *Development* **130**, 1367-1379.

Cheng, L., Hunke, L. & Hardy, C. F. (1998). Cell cycle regulation of the Saccharomyces cerevisiae polo-like kinase cdc5p. *Mol Cell Biol* **18**, 7360-7370.

Chowdhury, D., Keogh, M. C., Ishii, H., Peterson, C. L., Buratowski, S. & Lieberman, J. (2005). gamma-H2AX dephosphorylation by protein phosphatase 2A facilitates DNA double-strand break repair. *Mol Cell* **20**, 801-809.

Christianson, T. W., Sikorski, R. S., Dante, M., Shero, J. H. & Hieter, P. (1992). Multifunctional yeast high-copy-number shuttle vectors. *Gene* **110**, 119-122.

Chuang, R. Y. & Kelly, T. J. (1999). The fission yeast homologue of Orc4p binds to replication origin DNA via multiple AT-hooks. *Proc Natl Acad Sci U S A* **96**, 2656-2661.

Chun, H. H. & Gatti, R. A. (2004). Ataxia-telangiectasia, an evolving phenotype. *DNA Repair (Amst)* **3**, 1187-1196.

Ciosk, R., Zachariae, W., Michaelis, C., Shevchenko, A., Mann, M. & Nasmyth, K. (1998). An ESP1/PDS1 complex regulates loss of sister chromatid cohesion at the metaphase to anaphase transition in yeast. *Cell* **93**, 1067-1076.

Ciosk, R., Shirayama, M., Shevchenko, A., Tanaka, T., Toth, A. & Nasmyth, K. (2000). Cohesin's binding to chromosomes depends on a separate complex consisting of Scc2 and Scc4 proteins. *Mol Cell* **5**, 243-254.

Clark, M. W., Yip, M. L., Campbell, J. & Abelson, J. (1990). SSB-1 of the yeast Saccharomyces cerevisiae is a nucleolar-specific, silver-binding protein that is associated with the snR10 and snR11 small nuclear RNAs. *J Cell Biol* **111**, 1741-1751.

Clerici, M., Paciotti, V., Baldo, V., Romano, M., Lucchini, G. & Longhese, M. P. (2001). Hyperactivation of the yeast DNA damage checkpoint by TEL1 and DDC2 overexpression. *Embo J* **20**, 6485-6498.

Clerici, M., Baldo, V., Mantiero, D., Lottersberger, F., Lucchini, G. & Longhese, M. P. (2004). A Tel1/MRX-dependent checkpoint inhibits the metaphase-to-anaphase transition after UV irradiation in the absence of Mec1. *Mol Cell Biol* **24**, 10126-10144.

Cobb, J. A., Bjergbaek, L., Shimada, K., Frei, C. & Gasser, S. M. (2003). DNA polymerase stabilization at stalled replication forks requires Mec1 and the RecQ helicase Sgs1. *Embo J* **22**, 4325-4336.

Cobb, J. A., Schleker, T., Rojas, V., Bjergbaek, L., Tercero, J. A. & Gasser, S. M. (2005). Replisome instability, fork collapse, and gross chromosomal rearrangements arise synergistically from Mec1 kinase and RecQ helicase mutations. *Genes Dev* **19**, 3055-3069.

Colombo, S., Ma, P., Cauwenberg, L. & other authors (1998). Involvement of distinct G-proteins, Gpa2 and Ras, in glucose- and intracellular acidification-induced cAMP signalling in the yeast Saccharomyces cerevisiae. *Embo J* **17**, 3326-3341.

Colombo, S., Ronchetti, D., Thevelein, J. M., Winderickx, J. & Martegani, E. (2004). Activation state of the Ras2 protein and glucose-induced signaling in Saccharomyces cerevisiae. *J Biol Chem* **279**, 46715-46722.

Corda, Y., Lee, S. E., Guillot, S., Walther, A., Sollier, J., Arbel-Eden, A., Haber, J. E. & Geli, V. (2005). Inactivation of Ku-Mediated End Joining Suppresses mec1{Delta} Lethality by Depleting the Ribonucleotide Reductase Inhibitor Sml1 through a Pathway Controlled by Tel1 Kinase and the Mre11 Complex. *Mol Cell Biol* **25**, 10652-10664.

Cortez, D., Guntuku, S., Qin, J. & Elledge, S. J. (2001). ATR and ATRIP: partners in checkpoint signaling. *Science* **294**, 1713-1716.

Costanzo, V., Avvedimento, E. V., Gottesman, M. E., Gautier, J. & Grieco, D. (1999). Protein kinase A is required for chromosomal DNA replication. *Curr Biol* **9**, 903-906.

Cotta-Ramusino, C., Fachinetti, D., Lucca, C., Doksani, Y., Lopes, M., Sogo, J. & Foiani, M. (2005). Exo1 processes stalled replication forks and counteracts fork reversal in checkpoint-defective cells. *Mol Cell* **17**, 153-159.

Covey, S. N. (1986). Amino acid sequence homology in gag region of reverse transcribing elements and the coat protein gene of cauliflower mosaic virus. *Nucleic Acids Res* **14**, 623-633.

Cox, M. M. (2002). The nonmutagenic repair of broken replication forks via recombination. *Mutat Res* **510**, 107-120.

Craven, R. J., Greenwell, P. W., Dominska, M. & Petes, T. D. (2002). Regulation of genome stability by TEL1 and MEC1, yeast homologs of the mammalian ATM and ATR genes. *Genetics* **161**, 493-507.

Crosio, C., Boyl, P. P., Loreni, F., Pierandrei-Amaldi, P. & Amaldi, F. (2000). La protein has a positive effect on the translation of TOP mRNAs in vivo. *Nucleic Acids Res* **28**, 2927-2934.

Cross, F. R. & Tinkelenberg, A. H. (1991). A potential positive feedback loop controlling CLN1 and CLN2 gene expression at the start of the yeast cell cycle. *Cell* **65**, 875-883.

Czajkowsky, D. M., Liu, J., Hamlin, J. L. & Shao, Z. (2008). DNA combing reveals intrinsic temporal disorder in the replication of yeast chromosome VI. *J Mol Biol* **375**, 12-19.

Darlix, J. L. & Spahr, P. F. (1982). Binding sites of viral protein P19 onto Rous sarcoma virus RNA and possible controls of viral functions. *J Mol Biol* **160**, 147-161.

Dart, D. A., Adams, K. E., Akerman, I. & Lakin, N. D. (2004). Recruitment of the cell cycle checkpoint kinase ATR to chromatin during S-phase. *J Biol Chem* **279**, 16433-16440.

de Bruin, R. A., Kalashnikova, T. I., Chahwan, C., McDonald, W. H., Wohlschlegel, J., Yates, J., 3rd, Russell, P. & Wittenberg, C. (2006). Constraining G1-specific transcription to late G1 phase: the MBF-associated corepressor Nrm1 acts via negative feedback. *Mol Cell* **23**, 483-496.

de la Torre Ruiz, M. A. & Lowndes, N. F. (2000). DUN1 defines one branch downstream of RAD53 for transcription and DNA damage repair in Saccharomyces cerevisiae. *FEBS Lett* **485**, 205-206.

De Virgilio, C., Hottiger, T., Dominguez, J., Boller, T. & Wiemken, A. (1994). The role of trehalose synthesis for the acquisition of thermotolerance in yeast. I. Genetic evidence that trehalose is a thermoprotectant. *Eur J Biochem* **219**, 179-186.

Desany, B. A., Alcasabas, A. A., Bachant, J. B. & Elledge, S. J. (1998). Recovery from DNA replicational stress is the essential function of the S-phase checkpoint pathway. *Genes Dev* **12**, 2956-2970.

Deshpande, A. M. & Newlon, C. S. (1996). DNA replication fork pause sites dependent on transcription. *Science* **272**, 1030-1033.

Dirick, L. & Nasmyth, K. (1991). Positive feedback in the activation of G1 cyclins in yeast. *Nature* **351**, 754-757.

Dirick, L., Moll, T., Auer, H. & Nasmyth, K. (1992). A central role for SWI6 in modulating cell cycle Start-specific transcription in yeast. *Nature* **357**, 508-513.

Domkin, V., Thelander, L. & Chabes, A. (2002). Yeast DNA damage-inducible Rnr3 has a very low catalytic activity strongly stimulated after the formation of a cross-talking Rnr1/Rnr3 complex. *J Biol Chem* **277**, 18574-18578.

Downs, J. A., Lowndes, N. F. & Jackson, S. P. (2000). A role for Saccharomyces cerevisiae histone H2A in DNA repair. *Nature* **408**, 1001-1004.

Downs, J. A., Allard, S., Jobin-Robitaille, O., Javaheri, A., Auger, A., Bouchard, N., Kron, S. J., Jackson, S. P. & Cote, J. (2004). Binding of chromatin-modifying activities to phosphorylated histone H2A at DNA damage sites. *Mol Cell* **16**, 979-990.

Du, Y. C. & Stillman, B. (2002). Yph1p, an ORC-interacting protein: potential links between cell proliferation control, DNA replication, and ribosome biogenesis. *Cell* **109**, 835-848.

Durnez, P., Pernambuco, M. B., Oris, E., Arguelles, J. C., Mergelsberg, H. & Thevelein, J. M. (1994). Activation of trehalase during growth induction by nitrogen sources in the yeast Saccharomyces cerevisiae depends on the free catalytic subunits of cAMP-dependent protein kinase, but not on functional Ras proteins. *Yeast* **10**, 1049-1064.

Elledge, S. J. & Davis, R. W. (1987). Identification and isolation of the gene encoding the small subunit of ribonucleotide reductase from Saccharomyces cerevisiae: DNA damage-inducible gene required for mitotic viability. *Mol Cell Biol* **7**, 2783-2793.

Elledge, S. J. & Davis, R. W. (1990). Two genes differentially regulated in the cell cycle and by DNA-damaging agents encode alternative regulatory subunits of ribonucleotide reductase. *Genes Dev* **4**, 740-751.

Elliott, B. & Futcher, B. (1993). Stress resistance of yeast cells is largely independent of cell cycle phase. *Yeast* **9**, 33-42.

Emili, A. (1998). MEC1-dependent phosphorylation of Rad9p in response to DNA damage. *Mol Cell* **2**, 183-189.

Engelberg, D., Zandi, E., Parker, C. S. & Karin, M. (1994). The yeast and mammalian Ras pathways control transcription of heat shock genes independently of heat shock transcription factor. *Mol Cell Biol* **14**, 4929-4937.

Engstrom, Y., Rozell, B., Hansson, H. A., Stemme, S. & Thelander, L. (1984). Localization of ribonucleotide reductase in mammalian cells. *Embo J* **3**, 863-867.

Engstrom, Y., Eriksson, S., Jildevik, I., Skog, S., Thelander, L. & Tribukait, B. (1985). Cell cycle-dependent expression of mammalian ribonucleotide reductase. Differential regulation of the two subunits. *J Biol Chem* **260**, 9114-9116.

Engstrom, Y. & Rozell, B. (1988). Immunocytochemical evidence for the cytoplasmic localization and differential expression during the cell cycle of the M1 and M2 subunits of mammalian ribonucleotide reductase. *Embo J* **7**, 1615-1620.

Falaschi, A. (2000). Eukaryotic DNA replication: a model for a fixed double replisome. *Trends Genet* **16**, 88-92.

Falck, J., Coates, J. & Jackson, S. P. (2005). Conserved modes of recruitment of ATM, ATR and DNA-PKcs to sites of DNA damage. *Nature* **434**, 605-611.

Feng, W., Collingwood, D., Boeck, M. E., Fox, L. A., Alvino, G. M., Fangman, W. L., Raghuraman, M. K. & Brewer, B. J. (2006). Genomic mapping of single-stranded DNA in hydroxyurea-challenged yeasts identifies origins of replication. *Nat Cell Biol* **8**, 148-155.

Flink, I. L. & Morkin, E. (1995). Alternatively processed isoforms of cellular nucleic acid-binding protein interact with a suppressor region of the human beta-myosin heavy chain gene. *J Biol Chem* **270**, 6959-6965.

Flink, I. L., Blitz, I. & Morkin, E. (1998). Characterization of cellular nucleic acid binding protein from Xenopus laevis: expression in all three germ layers during early development. *Dev Dyn* **211**, 123-130.

Foss, M., McNally, F. J., Laurenson, P. & Rine, J. (1993). Origin recognition complex (ORC) in transcriptional silencing and DNA replication in S. cerevisiae. *Science* **262**, 1838-1844.

Francois, J., Van Schaftingen, E. & Hers, H. G. (1984). The mechanism by which glucose increases fructose 2,6-bisphosphate concentration in Saccharomyces cerevisiae. A cyclic-AMP-dependent activation of phosphofructokinase 2. *Eur J Biochem* **145**, 187-193.

Friedman, K. L., Brewer, B. J. & Fangman, W. L. (1997). Replication profile of Saccharomyces cerevisiae chromosome VI. *Genes Cells* **2**, 667-678.

Furuya, K., Poitelea, M., Guo, L., Caspari, T. & Carr, A. M. (2004). Chk1 activation requires Rad9 S/TQ-site phosphorylation to promote association with C-terminal BRCT domains of Rad4TOPBP1. *Genes Dev* **18**, 1154-1164.

Garcia-Muse, T. & Boulton, S. J. (2005). Distinct modes of ATR activation after replication stress and DNA double-strand breaks in Caenorhabditis elegans. *Embo J* **24**, 4345-4355.

Gardner, R., Putnam, C. W. & Weinert, T. (1999). RAD53, DUN1 and PDS1 define two parallel G2/M checkpoint pathways in budding yeast. *Embo J* **18**, 3173-3185.

Gasch, A. P., Huang, M., Metzner, S., Botstein, D., Elledge, S. J. & Brown, P. O. (2001). Genomic expression responses to DNA-damaging agents and the regulatory role of the yeast ATR homolog Mec1p. *Mol Biol Cell* **12**, 2987-3003.

Gerald, J. N., Benjamin, J. M. & Kron, S. J. (2002). Robust G1 checkpoint arrest in budding yeast: dependence on DNA damage signaling and repair. *J Cell Sci* **115**, 1749-1757.

Geymonat, M., Spanos, A., Smith, S. J., Wheatley, E., Rittinger, K., Johnston, L. H. & Sedgwick, S. G. (2002). Control of mitotic exit in budding yeast. In vitro regulation of Tem1 GTPase by Bub2 and Bfa1. *J Biol Chem* **277**, 28439-28445.

Gietz, R. D. & Woods, R. A. (2002). Transformation of yeast by lithium acetate/single-stranded carrier DNA/polyethylene glycol method. *Methods Enzymol* **350**, 87-96.

Gilbert, C. S., Green, C. M. & Lowndes, N. F. (2001). Budding yeast Rad9 is an ATP-dependent Rad53 activating machine. *Mol Cell* **8**, 129-136.

Gilman, A. G. (1984). G proteins and dual control of adenylate cyclase. *Cell* **36**, 577-579.

Goldstein, A. L. & McCusker, J. H. (1999). Three new dominant drug resistance cassettes for gene disruption in Saccharomyces cerevisiae. *Yeast* **15**, 1541-1553.

Greenwell, P. W., Kronmal, S. L., Porter, S. E., Gassenhuber, J., Obermaier, B. & Petes, T. D. (1995). TEL1, a gene involved in controlling telomere length in S. cerevisiae, is homologous to the human ataxia telangiectasia gene. *Cell* **82**, 823-829.

Gregan, J. & Rumpf, C. (2006). How might DNA enter the cohesin ring? *Cell Cycle* **5**, 2553-2554.

Grieco, D., Avvedimento, E. V. & Gottesman, M. E. (1994). A role for cAMP-dependent protein kinase in early embryonic divisions. *Proc Natl Acad Sci U S A* **91**, 9896-9900.

Grieco, D., Porcellini, A., Avvedimento, E. V. & Gottesman, M. E. (1996). Requirement for cAMP-PKA pathway activation by M phase-promoting factor in the transition from mitosis to interphase. *Science* **271**, 1718-1723.

Gruber, M., Wellinger, R. E. & Sogo, J. M. (2000). Architecture of the replication fork stalled at the 3' end of yeast ribosomal genes. *Mol Cell Biol* **20**, 5777-5787.

Guo, Z., Kumagai, A., Wang, S. X. & Dunphy, W. G. (2000). Requirement for Atr in phosphorylation of Chk1 and cell cycle regulation in response to DNA replication blocks and UV-damaged DNA in Xenopus egg extracts. *Genes Dev* **14**, 2745-2756.

Haering, C. H., Lowe, J., Hochwagen, A. & Nasmyth, K. (2002). Molecular architecture of SMC proteins and the yeast cohesin complex. *Mol Cell* **9**, 773-788.

Hakansson, P., Dahl, L., Chilkova, O., Domkin, V. & Thelander, L. (2006a). The Schizosaccharomyces pombe replication inhibitor Spd1 regulates ribonucleotide reductase activity and dNTPs by binding to the large Cdc22 subunit. *J Biol Chem* **281**, 1778-1783.

Hakansson, P., Hofer, A. & Thelander, L. (2006b). Regulation of mammalian ribonucleotide reduction and dNTP pools after DNA damage and in resting cells. *J Biol Chem.*

Hall, D. D., Markwardt, D. D., Parviz, F. & Heideman, W. (1998). Regulation of the Cln3-Cdc28 kinase by cAMP in Saccharomyces cerevisiae. *Embo J* **17**, 4370-4378.

Hamilton, T. L., Stoneley, M., Spriggs, K. A. & Bushell, M. (2006). TOPs and their regulation. *Biochem Soc Trans* **34**, 12-16.

Hammet, A., Pike, B. L. & Heierhorst, J. (2002). Posttranscriptional regulation of the RAD5 DNA repair gene by the Dun1 kinase and the Pan2-Pan3 poly(A)-nuclease complex contributes to survival of replication blocks. *J Biol Chem* **277**, 22469-22474.

Harrison, J. C. & Haber, J. E. (2006). Surviving the breakup: the DNA damage checkpoint. *Annu Rev Genet* **40**, 209-235.

Hartman, J. L. t. (2007). Buffering of deoxyribonucleotide pool homeostasis by threonine metabolism. *Proc Natl Acad Sci U S A* **104**, 11700-11705.

Hartwell, L. H., Culotti, J. & Reid, B. (1970). Genetic control of the cell-division cycle in yeast. I. Detection of mutants. *Proc Natl Acad Sci U S A* **66**, 352-359.

Hartwell, L. H. (1974). Saccharomyces cerevisiae cell cycle. *Bacteriol Rev* **38**, 164-198.

Hartwell, L. H. & Weinert, T. A. (1989). Checkpoints: controls that ensure the order of cell cycle events. *Science* **246**, 629-634.

Hekmat-Nejad, M., You, Z., Yee, M. C., Newport, J. W. & Cimprich, K. A. (2000). Xenopus ATR is a replication-dependent chromatin-binding protein required for the DNA replication checkpoint. *Curr Biol* **10**, 1565-1573.

Heo, S. J., Tatebayashi, K. & Ikeda, H. (1999). The budding yeast cohesin gene SCC1/MCD1/RHC21 genetically interacts with PKA, CDK and APC. *Curr Genet* **36**, 329-338.

Herman, P. K. (2002). Stationary phase in yeast. *Curr Opin Microbiol* **5**, 602-607.

Herschlag, D. (1995). RNA chaperones and the RNA folding problem. *J Biol Chem* **270**, 20871-20874.

Herskowitz, I. (1988). Life cycle of the budding yeast Saccharomyces cerevisiae. *Microbiol Rev* **52**, 536-553.

Hiraga, S., Hagihara-Hayashi, A., Ohya, T. & Sugino, A. (2005). DNA polymerases alpha, delta, and epsilon localize and function together at replication forks in Saccharomyces cerevisiae. *Genes Cells* **10**, 297-309.

Hirimburegama, K., Durnez, P., Keleman, J., Oris, E., Vergauwen, R., Mergelsberg, H. & Thevelein, J. M. (1992). Nutrient-induced activation of trehalase in nutrient-starved cells of the yeast Saccharomyces cerevisiae: cAMP is not involved as second messenger. *J Gen Microbiol* **138**, 2035-2043.

Ho, J. & Bretscher, A. (2001). Ras regulates the polarity of the yeast actin cytoskeleton through the stress response pathway. *Mol Biol Cell* **12**, 1541-1555.

Hodgson, B., Calzada, A. & Labib, K. (2007). Mrc1 and Tof1 regulate DNA replication forks in different ways during normal S phase. *Mol Biol Cell* **18**, 3894-3902.

Hottiger, T., De Virgilio, C., Hall, M. N., Boller, T. & Wiemken, A. (1994). The role of trehalose synthesis for the acquisition of thermotolerance in yeast. II. Physiological concentrations of trehalose increase the thermal stability of proteins in vitro. *Eur J Biochem* **219**, 187-193.

Hu, F., Wang, Y., Liu, D., Li, Y., Qin, J. & Elledge, S. J. (2001). Regulation of the Bub2/Bfa1 GAP complex by Cdc5 and cell cycle checkpoints. *Cell* **107**, 655-665.

Huang, M. & Elledge, S. J. (1997). Identification of RNR4, encoding a second essential small subunit of ribonucleotide reductase in Saccharomyces cerevisiae. *Mol Cell Biol* **17**, 6105-6113.

Huang, M., Zhou, Z. & Elledge, S. J. (1998). The DNA replication and damage checkpoint pathways induce transcription by inhibition of the Crt1 repressor. *Cell* **94**, 595-605.

Hubler, L., Bradshaw-Rouse, J. & Heideman, W. (1993). Connections between the Ras-cyclic AMP pathway and G1 cyclin expression in the budding yeast Saccharomyces cerevisiae. *Mol Cell Biol* **13**, 6274-6282.

Iida, H. (1988). Multistress resistance of Saccharomyces cerevisiae is generated by insertion of retrotransposon Ty into the 5' coding region of the adenylate cyclase gene. *Mol Cell Biol* **8**, 5555-5560.

Ira, G., Pellicioli, A., Balijja, A. & other authors (2004). DNA end resection, homologous recombination and DNA damage checkpoint activation require CDK1. *Nature* **431**, 1011-1017.

Irniger, S., Baumer, M. & Braus, G. H. (2000). Glucose and ras activity influence the ubiquitin ligases APC/C and SCF in Saccharomyces cerevisiae. *Genetics* **154**, 1509-1521.

Ivessa, A. S., Zhou, J. Q. & Zakian, V. A. (2000). The Saccharomyces Pif1p DNA helicase and the highly related Rrm3p have opposite effects on replication fork progression in ribosomal DNA. *Cell* **100**, 479-489.

Ivessa, A. S., Zhou, J. Q., Schulz, V. P., Monson, E. K. & Zakian, V. A. (2002). Saccharomyces Rrm3p, a 5' to 3' DNA helicase that promotes replication fork progression through telomeric and subtelomeric DNA. *Genes Dev* **16**, 1383-1396.

Ivessa, A. S., Lenzmeier, B. A., Bessler, J. B., Goudsouzian, L. K., Schnakenberg, S. L. & Zakian, V. A. (2003). The Saccharomyces cerevisiae helicase Rrm3p facilitates replication past nonhistone protein-DNA complexes. *Mol Cell* **12**, 1525-1536.

Jaspersen, S. L., Charles, J. F., Tinker-Kulberg, R. L. & Morgan, D. O. (1998). A late mitotic regulatory network controlling cyclin destruction in Saccharomyces cerevisiae. *Mol Biol Cell* **9**, 2803-2817.

Jazayeri, A., Falck, J., Lukas, C., Bartek, J., Smith, G. C., Lukas, J. & Jackson, S. P. (2006). ATM- and cell cycle-dependent regulation of ATR in response to DNA double-strand breaks. *Nat Cell Biol* **8**, 37-45.

Jeggo, P. A., Carr, A. M. & Lehmann, A. R. (1998). Splitting the ATM: distinct repair and checkpoint defects in ataxia-telangiectasia. *Trends Genet* **14**, 312-316.

Jelinsky, S. A. & Samson, L. D. (1999). Global response of Saccharomyces cerevisiae to an alkylating agent. *Proc Natl Acad Sci U S A* **96**, 1486-1491.

Johnson, K. E., Cameron, S., Toda, T., Wigler, M. & Zoller, M. J. (1987). Expression in Escherichia coli of BCY1, the regulatory subunit of cyclic AMP-dependent protein kinase from Saccharomyces cerevisiae. Purification and characterization. *J Biol Chem* **262**, 8636-8642.

Johnston, G. C., Pringle, J. R. & Hartwell, L. H. (1977). Coordination of growth with cell division in the yeast Saccharomyces cerevisiae. *Exp Cell Res* **105**, 79-98.

Johnston, G. C., Ehrhardt, C. W., Lorincz, A. & Carter, B. L. (1979). Regulation of cell size in the yeast Saccharomyces cerevisiae. *J Bacteriol* **137**, 1-5.

Johnston, M. (1987). A model fungal gene regulatory mechanism: the GAL genes of Saccharomyces cerevisiae. *Microbiol Rev* **51**, 458-476.

Jones, S., Vignais, M. L. & Broach, J. R. (1991). The CDC25 protein of Saccharomyces cerevisiae promotes exchange of guanine nucleotides bound to ras. *Mol Cell Biol* **11**, 2641-2646.

Kamimura, Y., Tak, Y. S., Sugino, A. & Araki, H. (2001). Sld3, which interacts with Cdc45 (Sld4), functions for chromosomal DNA replication in Saccharomyces cerevisiae. *Embo J* **20**, 2097-2107.

Kashlan, O. B. & Cooperman, B. S. (2003). Comprehensive model for allosteric regulation of mammalian ribonucleotide reductase: refinements and consequences. *Biochemistry* **42**, 1696-1706.

Kataoka, T., Powers, S., McGill, C., Fasano, O., Strathern, J., Broach, J. & Wigler, M. (1984). Genetic analysis of yeast RAS1 and RAS2 genes. *Cell* **37**, 437-445.

Kataoka, T., Powers, S., Cameron, S., Fasano, O., Goldfarb, M., Broach, J. & Wigler, M. (1985). Functional homology of mammalian and yeast RAS genes. *Cell* **40**, 19-26.

Kato, R. & Ogawa, H. (1994). An essential gene, ESR1, is required for mitotic cell growth, DNA repair and meiotic recombination in Saccharomyces cerevisiae. *Nucleic Acids Res* **22**, 3104-3112.

Katou, Y., Kanoh, Y., Bando, M., Noguchi, H., Tanaka, H., Ashikari, T., Sugimoto, K. & Shirahige, K. (2003). S-phase checkpoint proteins Tof1 and Mrc1 form a stable replication-pausing complex. *Nature* **424**, 1078-1083.

Keogh, M. C., Kim, J. A., Downey, M. & other authors (2005). A phosphatase complex that dephosphorylates gammaH2AX regulates DNA damage checkpoint recovery. *Nature*.

Kim, S. M., Kumagai, A., Lee, J. & Dunphy, W. G. (2005). Phosphorylation of Chk1 by ATM- and Rad3-related (ATR) in Xenopus Egg Extracts Requires Binding of ATRIP to ATR but Not the Stable DNA-binding or Coiled-coil Domains of ATRIP. *J Biol Chem* **280**, 38355-38364.

Kitamura, E., Blow, J. J. & Tanaka, T. U. (2006). Live-cell imaging reveals replication of individual replicons in eukaryotic replication factories. *Cell* **125**, 1297-1308.

Klein, C. & Struhl, K. (1994). Protein kinase A mediates growth-regulated expression of yeast ribosomal protein genes by modulating RAP1 transcriptional activity. *Mol Cell Biol* **14**, 1920-1928.

Knapp, D., Bhoite, L., Stillman, D. J. & Nasmyth, K. (1996). The transcription factor Swi5 regulates expression of the cyclin kinase inhibitor p40SIC1. *Mol Cell Biol* **16**, 5701-5707.

Kobayashi, J., Tauchi, H., Sakamoto, S. & other authors (2002). NBS1 localizes to gamma-H2AX foci through interaction with the FHA/BRCT domain. *Curr Biol* **12**, 1846-1851.

Kobayashi, T. & Horiuchi, T. (1996). A yeast gene product, Fob1 protein, required for both replication fork blocking and recombinational hotspot activities. *Genes Cells* **1**, 465-474.

Koc, A., Wheeler, L. J., Mathews, C. K. & Merrill, G. F. (2003). Replication-independent MCB gene induction and deoxyribonucleotide accumulation at G1/S in Saccharomyces cerevisiae. *J Biol Chem* **278**, 9345-9352.

Koc, A., Wheeler, L. J., Mathews, C. K. & Merrill, G. F. (2004). Hydroxyurea arrests DNA replication by a mechanism that preserves basal dNTP pools. *J Biol Chem* **279**, 223-230.

Koc, A., Mathews, C. K., Wheeler, L. J., Gross, M. K. & Merrill, G. F. (2006). Thioredoxin is required for deoxyribonucleotide pool maintenance during S phase. *J Biol Chem* **281**, 15058-15063.

Koch, C., Moll, T., Neuberg, M., Ahorn, H. & Nasmyth, K. (1993). A role for the transcription factors Mbp1 and Swi4 in progression from G1 to S phase. *Science* **261**, 1551-1557.

Konicek, B. W., Xia, X., Rajavashisth, T. & Harrington, M. A. (1998). Regulation of mouse colony-stimulating factor-1 gene promoter activity by AP1 and cellular nucleic acid-binding protein. *DNA Cell Biol* **17**, 799-809.

Kotani, S., Tugendreich, S., Fujii, M., Jorgensen, P. M., Watanabe, N., Hoog, C., Hieter, P. & Todokoro, K. (1998). PKA and MPF-activated polo-like kinase regulate anaphase-promoting complex activity and mitosis progression. *Mol Cell* **1**, 371-380.

Kraakman, L., Lemaire, K., Ma, P., Teunissen, A. W., Donaton, M. C., Van Dijck, P., Winderickx, J., de Winde, J. H. & Thevelein, J. M. (1999). A Saccharomyces cerevisiae G-protein coupled receptor, Gpr1, is specifically required for glucose activation of the cAMP pathway during the transition to growth on glucose. *Mol Microbiol* **32**, 1002-1012.

Kramer, K. M., Fesquet, D., Johnson, A. L. & Johnston, L. H. (1998). Budding yeast RSI1/APC2, a novel gene necessary for initiation of anaphase, encodes an APC subunit. *Embo J* **17**, 498-506.

Krogan, N. J., Cagney, G., Yu, H. & other authors (2006). Global landscape of protein complexes in the yeast Saccharomyces cerevisiae. *Nature* **440**, 637-643.

Kumagai, A., Lee, J., Yoo, H. Y. & Dunphy, W. G. (2006). TopBP1 activates the ATR-ATRIP complex. *Cell* **124**, 943-955.

Lambert, S. & Carr, A. M. (2005). Checkpoint responses to replication fork barriers. *Biochimie* **87**, 591-602.

Lambert, S., Watson, A., Sheedy, D. M., Martin, B. & Carr, A. M. (2005). Gross chromosomal rearrangements and elevated recombination at an inducible site-specific replication fork barrier. *Cell* **121**, 689-702.

Lee, J. H. & Paull, T. T. (2004). Direct activation of the ATM protein kinase by the Mre11/Rad50/Nbs1 complex. *Science* **304**, 93-96.

Lee, J. H. & Paull, T. T. (2005). ATM activation by DNA double-strand breaks through the Mre11-Rad50-Nbs1 complex. *Science* **308**, 551-554.

Lee, Y. D. & Elledge, S. J. (2006). Control of ribonucleotide reductase localization through an anchoring mechanism involving Wtm1. *Genes Dev* **20**, 334-344.

Lei, M., Kawasaki, Y., Young, M. R., Kihara, M., Sugino, A. & Tye, B. K. (1997). Mcm2 is a target of regulation by Cdc7-Dbf4 during the initiation of DNA synthesis. *Genes Dev* **11**, 3365-3374.

Lemoine, F. J., Degtyareva, N. P., Lobachev, K. & Petes, T. D. (2005). Chromosomal translocations in yeast induced by low levels of DNA polymerase a model for chromosome fragile sites. *Cell* **120**, 587-598.

Lengauer, C., Kinzler, K. W. & Vogelstein, B. (1998). Genetic instabilities in human cancers. *Nature* **396**, 643-649.

Leroy, C., Lee, S. E., Vaze, M. B., Ochsenbien, F., Guerois, R., Haber, J. E. & Marsolier-Kergoat, M. C. (2003). PP2C phosphatases Ptc2 and Ptc3 are required for DNA checkpoint inactivation after a double-strand break. *Mol Cell* **11**, 827-835.

Li, J. M., Li, Y. & Elledge, S. J. (2005). Genetic analysis of the kinetochore DASH complex reveals an antagonistic relationship with the ras/protein kinase A pathway and a novel subunit required for Ask1 association. *Mol Cell Biol* **25**, 767-778.

Liang, B., Qiu, J., Ratnakumar, K. & Laurent, B. C. (2007). RSC functions as an early double-strand-break sensor in the cell's response to DNA damage. *Curr Biol* **17**, 1432-1437.

Liang, C. & Stillman, B. (1997). Persistent initiation of DNA replication and chromatin-bound MCM proteins during the cell cycle in cdc6 mutants. *Genes Dev* **11**, 3375-3386.

Liang, F. & Wang, Y. (2007). DNA damage checkpoints inhibit mitotic exit by two different mechanisms. *Mol Cell Biol* **27**, 5067-5078.

Lieber, M. R., Ma, Y., Pannicke, U. & Schwarz, K. (2003). Mechanism and regulation of human non-homologous DNA end-joining. *Nat Rev Mol Cell Biol* **4**, 712-720.

Lisby, M., Barlow, J. H., Burgess, R. C. & Rothstein, R. (2004). Choreography of the DNA damage response: spatiotemporal relationships among checkpoint and repair proteins. *Cell* **118**, 699-713.

Liu, C., Powell, K. A., Mundt, K., Wu, L., Carr, A. M. & Caspari, T. (2003). Cop9/signalosome subunits and Pcu4 regulate ribonucleotide reductase by both checkpoint-dependent and -independent mechanisms. *Genes Dev* **17**, 1130-1140.

Lombardo, V. A., Armas, P., Weiner, A. M. & Calcaterra, N. B. (2007). In vitro embryonic developmental phosphorylation of the cellular nucleic acid binding protein by cAMP-dependent protein kinase, and its relevance for biochemical activities. *Febs J* **274**, 485-497.

Longhese, M. P., Neecke, H., Paciotti, V., Lucchini, G. & Plevani, P. (1996). The 70 kDa subunit of replication protein A is required for the G1/S and intra-S DNA damage checkpoints in budding yeast. *Nucleic Acids Res* **24**, 3533-3537.

Longhese, M. P., Clerici, M. & Lucchini, G. (2003). The S-phase checkpoint and its regulation in Saccharomyces cerevisiae. *Mutat Res* **532**, 41-58.

Longtine, M. S., McKenzie, A., 3rd, Demarini, D. J., Shah, N. G., Wach, A., Brachat, A., Philippsen, P. & Pringle, J. R. (1998). Additional modules for versatile and economical PCR-based gene deletion and modification in Saccharomyces cerevisiae. *Yeast* **14**, 953-961.

Lopes, M., Cotta-Ramusino, C., Pellicioli, A., Liberi, G., Plevani, P., Muzi-Falconi, M., Newlon, C. S. & Foiani, M. (2001). The DNA replication checkpoint response stabilizes stalled replication forks. *Nature* **412**, 557-561.

Lopes, M., Foiani, M. & Sogo, J. M. (2006). Multiple mechanisms control chromosome integrity after replication fork uncoupling and restart at irreparable UV lesions. *Mol Cell* **21**, 15-27.

Lowndes, N. F., Johnson, A. L. & Johnston, L. H. (1991). Coordination of expression of DNA synthesis genes in budding yeast by a cell-cycle regulated trans factor. *Nature* **350**, 247-250.

Lu, X., Nannenga, B. & Donehower, L. A. (2005). PPM1D dephosphorylates Chk1 and p53 and abrogates cell cycle checkpoints. *Genes Dev* **19**, 1162-1174.

Lucca, C., Vanoli, F., Cotta-Ramusino, C., Pellicioli, A., Liberi, G., Haber, J. & Foiani, M. (2004). Checkpoint-mediated control of replisome-fork association and signalling in response to replication pausing. *Oncogene* **23**, 1206-1213.

Ma, J. L., Lee, S. J., Duong, J. K. & Stern, D. F. (2006). Activation of the checkpoint kinase Rad53 by the phosphatidyl inositol kinase-like kinase Mec1. *J Biol Chem* **281**, 3954-3963.

Marchler, G., Schuller, C., Adam, G. & Ruis, H. (1993). A Saccharomyces cerevisiae UAS element controlled by protein kinase A activates transcription in response to a variety of stress conditions. *Embo J* **12**, 1997-2003.

Marheineke, K. & Hyrien, O. (2004). Control of replication origin density and firing time in Xenopus egg extracts: role of a caffeine-sensitive, ATR-dependent checkpoint. *J Biol Chem* **279**, 28071-28081.

Marini, F., Pellicioli, A., Paciotti, V., Lucchini, G., Plevani, P., Stern, D. F. & Foiani, M. (1997). A role for DNA primase in coupling DNA replication to DNA damage response. *Embo J* **16**, 639-650.

Marsolier, M. C., Roussel, P., Leroy, C. & Mann, C. (2000). Involvement of the PP2C-like phosphatase Ptc2p in the DNA checkpoint pathways of Saccharomyces cerevisiae. *Genetics* **154**, 1523-1532.

Marti, T. M., Hefner, E., Feeney, L., Natale, V. & Cleaver, J. E. (2006). H2AX phosphorylation within the G1 phase after UV irradiation depends on nucleotide excision repair and not DNA double-strand breaks. *Proc Natl Acad Sci U S A* **103**, 9891-9896.

Martinez-Pastor, M. T., Marchler, G., Schuller, C., Marchler-Bauer, A., Ruis, H. & Estruch, F. (1996). The Saccharomyces cerevisiae zinc finger proteins Msn2p and Msn4p are required for transcriptional induction through the stress response element (STRE). *Embo J* **15**, 2227-2235.

Martomo, S. A. & Mathews, C. K. (2002). Effects of biological DNA precursor pool asymmetry upon accuracy of DNA replication in vitro. *Mutat Res* **499**, 197-211.

Mathews, C. K. & Slabaugh, M. B. (1986). Eukaryotic DNA metabolism. Are deoxyribonucleotides channeled to replication sites? *Exp Cell Res* **162**, 285-295.

Mathews, C. K., Sjoberg, B. M. & Reichard, P. (1987). Ribonucleotide reductase of Escherichia coli. Cross-linking agents as probes of quaternary and quinary structure. *Eur J Biochem* **166**, 279-285.

Mathews, C. K. (1993). Enzyme organization in DNA precursor biosynthesis. *Prog Nucleic Acid Res Mol Biol* **44**, 167-203.

Mathews, C. K. (2006). DNA precursor metabolism and genomic stability. *Faseb J* **20**, 1300-1314.

Matsuoka, S., Ballif, B. A., Smogorzewska, A. & other authors (2007). ATM and ATR substrate analysis reveals extensive protein networks responsive to DNA damage. *Science* **316**, 1160-1166.

Melo, J. A., Cohen, J. & Toczyski, D. P. (2001). Two checkpoint complexes are independently recruited to sites of DNA damage in vivo. *Genes Dev* **15**, 2809-2821.

Mendenhall, M. D. & Hodge, A. E. (1998). Regulation of Cdc28 cyclin-dependent protein kinase activity during the cell cycle of the yeast Saccharomyces cerevisiae. *Microbiol Mol Biol Rev* **62**, 1191-1243.

Merrill, B. J. & Holm, C. (1998). The RAD52 recombinational repair pathway is essential in pol30 (PCNA) mutants that accumulate small single-stranded DNA fragments during DNA synthesis. *Genetics* **148**, 611-624.

Merrill, B. J. & Holm, C. (1999). A requirement for recombinational repair in Saccharomyces cerevisiae is caused by DNA replication defects of mec1 mutants. *Genetics* **153**, 595-605.

Michaelis, C., Ciosk, R. & Nasmyth, K. (1997). Cohesins: chromosomal proteins that prevent premature separation of sister chromatids. *Cell* **91**, 35-45.

Michelotti, E. F., Tomonaga, T., Krutzsch, H. & Levens, D. (1995). Cellular nucleic acid binding protein regulates the CT element of the human c-myc protooncogene. *J Biol Chem* **270**, 9494-9499.

Mohanty, B. K., Bairwa, N. K. & Bastia, D. (2006). The Tof1p-Csm3p protein complex counteracts the Rrm3p helicase to control replication termination of Saccharomyces cerevisiae. *Proc Natl Acad Sci U S A* **103**, 897-902.

Moldovan, G. L., Pfander, B. & Jentsch, S. (2007). PCNA, the maestro of the replication fork. *Cell* **129**, 665-679.

Morgan, D. O. (1999). Regulation of the APC and the exit from mitosis. *Nat Cell Biol* **1**, E47-53.

Morishita, T., Mitsuzawa, H., Nakafuku, M., Nakamura, S., Hattori, S. & Anraku, Y. (1995). Requirement of Saccharomyces cerevisiae Ras for completion of mitosis. *Science* **270**, 1213-1215.

Morrison, A., Araki, H., Clark, A. B., Hamatake, R. K. & Sugino, A. (1990). A third essential DNA polymerase in S. cerevisiae. *Cell* **62**, 1143-1151.

Morrow, D. M., Tagle, D. A., Shiloh, Y., Collins, F. S. & Hieter, P. (1995). TEL1, an S. cerevisiae homolog of the human gene mutated in ataxia telangiectasia, is functionally related to the yeast checkpoint gene MEC1. *Cell* **82**, 831-840.

Mosch, H. U., Roberts, R. L. & Fink, G. R. (1996). Ras2 signals via the Cdc42/Ste20/mitogen-activated protein kinase module to induce filamentous growth in Saccharomyces cerevisiae. *Proc Natl Acad Sci U S A* **93**, 5352-5356.

Mosch, H. U., Kubler, E., Krappmann, S., Fink, G. R. & Braus, G. H. (1999). Crosstalk between the Ras2p-controlled mitogen-activated protein kinase and cAMP pathways during invasive growth of Saccharomyces cerevisiae. *Mol Biol Cell* **10**, 1325-1335.

Motoyama, N. & Naka, K. (2004). DNA damage tumor suppressor genes and genomic instability. *Curr Opin Genet Dev* **14**, 11-16.

Moyer, S. E., Lewis, P. W. & Botchan, M. R. (2006). Isolation of the Cdc45/Mcm2-7/GINS (CMG) complex, a candidate for the eukaryotic DNA replication fork helicase. *Proc Natl Acad Sci U S A* **103**, 10236-10241.

Muller, E. G. (1994). Deoxyribonucleotides are maintained at normal levels in a yeast thioredoxin mutant defective in DNA synthesis. *J Biol Chem* **269**, 24466-24471.

Myung, K., Datta, A. & Kolodner, R. D. (2001). Suppression of spontaneous chromosomal rearrangements by S phase checkpoint functions in Saccharomyces cerevisiae. *Cell* **104**, 397-408.

Nakada, D., Hirano, Y. & Sugimoto, K. (2004). Requirement of the Mre11 complex and exonuclease 1 for activation of the Mec1 signaling pathway. *Mol Cell Biol* **24**, 10016-10025.

Nakada, D., Hirano, Y., Tanaka, Y. & Sugimoto, K. (2005). Role of the C terminus of mec1 checkpoint kinase in its localization to sites of DNA damage. *Mol Biol Cell* **16**, 5227-5235.

Nakafuku, M., Obara, T., Kaibuchi, K. & other authors (1988). Isolation of a second yeast Saccharomyces cerevisiae gene (GPA2) coding for guanine nucleotide-binding regulatory protein: studies on its structure and possible functions. *Proc Natl Acad Sci U S A* **85**, 1374-1378.

Nasmyth, K. & Dirick, L. (1991). The role of SWI4 and SWI6 in the activity of G1 cyclins in yeast. *Cell* **66**, 995-1013.

Natale, D. A., Li, C. J., Sun, W. H. & DePamphilis, M. L. (2000). Selective instability of Orc1 protein accounts for the absence of functional origin recognition complexes during the M-G(1) transition in mammals. *Embo J* **19**, 2728-2738.

Neecke, H., Lucchini, G. & Longhese, M. P. (1999). Cell cycle progression in the presence of irreparable DNA damage is controlled by a Mec1- and Rad53-dependent checkpoint in budding yeast. *Embo J* **18**, 4485-4497.

Neuman-Silberberg, F. S., Bhattacharya, S. & Broach, J. R. (1995). Nutrient availability and the RAS/cyclic AMP pathway both induce expression of ribosomal protein genes in Saccharomyces cerevisiae but by different mechanisms. *Mol Cell Biol* **15**, 3187-3196.

Newlon, C. S. & Theis, J. F. (1993). The structure and function of yeast ARS elements. *Curr Opin Genet Dev* **3**, 752-758.

Nikawa, J., Cameron, S., Toda, T., Ferguson, K. M. & Wigler, M. (1987). Rigorous feedback control of cAMP levels in Saccharomyces cerevisiae. *Genes Dev* **1**, 931-937.

Nordlund, P. & Reichard, P. (2006). Ribonucleotide reductases. *Annu Rev Biochem* **75**, 681-706.

Nurse, P. & Thuriaux, P. (1980). Regulatory genes controlling mitosis in the fission yeast Schizosaccharomyces pombe. *Genetics* **96**, 627-637.

O'Driscoll, M., Ruiz-Perez, V. L., Woods, C. G., Jeggo, P. A. & Goodship, J. A. (2003). A splicing mutation affecting expression of ataxia-telangiectasia and Rad3-related protein (ATR) results in Seckel syndrome. *Nat Genet* **33**, 497-501.

Osborn, A. J. & Elledge, S. J. (2003). Mrc1 is a replication fork component whose phosphorylation in response to DNA replication stress activates Rad53. *Genes Dev* **17**, 1755-1767.

Paciotti, V., Lucchini, G., Plevani, P. & Longhese, M. P. (1998). Mec1p is essential for phosphorylation of the yeast DNA damage checkpoint protein Ddc1p, which physically interacts with Mec3p. *Embo J* **17**, 4199-4209.

Paciotti, V., Clerici, M., Lucchini, G. & Longhese, M. P. (2000). The checkpoint protein Ddc2, functionally related to S. pombe Rad26, interacts with Mec1 and is regulated by Mec1-dependent phosphorylation in budding yeast. *Genes Dev* **14**, 2046-2059.

Paciotti, V., Clerici, M., Scotti, M., Lucchini, G. & Longhese, M. P. (2001). Characterization of mec1 kinase-deficient mutants and of new hypomorphic mec1 alleles impairing subsets of the DNA damage response pathway. *Mol Cell Biol* **21**, 3913-3925.

Pandita, T. K. (2002). ATM function and telomere stability. *Oncogene* **21**, 611-618.

Paull, T. T., Rogakou, E. P., Yamazaki, V., Kirchgessner, C. U., Gellert, M. & Bonner, W. M. (2000). A critical role for histone H2AX in recruitment of repair factors to nuclear foci after DNA damage. *Curr Biol* **10**, 886-895.

Paulovich, A. G. & Hartwell, L. H. (1995). A checkpoint regulates the rate of progression through S phase in S. cerevisiae in response to DNA damage. *Cell* **82**, 841-847.

Pedruzzi, I., Burckert, N., Egger, P. & De Virgilio, C. (2000). Saccharomyces cerevisiae Ras/cAMP pathway controls post-diauxic shift element-dependent transcription through the zinc finger protein Gis1. *Embo J* **19**, 2569-2579.

Peeters, T., Louwet, W., Gelade, R., Nauwelaers, D., Thevelein, J. M. & Versele, M. (2006). Kelch-repeat proteins interacting with the Galpha protein Gpa2 bypass adenylate cyclase for direct regulation of protein kinase A in yeast. *Proc Natl Acad Sci U S A* **103**, 13034-13039.

Pellicioli, A., Lucca, C., Liberi, G., Marini, F., Lopes, M., Plevani, P., Romano, A., Di Fiore, P. P. & Foiani, M. (1999). Activation of Rad53 kinase in response to DNA damage and its effect in modulating phosphorylation of the lagging strand DNA polymerase. *Embo J* **18**, 6561-6572.

Pellicioli, A., Lee, S. E., Lucca, C., Foiani, M. & Haber, J. E. (2001). Regulation of Saccharomyces Rad53 checkpoint kinase during adaptation from DNA damage-induced G2/M arrest. *Mol Cell* **7**, 293-300.

Pellizzoni, L., Lotti, F., Maras, B. & Pierandrei-Amaldi, P. (1997). Cellular nucleic acid binding protein binds a conserved region of the 5' UTR of Xenopus laevis ribosomal protein mRNAs. *J Mol Biol* **267**, 264-275.

Pellizzoni, L., Lotti, F., Rutjes, S. A. & Pierandrei-Amaldi, P. (1998). Involvement of the Xenopus laevis Ro60 autoantigen in the alternative interaction of La and CNBP proteins with the 5'UTR of L4 ribosomal protein mRNA. *J Mol Biol* **281**, 593-608.

Perlstein, D. L., Ge, J., Ortigosa, A. D., Robblee, J. H., Zhang, Z., Huang, M. & Stubbe, J. (2005). The active form of the Saccharomyces cerevisiae ribonucleotide reductase small subunit is a heterodimer in vitro and in vivo. *Biochemistry* **44**, 15366-15377.

Pernambuco, M. B., Winderickx, J., Crauwels, M., Griffioen, G., Mager, W. H. & Thevelein, J. M. (1996). Glucose-triggered signalling in Saccharomyces cerevisiae: different requirements for sugar phosphorylation between cells grown on glucose and those grown on non-fermentable carbon sources. *Microbiology* **142 (Pt 7)**, 1775-1782.

Peterson, C. L. & Cote, J. (2004). Cellular machineries for chromosomal DNA repair. *Genes Dev* **18**, 602-616.

Piatti, S., Bohm, T., Cocker, J. H., Diffley, J. F. & Nasmyth, K. (1996). Activation of S-phase-promoting CDKs in late G1 defines a "point of no return" after which Cdc6 synthesis cannot promote DNA replication in yeast. *Genes Dev* **10**, 1516-1531.

Polymenis, M. & Schmidt, E. V. (1997). Coupling of cell division to cell growth by translational control of the G1 cyclin CLN3 in yeast. *Genes Dev* **11**, 2522-2531.

Prem veer Reddy, G. & Pardee, A. B. (1980). Multienzyme complex for metabolic channeling in mammalian DNA replication. *Proc Natl Acad Sci U S A* **77**, 3312-3316.

Raghuraman, M. K., Winzeler, E. A., Collingwood, D. & other authors (2001). Replication dynamics of the yeast genome. *Science* **294**, 115-121.

Rajavashisth, T. B., Taylor, A. K., Andalibi, A., Svenson, K. L. & Lusis, A. J. (1989). Identification of a zinc finger protein that binds to the sterol regulatory element. *Science* **245**, 640-643.

Reichard, P. (1988). Interactions between deoxyribonucleotide and DNA synthesis. *Annu Rev Biochem* **57**, 349-374.

Reichard, P., Eliasson, R., Ingemarson, R. & Thelander, L. (2000). Cross-talk between the allosteric effector-binding sites in mouse ribonucleotide reductase. *J Biol Chem* **275**, 33021-33026.

Reynolds, A. E., McCarroll, R. M., Newlon, C. S. & Fangman, W. L. (1989). Time of replication of ARS elements along yeast chromosome III. *Mol Cell Biol* **9**, 4488-4494.

Rhind, N. & Russell, P. (1998). Mitotic DNA damage and replication checkpoints in yeast. *Curr Opin Cell Biol* **10**, 749-758.

Ricke, R. M. & Bielinsky, A. K. (2004). Mcm10 regulates the stability and chromatin association of DNA polymerase-alpha. *Mol Cell* **16**, 173-185.

Ritchie, K. B., Mallory, J. C. & Petes, T. D. (1999). Interactions of TLC1 (which encodes the RNA subunit of telomerase), TEL1, and MEC1 in regulating telomere length in the yeast Saccharomyces cerevisiae. *Mol Cell Biol* **19**, 6065-6075.

Rogakou, E. P., Pilch, D. R., Orr, A. H., Ivanova, V. S. & Bonner, W. M. (1998). DNA double-stranded breaks induce histone H2AX phosphorylation on serine 139. *J Biol Chem* **273**, 5858-5868.

Rogakou, E. P., Boon, C., Redon, C. & Bonner, W. M. (1999). Megabase chromatin domains involved in DNA double-strand breaks in vivo. *J Cell Biol* **146**, 905-916.

Rolland, F., De Winde, J. H., Lemaire, K., Boles, E., Thevelein, J. M. & Winderickx, J. (2000). Glucose-induced cAMP signalling in yeast requires

both a G-protein coupled receptor system for extracellular glucose detection and a separable hexose kinase-dependent sensing process. *Mol Microbiol* **38**, 348-358.

Roosen, J., Engelen, K., Marchal, K. & other authors (2005). PKA and Sch9 control a molecular switch important for the proper adaptation to nutrient availability. *Mol Microbiol* **55**, 862-880.

Rouse, J. & Jackson, S. P. (2002). Lcd1p recruits Mec1p to DNA lesions in vitro and in vivo. *Mol Cell* **9**, 857-869.

Sancar, A., Lindsey-Boltz, L. A., Unsal-Kacmaz, K. & Linn, S. (2004). Molecular mechanisms of mammalian DNA repair and the DNA damage checkpoints. *Annu Rev Biochem* **73**, 39-85.

Sanchez, Y., Desany, B. A., Jones, W. J., Liu, Q., Wang, B. & Elledge, S. J. (1996). Regulation of RAD53 by the ATM-like kinases MEC1 and TEL1 in yeast cell cycle checkpoint pathways. *Science* **271**, 357-360.

Santocanale, C. & Diffley, J. F. (1998). A Mec1- and Rad53-dependent checkpoint controls late-firing origins of DNA replication. *Nature* **395**, 615-618.

Sass, P., Field, J., Nikawa, J., Toda, T. & Wigler, M. (1986). Cloning and characterization of the high-affinity cAMP phosphodiesterase of Saccharomyces cerevisiae. *Proc Natl Acad Sci U S A* **83**, 9303-9307.

Schaarschmidt, D., Baltin, J., Stehle, I. M., Lipps, H. J. & Knippers, R. (2004). An episomal mammalian replicon: sequence-independent binding of the origin recognition complex. *Embo J* **23**, 191-201.

Schimmang, T., Tollervey, D., Kern, H., Frank, R. & Hurt, E. C. (1989). A yeast nucleolar protein related to mammalian fibrillarin is associated with small nucleolar RNA and is essential for viability. *Embo J* **8**, 4015-4024.

Schneider, B. L., Seufert, W., Steiner, B., Yang, Q. H. & Futcher, A. B. (1995). Use of polymerase chain reaction epitope tagging for protein tagging in Saccharomyces cerevisiae. *Yeast* **11**, 1265-1274.

Schuller, H. J. (2003). Transcriptional control of nonfermentative metabolism in the yeast Saccharomyces cerevisiae. *Curr Genet* **43**, 139-160.

Schwab, M., Lutum, A. S. & Seufert, W. (1997). Yeast Hct1 is a regulator of Clb2 cyclin proteolysis. *Cell* **90**, 683-693.

Schwartz, M., Zlotorynski, E. & Kerem, B. (2006). The molecular basis of common and rare fragile sites. *Cancer Lett* **232**, 13-26.

Schwartz, M. F., Duong, J. K., Sun, Z., Morrow, J. S., Pradhan, D. & Stern, D. F. (2002). Rad9 phosphorylation sites couple Rad53 to the Saccharomyces cerevisiae DNA damage checkpoint. *Mol Cell* **9**, 1055-1065.

Sclafani, R. A. & Holzen, T. M. (2007). Cell cycle regulation of DNA replication. *Annu Rev Genet* **41**, 237-280.

Searle, J. S., Schollaert, K. L., Wilkins, B. J. & Sanchez, Y. (2004). The DNA damage checkpoint and PKA pathways converge on APC substrates and Cdc20 to regulate mitotic progression. *Nat Cell Biol* **6**, 138-145.

Shechter, D., Costanzo, V. & Gautier, J. (2004). ATR and ATM regulate the timing of DNA replication origin firing. *Nat Cell Biol* **6**, 648-655.

Shen, C., Lancaster, C. S., Shi, B., Guo, H., Thimmaiah, P. & Bjornsti, M. A. (2007). TOR Signaling Is a Determinant of Cell Survival in Response to DNA Damage. *Mol Cell Biol* **27**, 7007-7017.

Shimada, K., Pasero, P. & Gasser, S. M. (2002). ORC and the intra-S-phase checkpoint: a threshold regulates Rad53p activation in S phase. *Genes Dev* **16**, 3236-3252.

Shimada, K. & Gasser, S. M. (2007). The origin recognition complex functions in sister-chromatid cohesion in Saccharomyces cerevisiae. *Cell* **128**, 85-99.

Shimizu, K., Chen, W., Ashique, A. M., Moroi, R. & Li, Y. P. (2003). Molecular cloning, developmental expression, promoter analysis and functional characterization of the mouse CNBP gene. *Gene* **307**, 51-62.

Sidorova, J. M. & Breeden, L. L. (1997). Rad53-dependent phosphorylation of Swi6 and down-regulation of CLN1 and CLN2 transcription occur in response to DNA damage in Saccharomyces cerevisiae. *Genes Dev* **11**, 3032-3045.

Siede, W., Friedberg, A. S. & Friedberg, E. C. (1993). RAD9-dependent G1 arrest defines a second checkpoint for damaged DNA in the cell cycle of Saccharomyces cerevisiae. *Proc Natl Acad Sci U S A* **90**, 7985-7989.

Slater, M. L. (1973). Effect of reversible inhibition of deoxyribonucleic acid synthesis on the yeast cell cycle. *J Bacteriol* **113**, 263-270.

Smith, A., Ward, M. P. & Garrett, S. (1998). Yeast PKA represses Msn2p/Msn4p-dependent gene expression to regulate growth, stress response and glycogen accumulation. *Embo J* **17**, 3556-3564.

Smogorzewska, A. & de Lange, T. (2004). Regulation of telomerase by telomeric proteins. *Annu Rev Biochem* **73**, 177-208.

Smolka, M. B., Albuquerque, C. P., Chen, S. H. & Zhou, H. (2007). Proteome-wide identification of in vivo targets of DNA damage checkpoint kinases. *Proc Natl Acad Sci U S A* **104**, 10364-10369.

Sogo, J. M., Lopes, M. & Foiani, M. (2002). Fork reversal and ssDNA accumulation at stalled replication forks owing to checkpoint defects. *Science* **297**, 599-602.

Stegmeier, F., Visintin, R. & Amon, A. (2002). Separase, polo kinase, the kinetochore protein Slk19, and Spo12 function in a network that controls Cdc14 localization during early anaphase. *Cell* **108**, 207-220.

Stegmeier, F. & Amon, A. (2004). CLOSING MITOSIS: The Functions of the Cdc14 Phosphatase and Its Regulation. *Annu Rev Genet* **38**, 203-232.

Strahl-Bolsinger, S., Hecht, A., Luo, K. & Grunstein, M. (1997). SIR2 and SIR4 interactions differ in core and extended telomeric heterochromatin in yeast. *Genes Dev* **11**, 83-93.

Suka, N., Nakashima, E., Shinmyozu, K., Hidaka, M. & Jingami, H. (2006). The WD40-repeat protein Pwp1p associates in vivo with 25S ribosomal chromatin in a histone H4 tail-dependent manner. *Nucleic Acids Res* **34**, 3555-3567.

Sullivan, M. & Uhlmann, F. (2003). A non-proteolytic function of separase links the onset of anaphase to mitotic exit. *Nat Cell Biol* **5**, 249-254.

Sun, Z., Fay, D. S., Marini, F., Foiani, M. & Stern, D. F. (1996). Spk1/Rad53 is regulated by Mec1-dependent protein phosphorylation in DNA replication and damage checkpoint pathways. *Genes Dev* **10**, 395-406.

Surana, U., Amon, A., Dowzer, C., McGrew, J., Byers, B. & Nasmyth, K. (1993). Destruction of the CDC28/CLB mitotic kinase is not required for the metaphase to anaphase transition in budding yeast. *Embo J* **12**, 1969-1978.

Tadi, D., Hasan, R. N., Bussereau, F., Boy-Marcotte, E. & Jacquet, M. (1999). Selection of genes repressed by cAMP that are induced by nutritional limitation in Saccharomyces cerevisiae. *Yeast* **15**, 1733-1745.

Takayama, Y., Kamimura, Y., Okawa, M., Muramatsu, S., Sugino, A. & Araki, H. (2003). GINS, a novel multiprotein complex required for chromosomal DNA replication in budding yeast. *Genes Dev* **17**, 1153-1165.

Tanaka, H., Arakawa, H., Yamaguchi, T., Shiraishi, K., Fukuda, S., Matsui, K., Takei, Y. & Nakamura, Y. (2000). A ribonucleotide reductase gene involved in a p53-dependent cell-cycle checkpoint for DNA damage. *Nature* **404**, 42-49.

Tanaka, S., Umemori, T., Hirai, K., Muramatsu, S., Kamimura, Y. & Araki, H. (2007). CDK-dependent phosphorylation of Sld2 and Sld3 initiates DNA replication in budding yeast. *Nature* **445**, 328-332.

Tatchell, K., Robinson, L. C. & Breitenbach, M. (1985). RAS2 of Saccharomyces cerevisiae is required for gluconeogenic growth and proper response to nutrient limitation. *Proc Natl Acad Sci U S A* **82**, 3785-3789.

Taylor, S. S., Buechler, J. A. & Yonemoto, W. (1990). cAMP-dependent protein kinase: framework for a diverse family of regulatory enzymes. *Annu Rev Biochem* **59**, 971-1005.

Tercero, J. A. & Diffley, J. F. (2001). Regulation of DNA replication fork progression through damaged DNA by the Mec1/Rad53 checkpoint. *Nature* **412**, 553-557.

Thelander, L. & Reichard, P. (1979). Reduction of ribonucleotides. *Annu Rev Biochem* **48**, 133-158.

Thevelein, J. M. & de Winde, J. H. (1999). Novel sensing mechanisms and targets for the cAMP-protein kinase A pathway in the yeast Saccharomyces cerevisiae. *Mol Microbiol* **33**, 904-918.

Thevelein, J. M., Cauwenberg, L., Colombo, S. & other authors (2000). Nutrient-induced signal transduction through the protein kinase A pathway and its role in the control of metabolism, stress resistance, and growth in yeast. *Enzyme Microb Technol* **26**, 819-825.

Thevelein, J. M., Gelade, R., Holsbeeks, I. & other authors (2005). Nutrient sensing systems for rapid activation of the protein kinase A pathway in yeast. *Biochem Soc Trans* **33**, 253-256.

Toda, T., Uno, I., Ishikawa, T. & other authors (1985). In yeast, RAS proteins are controlling elements of adenylate cyclase. *Cell* **40**, 27-36.

Toda, T., Cameron, S., Sass, P., Zoller, M., Scott, J. D., McMullen, B., Hurwitz, M., Krebs, E. G. & Wigler, M. (1987a). Cloning and characterization of BCY1, a locus encoding a regulatory subunit of the cyclic AMP-dependent protein kinase in Saccharomyces cerevisiae. *Mol Cell Biol* **7**, 1371-1377.

Toda, T., Cameron, S., Sass, P., Zoller, M. & Wigler, M. (1987b). Three different genes in S. cerevisiae encode the catalytic subunits of the cAMP-dependent protein kinase. *Cell* **50**, 277-287.

Toda, T., Cameron, S., Sass, P. & Wigler, M. (1988). SCH9, a gene of Saccharomyces cerevisiae that encodes a protein distinct from, but functionally and structurally related to, cAMP-dependent protein kinase catalytic subunits. *Genes Dev* **2**, 517-527.

Tokiwa, G., Tyers, M., Volpe, T. & Futcher, B. (1994). Inhibition of G1 cyclin activity by the Ras/cAMP pathway in yeast. *Nature* **371**, 342-345.

Tollervey, D., Lehtonen, H., Carmo-Fonseca, M. & Hurt, E. C. (1991). The small nucleolar RNP protein NOP1 (fibrillarin) is required for pre-rRNA processing in yeast. *Embo J* **10**, 573-583.

Toone, W. M., Aerne, B. L., Morgan, B. A. & Johnston, L. H. (1997). Getting started: regulating the initiation of DNA replication in yeast. *Annu Rev Microbiol* **51**, 125-149.

Tourriere, H. & Pasero, P. (2007). Maintenance of fork integrity at damaged DNA and natural pause sites. *DNA Repair (Amst)* **6**, 900-913.

Traven, A., Hammet, A., Tenis, N., Denis, C. L. & Heierhorst, J. (2005). Ccr4-not complex mRNA deadenylase activity contributes to DNA damage responses in Saccharomyces cerevisiae. *Genetics* **169**, 65-75.

Trenz, K., Smith, E., Smith, S. & Costanzo, V. (2006). ATM and ATR promote Mre11 dependent restart of collapsed replication forks and prevent accumulation of DNA breaks. *Embo J* **25**, 1764-1774.

Tyers, M., Tokiwa, G. & Futcher, B. (1993). Comparison of the Saccharomyces cerevisiae G1 cyclins: Cln3 may be an upstream activator of Cln1, Cln2 and other cyclins. *Embo J* **12**, 1955-1968.

Uchiki, T., Dice, L. T., Hettich, R. L. & Dealwis, C. (2004). Identification of phosphorylation sites on the yeast ribonucleotide reductase inhibitor Sml1. *J Biol Chem* **279**, 11293-11303.

Uhlmann, F. & Nasmyth, K. (1998). Cohesion between sister chromatids must be established during DNA replication. *Curr Biol* **8**, 1095-1101.

Uhlmann, F., Lottspeich, F. & Nasmyth, K. (1999). Sister-chromatid separation at anaphase onset is promoted by cleavage of the cohesin subunit Scc1. *Nature* **400**, 37-42.

Unal, E., Arbel-Eden, A., Sattler, U., Shroff, R., Lichten, M., Haber, J. E. & Koshland, D. (2004). DNA damage response pathway uses histone modification to assemble a double-strand break-specific cohesin domain. *Mol Cell* **16**, 991-1002.

Uno, I., Matsumoto, K., Adachi, K. & Ishikawa, T. (1983). Genetic and biochemical evidence that trehalase is a substrate of cAMP-dependent protein kinase in yeast. *J Biol Chem* **258**, 10867-10872.

Unsal-Kacmaz, K. & Sancar, A. (2004). Quaternary structure of ATR and effects of ATRIP and replication protein A on its DNA binding and kinase activities. *Mol Cell Biol* **24**, 1292-1300.

Urban, J., Soulard, A., Huber, A. & other authors (2007). Sch9 is a major target of TORC1 in Saccharomyces cerevisiae. *Mol Cell* **26**, 663-674.

Usui, T., Ogawa, H. & Petrini, J. H. (2001). A DNA damage response pathway controlled by Tel1 and the Mre11 complex. *Mol Cell* **7**, 1255-1266.

Uziel, T., Lerenthal, Y., Moyal, L., Andegeko, Y., Mittelman, L. & Shiloh, Y. (2003). Requirement of the MRN complex for ATM activation by DNA damage. *Embo J* **22**, 5612-5621.

Vallen, E. A. & Cross, F. R. (1999). Interaction between the MEC1-dependent DNA synthesis checkpoint and G1 cyclin function in Saccharomyces cerevisiae. *Genetics* **151**, 459-471.

van Heumen, W. R., Claxton, C. & Pickles, J. O. (1997). Sequence and tissue distribution of chicken cellular nucleic acid binding protein cDNA. *Comp Biochem Physiol B Biochem Mol Biol* **118**, 659-665.

Vas, A. C., Andrews, C. A., Kirkland Matesky, K. & Clarke, D. J. (2007). In vivo analysis of chromosome condensation in Saccharomyces cerevisiae. *Mol Biol Cell* **18**, 557-568.

Vaze, M. B., Pellicioli, A., Lee, S. E., Ira, G., Liberi, G., Arbel-Eden, A., Foiani, M. & Haber, J. E. (2002). Recovery from checkpoint-mediated arrest after repair of a double-strand break requires Srs2 helicase. *Mol Cell* **10**, 373-385.

Visintin, R., Prinz, S. & Amon, A. (1997). CDC20 and CDH1: a family of substrate-specific activators of APC-dependent proteolysis. *Science* **278**, 460-463.

Visintin, R., Craig, K., Hwang, E. S., Prinz, S., Tyers, M. & Amon, A. (1998). The phosphatase Cdc14 triggers mitotic exit by reversal of Cdk-dependent phosphorylation. *Mol Cell* **2**, 709-718.

Visintin, R., Hwang, E. S. & Amon, A. (1999). Cfi1 prevents premature exit from mitosis by anchoring Cdc14 phosphatase in the nucleolus. *Nature* **398**, 818-823.

Wach, A., Brachat, A., Pohlmann, R. & Philippsen, P. (1994). New heterologous modules for classical or PCR-based gene disruptions in Saccharomyces cerevisiae. *Yeast* **10**, 1793-1808.

Waga, S. & Stillman, B. (1998). The DNA replication fork in eukaryotic cells. *Annu Rev Biochem* **67**, 721-751.

Wakayama, T., Kondo, T., Ando, S., Matsumoto, K. & Sugimoto, K. (2001). Pie1, a protein interacting with Mec1, controls cell growth and checkpoint responses in Saccharomyces cerevisiae. *Mol Cell Biol* **21**, 755-764.

Wang, H. & Elledge, S. J. (1999). DRC1, DNA replication and checkpoint protein 1, functions with DPB11 to control DNA replication and the S-phase checkpoint in Saccharomyces cerevisiae. *Proc Natl Acad Sci U S A* **96**, 3824-3829.

Wang, H., Liu, D., Wang, Y., Qin, J. & Elledge, S. J. (2001). Pds1 phosphorylation in response to DNA damage is essential for its DNA damage checkpoint function. *Genes Dev* **15**, 1361-1372.

Wang, P. J., Chabes, A., Casagrande, R., Tian, X. C., Thelander, L. & Huffaker, T. C. (1997). Rnr4p, a novel ribonucleotide reductase small-subunit protein. *Mol Cell Biol* **17**, 6114-6121.

Wang, Y., Xu, H. P., Riggs, M., Rodgers, L. & Wigler, M. (1991). byr2, a Schizosaccharomyces pombe gene encoding a protein kinase capable of partial suppression of the ras1 mutant phenotype. *Mol Cell Biol* **11**, 3554-3563.

Warden, C. H., Krisans, S. K., Purcell-Huynh, D., Leete, L. M., Daluiski, A., Diep, A., Taylor, B. A. & Lusis, A. J. (1994). Mouse cellular nucleic acid binding proteins: a highly conserved family identified by genetic mapping and sequencing. *Genomics* **24**, 14-19.

Warner, J. R. (1999). The economics of ribosome biosynthesis in yeast. *Trends Biochem Sci* **24**, 437-440.

Weiner, A. M., Allende, M. L., Becker, T. S. & Calcaterra, N. B. (2007). CNBP mediates neural crest cell expansion by controlling cell proliferation and cell survival during rostral head development. *J Cell Biochem* **102**, 1553-1570.

Weinert, T. A., Kiser, G. L. & Hartwell, L. H. (1994). Mitotic checkpoint genes in budding yeast and the dependence of mitosis on DNA replication and repair. *Genes Dev* **8**, 652-665.

Weinreich, M. & Stillman, B. (1999). Cdc7p-Dbf4p kinase binds to chromatin during S phase and is regulated by both the APC and the RAD53 checkpoint pathway. *Embo J* **18**, 5334-5346.

West, S. C. (2003). Molecular views of recombination proteins and their control. *Nat Rev Mol Cell Biol* **4**, 435-445.

White, J. H., Green, S. R., Barker, D. G., Dumas, L. B. & Johnston, L. H. (1987). The CDC8 transcript is cell cycle regulated in yeast and is expressed coordinately with CDC9 and CDC21 at a point preceding histone transcription. *Exp Cell Res* **171**, 223-231.

Wigler, M., Field, J., Powers, S. & other authors (1988). Studies of RAS function in the yeast Saccharomyces cerevisiae. *Cold Spring Harb Symp Quant Biol* **53 Pt 2**, 649-655.

Winey, M. & O'Toole, E. T. (2001). The spindle cycle in budding yeast. *Nat Cell Biol* **3**, E23-27.

Woollard, A., Basi, G. & Nurse, P. (1996). A novel S phase inhibitor in fission yeast. *Embo J* **15**, 4603-4612.

Woolstencroft, R. N., Beilharz, T. H., Cook, M. A., Preiss, T., Durocher, D. & Tyers, M. (2006). Ccr4 contributes to tolerance of replication stress through control of CRT1 mRNA poly(A) tail length. *J Cell Sci* **119**, 5178-5192.

Wullschleger, S., Loewith, R. & Hall, M. N. (2006). TOR signaling in growth and metabolism. *Cell* **124**, 471-484.

Xie, A., Puget, N., Shim, I., Odate, S., Jarzyna, I., Bassing, C. H., Alt, F. W. & Scully, R. (2004). Control of sister chromatid recombination by histone H2AX. *Mol Cell* **16**, 1017-1025.

Xu, H. P., Rajavashisth, T., Grewal, N., Jung, V., Riggs, M., Rodgers, L. & Wigler, M. (1992). A gene encoding a protein with seven zinc finger domains acts on the sexual differentiation pathways of Schizosaccharomyces pombe. *Mol Biol Cell* **3**, 721-734.

Xue, L., Zhou, B., Liu, X., Qiu, W., Jin, Z. & Yen, Y. (2003). Wild-type p53 regulates human ribonucleotide reductase by protein-protein interaction with p53R2 as well as hRRM2 subunits. *Cancer Res* **63**, 980-986.

Xue, Y., Batlle, M. & Hirsch, J. P. (1998). GPR1 encodes a putative G protein-coupled receptor that associates with the Gpa2p Galpha subunit and functions in a Ras-independent pathway. *Embo J* **17**, 1996-2007.

Yamada, H., Kumada, K. & Yanagida, M. (1997). Distinct subunit functions and cell cycle regulated phosphorylation of 20S APC/cyclosome required for anaphase in fission yeast. *J Cell Sci* **110 (Pt 15)**, 1793-1804.

Yao, R., Zhang, Z., An, X., Bucci, B., Perlstein, D. L., Stubbe, J. & Huang, M. (2003). Subcellular localization of yeast ribonucleotide reductase regulated by the DNA replication and damage checkpoint pathways. *Proc Natl Acad Sci U S A* **100**, 6628-6633.

Yasuda, J., Mashiyama, S., Makino, R., Ohyama, S., Sekiya, T. & Hayashi, K. (1995). Cloning and characterization of rat cellular nucleic acid binding protein (CNBP) cDNA. *DNA Res* **2**, 45-49.

Yoshida, S., Ichihashi, R. & Toh-e, A. (2003). Ras recruits mitotic exit regulator Lte1 to the bud cortex in budding yeast. *J Cell Biol* **161**, 889-897.

Yoshioka, K., Yoshioka, Y. & Hsieh, P. (2006). ATR kinase activation mediated by MutSalpha and MutLalpha in response to cytotoxic O6-methylguanine adducts. *Mol Cell* **22**, 501-510.

You, Z., Chahwan, C., Bailis, J., Hunter, T. & Russell, P. (2005). ATM Activation and Its Recruitment to Damaged DNA Require Binding to the C Terminus of Nbs1. *Mol Cell Biol* **25**, 5363-5379.

You, Z., Bailis, J. M., Johnson, S. A., Dilworth, S. M. & Hunter, T. (2007). Rapid activation of ATM on DNA flanking double-strand breaks. *Nat Cell Biol* **9**, 1311-1318.

Zachariae, W. & Nasmyth, K. (1999). Whose end is destruction: cell division and the anaphase-promoting complex. *Genes Dev* **13**, 2039-2058.

Zegerman, P. & Diffley, J. F. (2007). Phosphorylation of Sld2 and Sld3 by cyclin-dependent kinases promotes DNA replication in budding yeast. *Nature* **445**, 281-285.

Zhang, W., Morris, Q. D., Chang, R. & other authors (2004). The functional landscape of mouse gene expression. *J Biol* **3**, 21.

Zhang, Z., An, X., Yang, K., Perlstein, D. L., Hicks, L., Kelleher, N., Stubbe, J. & Huang, M. (2006). Nuclear localization of the Saccharomyces cerevisiae ribonucleotide reductase small subunit requires a karyopherin and a WD40 repeat protein. *Proc Natl Acad Sci U S A.*

Zhang, Z., Yang, K., Chen, C. C., Feser, J. & Huang, M. (2007). Role of the C terminus of the ribonucleotide reductase large subunit in enzyme regeneration and its inhibition by Sml1. *Proc Natl Acad Sci U S A* **104**, 2217-2222.

Zhao, X., Muller, E. G. & Rothstein, R. (1998). A suppressor of two essential checkpoint genes identifies a novel protein that negatively affects dNTP pools. *Mol Cell* **2**, 329-340.

Zhao, X., Chabes, A., Domkin, V., Thelander, L. & Rothstein, R. (2001). The ribonucleotide reductase inhibitor Sml1 is a new target of the Mec1/Rad53 kinase cascade during growth and in response to DNA damage. *Embo J* **20**, 3544-3553.

Zhao, X. & Rothstein, R. (2002). The Dun1 checkpoint kinase phosphorylates and regulates the ribonucleotide reductase inhibitor Sml1. *Proc Natl Acad Sci U S A* **99**, 3746-3751.

Zhao, Z. S., Leung, T., Manser, E. & Lim, L. (1995). Pheromone signalling in Saccharomyces cerevisiae requires the small GTP-binding protein Cdc42p and its activator CDC24. *Mol Cell Biol* **15**, 5246-5257.

Zhou, Z. & Elledge, S. J. (1993). DUN1 encodes a protein kinase that controls the DNA damage response in yeast. *Cell* **75**, 1119-1127.

Zou, L. & Elledge, S. J. (2003). Sensing DNA damage through ATRIP recognition of RPA-ssDNA complexes. *Science* **300**, 1542-1548.

Zou, L., Liu, D. & Elledge, S. J. (2003). Replication protein A-mediated recruitment and activation of Rad17 complexes. *Proc Natl Acad Sci U S A* **100**, 13827-13832.